Sulfur-Containing Polymers for Surface Attachment

Dissertation
zur Erlangung des Grades
„Doktor der Naturwissenschaften“
im Promotionsfach Chemie

am Fachbereich Chemie, Pharmazie und Geowissenschaften
der Johannes Gutenberg-Universität
in Mainz

Jasmin Preis

geboren in Rockenhausen

Mainz 2012

Dekan:

1. Berichterstatter:
2. Berichterstatter:

Tag der mündlichen Prüfung: 26.07.2012

Hiermit versichere ich gemäß §10 Abs. 3d der Promotionsordnung vom 24.07.2007, dass ich die als Dissertation vorgelegte Arbeit selbst angefertigt und alle benutzten Hilfsmittel (Literatur, Apparaturen, Material) in der Arbeit angegeben habe.

Die vorliegende Arbeit wurde in der Zeit von November 2008 bis Juli 2012 am Institut für Organische Chemie der Johannes Gutenberg-Universität Mainz angefertigt.

Contents

Chapter 1

Abstract & Zusammenfassung

1.1 Abstract

Different concepts for the synthesis of sulfur-containing polymers as well as their adsorption onto gold surfaces were studied. The present work is divided into three parts. The main part focuses on the synthesis of poly(1,2-alkylene sulfides) ("polysulfides") with complex architectures on the basis of polyether-based macroinitiators by the anionic ring-opening polymerization of ethylene sulfide and propylene sulfide. This synthetic tool kit allowed the synthesis of star-shaped, brush-like, comb-like and pom-pom-like polysulfides, the latter two with an additional poly(ethylene glycol) chain. Additionally, the number of polysulfide arms as well as the monomer composition could be varied over a wide range to obtain copolymers with multiple thioether functionalities.

The second section deals with the synthesis of a novel lipoic acid-based initiator for ring-opening polymerizations for lactones and epoxides. A straightforward approach was selected to accomplish the ability to obtain tailored polymers with a common used disulfide-anchoring group, without the drawbacks of post-polymerization functionalization.

In the third part, a new class of block-copolymers consisting of polysulfides and polyesters were investigated. For the first time this approach enabled the use of hydroxyl-terminated poly(propylene sulfide) as macroinitiator for the synthesis of a second block.

The adsorption efficiency of those different polymer classes onto gold nanoparticles as well as gold supports was studied via different methods.

1.2 Zusammenfassung

Unterschiedliche Synthesekonzepte für schwefelhaltig Polymere sowie deren Adsorption an Goldoberflächen wurde untersucht. Die vorliegende Arbeit ist dabei in drei Teile gegliedert. Der Hauptteil der Arbeit beschäftigt sich mit der Synthese von Poly(1,2-alkenylsulfiden) („Polysulfide") anspruchsvoller Architekturen. Dies wurde mittels polyether-basierten Makroinitiatoren und anionischer ringöffnender Polymerisation von Ethylensulfid und Propylensulfid realisiert. Dieser vielseitig Ansatz ermöglicht einerseits die Synthese von sternförmigen sowie bürstenartigen Polysulfiden und andererseits die Synthese von kammartigen sowie pompom-förmigen Polysulfiden, die zusätzlich eine Polyethylenglykolkette tragen. Des Weiteren kann die Anzahl sowie die Monomerzusammensetzung der Polysulfidketten über einen sehr breiten Bereich variiert werden, um so Copolymere mit unzähligen Thioetherfunktionalitäten zu erhalten.

Der zweite Abschnitt behandelt die Synthese von einem neuen liponsäure-basiertem Initiator für die ringöffnende Polymerisation von Lactonen und Epoxiden. Hierfür wurde ein unkompliziertes Konzept gewählt, um maßgeschneiderte Polymere mit einer weitverbreitete Bindungsstelle zu erhalten, ohne die üblichen Nachteile einer polymeranalogen Funktionalisierung.

Im dritten Teil der Arbeit wiederum wird eine neue Blockcopolymer Klasse, bestehend aus Polyestern und Polysulfiden, untersucht. Dabei wurde zum ersten Mal ein hydroxyl-terminiertes Polysulfid als Makroinitiator benutzt, um einen weiteren Polymerblock zu synthetisieren.

Die Absorptionseffektivität dieser verschiedenen Polymerklassen an Goldnanopartikel und Goldträger wurde anschließend mittels verschiedener Methoden analysiert.

Chapter 2

Objectives of this Thesis

2.1 Introduction

The investigation of sulfur-containing polymers was motivated by the request to study the behavior of polymers, which were attached to surfaces. The strong attraction between sulfur and gold seemed suitable for this issue. The aim of this work was to study polymers, which were commonly investigated by Frey et al. or related to those, such as polyethers, polyether-polyols as well as polyesters. The intension was realized by two main concepts. The first concept was based on polysulfides with multiple sulfide functionalities and the second concept incorporated the use of a disulfide anchoring group.

2.2 Polysulfides

The study of polysulfides was inspired by the structural relationship between episulfides and epoxides, which are common monomers for preparation of polyethers. The results of Tirelli and Hubbell on poly(propylene sulfide) homopolymers as well as poly(propylene sulfide)-poly(ethylene glycol) block-copolymers and their numerous useful applications especially in the field of biomedicine as well as the ability to adsorb on gold substrates, which are described in the introduction of chapter 4 in more detail, supported the research intention.

Two different strategies concerning polysulfides were targeted in this thesis: The use of macroinitiators for thiiranes as well as the use of a polysulfide as macroinitiator. The first concept used different well-known polyethers as macroinitiators for thiiranes to accomplish the synthesis of sulfur-containing polymers with complex architectures and a variable number of polysulfide arms. The anionic ring-opening polymerization of thiiranes requires a thiol as initiating group and an effective synthetic route to convert polyether-polyols into polythiols, which was based on post-polymerization modifications, was investigated first. The use of such macroinitiators enabled the synthesis of star-shaped, brush- as well as comb-like and pom-pom-like polysulfides. Comb- and pom-pom-like structures carried an additional PEG chain (**Figure 2.1**).

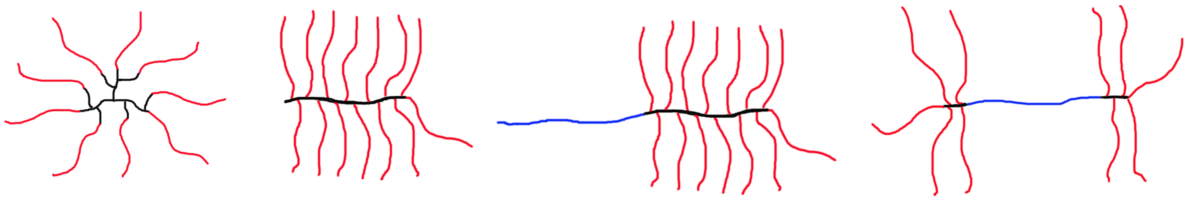

Figure 2.1: Scheme of the different polymer architectures: (from right to left) star-shaped, brush-like, comb-like, pom-pom-like) (red = polysulfide; black = PG / PAGE; blue = PEG).

The polymerization conditions of ethylene sulfide and propylene sulfide with polyether-based macroinitiators were prospected. Three different approaches were applied: a) the homopolymerization of ethylene sulfide, b) the homopolymerization of propylene sulfide and c) the copolymerization of both episulfides. Poly(ethylene sulfide) is highly crystalline and hence insoluble in common organic solvents under ambient conditions. The polymerization of short poly(ethylene sulfide) chains on a macroinitiator with multiple initiating groups was addressed to obtain soluble copolymers. This strategy was similarly used by Wolf et al. to synthesize soluble polyglycolides.[224] The random copolymerization of both thiiranes should also led to soluble poly(ethylene sulfide)-containing polymers.

The different polymer architectures, the number of polysulfide arms as well as their monomer composition and chain length were analyzed regarding their thermal behavior as well as their adsorption efficiency to gold surfaces and the obtained characteristics were compared among each other.

The second strategy, which is based on polysulfides, was the synthesis of poly(propylene sulfide) with a terminal functionality. This functionality should by addressable in a second polymerization to synthesize polysulfide-containing block-copolymers without post-polymerization modification.
In this thesis, 2-bromoethanol was used as termination reagent for poly(propylene sulfide) to obtain a terminal hydroxyl functionality, which should initiate the ring-opening polymerization of lactide. This approach led to a novel class of block-copolymers composed of polyester and polysulfides. The synthetic route is illustrated in **Figure 2.2**. The structure as well as the efficiency as absorbents for gold supports and gold nanoparticles was investigated.

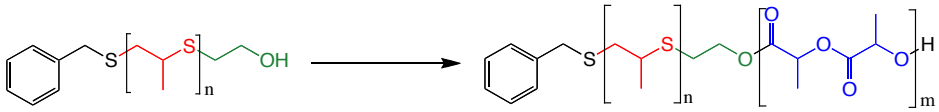

Figure 2.2: Synthetic route to synthesize poly(propylene sulfide)-*block*-poly(lactide) copolymers

2.3 Polymers with a lipoic acid anchoring group

The second strategy was inspirited by numerous publications with various applications, which applied lipoic acid or its derivatives as anchoring group to attach small molecules as well as polymers to gold and other metal surfaces. In the introduction of chapter 5 several approaches are descript in detail. The common procedure to tie the dithiolane motif onto polymers is the post-polymerization modification with lipoic acid derivatives. This method held the disadvantage of a difficult purification to separate functionalized polymers from unreacted polymers and the excess of the lipoic acid derivative. Furthermore, entirely a statistically conversion can be achieved if the polymer carries more than one active functionality, for example the esterification of hyperbranched polyglycerol by Haag et al.[287,288]
Walker and Gupta introduced an amide derivative of lipoic acid as initiator for the preparation of lipoic acid-functionalized poly(amino acids).[278,279] This approach motivated the development of a lipoic acid derivative as initiator for the ring-opening polymerization of epoxides and lactones. The use of an initiator, which carries the desired anchoring group, facilitates the synthesis of tailored polymers in a straightforward approach, without the named drawbacks of post-polymerization modifications.
The second part of this thesis perused this synthetic route. First a novel lipoic acid derivative with a terminal hydroxyl functionality was designed and characterized. Subsequently, the ring-opening polymerization of lactones and epoxides was investigated and further improved. **Figure 2.3** shows the synthesized lipoic acid derivative and the targeted functionalized polymers.

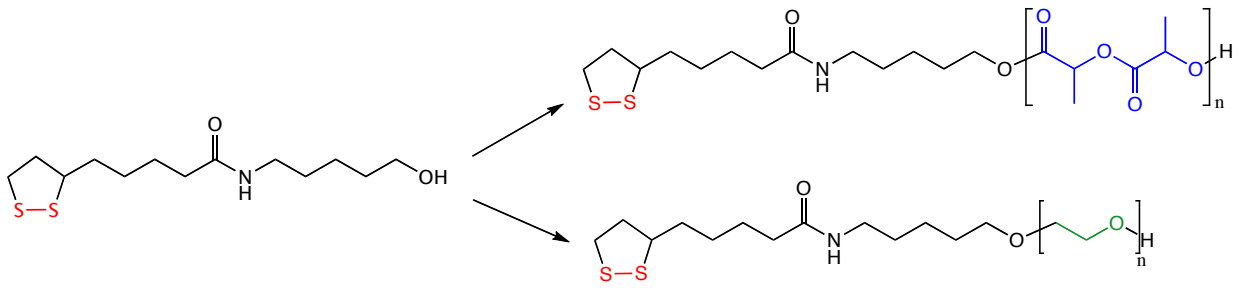

Figure 2.3: Synthetic route to obtain lipoic acid-modified polymers

A set of polyesters and polyethers with different block lengths were synthesized and the structure of the obtained polyester and polyether moieties were analyzed. As proof of principal, the disulfide-modified polymer sets were used to adsorb onto gold surfaces.

Chapter 3

General Introduction

3.1 Self-assembled monolayers (SAMs) on gold[1-35]

The adsorption of sulfur containing molecules, mostly thiols, disulfides and sulfides, on bare gold as SAMs (**Figure 3.1**) is descripted since the early nineties and, since then, widely used.[1-20] The free energy on the interface between the metal and the surroundings is lowered through the adsorption of organic molecules on gold surfaces.[3] The lone pair of the sulfur atoms is taken by the metal surface, which acts as an acceptor.[4]

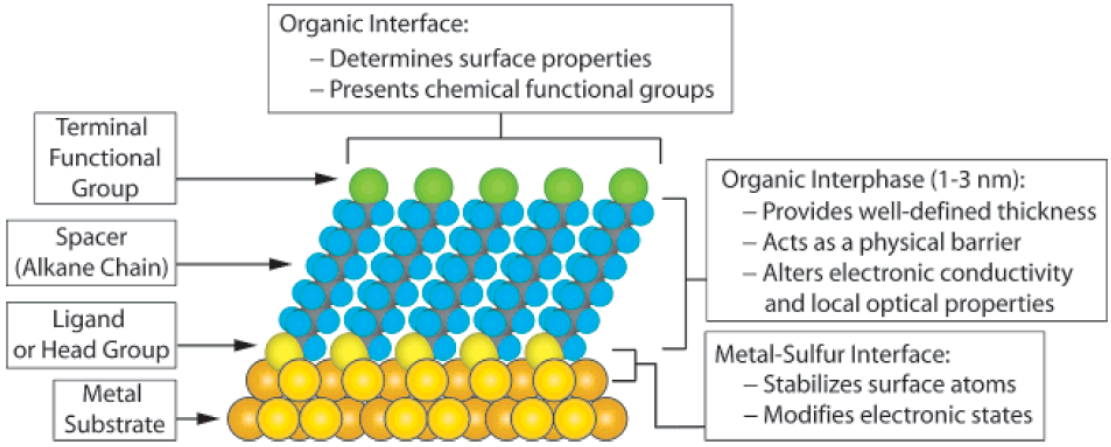

Figure 3.1: Schematic illustration of an ideal, single-crystalline SAM of alkanethiolates on Au (111) [scheme taken from[2]].

3.1.1 Small organic molecules[5-20]

In one of the very first publications, a gold electrode was coated with bis(4-pyridyl) disulfide to enhance the electron transfer between the electrode and Cytochrome c.[5] In 1983, Nuzzo and Allara started the systematic investigation of the spontaneous adsorption of divergent substituted organic disulfides onto gold substrates to oriented monolayers.[6,7]

In the following years, SAMs were explored by numerous groups with different prospects and the following publications are only a short selection of a broad field of research. As a main point the influence of electron transfer on metal surfaces,[8,9] with special attention to electrodes,[10,11] was investigated under different considerations. As started with the work by Nuzzo und Allara, the spontaneously organized assembly of *n*-alkyl thiols $CH_3(CH_2)_nSH$ with n = 1, 3, 5, 7, 9, 11, 15, 17, 21 on gold was studied methodically with optical ellipsometry, infrared (IR) spectroscopy and electrochemistry.[12] Similar work was done in the group of Whitesides with long-chain ω-hydroxyalkanethiols $HS(CH_2)_nOH$ with n = 11, 19, who additionally also investigated the wettability.[13] In a following study, alkanethiols $HS(CH_2)_nX$ with n = 11, 19 and different functional groups (X = CH_3, Br, Cl or $OCH_2C_2F_5$) were used.[14] The adsorption of those functional thiols changes the surface properties. The terminal functional group of the used thiols is exposed on the top of the formed monolayer (**Figure 3.1**).

Furthermore, unsymmetrical disulfides $HO(CH_2)_{16}SS(CH_2)_3CF_3$ were adsorbed to gold supports.[15] The sulfur-sulfur bond was cleaved, thiolates were formed and enabled to react independently. This was shown by the replacement of the $S(CH_2)_{16}CF_3$ of the mixed monolayer with $HS(CH_2)_{16}CN$. This exchange reaction was 1000 times faster than the replacement of the $S(CH_2)_{16}OH$.

The adsorption behavior of dialkyl sulfides was investigated with $R(CH_2)_mS(CH_2)_nR'$ with R, R′ = CH_3 or COOH by Troughton et al.[16] The resulting SAMs were analyzed via X-ray photoelectron spectroscopy (XPS), IR spectroscopy, elliposmetry and contact angle measurements. The films were proved to be robust against neutral water, but were sensitive to aqueous basic media in a pH range from 8-13. The organic sulfides appeared to be mounted through a coordinative bond between sulfur and gold. Furthermore, they were relatively disordered layers compared to SAMs of alkylthiols.

In summary, the kinetic of the film formation of dialkyl sulfides was more than three orders of magnitude smaller compared to alkylthiols and alkyl disulfides.[17] The proposed adsorption mechanism in this study negated the rupture of the sulfur-carbon bond. The maximum surface coverage was also significantly lower. The film formation was sensitive to contamination with sulfur compounds of the environment. In contrast, the SAMs of thiols and disulfides were relatively robust against contamination.

In further studies, the used adsorbents were enlarged, for example, to aryl sulfur species and the formed SAMs were characterized by surface enhanced Raman (SER) spectroscopy.[18] It was found that the aryl sulfinate ($ArSO_2^-$) monolayer was subjected to reversible oxidation to sulfonate ($ArSO_3^-$) monolayers. The examination of SAMs is still a significant field of interest, which is shown by some recent publications in this area. For example, the investigation of the bonding geometry and rotational dynamics of butyl methyl sulfide[19] or the molecular dynamic study of SAM formation.[20] The main attention is shifted towards on theoretical investigations nowadays.

3.1.2 Oligomers and polymers[21-35]

The attraction between sulfur and gold is also used to fix polymers on metal surfaces.[21-35] In principle, there are two main procedures to bind polymers to bare gold surfaces. The first strategy involves the use of a sulfur containing linker group to adsorb the polymer onto metal surfaces.[21-30] In the second strategy, the polymers are attached through sulfur atoms along the polymer backbone.[30-35] It is a widely used technique and the publications listed below represent only an overview of different polymers with various applications.

Common linker molecules of the first strategy are thiols,[21-28] disulfides, and sulfides.[30] Oligo(ethylene glycol)s for example, were fixed to gold by an alkanethiol linker.[21,22] Various mercapto-terminated polymers were described in literature. Poly(ethylene glycol) (PEG) with a thiol functionality in α- or in α- and ω-position was used to adsorb on gold.[23,24] These SAMs have several potential applications, e. g. they show antifouling effects[23] and an inactivation of antibody fragments.[24] Oligoimide monolayers on gold were achieved by the use of thiophenol-terminated oligoimides as adsorbants.[25] The molecular structure of monolayers of this oligomer was also focused in simulation study.[26] A further example of a thiol end-functionalized polymer was poly(ferrocenyldimethylsilane).[27,28] The end-functionalization was achieved by the reaction between ethylene sulfide and the living polymer. A typical disulfide linker molecule for surface attachment is α-lipoic acid, which is discussed in more detail in chapter five. In a recent study, the adsorption behavior of several sulfur-containing polymers were investigated via quartz crystal microbalance with dissipation monitoring (QCM-D).[29] In this study, the thio-functional oligo(ethylene glycol) polymers with disulfides, dithio, trithio or thiol groups were synthesized via radical addition-fragmentation chain transfer (RAFT) polymerization. The polymers with a free thiol were obtained by reduction of the RAFT agent in the polymer and the disulfide containing polymers were formed through exposition to air after the reduction.

The second adsorption strategy is represented, for example, by organic polythioethers (polysulfides) such as the aromatic poly(phenylene sulfide) as well as the aliphatic poly(ethylene sulfide) (PES) and poly(propylene sulfide) (PPS), which are described in chapter four more briefly.[30] A further polymer class is presented by the sulfide-derivatized poly(methyl methacrylate) copolymers.[31,32] The spontaneous adsorption of these polymers from solution on gold was investigated with IR, X-ray photoelectron spectroscopy (XPS) and scanning tunneling microscopy (STM).[31] A similar copolymer consisting of a poly(methyl methacrylate) block with a sulfide substituent and a poly(acrylamide) block, was used as hydrogel.[32] The thermosensitive extraction of gold(III) ions with this hydrogel was prospected under different pH conditions. Furthermore,

sulfur containing siloxane copolymers were also used to adsorb on surfaces.[33,34] Mercapto-functionalized siloxane oligomers were adsorbed to gold. It was found that only a fraction of all available thiol groups generated a bond to gold. The unbound thiols of the fixed oligomers were functionalized via a photo- and AIBN (azobisisobutyronitrile)-initiated thiol-ene reaction with different terminal alkene compounds.[33] In another approach, protein-resistant surfaces were obtained via coating with PEG-grafted siloxane copolymers with disulfide chains. The disulfides acted as linkers to the gold surface and the PEG chains were exposed on the outer surface to ensure the antifouling behavior.[34]

Liebau et al. used a versatile approach, which can be defined according to both strategies that are mentioned above. The definition as a polymer with sulfur carrying linker groups is possible, as well as the definition as a polymer with sulfur as part of the backbone. The synthesized poly(propylene imine) (PEI) dendrimers contained between 4 and 64 dialkyl sulfide chains according to generation 1-5 (**Figure 3.2**). These polymers were used to investigate the self-assembly on the interface between air or water and a gold surface.[35]

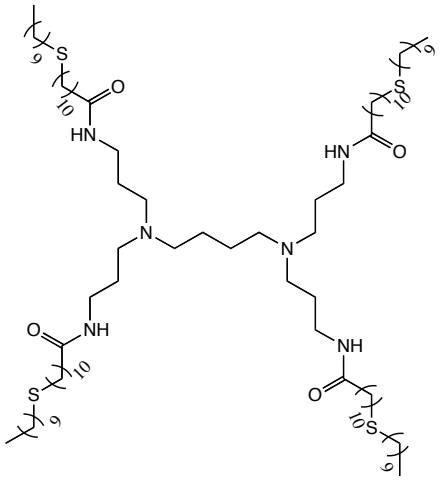

Figure 3.2: Dendrimer of the first generation with four dialkyl sulfide chains (G1-sulfide$_4$).[35]

3.2 Gold nanoparticles (Au NPs)[36-74]

Nanoparticles (NPs) are defined as objects with a size between 1 and 100 nm in two or three dimensions.[36,37] Typically, their physical and chemical properties are different from a single molecule and the bulk material, which is caused by a large surface-to-volume ratio and discrete electronic energy states.[38] Due to their high surface energy NP dispersions tend to aggregate and have to be stabilized.

In here, only gold nanoparticles are considered. The use of colloidal gold started very early and was already, unknowingly, used in antiquity to make red colored glasses and ceramics.[39] Faraday was the first scientist in 1857 to reported the synthesis of Au NPs by the reduction of aqueous chloroaurate ($AuCl_4^-$) solution with phosphorus and carbon disulfide in a two phase system in 1857.[40] Nowadays, there are several different synthesis protocols. In 1951, Turkevitch published the synthesis of gold nanoparticles with a size of about 20 nm.[41] He used citrate as a reduction agent for chloroaurate in aqueous solution. This procedure was further developed by Frens, who introduced gold nanoparticles with adjustable size via the variation of the ratio between gold and trisodium citrate.[42] The method of Brust and Schiffrin was based on the Faraday protocol in a two phase system.[43] Toluene was used as organic phase and a phase-transfer catalyst was liable to transport the chloroaurate into the organic solvent. In this case, sodium borohydrate was used as reducing agent and dodecanthiol acted as a stabilizer. All these approaches allowed the synthesis of stable Au NPs in a controlled fashion. The introduced methods are the main protocols, but the use of seeds[44] and different

physical methods such as ultrasound,[45] was also described. As already mentioned, the size of the nanoparticles has a large influence on their physical properties, for example, on the color of the colloidal solution (**Figure 3.3**).[46]

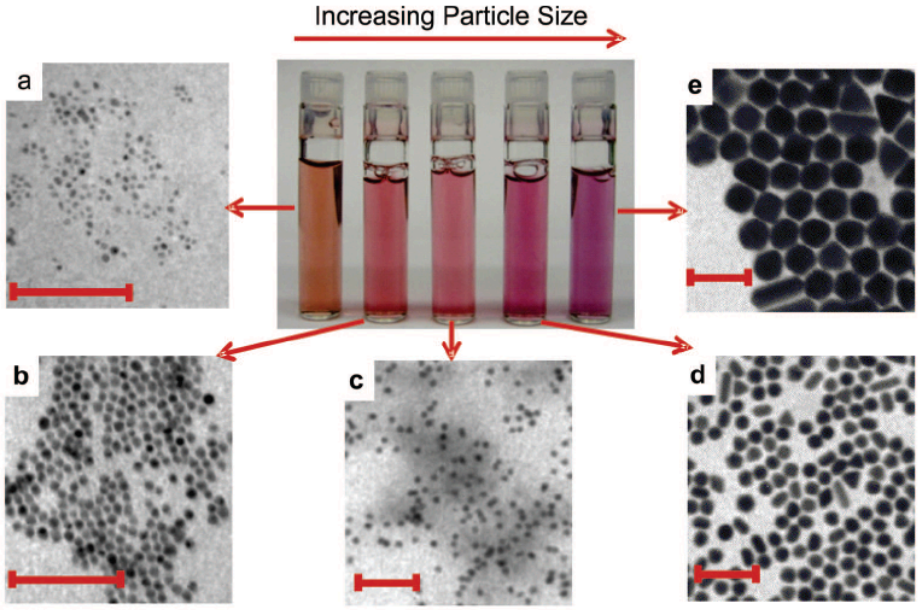

Figure 3.3: Photographs of gold nanoparticles of different sizes (4 to 40 nm) in aqueous solution and TEM (transmission electron microscopy) images of the nanoparticle solutions [scheme taken from[46]].

The qualitative explanation of these phenomena is coherent. Au NPs (5-200 nm) have a conduction band of about 100 nm at room temperature. In comparison with visible light (400 - 750 nm), this is relatively small and irradiation leads to a collective oscillation of the electrons ("plasmons"[47]). In case of gold, the resonance of the collective oscillation is often in the visible range of the electromagnetic spectrum. Due to the large surface-to-volume ratio of the NPs, the plasmon frequency is very sensitive to any change in the surroundings like aggregation, surface modification, and furthermore the refractive index of the media.[48] For example, the adsorption wavelength of gold nanoparticles of the same size linearly depends on the refractive index of the used solvent (**Figure 3.4**).

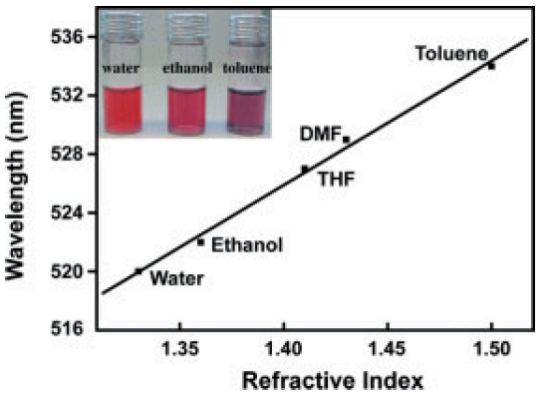

Figure 3.4: Photographs of Au[5]-PNIPMAA (poly(*N*-isopropylacrylamide-*co*-methacrylic acid)) hydrogel spheres (12nm) in different solvents (inset) and plot of the adsorption wavelength against the refractive index of the Au[5]-PNIPMAA in different solvents [scheme taken from[48]].

The aggregation of particles, for example, triggers the coupling of plasmons, which leads to a shift of the plasmon frequency. In addition, with increasing particle size a higher content of the emitted light is scattered.[46] Furthermore, Au NPs have a high contrast in electron microscopy, which allows visualization in a high quality.[49] As described before, the Au NPs have to be stabilized to avoid aggregation. Various small molecules are known as stabilizers for Au NPs, mostly thiols or amines.[39] The introduction of these stabilizers occurred either directly during the synthesis like citrate,[41,42] which acted as reducing agent and stabilizer or the thiols in the Burst method.[43] A further possibility was presented by a ligand exchange after synthesis.[50,51] Besides further sulfur containing species, such as disulfides,[52] dithiols and trithiols,[50,53,54] different phosphorous species[55,56] and acetone[57] are also used.

In here, the main focus lies on polymer-coated gold nanoparticles.[58] The surface functionalization of gold nanoparticles with polymers is available through three strategies[37]: (i) the polymer was directly used as a stabilizer during the synthesis of the Au NPs,[59-63] (ii) the stabilizers were exchanged with a polymer after NP preparation[64-72] or (iii) a suitable initiator was absorbed onto the gold nanoparticles, which allowed a grafting-from approach.[73-74] Merely sulfur-containing polymers or at least polymers with a sulfur linker group should be contemplated in this introduction.

The first strategy - the direct adsorption of the polymer during the Au NP synthesis, was used to coat thiol-terminated poly[(methyl methacrylate-*r*-styrene)-*b*-azidostyrene] to gold nanoparticles. These hybrid materials were introduced to control the orientation of microdomains in block-copolymer thin films.[59] In a similar approach, polypropylene, end-functionalized with ethylene sulfide, stabilized gold nanoparticles.[60] The direct method was also utilized in an approach, where the sulfur-containing polymer were immobilized on a surface and the Au NPs were subsequently synthesized on this substrate. Thus, the nanoparticles were tightly fixed on the surface and could not be removed by scotch tape test.[61] In a further study, hyperbranched polyglycerol was converted to an amphiphilic polymer with long alkylsulfide chains. This polymer was also used as a stabilizer of gold nanoparticles, prepared in direct fashion.[62] The use of thioethers as stabilizing agent for Au NPs were also investigated.[63] It was found, that the stability of the Au NPs increased with the number of sulfur atoms per ligand. This lead to the use of poly(thioether)s, which is described in more detail in chapter four.

The second strategy - the exchange of the linker groups of the synthesized gold nanoparticles, was applied in many publications to adsorb thiol-functionalized PEG on Au NPs.[64-69] In one approach, the size-dependent kinetic of PEG-coated NPs was investigated *in vivo* in mice.[65] In a further *in vivo* study, the blood circulation time of PEG-protected gold clusters was prospected.[66] The fabrication of stable PEG nanoparticle conjugates with different functional groups was achieved by femtosecond laser ablation in water just recently.[67] PEG-SH adsorbed on the surface of Au NPs was also used in an investigation of surface-immobilized antibodies, and the synthesis of optical contrast agents with delivery and targeting moieties.[68] In addition, such polymer hybrids played a role in the encapsulation process with a temperature-responsive polymer, as a system for intelligent therapeutics.[69] The second strategy was further used to adsorb sulfur containing conducting copolymers to Au NPs to increase their electrocatalytic activity.[70] A set of copoly(oligoethylene oxide) acrylates were synthesized via RAFT and subsequently bound to gold nanoparticles via the trithiocarbonate linker of the polymer. Both of these polymers showed thermoresponsiveness and antifouling behavior.[71] Au NPs capped with thiol and amine-containing peptides were also produced through the exchange of the stabilizers on the surface of the nanoparticles.[72]

The third synthetic strategy - the grafting from approach, will be illustrated by two examples. An initiator for ATRP (atom-transfer radical polymerization) with a disulfide based linker group was adsorbed on Au

NPs.[73] In a second step, two acrylamide monomers were directly polymerized on the nanoparticle surface. A similar approach was described with RAFT as polymerization technique, which resulted in Au NPs coated with thermoresponsive polymers.[74] The synthesized nanoparticles were stabilized with long-chain ω-hydroxyalkanethiols and the hydroxyl function was subsequently converted to an initiator for RAFT in an esterification reaction.

3.3 Atomic force microscope (AFM)[75-85]

In 1986, Binnig, Quate and Gerber introduced the atomic force microscope (AFM) as a combination of scanning tunneling microscopy (STM) and stylus profiler.[75] AFM builds together with magnetic force, electric force, and Kelvin probe microscope[78] the class of scanning probe microscopes.[76] In some cases AFM enables resolution of surface topographies up to the atomic level.[76] A schematic illustration of an AFM is shown in **Figure 3.5**.

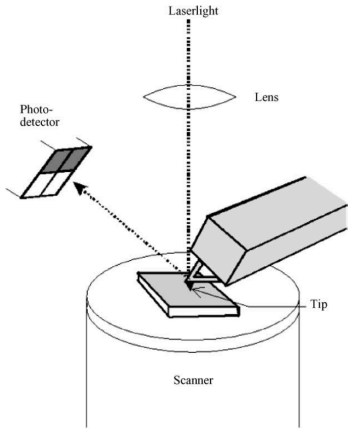

Figure 3.5: Schematic illustration of an AFM [scheme taken from[76]].

The surface of a sample is scanned with a cantilever spring, which has a very sharp tip at its end. The commercially available cantilevers usually consist of silicon or silicon nitride, but for special applications different modifications are used. The cantilever deflection is measured in different ways to map the topology of the sample. In most cases, an optical method was used to detect the cantilever deflection. For this purpose, a laser beam is focused on the cantilever and the reflected laser beam was measured by a quatered photodiode. The sample has to be moved according to the tip, which is done by a piezo actuator. The piezo actuator enables a minimal displacement order of 1 Å. Both, the displacement of the sample and the dislocation of the tip is used in common AFMs.[76,77]

AFM provides access to a wide range of applications because the characterization of both conducting and insulating surfaces is possible. Furthermore, the measurement is accomplished under ambient conditions, in different gases, in vacuum and in liquids as well as at higher or lower temperatures, by the use of special measurement cells.[76,77] The ability to measure in liquids lead to various applications in the biological field.[79]

In principal, there are two main operating modes for the topographic imaging of different samples via AFM, the static mode and the dynamic mode. In the static contact mode, the tip is in contact with the sample surface during the scanning. A topological image is maintained through a plot of the cantilever deflection against the position on the sample. This mode is only suitable for very hard samples. Soft matter like polymers would be damaged.[80]

The dynamic mode is divided into the tapping mode and the non-contact mode. In the dynamic mode, the cantilever is vibrated via an additional piezoelectric device. The amplitude of the oscillating cantilever is measured in dependency of the distance between the tip and the sample. In the tapping mode, the surface is approached and withdrawn. This method is gentle enough to image soft matter.[80]

In the non-contact mode, the tip does not touch the surface at all. Thereby the van-der-Waals force between the tip and the surface atoms is used. The implementation of the measurement under high vacuum conditions improves the resolution.[76,77]

Besides the topographic imaging, AFM is used to define nanoindentation.[81,82] The micro- and nanomechanical properties of a surface are described by Young´s modulus - the deformation on the length scale and the stiffness.[83] This parameters are obtained by force-distance measurements with an AFM.

Due to the chemical functionalization of an AFM tip, the force measurement between two molecules is possible. In 1994, the single bond rupture between biotin and streptavidin was reported.[84, 85] Since then, the single molecule spectroscopy is a widely used technique.[86]

3.4 References

(1) Bain, C. B.; Whitesides, G. M.; *Angewandte Chemie International Edition* **1989**, *4*, 506.
(2) Love, J. C.; Estroff, L. A.; Kriebel, J. K.; Nuzzo, R. G.; Whitesides, G. M.; *Chemical Reviews* **2005**, *105*, 1103.
(3) Adamson, A. W.; Gast, A. P.; *Physical Chemistry of Surfaces*, 6th edition; Wiley-Interscience: New York, 1997.
(4) Barclay, D. J.; Caja, J.; *Croatica Chemica Acta* **1971**, *43*, 221.
(5) Taniguchi, I.; Toyosawa, K.; Yamaguchi, H.; Yasukouchi, K.; *Journal of the Chemical Society, Chemical Communications* **1982**, *18*, 1032.
(6) Nuzzo, R. G.; Allara, D. L.; *Journal of the American Chemical Society* **1983**, *105*, 4481.
(7) Nuzzo, R. G.; Fusco, F. A.; Allara, D. L.; *Journal of the American Chemical Society* **1987**, *109*, 2358.
(8) Li, T. T.-T.; Liu, H. Y.; Weaver, M.J.; *Journal of the American Chemical Society* **1984**, *106*, 1233.
(9) Li, T. T.-T.; Weaver, M.J.; *Journal of the American Chemical Society* **1984**, *106*, 6107.
(10) Finklea, H. O.; Avery, S.; Lynch, M.; Furtsch, T.; *Langmuir* **1987**, *3*, 409.
(11) Hickman, J. J.; Ofer, D.; Laibinis, P. E.; Whitesides, G. M.; Wrighton, M. S.; *Science* **1991**, *252*, 688.
(12) Porter, M. D.; Bright, T. B.; Allara, D. L.; Chidsey, C. E. D.; *Journal of the American Chemical Society* **1987**, *109*, 3559.
(13) Bain, C. D.; Whitesides, G. M.; *Science* **1988**, *240*, 62.
(14) Laibinis, P. E.; Hickman, J. J.; Wrighton, M. S.; Whitesides, G. M.; *Science* **1989**, *245*, 845.
(15) Biebuyck, H. A.; Whitesides, G. M.; *Langmuir* **1993**, *9*, 1766.
(16) Troughton, E. B.; Bain, C. D.; Whitesides, G. M.; Nuzzo, R. G.; Allara, D. L.; Porter, M.D.; *Langmuir* **1988**, *4*, 365.
(17) Jung, C.; Dannenberger, O.; Xu, Y.; Buck, M.; Grunze, M; *Langmuir* **1998**, *14*, 1103.
(18) Garrell, R. L.; Chadwick, J. E.; Severance, D. L.; McDonald, N. A.; Myles, D. C.; *Journal of the American Chemical Society* **1995**, *117*, 11563.
(19) Tierney, H. L.; Han, J. W.; Jewell, A. D.; Iski, E. V.; Baber, A. E.; Sholl, D. S.; Sykes, C. H.; *The Journal of Physical Chemistry C* **2011**, *115*, 897.
(20) Ahn, Y.; Saha, J. K.; Schatz, G. C.; Jang, J.; *The Journal of Physical Chemistry C* **2011**, *115*, 10668.
(21) Bain, C. B.; Whitesides, G. M.; *Journal of the American Chemical Society* **1988**, *110*, 5897.
(22) Pale-Grosdemange, C.; Simon, E. S.; Prime, K. L.; Whitesides, G.M.; *Journal of the American Chemical Society* **1991**, *113*, 12.
(23) Yoshimoto, K.; Hirase, T.; Nemoto, S.; Hatta, T.; Nagasaki, Y.; *Langmuir* **2008**, 24, 9623.
(24) Yoshimoto K.; Nishio, M.; Sugasawa, H.; Nagasaki, Y.; *Journal of the American Chemical Society* **2010**, *132*, 7982.
(25) Kwan, W. S. V.; Atanasoska, L.; Miller, L.L.; *Langmuir* **1991**, 7, 1419.
(26) Zhang, Z.; Beck, T. L.; Young, J. T.; Boerio, F. J.; *Langmuir* **1996**, *12*, 1227.
(27) Peter, M.; Lammertink, R. G. H.; Hempenius, M. A.; van Os, M.; Beulen, M. W. J.; Reinhouldt, D. N.; Knoll, W.; Vancso, G. J.; *Chemical Communications* **1999**, *4*, 359.
(28) Song, J.; Vancso, G. J.; *Langmuir* **2011**, *27*, 6822.
(29) Slavin, S.; Soeriyadi, A. H.; Voorhaar, L.; Whittaker, M. R.; Becer, C. R.; Boyer, C.; Davis, T. P.; Haddleton, D. M.; *Soft Matter* **2011**, *8*, 118.
(30) Roman, T.; Diño, W. A.; Nakanishi, H.; Kasai, H.; Miyako, Y.; Naritomi, M.; *Solid State Communications* **2004**, *132*, 405.
(31) Lenk, T. J.; Hallmark, V. M.; Rabolt, J. F.; Häussling, L.; Ringsdorf, H.; *Macromolecules* **1993**, *26*, 1230.
(32) Hemvasdukij, S.; Ngeontae, W.; Imyim, A.; *Journal of Applied Polymer Science* **2011**, *120*, 3098.
(33) Sun, F.; Grainger, D. W.; Castner, D. G.; Leach-Scampavia, D. K.; *Macromolecules* **1994**, *27*, 3053.
(34) Zhou, C.; Khlestkin, V. K.; Braeken, D.; De Keersmaecker, K.; Laureyn, W.; Engelborghs, Y.; Borghs, G.; *Langmuir* **2005**, *21*, 5988.
(35) Liebau, M.; Janssen, H. M.; Inoue, K.; Shinkai, S.; Huskens, J.; Sijbesma, R. P.; Meijer, E. W.; Reinhouldt, D. N.; *Langmuir* **2002**, *18*, 674.
(36) Auffan, M.; Rose, J.; Bottero, J.-Y.; Lowry, G. V.; Jolivet, J.-P.; Wiesner, M. R.; *Nature Nanotechnology* **2009**, *4*, 634.
(37) Hu, X.; Zhou, L.; Gao, C.; *Colloid and Polymer Science* **2011**, *289*, 1299.
(38) El-Sayed, M. A.; *Accounts of Chemical Research* **2004**, *37*, 326.
(39) Daniel, M.-C.; Astruc, D.; *Chemical Reviews* **2004**, *104*, 293.

(40) Faraday, M.; *Philosophical Transactions of the Royal Society* **1857**, *147*, 145.
(41) Turkevich, J.; Stevenson, P. C.; Hillier, J.; *Discussion of the Faraday Society* **1951**, *11*, 55.
(42) Frens, G.; *Nature Physical Science* **1973**, *241*, 20.
(43) Brust, M.; Walker, M.; Bethell, D.; Schiffrin, D. J.; Whyman, R. J.; *Journal of the Chemical Society, Chemical Communications* **1994**, *7*, 802.
(44) Jana, N. R.; Gearheart, L.; Murphy, C. J.; *Chemistry of Materials* **2001**, *13*, 2313.
(45) Zhou, Y.; Wang, C. Y.; Zhu, Y. R.; Chen, Z. Y.; *Chemistry of Materials* **1999**, *11*, 2310.
(46) Murphy, C. J.; Gole, A. M.; Stone, J. W.; Sisco, P. N.; Alkilany, A. M.; Goldsmith, E. C.; Baxter, S. C.; *Accounts of Chemical Research* **2008**, *41*, 1721.
(47) El-Sayed, M. A.; *Accounts of Chemical Research* **2001**, *34*, 257.
(48) Kuang, M.; Wang, D.; Möhwald, H.; *Advanced Functional Materials* **2005**, *15*, 1611.
(49) Karakoti, A. S.; Das, S.; Thevuthasan, S.; Seal, S.; *Angewandte Chemie International Edition* **2011**, *50*, 1980.
(50) Zhang, S.; Leem, G.; Srisombat, L.; Lee, T. R.; *Journal of the American Chemical Society* **2008**, *130*, 113.
(51) Weisbecker, C. S.; Merritt, M. V.; Whitesides, G. M.; *Langmuir* **1996**, *12*, 3763.
(52) Porter, L. A., Jr.; Ji, D.; Westcott, S. L.; Graupe, M.; Czernuszewicz, R. S.; Halas, N. J.; Lee, T. R.; *Langmuir* **1998**, *14*, 7378.
(53) Srisombat, L.; Park, J.-S.; Zhang, S.; Lee, T. R.; *Langmuir* **2008**, *24*, 7750.
(54) Perumal, S.; Hofmann, A.; Scholz, N.; Rühl, E.; Graf, C.; *Langmuir* **2011**, *27*, 4456.
(55) Weare, W. W.; Reed, S. M.; Warner, M. G.; Hutchison, J. E.; *Journal of the American Chemical Society* **2000**, *122*, 12890.
(56) Green, M.; O'Brien, P.; *Chemical Communications* **2000**, *3*, 183.
(57) Li, G.; Lauer, M.; Schulz, A.; Boettcher, C.; Li, F.; Fuhrhop, J.-H.; *Langmuir* **2003**, *19*, 6483.
(58) Shan, J.; Tenhu, H.; *Chemical Communications* **2007**, *44*, 4580.
(59) Yoo, M.; Kim, S.; Jang, S. G.; Choi, S.-H.; Yang, H.; Kramer, E. J.; Lee, W. B.; Kim, B. J.; Bang, J.; *Macromolecules* **2011**, *44*, 9356.
(60) Yeh, J.-R.; Tseng, F.-Y.; Yeh, J.-Y.; Tsai, J.-C.; Tsiang, R. C.-C.; *Journal of Polymer Science: Part A: Polymer Chemistry* **2010**, *48*, 4400.
(61) Intelmann, C. M.; Dietz, H.; Plieth, W.; *European Journal of Inorganic Chemistry* **2005**, *18*, 3711.
(62) Wan, D.; Fu, Q.; Huang, J.; *Journal of Applied Polymer Science* **2006**, *101*, 509.
(63) Li, X.-M.; de Jong, M. R.; Inoue, K.; Shinkai, S.; Huskens, J.; Reinhouldt, D. N.; *Journal of Materials Chemistry* **2001**, *11*, 1919.
(64) Karakoti, A. S.; Das, S.; Thevuthasan, S.; Seal, S.; *Angewandte Chemie International Edition* **2011**, *50*, 1980.
(65) Cho, W.-S.; Cho, M.; Jeong, J.; Choi, M.; Han, B. S.; Shin, H.-S.; Hong, J.; Chung, B. H.; Jeong, J.; Cho, M.-H.; *Toxicology and Applied Pharmacology* **2010**, *245*, 116.
(66) Simpson, C. A.; Agrawal, A. C.; Balinski, A.; Harkness, K. M.; Cliffel, D. E.; *ACS Nano* **2011**, *5*, 3577.
(67) Qian, W.; Murakami, M.; Ichikawa, Y.; Che, Y.; *The Journal of Physical Chemistry C* **2011**, *115*, 23293.
(68) Kumar, S.; Aaron, J.; Sokolov, K.; *Nature Protocols* **2008**, *3*, 314.
(69) Owens III, D. E.; Eby, J. K.; Jian, Y.; Peppas, N. A.; *Journal of Biomedical Materials Research Part A* **2007**, *83A*, 692.
(70) Ferreira, V. C.; Melato, A. I.; Silva, A. F.; Abrantes, L. M.; *Electrochimica Acta* **2011**, *56*, 3567.
(71) Boyer, C.; Whittaker, M. R.; Luzon, M.; Davis, T. P.; *Macromolecules* **2009**, *42*, 6917.
(72) Porta, F.; Speranza, G.; Krpetić, Ž.; Santo, V. D.; Francescato, P.; Scarì, G.; *Materials Science and Engineering B* **2007**, *140*, 187.
(73) Li, D.; He, Q.; Cui, Y.; Wang, K.; Zhang, X.; Li, J.; *Chemistry – A European Journal* **2007**, *13*, 2224.
(74) Raula, J.; Shan, J.; Nuopponen, M.; Niskanen, A.; Jiang, H.; Kauppinen, E. I.; Tenhu, H.; *Langmuir* **2003**, 19, 3499.
(75) Binnig, G.; Quate, C. F.; Gerber, Ch.; *Physical Review Letters* **1986**, *56*, 930.
(76) Butt, H.-J.; Cappella, B.; Kappl, M.; *Surface Science Reports* **2005**, *59*, 1.
(77) Capella, B.; Dietler, G.; *Surface Science Reports* **1999**, *34*, 1.
(78) Berger, R.; Butt, H.-J.; Retschke, M. B.; Weber, S. A. L.; *Macromolecular Rapid Communications* **2009**, *30*, 1167.
(79) Cohen, S. R.; Bitler, A.; *Current Opinion in Colloid & Interface Science* **2008**, *13*, 316.
(80) Palermo, V.; Schwartz, E; Liscio, A.; Otten, M. B. J.; Müllen, K.; Nolte, R. J. M.; Rowan, A. E.; Samorì, P.; *Soft Matter* **2009**, *5*, 4680.

(81) Kurland, N. E.; Drira, Z.; Yadavalli, V. K.; *Micron* **2012**, *43*, 116. (82) Kurland, N. E.; Drira, Z.; Yadavalli, V. K.; *Micron* **2012**, *43*, 116.
(82) Tang, B.; Aifantis, K. E.; Ngan, A. H. W.; *Materials Letters* **2012**, *67*, 237.
(83) Ebenstein, D. M.; Pruitt, L. A.; *Nano Today* **2006**, *1*, 26.
(84) Florin, E.-L.; Moy, V. T.; Gaub, H. E.; *Science* **1994**, *264*, 415.
(85) Lee, G. U.; Kidwell, D. A.; Colton, R. J.; *Langmuir* **1994**, *10*, 354.
(86) Janshoff, A.; Neitzert, M.; Oberdörfer, Y.; Fuchs, H.; *Angewandte Chemie International Edition* **2000**, *39*, 3212.

Chapter 4

Synthesis and Characterization of Polysulfides

4.1 Introduction[87-222]

Ethylene sulfide (ES) and propylene sulfide (PS) are thiiranes and hence the sulfur analog of the epoxides, ethylene oxide (EO) and propylene oxide (PO), which are widely used as monomers in polymer science for the synthesis of aliphatic polyethers. In the following, typical characteristics and polymerization methods of thiiranes are summarized. Furthermore, homopolymer and copolymer structures of polysulfides are explained.

4.1.1 Ethylene sulfide (ES)[87-105]

4.1.1.1 Historical Retrospect

ES is the simplest three-membered ring with sulfur as heteroatom. The structure of ethylene sulfide is shown in **Figure 4.1**. The first pure ethylene sulfide was synthesized by Delépine in 1920.[89]

Figure 4.1: Structure of ES.

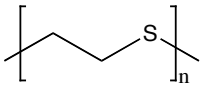

Figure 4.2: Structure of PES.

In 1951, various observations of the polymerization of ES were summarized in a review.[90] The structure of the formed poly(ethylene sulfide) (PES) is shown in **Figure 4.2**. ES is described to polymerize even in the dark under ambient conditions.[91] Ionic polymerization of the strained ring was also published very early. Cationic ring-opening polymerization was initiated with mineral acids like hydrochloric acid and sulfuric acid. Anionic ring-opening polymerization was catalyzed with ammonia in alcoholic or aqueous solution. The obtained degrees of polymerization (DPs) were rather low with six for ammonia and twelve for acetic acid.[89,91,92] More than thirty years later, Boileau and Sigwalt obtained PES, which was polymerized in an anionic fashion with sodium naphthalide with a melting point of 208-210°C. The polymer obtained with boron fluoride melted significantly lower at 192-195°C.[93] It was deducted that the anionic ring-opening polymerization led to higher DPs. A further synthesis method for poly(ethylene sulfide) was introduced by Gobran and Larsen in 1970. They applied a seed polymerization to synthesize an "immortal" polymer by the use of diethylzinc in water as a coordination catalyst.[94]

The properties of PES were noted in several other publications. PES has been characterized as a colorless solid matter. Due to its high degree of crystallization, it was insoluble in all common organic solvents at room temperature.[88,97] It has been described to dissolve solely in α-methylnaphthalene, nitrobenzene, *o*-dichlorobenzene, dithiolane and dimethyl sulfoxide above 140°C. At these temperature values the thermal degradation already started for low molecular weight PES.[95] The degradation of high molecular weight PES with a melting point above 200°C is observed at 220-260°C, which was detected by gas evolution.[96] Melt rheology was used to determine the molecular weight of the synthesized polymers, which seemed the only method for such an insoluble material.[97] Furthermore, the oxidative degradation[98] and the electron diffraction structure[99] of PES were investigated in more detail.

4.1.1.2 Comparison to the analog polyether

Poly(ethylene oxide) (PEO) or poly(ethylene glycol) (PEG), the oxygen analog of PES, melts at 70°C, which is significantly lower compared to PES.[100] The dipole moment of the C-S bond is larger than the one of the C-O bond and the bond length in PEG is smaller compared to PES. Owing to these results, the partial charges in the two polymers should be similar.[101] However, the C-S bond is unusually long with 181.5 pm and the PES

chain is more flexible with a rather large enthalpy of fusion, which leads to the rather high melting point of poly(ethylene sulfide).[100]

4.1.1.3 State of the art

The conformational characteristics of PES were in focus of theoretical studies.[102,103] Due to the high degree of crystallization of PES and its insolubility in common organic solvents, the use is highly restricted. But as shown in one approach, PES could be used as a precursor for poly(ethylene sulfoxide), which is a kind of polymer homologue of dimethyl sulfoxide (DMSO). Poly(ethylene sulfoxide) was synthesized via selective oxidation of PES with HNO_3/CH_3SO_3H and it was shown to be a soluble material, even in acidic media.[104] In addition, the electrochemical ring-opening polymerization of ethylene sulfide on platinum surfaces was described. The resulting crystalline-doped PES films were partially oxidized, with about 25% of the sulfur atoms of the polymer backbone being positively charged. The electrical conductivity of these polymers was comparable to semi-conductors.[105]

4.1.2 Propylene sulfide (PS)[87,88,90,105-131]

4.1.2.1 Historical Retrospect

Propylene sulfide is a thiirane substituted with one methyl group (**Figure 4.3**). In 1921, Delépine was again the first to describe the synthesis of PS by the reaction of 2-halo thiocyanates with sodium sulfide.[106]

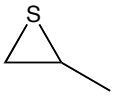

Figure 4.3: Structure of PS.

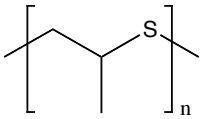

Figure 4.4: Structure of PPS.

Similar to substituted epoxides, PS polymerizes through ionic ring-opening mechanisms to poly(propylene sulfide) (PPS).[87] The structure of the polymer is shown in **Figure 4.4**. Propylene sulfide is less reactive compared to ethylene sulfide and stable under storage for months.[106] Only the use of concentrated sulfuric acid resulted in polymerization. With acetic acid no reaction was observed, which confirms also the lower reactivity in comparison to ES. The use of ammonia and alkali led to slower polymerization rates, and the formed polymer was more viscous in comparison to the product generated in the polymerization with sulfuric acid.[106] PPS is amorphous and characterized as a viscous oil, which is soluble in chloroform and dioxane.[107] Boileau and Sigwalt investigated the polymerization reactions of propylene sulfide systematically and in fact created the research area of polysulfides. They used $TiCl_4$ and $AlCl_3$ as catalysts for the cationic ring-opening polymerization, but they obtained rather low molecular weight polymers via this technique. The anionic ring-opening polymerization with $NaNH_2$, KOH or Na yielded high molecular weight products and the highest molecular weights were achieved with sodium metal. Approaches with butyllithium and $Al(C_2H_5)_3$ as catalyst failed.[88,108] The use of sodium naphthalide as initiator for propylene sulfide in THF (tetrahydrofuran) led to high molecular weight polymers with up to 320 000 $g \cdot mol^{-1}$ and narrow molecular weight distribution. To avoid oxidation of the terminal thiols to disulfides and the dimerization of two polymers, 1-chloromethyl naphthalene was used as an end-capping reagent (**Figure 4.5**).[109] The same group studied the kinetics of the anionic ring-opening polymerization of propylene sulfide in tetrahydrofuran and tetrahydropyran at different temperatures with sodium and tetrabutylammonium as counter-ions.[110] Furthermore, the use of cryptates to chelate the counter-ions was investigated, which led to an increasing activity of the living center.[111] The range of initiators was further extended, for example, to thiols.[112,113]

Owing to the methyl group, the three-membered ring of propylene sulfide possesses a chiral carbon atom. In principle, there are two strategies to obtain an optically active polymer: (i) the use of a pure cyclic enantiomer as a monomer or (ii) a racemic monomer and a chiral initiator. The stereoelection and the stereoselection of the ring-opening polymerization of propylene sulfide was described in several publications.[113-117] In a later work, for example, racemic propylene sulfide was polymerized in a stereoselective polymerization with bis(isopropyl-*S*-cysteinato) cadmium as an enantiopure initiator. At partial conversation, the obtained products were isotactic and optically active.[118]

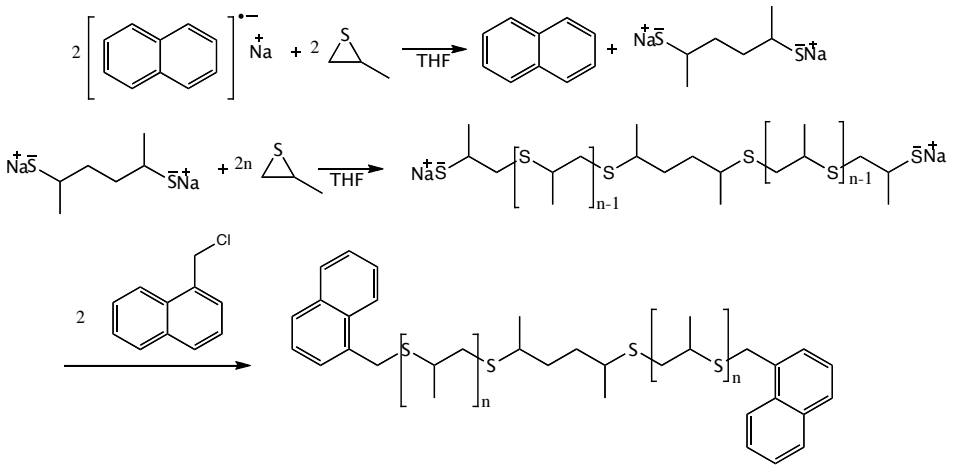

Figure 4.5: Polymerization of PS with sodium naphthalide and 1-chloromethyl naphthalene as an end-capping reagent.[109]

4.1.2.2 Comparison to the analog polyether

Poly(propylene oxide) (PPO) is the polyether analog to PPS, however, the sulfur atoms at the polymer backbone are replaced by oxygen atoms. Despite the similar structure of the two polymers, the analysis of the conformational characteristics of poly(propylene sulfide) with *ab initio* molecular orbital (MO) calculations and NMR (nuclear magnetic resonance) spectroscopy of monomeric model compounds showed a significant difference between PPO and PPS. In case of the conformational characteristics PPS appeared to be similar to PES.[119] In a further investigation the dynamic properties of PPS were studied with dielectric spectroscopy and dynamic mechanical measurements. In principle, the dynamic of poly(propylene sulfide) was similar to that of poly(propylene oxide). Solely the glass transition temperature (T_g) of PPO is almost independent of the molecular weight of the polymer. In contrast, a significant interrelation was reported for PPS. In PPO strong hydrogen bonding is present, which lowers the mobility of the chain ends and thus the influence on the T_g. In comparison to PPO, hydrogen bonding in PPS is much weaker and the molecular mass has an explicit influence on the glass temperature, as noted for most polymers. The T_g of poly(propylene sulfide) increases with increasing molecular weight of the polymer. [120] In stereoselective polymerizations a similar behavior of propylene sulfide and propylene oxides was reported.[114,121]

4.1.2.3 State of the art

The polymerization of propylene sulfide under influence of cationic catalysts such as triethyl oxonium tetrafluoroborate or boron trifluoride etherate was described, but the formed polymers exhibited a low molecular mass and a significant amount of oligomers was formed in the polymerization, as mentioned before. These side-products were the result of a depolymerization mechanism, which was also catalyzed by the polymerization promoters, although with slower kinetic.[122] Due to this fact, the cationic ring-opening polymerization of PS has been almost abandoned. In contrast, the anionic ring-opening polymerization led

to high molecular mass polymers with narrow molecular weight distributions. The anionic ring-opening polymerization of propylene sulfide was revitalized in the last fifteen to twenty years. In 1999, the group of Levesque introduced the use of a thiol/thiolate system to initiate the anionic ring-opening polymerization of PS. This approach was achieved with different thiols, for example hexanethiol as well as 1,6-hexanedithiol and 1,8-diazabicyclo[5.4.0]undec-7-ene (DBU) as a deprotonating agent. The initiator system allowed fast proton exchange and thus a living polymerization of propylene sulfide.[123] In a follow-up work, the same group described the synthesis of end-functionalized poly(propylene sulfide) star polymers. A prerequisite for the controlled synthesis of star-shaped polymers is the living character of the polymerization. In principle, star polymers are attainable through two strategies, the "core first" method, via a multi-functional initiator, and the "arm first" strategy, via a multi-functional coupling reagent. Both methods were used in the synthesis of PPS star polymers. The "arm first" approach was carried out with hexanethiol, mercapotopropane-1,2 diol as well as methyl thioglycolate as initiators for propylene sulfide and 1,2,4,5-tetrakis (bromomethyl) benzene as coupling agent. This approach resulted in a product mixture of mono- to tetra-arm polymers, which was shown by size-exclusion chromatography (SEC). The "core first" strategy was enabled to avoid the known drawbacks of the "arm first" strategy. Tri- and tetrathiols acted as multi-functional initiators, which immediately led to star-shaped poly(propylene sulfide)s. As expected, the polymers with a thiol as a terminal group were oxidized to disulfides under dimerization. This reaction was easily reversible through reduction with $LiAlH_4$. Nevertheless, this was eliminated by the use of an end-capping reagent after the polymerization. The star-shaped polymers were end-capped with (α-naphthyl)-methyl groups, bromo acetoacetate or 3-bromopropane-1,2-diol to achieve further functionalization. The synthesized end-functionalized star polymers are shown in **Figure 4.6**.[124]

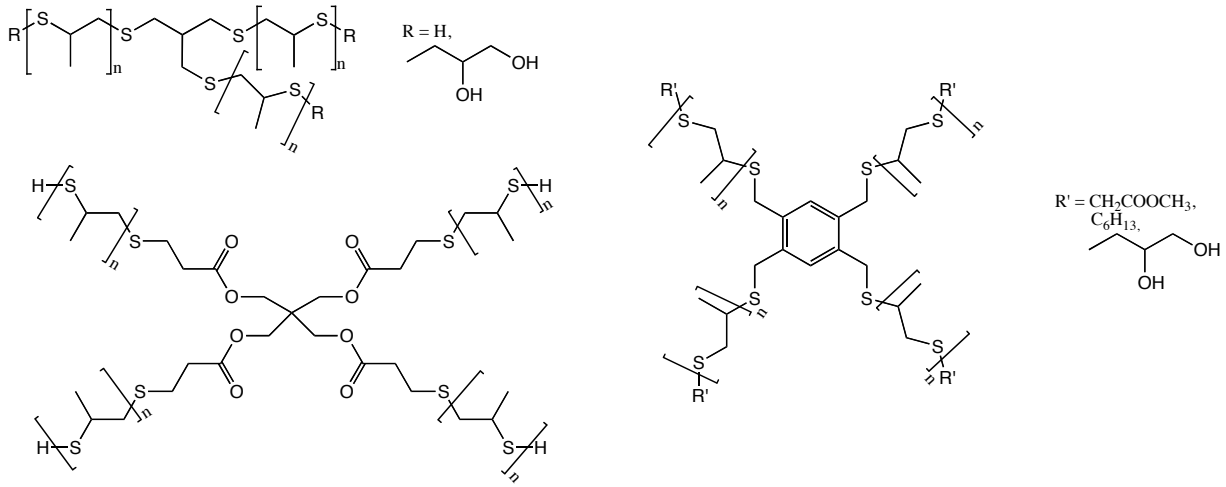

Figure 4.6: PPS star polymers, synthesized by "arm first" and "core first" method.[124]

Star-shaped PPS was also synthesized in a different approach with a tri-functional initiator based on a tri-functional five-membered cyclic dithiocarbonate. This compound was reacted quantitatively with amines to mercapto-thiourethanes by selective cleavage of the dithiocarbonates. Subsequently, the thiol functionalities were deprotonated with DBU and propylene sulfide was added. After the polymerization 1-chloromethyl naphthalene or methyl iodate were enclosed to terminate the living PPS chains (**Figure 4.7**).[125]

Tirelli et al. investigated the reaction conditions in more detail and introduced an improved procedure for well-defined polymers with low polydispersity. They prospected the effect of the thiolate/disulfide

exchange[126] as well as the initiation and termination[127] reaction in the anionic ring-opening polymerization of propylene sulfide in more detail.

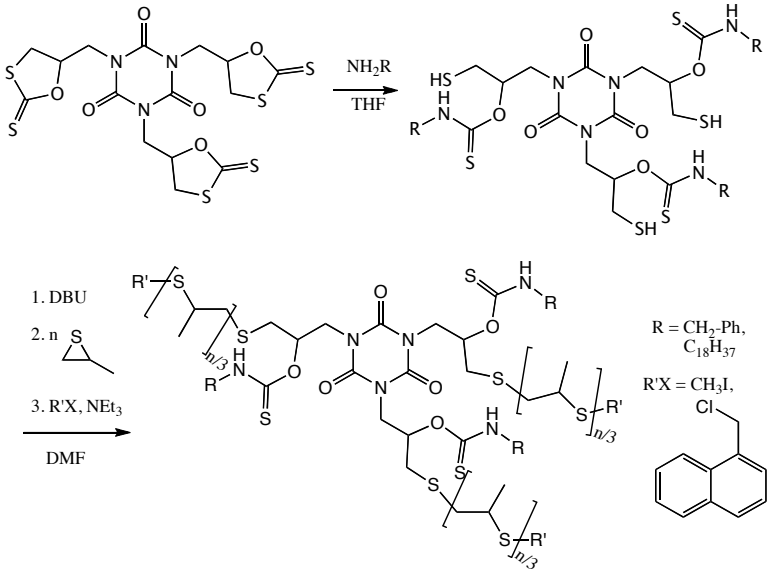

Figure 4.7: Reaction scheme of the synthesis of the dithiocarbamate-based initiator and the polymerization of PS.[125]

Common initiator systems for propylene sulfide are thiols, as mentioned before, although thiols are readily oxidized to disulfides by oxygen in the air. Thiols are often contaminated with disulfides in different degrees. If thiols are used as initiators of PS, disulfides are often present in the polymerization. Such impurities are enabled to act as chain transfer as well as end-capping reagent, which resultes in polymers with terminal and in-chain disulfides (**Figure 4.8**).[126]

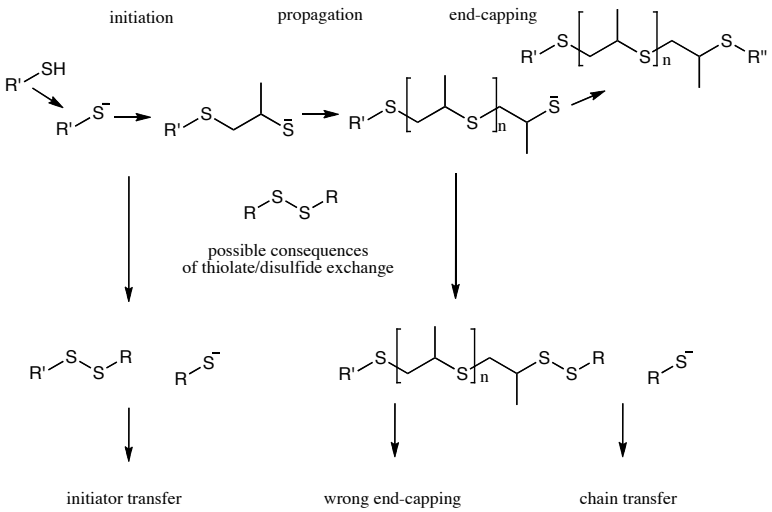

Figure 4.8: Possible side-reactions of disulfides in PS polymerization.[126]

Due to these facts, in a following work the polymerization conditions for propylene sulfide were optimized to avoid the presence and formation of disulfides in the polymerization. Further on a protected thiol, namely a thioacetate, was used as an initiator. The thioester was *in-situ* cleaved by sodium methoxide solution. Furthermore, the formation of disulfides in the polymerization was inhibited by the addition of tributyl phosphine (TBP) as reduction agent, which inverted the formed disulfides rapidly back to thiols. The end-

capping reaction was also improved to ensure a complete and fast termination of the synthesized polymers. Ethyl bromoacetate is a common used end-capping reagent and it is described to be sensitive against transesterification caused by the methoxide solution, which was added at the beginning of the polymerization in slight excess to guaranty complete deprotection of the initiator. Hence, the reaction mixture was buffered with acetic acid (AA) and DBU after the polymerization to achieve a quantitative and rapid end-capping of the poly(propylene sulfide).[127]

The improved recipe (**Figure 4.9**) was used to synthesize linear and star-shaped polymers (**Figure 4.10**). Different initiators with up to four thioacetates were synthesized, which subsequently initiated the PS polymerization.[128,129]

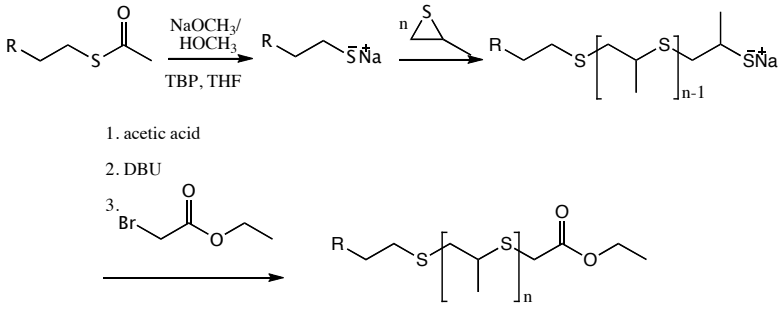

Figure 4.9: Optimized polymerizations conditions for propylene sulfide.[128,129]

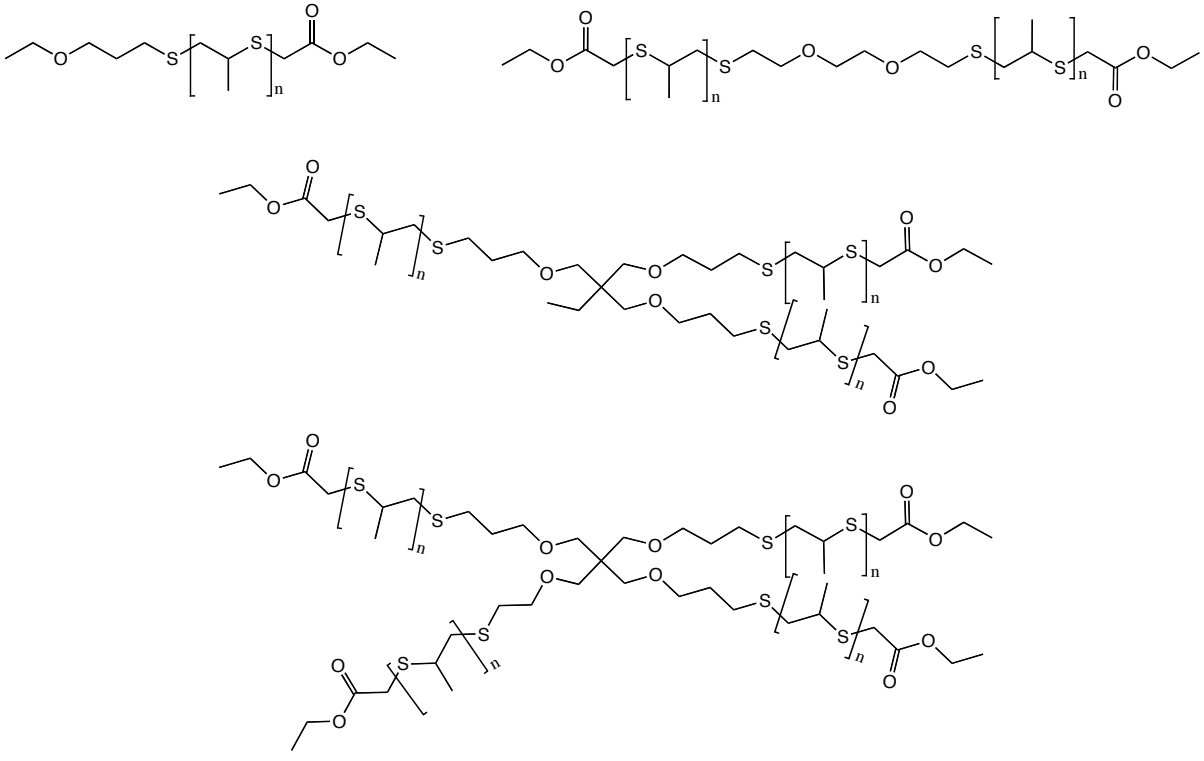

Figure 4.10: Synthesized linear and star-shaped polymers.[128,129]

An elastic polysulfide network was accomplished by use of a bifunctional initiator, 1,3-dimercatopropane, for propylene sulfide. After the polymerization the two living terminal groups of the PPS were end-capped in two steps. First with ethyl bromoacetate and subsequently with 2-(bromoacetoxy) ethyl methacrylate, to gain a mixture of PPS polymers with two terminal ethyl acetate functions and PPS with one ethyl acetate and one methacrylate functionality. The polysulfide three-dimensional network was formed through

photopolymerization of the terminal methacrylate groups of the PPS macromonomers. The obtained materials showed elastic behavior and the properties were tunable via the number of methacrylate end-groups.[130]

However, there were more strategies to polymerize propylene sulfide. The Inoue group introduced the living and immortal polymerization of episulfides with zinc *N*-substituted porphyrins in 1990. An initiator with a propyl thiol in axial positions was the effective one (**Figure 4.11**).[131]

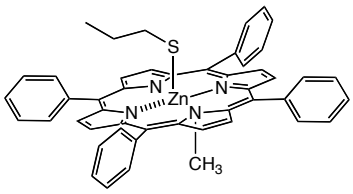

Figure 4.11: Used zinc *N*-substituted porphyrin-based initiator.[131]

The polymerization was initiated through the reaction of the zinc-polythio group with propylene sulfide to the growing species. The molecular weight of the formed polymers was tailored by the molar ratio of propylene sulfide reacting with the zinc porphyrin. The polymerization showed a living as well as immortal character and led to polysulfides with narrow molecular weight distributions below 1.10.[131]

Furthermore, the ring-expansion polymerization was investigated for propylene sulfide. The reaction was carried out in the presence of a cyclic bi-functional initiator. An insertion reaction of the monomer occurred into thioester bonds under catalysis of tetrabutylammonium chloride (TBAC). These polymerization conditions provided merely unsatisfying results. The reaction in a pressure-proof polymerization tube at 90°C for 24 h resulted in only 56% conversion and a bimolecular weight distribution in SEC.[132] In contrast, the insertion reaction of PS into carbamothiolates led to well-defined polysulfides with narrow molecular weight distributions below 1.10. The polymerization was also catalyzed by TBAC and exhibited a living character. Hence, the use of a tri-functional carbamothiolate as initiator allowed the synthesis of well-defined three-arm star polymers (**Figure 4.12**).[133]

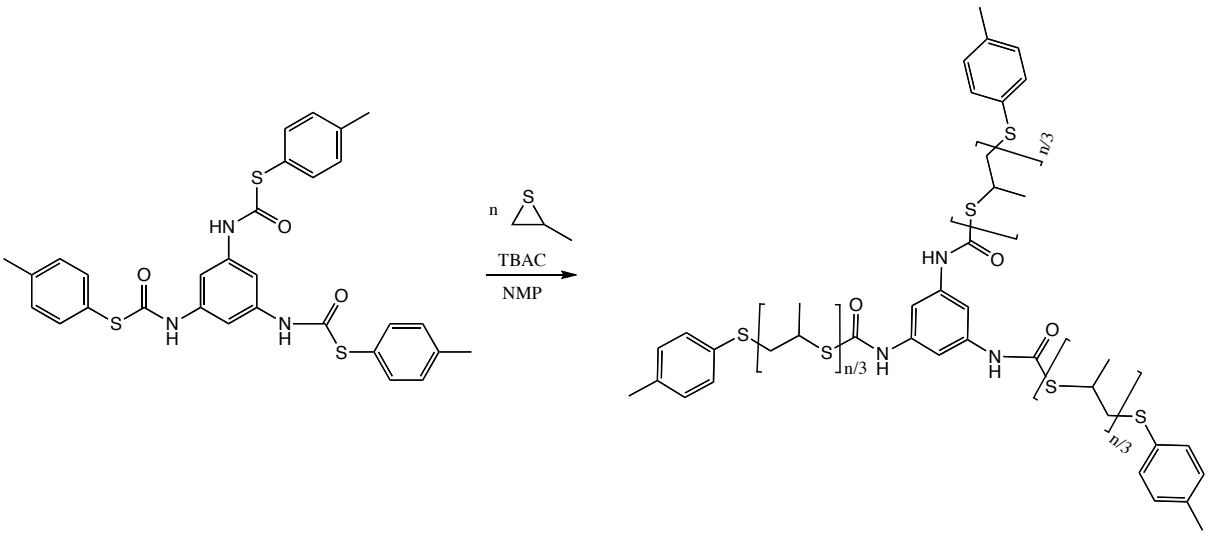

Figure 4.12: Three-arm star polymers via insertion reaction.[133]

In analogy to ethylene sulfide, the electrochemical ring-opening polymerization of propylene sulfide was realized. The PPS films behaved also similar to semi-conductors and the heteroatoms were partly positively charged due to electrochemical oxidation.[105]

4.1.3 Copolymer structures with thiiranes[134-191]

4.1.3.1 Copolymers with poly(ethylene sulfide)

Poly(ethylene sulfide) is known in some copolymer structures, although it is difficult to process due to the high degree of crystallization and the resulting insolubility.

Sigwalt and Boileau synthesized PEG-PES block-copolymers via the addition of ethylene sulfide to a living poly(ethylene glycol), prepared in anionic ring-opening polymerization with 9-carbazolyl potassium as initiator.[134] For the synthesis of telechelic polymers with thiol functionalities, living polystyrene was terminated with ethylene sulfide. However, the formation of poly(ethylene sulfide)-polystyrene-poly(ethylene sulfide) triblock-copolymers was not avoidable. These synthesized polymers were successfully used to stabilize cadmium sulfide semiconductors in a size range of 5-30 nm.[135] The transfer from living polymers, synthesized via carbanionic polymerization, was often used to generate block-copolymer structures with ethylene sulfide. This approach was used to form AB block-copolymers and ABA triblock-copolymers with ethylene sulfide and styrene, α-methylstyrene or methyl methacrylate, respectively (**Figure 4.13**). For the di-block-copolymers butyllithium was used as initiator and for the ABA polymers sodium naphthalide, which generated a dual anion with two living centers.[136]

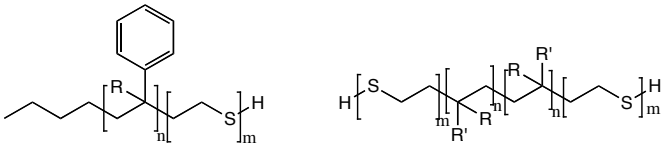

Figure 4.13: Synthesized AB and ABA copolymers.[136]

A similar approach was described for styrene, isoprene or butadiene and ethylene sulfide. The ABA copolymers with ES and isoprene were also initiated with a naphthalide species and the ABC structures were started with *n*-butyllithium-anisol as initiator. Styrene was added first, then isoprene or butadiene and the thiirane was introduced last. The formed AB samples with isoprene were good elastomers with good temperature stability, but the handling was challenging without partial oxidation of the polysulfide segments. However, the triblock-copolymers with styrene were described to be strong resilient elastomers with improved thermal stability compared to common poly(styrene-*b*-butadiene). The preparation of the ABC copolymers was more difficult, but the processing was easier. Vulcanization with accelerated sulfur systems was also affected and the products showed good physical properties.[137,138] Poly(ethylene sulfide) is also known in copolymers with substituted thiiranes. The random and block-copolymer of ES and isobutylene sulfide (IBS) as well as the unsaturated terpolymers of ES, IBS and allyl thioglycidyl ether (ATE) were introduced by Roggero et al. in 1975. For this, anionic ring-opening polymerization with metalated sulfoxides and sulfones as initiators were used. In **Figure 4.14** the synthesized copolymers are shown. [139,140]

The ES-IBS-ATE terpolymers were vulcanized and the formed materials had improved oil-resistance.[140] Random and block-copolymers of ethylene sulfide and isobutylene sulfide were investigated in more detail. A further study introduced a comprehensive NMR investigation of such polysulfide copolymers, which

included the assignment of the diads and triads in carbon NMR. Additionally, the obtained results led to the consumption of a higher reactivity of ES compared to IBS and thus led in case of high conversion in random copolymerization towards a block-like structure.[141,142] In addition the glass transition temperature and the crystallization was explored. PES and PIBS are both highly crystalline with melting points above 200°C.[143] The glass transition temperature decreased with increasing ethylene sulfide content, from -14°C for pure PIBS to -50°C for neat PES.[144]

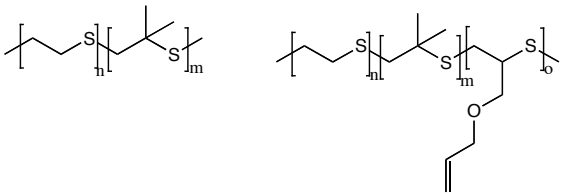

Figure 4.14: Synthesized block-copolymers and terpolymers.[139,140]

Furthermore, ES was copolymerized with a germylene in an oxidation-reduction-copolymerization procedure. The resulting organometallic polymer carried germanium (IV) along the polymer backbone. The 1:1:α periodical copolymer was developed via the confusion of two thiiranes to a dithioether unit under elimination of ethylene (**Figure 4.15**).[145]

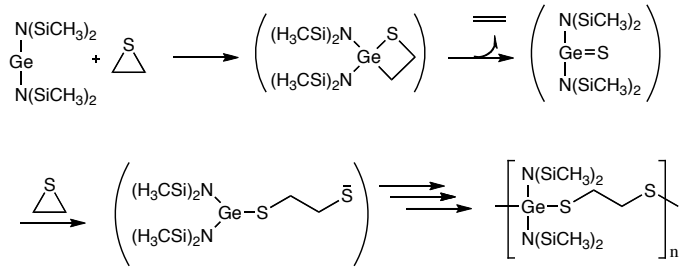

Figure 4.15: Mechanism of the oxidation-reduction polymerization.[145]

The conformational as well as configurational characteristics of poly(ethylene oxide-*alt*-ethylene sulfide)[146] and of poly(ethylene imine-*alt*-ethylene sulfide)[147] were investigated via NMR analysis of synthesized small molecular model compounds and additionally, with *ab initio* molecular orbital calculations.

Beside the ring-opening polymerization of ethylene sulfide, PES containing copolymers were obtained by polycondensation. Poly(ethylene sulfide), generated by this method, was known about 80 years before pure ethylene sulfide was synthesized by Delépine.[89] In 1839, Löwig and Weidmann described the reaction between potassium sulfide and a halogen compound.[148] A similar observation was published by Meyer in 1886.[149] Compared to the ring-opening polymerization, the polycondensation reveales some drawbacks. The molecular weight distribution is rather broad and it is quite challenging to obtain high molecular weight polymers, but it is still a used process as shown by two more recent studies. In 2003, the phase-transfer catalyzed polycondensation of ethylene dibromide with styrene dibromide and sodium sulfide to poly(ethylene sulfide-*co*-styrene sulfide) was introduced. The obtained copolymers had a random structure, due to the higher reactivity of ethylene bromide towards sodium sulfide (**Figure 4.16**).[150]

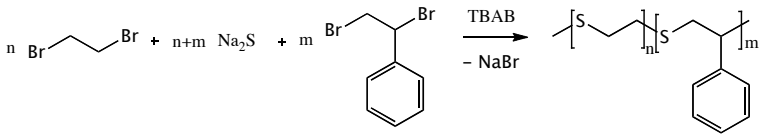

Figure 4.16: Polycondensation of ethylene dibromide with styrene dibromide and sodium sulfide.[150]

In a similar approach, poly(ethylene oxide-*co*-ethylene sulfide) copolymers with different oxygen to sulfur ratios were synthesized by polycondensation. Several dithiols and bischloro ethers were used as monomers to accomplish the targeted ratios. The reaction was carried out in buffered solution to accomplish the synthesis of high molecular weight polymers. Subsequently, the polysulfide copolymers were oxidized with 3-chloroperoxybenzoic acid to obtain poly(ethylene oxide *co*-ethylene sulfone) copolymers.[151]

4.1.3.2 Copolymers with poly(propylene sulfide)

Poly(propylene sulfide) has been described in various copolymer structures. The most common ones contain PEG, although the synthesis via addition of propylene sulfide to a living poly(ethylene glycol) species, in analogy to the approach with ES, failed. A proton of the methyl group of PS was abstracted by the alkoxide of the living PEG chain and the targeted copolymers were not obtained.[134] Three strategies were introduced to circumvent this phenomenon: (i) post-polymerization modification, (ii) the use of PEG derivatives as initiator or/and (iii) end-capping reagent for PPS. The latter two were both published in 2001. The group of Levesque used PEG bromo acetate as end-capping reagent for the synthesis of star-polymers, obtained by "core-first" method (compare **Figure 4.6**).[124] The architecture of PEG-PPS was further varied in a following approach. Synthesis of AB, ABA and BAB as well as tri-arm star polymers with a PEG core and polysulfide arms was achieved by two methods. The first method involved coupling reactions and was similar to the "arm-first" strategy. Hexanethiol acted as initiator for propylene sulfide and the living polymer chain was either end-capped with PEG bromoacetate to yield AB copolymers, with PEG-α,ω-dibromoacetate to obtain ABA copolymer or with star-shaped PEG, consisting of three bromoacetates as terminal groups, to result in a tri-arm star architecture. The use of hexanedithiol as initiator and PEG bromoacetate as terminating reagent led to the vice versa triblock-copolymer with a BAB structure. The second strategy was based on a PEG-based macroinitiator route. PEG thiol, PEG-α,ω-dithiol and a PEG tri-arm star with thiol groups as terminal functionality were used as macroinitiators for the polymerization of thiiranes, which resulted in an identical copolymer architectures. A reversed triblock-copolymer structure was obtained by the use of a mono functional PEG-based macroinitiator and a PEG bromoacetate as end-capping reagent after the polymerization of PS. The synthesis of different PEG-PPS copolymers with various block lengths was in both methods controlled, but the macroinitiator strategy exhibited a larger amount of disulfide formation.[152]

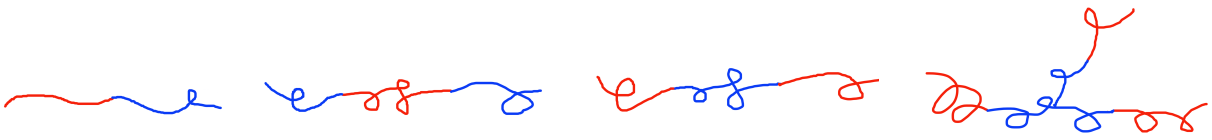

Figure 4.17a: Scheme of PEG-PPS copolymers with different architecture (red = PPS; blue = PEG).[152]

The group around Hubbell and Tirelli provided PEG with a thioacetate function and applied this as macroinitiator for PPS. The termination step enabled the synthesis of different amphiphilic polymer structures (**Figure 4.17a** and **b**). An AB block-copolymer was obtained by end-capping with small molecules like iodoacetamide. The exposure to air after the polymerization led to oxidation of the terminal thiols to disulfide and the formed ABA copolymers contained a concentric disulfide in the polymer backbone. Copolymers with an ABA' structure resulted in the termination with PEG monoacrylate, which was analog to the mentioned route by Levesque.[153]

The aggregation behavior of these amphiphilic copolymers in aqueous solution was studied in more detail. Cryo-TEM after the direct hydration of polymer films imaged several different morphologies of PEG-PPS-PEG triblock-copolymers. The variety included spherical and worm-like micelles, Y-junctions, blackberry micelles and vesicles. These aggregates were non-equilibrium species and transformed with time into uniform micelles with a wormlike or spherical shape. The preparation with organic solvents led immediately to consistent structures, which were closer to the equilibrium topology.[154]

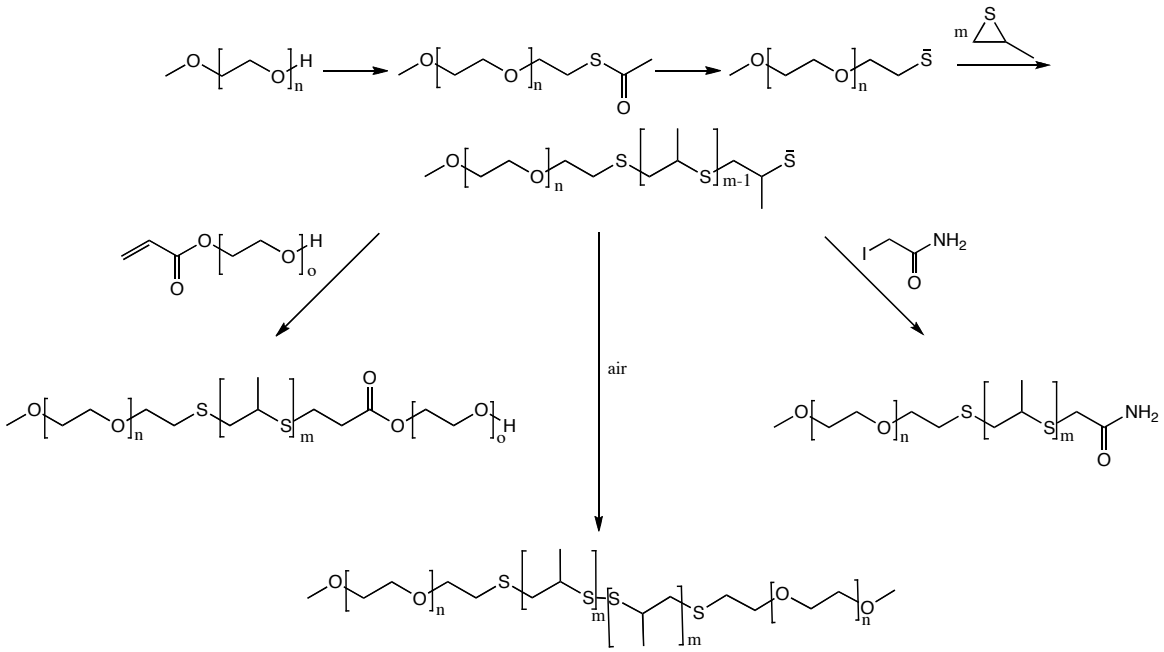

Figure 4.17b: Synthesis of AB, ABA, ABA' PEG-PPS copolymers.[153]

The morphology of the equilibrium shape was controlled by the relative block values of PEG and PPS. Polymer compositions, which were rich in PEG, generally developed micelles and copolymers with small amounts of PEG always formed vesicle. However, the stability of the aggregates was assigned by the length of the hydrophobic PPS block. In general, PPS-PEG copolymers formed rather stable aggregates. In comparison to the aggregates of the polyether analog Pluronics (PEG-*b*-PPO-*b*-PEG), they are one order of magnitude more stable.[155] In a further study, a nonionic surfactant Triton X-100 (poly(ethylene glycol) p-(1,1,3,3-tetramethylbutyl)-phenyl ether) was used to investigated the stability of micelles. The surfactant interacted strongly with hydrophobic polymers by intercalation into the core of the micelles. The obtained results confirmed the stability, which was defined by the hydrophilic polymer segment.[156]

The lyotropic behavior of ABA triblock-copolymers and AB copolymers with up to four branching points was explored via polarized light optical microscopy, rheometry, freeze-fracture TEM and surface pressure isotherm investigations. PPS-PEG copolymers are more hydrophobic than the analog Pluronic, due to the sulfur atoms in the polymer backbone. The different hydrophobicity of the polyether block and the polysulfide block was responsible for the organization of stable lyotropic mesophases in water for several linear block compositions. Furthermore, the formed lamellar gels were transformed to micelle suspensions and were stable under storage for months. In addition, these lyotropic structures were sensitive to temperature.[157] To investigate the influence of branching, a set of different PEG-PPS samples were prepared by the Tirelli group. They initiated the polymerization of propylene sulfide with different initiators, which bore up to four initiating groups (compare **Figure 4.10**) and used PEG bromoacetate as terminator (**Figure**

4.18).[128,129] These star polymers showed in rheology a dependency between the number of arms and the lyotropic phases as well as interfacial dimensions. The ratio of PPS to PEG indicated no influence on these parameters. With increasing number of branching points, the PEG chains appeared to be more compact and in a less hydrated conformation.[129] These polymer aggregates were also explored concerning their sensitivity towards oxidizing agents in aqueous solution. The response to oxidants seemed not to be influenced by the degree of branching. These results might be caused by the investigated polymers, which were rather large in size.[128]

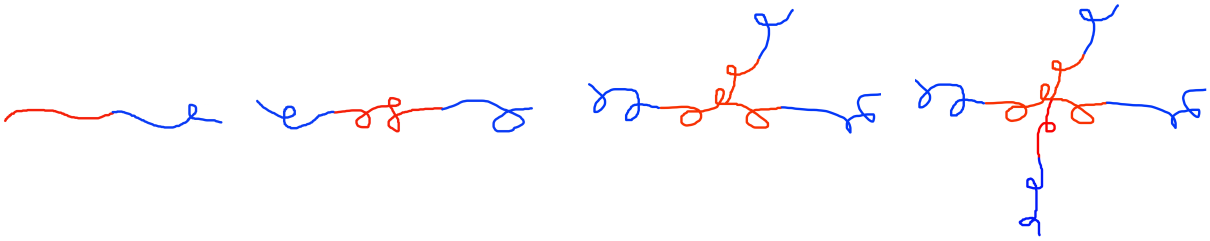

Figure 4.18: Scheme of PEG-PPS copolymers with different architecture (red = PPS; blue = PEG).[128,129]

In a follow-up publication, the oxidation-sensitive response of PEG-PPS copolymer aggregates was analyzed. The amphiphilic polysulfide-polyether copolymers with a vinyl sulfone end-group were provided with an enzyme, superoxide dismutase (SOD). Conjugation with the biomolecule was realized in a Michael-type reaction between the vinyl sulfone functionality of the polymer and a thiol group of a cysteine or an amine group of a lysine of the SOD (**Figure 4.19**).[158]

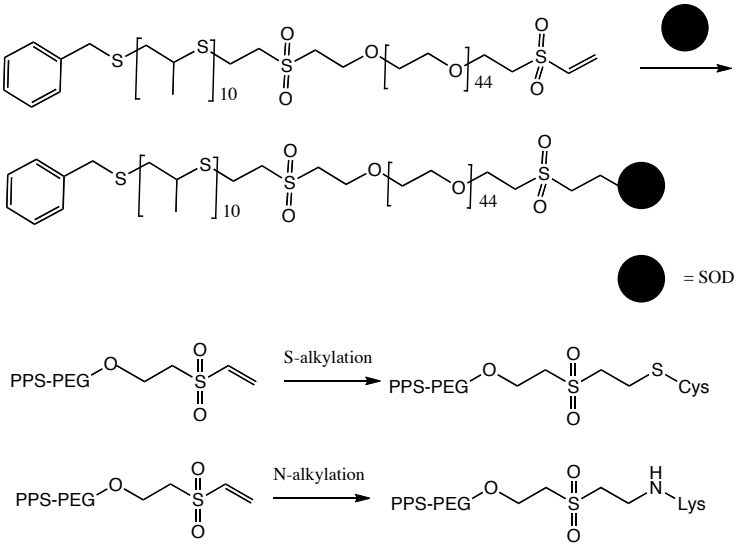

Figure 4.19: PPS-PEG-SOD conjugates (top), conjugation possibilities between polymer and SOD (bottom).[158]

These polymer-enzyme conjugates were sensitive against two reactive oxygen species, superoxide and hydrogen peroxide, which are essential compounds in inflammatory diseases. The polysulfide block was reactive against hydrogen peroxide and the SOD captures effective the superoxide ions. Simultaneously, these materials could act as drug carriers and released the carriage after inflammatory-response.[158]

Vinyl terminated PEG-PPS copolymers were also used to explore the exchange phenomena of micelles via fluorescence resonance energy transfer experiments. The copolymer was converted at the terminal end with a dansyl group as fluorophore or a dabsyl group as quencher. Alternatively, either the fluorophore or the quencher was encapsulated into micelles. The exchange reaction was indicated by an increase of the

fluorescence quenching efficiency. Within 24 hours no rapid exchange phenomena occurred in the study. Furthermore, the exchange of the carriage was temperature sensitive and the aggregates were stable for days under storage at low temperatures.[159]

In a similar work, the synthesis of PEG-PPS-based polymer-biomolecule conjugates was introduced, which accomplished the production of polyether-polysulfide copolymers by post-polymerization modification. In this study, ethyl mercaptan acted as initiator for propylene sulfide, which was terminated with methyl acrylate. The ester function was cleaved under basic conditions to the corresponding carboxylic acid, which was subsequently reacted with a bi-functional PEG to enable the conjugation to biomolecules. The conducted synthesis is shown in (**Figure 4.20**).[160]

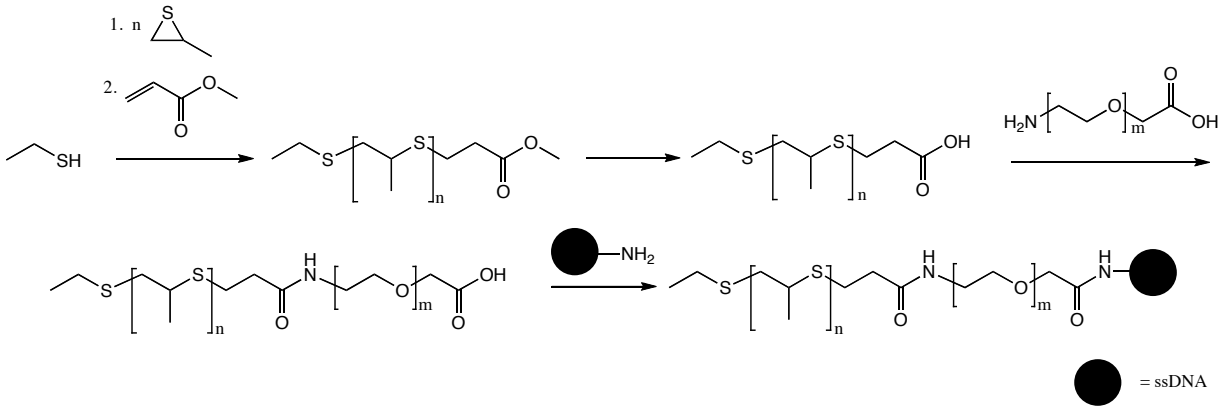

Figure 4.20: Synthesis of PEG-PPS-based polymer-biomolecule conjugates.[160]

PPS-PEG copolymers were conjugated to ssDNA and combined with hydrophobic ultrasmall superparamagnetic iron oxides (USPIO) to result in ssDNA-displaying USPIO micelles. These clusters were sensitive to temperature and enzymatic activity for applications in magnetic resonance imaging (MRI). The system was enabled to release the nanoparticles in a controlled fashion and the released USPIOs changed the magnetic relaxation in MRI and thus enzymatic activity was detected. In most diseases, even in cancer, enzymatic activity is an important benchmark.[160]

A disulfide end-capped PPS-PEG was converted with a positive charged protein via thiol/disulfide exchange between the disulfide terminus of the copolymer and a thiol group of a cysteine of the enzyme (**Figure 4.21**).[161]

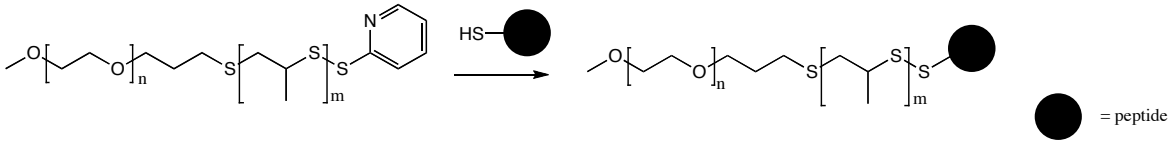

Figure 4.21: Synthesis of PEG-PPS-enzyme conjugates.[161]

The polymer-enzyme conjugates self-assembled with siRNA through hydrophobic interaction and electrostatics. The size of the formed aggregates depended on the length of the polysulfide block and the used amount of polymer, which meant the charge ratio. Those complexes were enabled to transport siRNA into cells and to achieve a down-regulation of gene expression. This effect is imported for the RNAi pathway in mammalian cells and essential in therapy.[161]

However, in drug delivery systems the encapsulation efficiency is the crucial issue. The use of PEG-PPS copolymers, with a low molecular weight PEG block, led to high encapsulation efficiency via direct

hydration of the mixture to polymersomes. The encapsulation amounted 37% for ovalbumin, 19% for bovine serum albumin and 15% for bovine γ-globulin. Furthermore, the encapsulation of proteinkinase K was successfully accomplished.[162] In addition, the encapsulation efficiency and release of the carriage in PPS-PEG drug delivery systems was studied with Cyclosporin A, an immunosuppressive drug. A loading level of 19% was achieved with amphiphilic copolymers and the release of Cyclosporin A continued for 9-12 days.[163]
In a further approach, PEG-PPO-PEG was functionalized with a sulfate group at the terminal position to mimic heparin and the facility to bind collagen of the extracellular matrix. This complex was encapsulated in PEG-PPS micelles. In addition, a drug was incorporated into this copolymers and the *in vitro* release was explored. Sirolimus, a therapeutic to suppress the immune response in cardiovascular diseases especially in coronary treatment, was used in this study. The encapsulation efficiency accomplished 90% at a loading of 20%. *In vitro* 60% of Sirolismus was released over 12 days at 37°C.[164]
Moreover, the use of PEG-PPS block-copolymers was realized in reduction-sensitive block-copolymer vesicles. The amphiphilic copolymer contained a disulfide, which is sensitive to reduction agents, as conjunction point of the polysulfide and the polyether block. This structure was obtained by oxidative coupling of the living PPS chain and a PEG with a thiolate as end-group. The formed polymer vesicles were enabled to encapsulate active agents and protected them from the extracellular environment. In cellular experiments an uptake via endocytosis was exhibited. They burst immediately in the early endosomes and thus they released their carriage. This prevented the release of the content under the harsh conditions beyond lysosomal fusion. The release occurred within ten minutes after exposure to cells, thereby PPS-PEG is a potential drug delivery system for peptides, oligonucleotides and DNA.[165]
In a recent publication, the group around Hubbell introduced novel PEG-PPS-PEI copolymer as non-viral vectors for plasmid DNA. The triblock-copolymers were obtained through a thiolate/disulfide exchange between the terminal thiol functionality of a living PEG-PPS species and a disulfide terminated protected PEI (**Figure 4.22**).[166]

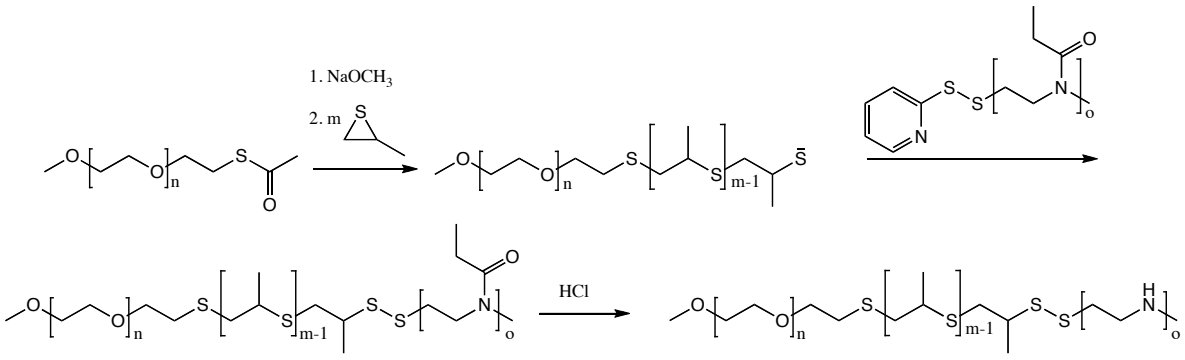

Figure 4.22: Synthesis of PEG-PPS-PEI triblock-copolymers.[166]

PEG-PPS macrophilics as well as a mixture of PEG-PPS and PEG-PPS-PEI copolymers formed positively charged micelles, which were used as non-viral vectors for plasmid DNA transfection in a tumor immunotoxicity model. The two formed carrier systems accomplished good results for the transfection of melanoma cells *in vitro* as well as *in vivo* after intratumoral injection. Plasmid DNA was released by cleavage of the triblock-copolymer under endosomal conditions in combination with rupture of the endosoms provided by the cationic PEI. Furthermore, tumors were transfected with an antigen transgene, which led to a significant reduction in tumor grows, an accumulation of cytokines and an increase of cytotoxic T

lymphocytes in intratumoral infiltration. These results implied an effective transfection with low cytotoxicity of the polysulfide-based carrier system.[166]

In a different approach, the use of PPS-PEG copolymers enabled the formation of single-walled carbon nanotubes in biocompatible dispersions. The stabilization of concentrated dispersions with PPS-PEG bi- and triblock-copolymers was more effective compared to the polyether analog PEG-PPO-PEG. The toxicity of the polymer-carbon nanotube dispersion in cellular tests was low, which indicated an effective functionality by the copolymer structures. The ratio between the hydrophilic block and the hydrophobic block, as well as the block length of the PPS influences the stability of the prepared dispersions. In addition, the polymer concentration and the sonication time during the formation controlled the dispersion stability.[167]

However, the PPS-PEG copolymers approached even a further range of applications. The sulfur atoms along the polymer backbone of the polysulfide block enabled the adsorption of this class of copolymers to metal surfaces. In 2003, Bearinger et al. published the chemisorption of PPS-PEG copolymers to gold surfaces. PEG-PPS-PEG triblock-copolymers exhibited a minimization of adsorption and adhesion of biomolecules. The protein adsorption was more than 95% reduced and the cell adhesion was reduced about 97%. Similar results were sustained after exposure to whole blood serum. Compared to common alkylthiols, the formed polymer layers were more stable against oxidation.[168] In a follow-up work, these results were confirmed. The same group investigated a set of PPS-PEG bi- and triblock-copolymers adsorbed to gold surfaces in more detail. By a dip- and rinse procedure a quantitative polymer surface coverage was obtained. The polymer architecture influenced significantly the measured protein resistance. Triblock-copolymers led to better results compared to the diblock-copolymers, presumably due to the higher PEG content in the triblock-copolymer.[169] A micropattering of gold substrates with the amphiphilic copolymer structures was also feasible. Patterned surfaces were achieved by molecular-assembly patterning by lift-off technique. This technique used a sharp pattern of a photoresist, which was obtained by spin coating of two positive photoresists. These photoresists were illuminated trough a chromium mask and rinsed afterwards to produce the patterned photoresist. The prepared gold substrate was dipped in the organic copolymer solution and subsequently the photoresist was removed via an intensive treatment process with mainly *N*-methyl-pyrrolidone. Protein adsorption tests were conducted on the prepared polymer layers. The PEG-PPS areas reduced the protein adsorption over 90%. In contrast, the areas without copolymer indicated no protein resistance at all.[170] In a further approach, patterning on micrometer and submicrometer scale of gold surfaces with polysulfide copolymers was attained with porphyrin-based photocatalytic lithography. In this method a polymer coated gold substrate was provided with a mask on the top. This mask determined the pattern. The excess PPS-PEG was removed by local oxidation via the activation of a photocatalyst through the polymeric photomask by exposure to red light. The activated photocatalyst was in contact with the sensitive organic polymer layer and the mask localized chemical reactivity to the areas, which were in contact with the polymer layer. Protein adsorption test confirmed again the nonfouling effect of the polymer-pattered areas.[171] Furthermore the protein-resistant PPS-PEG triblock-copolymers were adsorbed onto indium tin oxide as an electrically conductive substrate. The adsorption and electro-desorption of the copolymer from the substrate was investigated. An anodic electrical stimulus on the surface modified indium tin oxide samples led to a continuous desorption of the PPS-PEG copolymers.[172]

The immortal polymerization with a zinc *N*-methylated porphyrin complex (**Figure 4.11**) enabled the rapid synthesis of polysulfide-polyether copolymers. First the episulfide block was formed, followed by the polymerization of the epoxide mediated by visible light. The polymerization exhibited a living and immortal character and allowed the controlled synthesis of PPS-PPO copolymers with narrow molecular weight

distributions. As mentioned before, the polymer grew in axial position of the initiator. The photoexcitation led to an increased reactivity of the active center through the light absorption by the porphyrin ligand.[173] In the following publication, the same method was used to obtain PEG-PPS copolymers, in a random fashion. The initiator provided a much higher polymerization activity for sulfides compared to epoxides, which led with common polymerization techniques to a mixture of two homopolymers or to block-copolymers. In this study, the photoenhanced copolymerizability was introduced, which facilitated random copolymers despite different polymerizability.[174]

As shown, the synthesis of PEG-PPS copolymers with different structures and functional groups was feasible and introduced a wide range of different characteristics and thus several useful applications in the field of drug delivery and biomedicine.

In analogy to ethylene sulfide, propylene sulfide polymerization was initiated with living carbanionic polymers. In 1965, Boileau and Sigwalt synthesized polystyrene-poly(propylene sulfide) block-copolymers by addition of PS to a living polystyrene.[175] In the same year, the synthesis of copolymer structures with PS and styrene, α-methylstyrene or methyl methacrylate were published. Use of butyllithium for carbanionic polymerizations led to AB structures and polymers initiated by sodium naphthalide exhibit an ABA composition, while PPS provided the A block. The formed polymers were in analogy to those with ethylene sulfide, despite a methyl group along the polysulfide chain (compare to **Figure 4.13**).[135] Inverse ABA copolymers of α-methylstyrene and PS, while A was featured by α-methylstyrene, were introduced by Morton et al. Ethyllithium was used as initiator and α-methylstyrene was first introduced into the polymerization mixture. After full conversion of the styrene monomer, propylene sulfide was added to synthesize the second block. Subsequently, phosgene acted as coupling agent for the active thiolate end groups to provide the triblock-copolymers (**Figure 4.23**).[176,177]

In a further approach, PS was grafted onto crosslinked polystyrene beads as well as onto chloromethylated polystyrene beads. The crosslinked polystyrene beads were deprotonated with butyllithium/tetramethylethylenediamine and acted as macroinitiator for propylene sulfide. The grafted polysulfide was regularly distributed across the macroinitiator beads. Grafting approaches to chloromethylated polystyrene beads were realized by the coupling between the chloromethylene groups and the terminal thiolate groups of preformed poly(propylene sulfide) chains. After the grafting reaction the diameter of the beads increased as expected.[178]

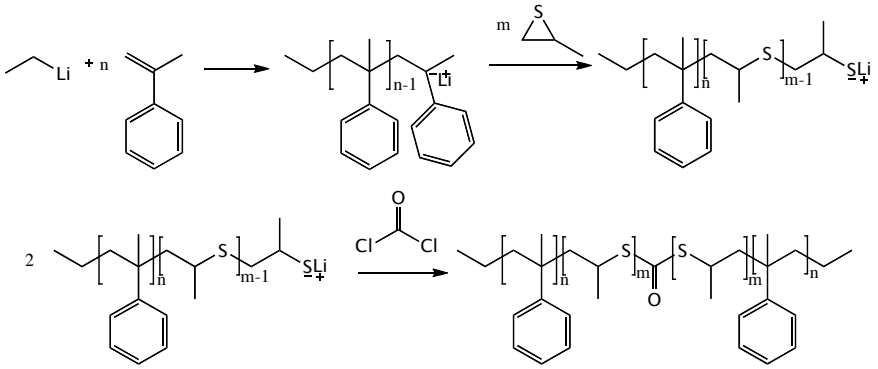

Figure 4.23: Synthesis of poly(α-methylstyrene)-poly(propylene sulfide)-poly(α-methylstyrene) triblock-copolymers.[176,177]

However, there were several copolymer structures with substituted thiiranes described. The random and block-copolymerization of isobutylene sulfide (IBS) and propylene sulfide was introduced in 1970. 9-carbazolyl sodium as starter led to AB copolymers and the use of sodium or potassium naphthalide

created polymers with two living centers and triblock-copolymers with an ABA structure were obtained. The A block was provided by isobutylene sulfide, which is described as highly crystalline polymer. AB block-copolymers as well as random copolymers are soluble in toluene. In contrast, the triblock-copolymers with two poly(isobutylene sulfide) chains are insoluble in toluene. **Figure 4.24** shows the syntheses of a poly(isobutylene sulfide)-poly(propylene sulfide)-poly(isobutylene sulfide) polymer with sodium naphthalide as starter and ethyl bromide as end-capping reagent.[179]

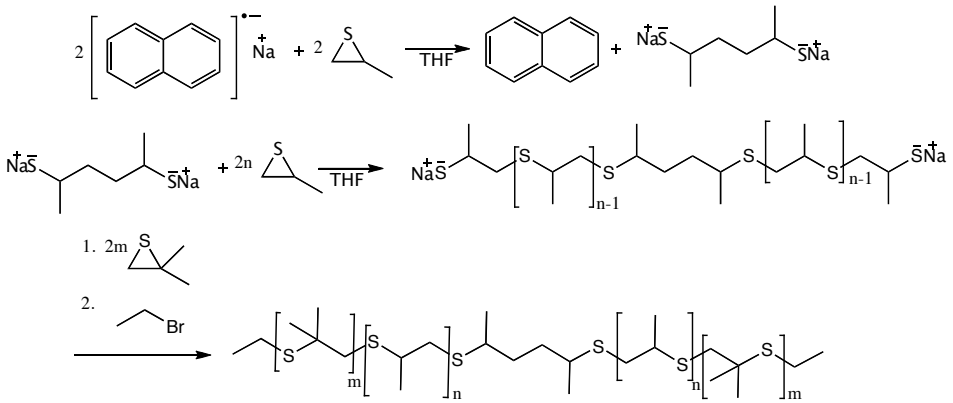

Figure 4.24: Synthesis of poly(isobutylene sulfide)-poly(propylene sulfide)-poly(isobutylene sulfide)triblock-copolymers.[179]

Copolymers with PS und IBS were also obtained by polymerizations initiated with metalated sulfones and sulfoxides. The synthesized copolymers were amorphous over a wide range with up to 70% PIBS content.[139] The detailed evaluation of the NMR signals of the PPS-PIBS copolymers and the assignment of the diad as well as triad signals of ^{13}C NMR was published by Corno et al.[141,142] In addition, the deprotonated sulfones und sulfoxides acted as starter for the synthesis of unsaturated terpolymers accomplished of PS, IBS and ATE (compare to **Figure 4.14**).[139] These terpolymers were explored in a further investigation, for example, by dynamo mechanical measurements.[143]

Bonnans-Plaisance et al. described the synthesis of random and block-copolymers consisting of propylene sulfide and hydroxymethylthiirane (HMT). Dithiobenzoic acid quaternary ammonium salts were utilized as initiators and the polymerization was conducted in DMF. The obtained polymers are colorless, amorphous and soluble in THF and chlorinated solvents. The molar content of HMT in the copolymers were analyzed with NMR spectroscopy and UV spectroscopy, after conversion of the hydroxyl functionalities with 1-naphthyl isocyanate.[180] In a further investigation, the molar ration of HMT was explored by proton NMR after acylation of the hydroxyl groups with acetyl chloride or benzoyl chloride.[181] In addition, the obtained copolymers were analyzed with carbon NMR spectroscopy. The homopolymerization of PS failed under the used conditions due to termination reactions. Hence, the block-copolymer synthesis was only successful, if the poly(hydroxymethylthiirane) block was formed first. The hydroxyl functionalities of the PHMT avoided partially the termination reaction and the PS polymerization was enabled. The homopolymerization of propylene sulfide was also achievable by addition of ethanol to the polymerization mixture.[182] In addition PS was copolymerized with methyl(2,3-epithiopropyl-thio) ethanoate and thiirane macromonomers with PEG side-chains.[215,217,218]

A further strategy to obtain polystyrene-poly(propylene sulfide) copolymer used a combination of RAFT and controlled thioacyl group transfer (TAGT) polymerization. RAFT polymerization of styrene or *N,N*-dimethyl acrylaminde was conducted first to result in polymers with a terminal dithiocarbonyl functionality.

In a second step, these macroCTAs acted as initiator for TAGT polymerization of PS. The synthesized polystyrene-poly(propylene sulfide) and poly(*N*,*N*-dimethyl acrylamind)-poly(propylene sulfide) block-copolymers exhibited narrow molecular weight distributions below 1.20. The synthesis is shown for poly(*N*,*N*-dimethyl acrylamind)-poly(propylene sulfide) block-copolymers in **Figure 4.25**.[183]

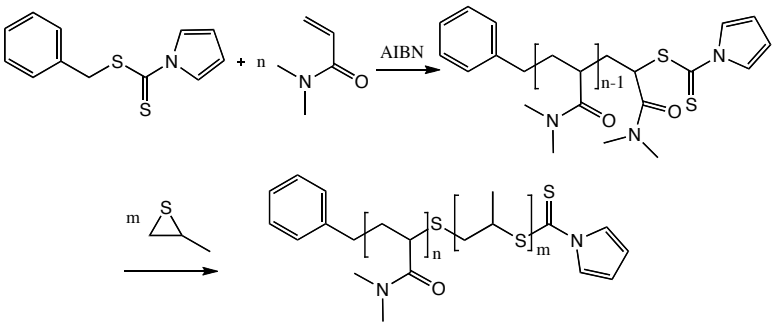

Figure 4.25: Synthesis of poly(*N*,*N*-dimethyl acrylamind)-poly(propylene sulfide) block-copolymers.[183]

In a further study the graft-copolymerization of propylene sulfide to human hair was explored. Human hair consists mainly of creatine, a protein produced in the human body, and exhibits a small amount of disulfide bonds. Prior, the disulfides were cleaved by reduction and the formed thiolats on the hair acted as initiator for propylene sulfide. The polymerization was successfully conducted in aqueous solution. After basic hydrolysis of the hair, the grafted polymer chains were isolated and investigated.[184]

The copolymerization of carbon disulfide and propylene sulfide was achieved with a chromium catalyst (**Figure 4.26**). The obtained poly(ethylene trithiocarbonate) exhibited a completely alternating structure. Although the formation of a side-product, a cyclic trithiocarbonate, always took place, the selectivity was influenced by the amount of carbon disulfide. Higher carbon disulfide contents shifted the product ratio towards the polymer formation.[185]

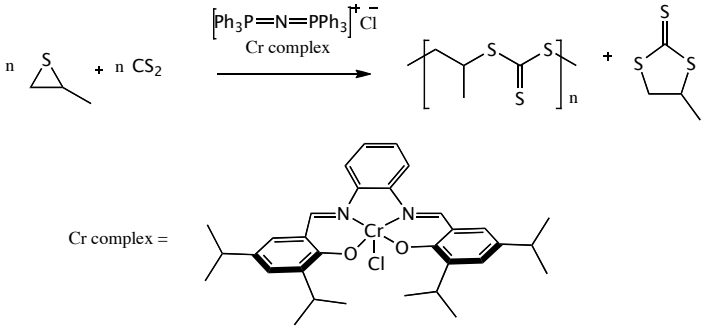

Figure 4.26: Copolymerization of propylene sulfide and carbon disulfide.[185]

Lautenschlaeger and Zeeman introduced the reaction of propylene sulfide with nitrogen containing polymer. The authors described a graft-copolymerization of PS onto poly(ethylene imine) and nylon 11. Primary, secondary and tertiary amines were enabled to initiate the ring-opening polymerization of PS, which led in case of PEI to a graft copolymer with mercapto and mercaptide groups (**Figure 4.27**).[186,187]

The oxidation-reduction copolymerization with a germylene was also investigated with propylene sulfide (compare to **Figure 4.15**). During the reaction propylene was evolved and a 1:1:α periodic copolymer was obtained.[145]

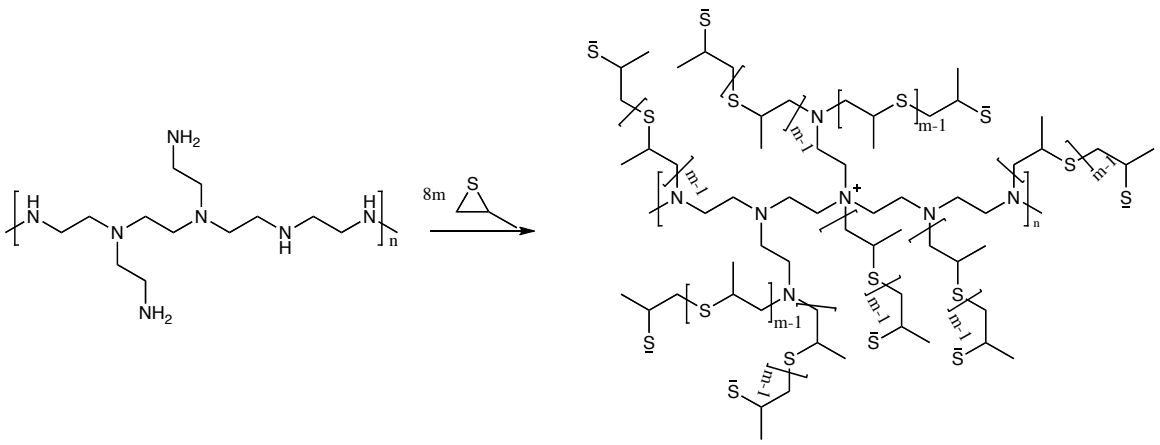

Figure 4.27: Graft-copolymerization of propylene sulfide onto poly(ethylene imine).[186,187]

4.1.3.3 Poly(ethylene sulfide)-poly(propylene sulfide) copolymers

Sigwalt and Boileau described the first block-copolymers consisting of ethylene sulfide and propylene sulfide in 1965. Sodium naphthalide was used as initiator for PS and afterwards ES was added to the living PPS polymer to yield ABA copolymers (**Figure 4.28**).[175]

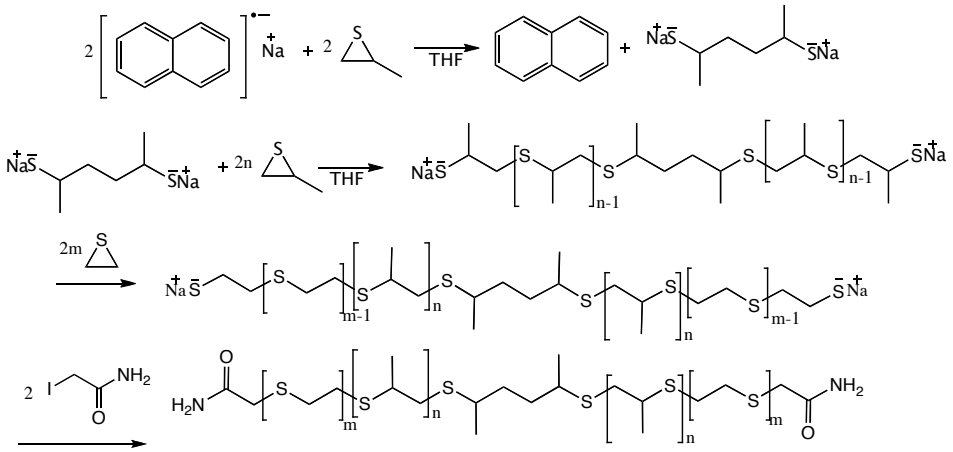

Figure 4.28: Synthesis of PES-PPS-PES block-copolymers.[175]

The same ABA structure was received in a similar approach with 1,2-ethandithiol as initiator. Although the formed samples were low molecular weight polymers, they showed thermoplastic behavior with rubbery properties below their softening point. The softening temperature increased with increasing ethylene sulfide content from 70-78°C for copolymers with 9% ES to 117-125°C for copolymers with 29% ES. Furthermore, they exhibited a good swelling resistance, which was comparable to other rubber materials.[188]

In addition, the random copolymerization of ES and PS with cadmium carbonate in aqueous media was investigated in detail.[189,190] The main focus of this study was on the reactivity ratios of the monomers. The reactivity ratio of PS was around 0.7 and of ES about 2.0, which was shifted under the influence of the cadmium salt in favor to PS.[190]

Roggero et al. synthesized AB and ABA block-copolymers as well as random copolymers of ethylene sulfide and propylene sulfide in presence of their metalated sulfoxides and sulfones. The investigation of the random copolymers by X-ray analysis and ^{13}C-NMR spectroscopy revealed a nearly random structure and amorphous structure up to an ES content of 45 %, samples with 54% ES content showed a low degree of

crystallization. Block-copolymers were explored by differential scanning calorimetry (DSC) to evidence the glass transition temperature of the amorphous PS part at -44°C as well as the melting point of the crystalline ES part at 204°C.[139] Furthermore, the same anionic initiators based on the metalation of sulfones and sulfoxides were used to synthesize ES-PS-ATE terpolymers, which were enabled for vulcanization. Compared to the vulcanized ES-IBS-ATE copolymers, the ES-PS-ATE terpolymers exhibited similar thermal and thermo-oxidative behavior as well as related vulcanization kinetics and processability. ES-PS-ATE copolymers are preferred if good mechanical properties are required.[139,140] Copolymers of ethylene sulfide and propylene sulfide were well investigated via NMR spectroscopy and the assignment of diad and triad signals in carbon NMR spectroscopy were also published.[141,142,191] In addition, carbon NMR was also used to prospect the microstructure of different episulfide copolymers, which indicated the block-copolymer character was more distinctive for ES-IBS copolymers than for ES-PS copolymer. This result also proved the reactivity graduation in anionic polymerization from ES to PS to IBS. The unsubstituted thiirane, ethylene sulfide, exhibits the highest reactivity, and isobutylene sulfide showed a lower reactivity than propylene sulfide.[140]

The block-copolymers of ethylene sulfide and propylene sulfides were also formed in cationic ring-opening polymerization of the episulfides with aluminum chloride.[192]

4.1.4 Polysulfide nanoparticles[193-198]

Living anionic ring-opening polymerization of thiiranes was successfully accomplished in emulsion to obtain polysulfide nanoparticles. The polymerization was conducted in aqueous solution with Pluronic as emulsifier and 1,3-dipropandithiol as bifunctional initiator as well as DBU as deprotonating agent. After the polymerization three different end-capping strategies were conducted. The first strategy involved the chain termination with iodoacetamide. In the second strategy divinyl sulfone as bifunctional end-capper was added to enable chain extension. The third strategy led also to chain extension via oxidation of the terminal thiolate to disulfides by air. The obtained nanoparticles exhibited a PEG corona caused by the Pluronic and they were stable against agglomeration. Conversion was limited, which might be caused by the increasing viscosity during the polymerization in the particles. The analog approach was also conducted with a mixture of ethylene sulfide and propylene sulfide. For block-copolymerization PS was polymerized first and afterwards the equivalent amount of ES was added. The obtained nanoparticles showed in proton NMR a monomer ratio of one to one, as targeted. Random copolymerization led to a low degree of polymerization, which might be caused by the faster incorporation of the more reactive ES and thus a partial crystallization of the growing chains and a hindered further polymerization. The emulsion polymerization of cyclohexene sulfide failed and solely a mixture of oligomers were yielded.[193]

Due to the PEG surface, the PPS nanoparticles have potential applications in biological systems. The described polymerization was adapted to pentaerythritol tetrathioacetate as initiator and the thioesters were cleaved in basic media. After the polymerization the living polymer chains were cross-linked by exposure to air and thus oxidation to disulfides or by Michael-type addition with tetra(ethylene glycol) diacrylate as bifunctional end-capping reagent, respectively. The size of the polysulfide nanoparticles was well controlled in the range of 25 nm to 250 nm by the used monomer to emulsifier ratio of the emulsion polymerization. Furthermore, the nanoparticles were fluorescent labeled on the surface by fluorescein labeled Pluronics. In cytotoxicity test with fibroblast cells a negligible cytotoxic effect was observed. In addition, the polysulfide nanoparticles were oxidation sensitive toward water-based oxidants such as hydrogen peroxide to enable the materials to swell and afterwards solubilize in water.[194]

In a further study, the PPS nanoparticles were investigated in an *in vivo* study of dendritic cells in lymph nodes. In a mice model the delivery of polysulfide nanoparticles with a diameter of 20, 45 and 100 nm to dendritic cells were explored. These nanoparticles were enabled to enclose hydrophobic drugs and to release the carriage in oxidative media. For the nanoparticles with 20 nm respectively 45 nm diameter a significant retention on lymph nodes was obtained with a stable presence until five days after injection. The number of nanoparticles containing dendritic cells increased from the measurement after 24 h to the analysis after 96 h. PPS nanoparticles might have potential applications in immunotherapeutics with targeted drug delivery to dendritic cells of nymph nodes.[195]

In the following investigation, the polysulfide nanoparticles were labeled to enable their detection. For this 5-iodoacetamido-fluorescein was used to terminate a small number of living polymer chains, and the remaining thiolates were reacted with *L*-cystein. The alternative strategy involved the formation of gold nanoparticles from chloroauric acid with sodium borohydride in the living polymer mixture. The gold nanoparticles were fixed to the sulfur atoms of the PPS nanoparticles. In addition, the used emulsifier was converted to Pluronic-α,ω-divenylsulfone, which allowed mild and rapid functionalization of the PPS nanoparticles with bioactive molecules. The concept is shown in **Figure 4.29**.[196]

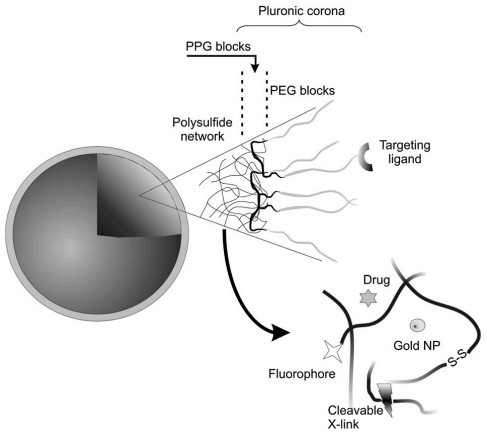

Figure 4.29: Concept of the labeled PPS nanoparticles with a targeting ligand of bioactive molecules [scheme taken from[196]].

The *in vivo* lifetime was controlled through the uptake by phagocytic cells, which was determined by its size and nature of the particle surface. Smaller nanoparticles with a diameter of 40 nm showed nearly no uptake by macrophages *in vitro*. For larger PPS nanoparticles (100 nm) an uptake was detected *in vitro* and furthermore the *in vivo* experiment showed a decreasing blood circulation half-life time. However, smaller polysulfide nanoparticle with a fixed RGD peptide on the surface were also incorporated.[196]

Furthermore, the poly(propylene sulfide) nanoparticles were possibly used as oxidation-responsive materials for inflammatory reactions. These materials showed bulk behavior with a homogeneous oxidation along the nanoparticles. This was investigated in a model reaction with hydrogen peroxide, where an autoaccelerating conduct was obtained. It was evidenced that one hydrogen peroxide molecule participate and hence, the oxidant concentration was not linear to the reaction rate. This might mean the PPS nanoparticles respond only to string inflammation with a high oxidant concentration.[197]

The encapsulation of hydrophobic molecules into PPS nanoparticles was investigated in a recent study. Nile red and Reichardt's dye were used as cargo for PPS nanoparticles and the chemically and enzymatically induced release was analyzed by spectroscopic methods. A sodium hypochlorite concentration in the ppm

range was sufficed to oxidize polysulfide nanoparticles to polysulfoxides and polysulfones, which were enabled to swell and solubilize in water. Furthermore, physiological relevant oxidoreductase enzymes such as chloroperoxidase and human myeloperoxidase facilitated the oxidation of the nanoparticles in the attendance of sodium chloride and hydrogen peroxide in low concentrations. The chloroperoxidase catalyzed the formation of sodium hypochlorite from sodium chloride and hydrogen peroxide. The catalytic amount of the oxidizing agent enabled the release of the encapsulated dyes.[198]

4.1.5 From substituted thiirane to functional polysulfides[199-222]

The following description of various thiirane derivatives should point out the diversity of substituted monomers and the access to functional polythioethers, which carry functional groups at every repeating unit along the polymer backbone. However, most thiiranes are less important and in most cases sporadically used. The following should be understood as an overview on substituted thiiranes.

4.1.5.1 Alkylene sulfides

In 1972, Vandenberg investigated the mechanism aspects of the ring-opening polymerization of *cis*- and *trans*-2-butene sulfide under cationic catalysis. *Cis*-2-butene sulfide formed crystalline racemic diisotactic polymers in asymmetrical synthesis and with coordination catalysts. Polymers obtained with *trans*-2-butene sulfide were nearly amorphous. The obtained results for the analog epoxides were convers. The *cis*-oxides led to amorphous disyndiotactic polymers and the *trans*-oxides yielded *meso*-diisotactic polymers, which were crystalline. The bond between carbon and sulfur is longer and a decreased steric hindrance results, hence an isomer selection at the growing chain end led to less stereoregular polymers in case of the *trans*-form. Different results for the *cis*-forms might occur due to distinguished coordination of the counterion. Polymerization of isobutylene sulfide with cationic catalyst was significantly slower. The formed product consisted of a crystalline and insoluble polymer fraction as well as a soluble and amorphous polymer. The amorphous part was obtained by structural irregularities of head-to-head and tail-to-tail combinations caused by the catalyst. The analog poly(isobutylene oxide) held neither a soluble fraction nor the presence of such irregular combinations.[199]

Furthermore, the polymerization of optically active thiiranes was investigated with different initiators. The results for ethyl thiirane, isopropyl thiirane and *tert*-butyl thiirane were compared to the corresponding oxiranes. Episulfides exhibited more stereospecific reactions compared to the epoxides. In most cases the racemic and optically active polymer had the identical physical properties. Poly(*tert*-butyl thiirane) was an exception, since the crystalline structure as well as the solubility is different and the isolation of the pure enantiomeric polymer was accessible.[200]

In addition, the living anionic polymerization of cyclohexene sulfide with lithium ethane thiolate was described (**Figure 4.30**).[201]

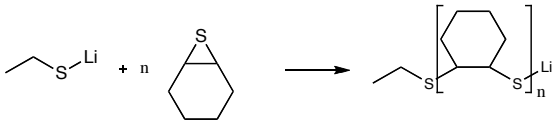

Figure 4.30: Anionic polymerization of cyclohexene sulfide.[201]

This monomer was enabled to polymerize via acyl group transfer polymerization, which is also described for propylene sulfide and phenoxy propylene sulfide.[202]

4.1.5.2 Unsaturated episulfides

The polymerization of vinylthiirane led to a mixture of two polymers with different repeating units. The 1,3-polymer as well as the polymer with the 1,5-repeating unit was formed (**Figure 4.31**).[203] Use of different initiators led to a variation of the ratio between 1,3- and 1,5-product. With ionic catalyst the 1,3-polymer was formed prevalently and with increasing temperature the content of the polymer with 1,3-repeating unit decreased linearly.

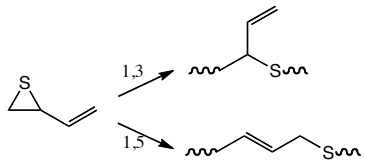

Figure 4.31: 1,3-polymer and 1,5-polymer of vinylthiirane.[203]

Use of a tertiary amine guided to low yield, but the 1,5-polymer was exclusively formed. The ratio of the polymer mixture was shifted towards the 1,3-product at lower temperature and shorter polymerization times.[203]

As a further unsaturated episulfide, norboreadiene episulfide was investigated. Polymerization of this monomer indicated low yields with boron trifluoride etherate and the rearranged structure was favored. Utilization of zinc initiator systems was not satisfying, either the polymerization failed completely or only 5% conversion were detected. In comparison to these results, the polymerization of cyclooctadiene-1,5-monoepisulfide held good conversions with boron trifluoride.[203]

4.1.5.3 Episulfides with heteroatom substituents

Bonnans-Plaisance and Levesque explored the reaction of epichlorohydrin with quaternary ammonium dithiobenzoates. Either the formation of a low molecular weight product or a mixture of different substituted polymers was controlled by temperature and concentration (**Figure 4.32**). Polymerization of methyl- or ethylthiirane results with the same initiating system in the corresponding poly(alkylene sulfides).[204]

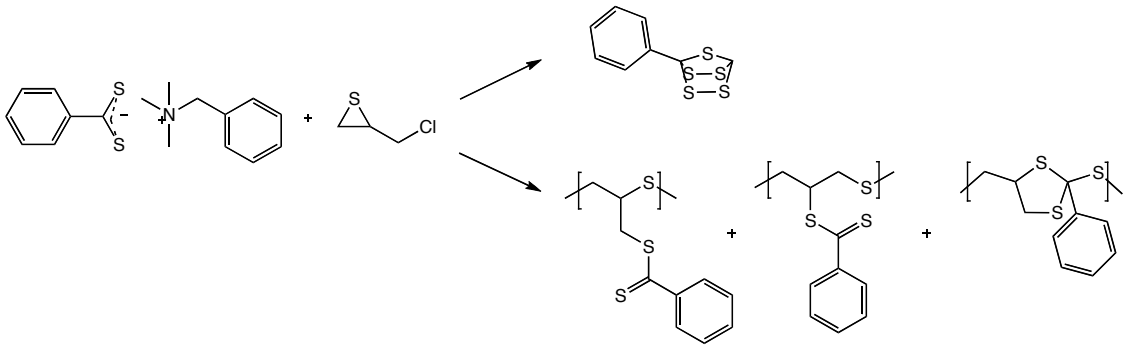

Figure 4.32: Reaction of epichlorohydrin with quaternary ammonium dithiobenzoate.[204]

The cationic ring-opening polymerization of choromethylthiirane with boron trifluoride etherate resulted in expected polymer structure, however a second product was formed by isomerization of the chloromethyl group (**Figure 4.33**).[204,205] Homopolymerization of 2-hydroxymethylthiirane was also introduced by Bonnans-Plaisance and Levesque. They used again benzyltrimethylammonium dithiobenzoate to initiate the ring-opening polymerization of the episulfide monomer. The formed polymer samples consisted of head-to-tail

combinations and were only soluble in highly polar solvents like dimethylformamide and dimethyl sulfoxide. The hydroxyl functionalities along the polymer chain were reacted in an acylation with acetyl chloride or benzoyl chloride to improve the solubility in THF and chlorinated solvents such as dichloromethane and chloroform. The transformation of the hydroxyl groups led to various modifications. Polymerization of the 2-hydroxymethylthiirane was enabled to form high molecular weight polymers and nearly no proton transfer reaction between the hydroxyl functionalities and the thiolate of the growing polymer chains occurs.[180,181]

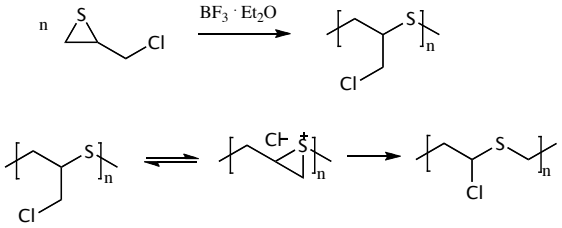

Figure 4.33: Cationic polymerization of epichlorohydrin (top) and isomerization of the formed polymer (bottom).[204,205]

There are several thiiranes with an ether substituent known in literature, the most common one is phenoxy propylene sulfide, which is probably the most famous episulfide beside ethylene sulfide and propylene sulfide. For this monomer the polymerization was conducted with different strategies. The first method was common ring-opening polymerization initiated by a deprotonated thiol. This reaction was carried out in DMF, with a monofunctional initiator (**Figure 4.34**) as well as a trifunctional initiating system to result in star-shaped polymers. The identical trifunctional initiator was used for the ring-opening polymerization of propylene sulfide (compare **Figure 4.7**) and the same reaction conditions were used to polymerize phenoxy propylene sulfide. The synthesized star polymers hold higher glass transition temperatures as the analog star polymers with propylene sulfide. This polymerization was well controlled under the described conditions and led to narrow molecular weight distributions below 1.30.[206]

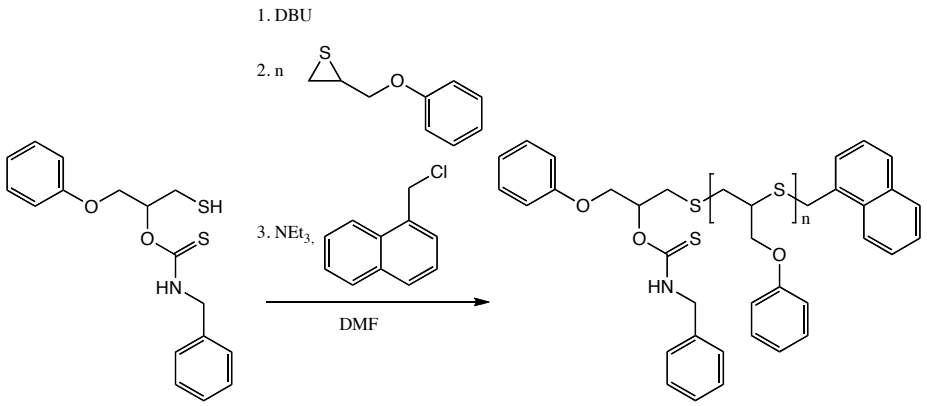

Figure 4.34: Anionic ring-opening polymerization of phenoxy propylene sulfide.[206]

In a following study, phenoxy propylene sulfide was polymerized with the same initiators and in addition with an initiator, which held two thiol functionalities and the polymers were end-capped with 4-chloromethyl styrene. In **Figure 4.35** the structure of the yielded polymer, initiated with the bifunctional starter is shown.[207]

In a second step, these synthesized polymers, cast on a silicon wafer, were crosslinked under photocuring conditions with 10wt% of poly(ethylene glycol) diacryate by UV irradiation. A negative photoresist pattern was formed by the use of a mask for the curing step. A defined patterning of the silicon wafer was observed and the crosslinked polymer film was not soluble in THF anymore after curring.[207]

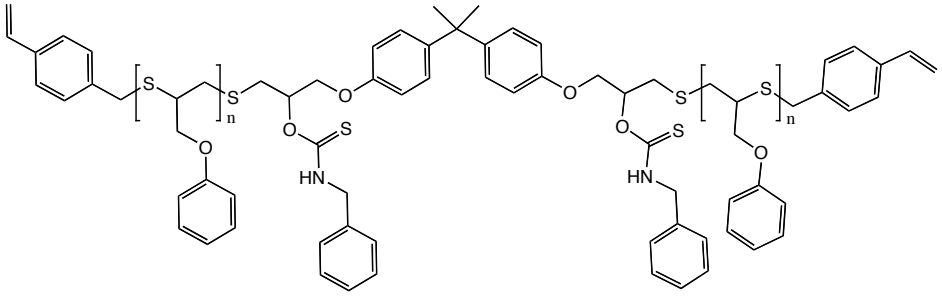

Figure 4.35: Poly(phenoxy propylene sulfide) di-arm star polymer functionalized with 4-chloromethyl styrene.[207]

The second strategy involved an insertion reaction of the thiirane moiety into a thioester bond under catalysis of quaternary salts such as TBAC and TBAB. In 1994, this acyl group transfer polymerization was explored with different thioesters as initiators. *S*-phenyl thioacetate was more effective compared to acyl chlorides like acetyl chloride or dodecanoyl choride. The formed polysulfides were enabled to act again as template for further insertion polymerization. However, a terminal thioester function was mandatory (**Figure 4.36)**.[202,208]

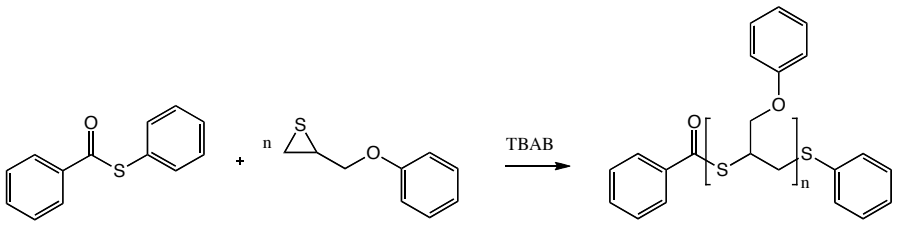

Figure 4.36: Acyl group transfer polymerization of poly(phenoxy propylene sulfide).[202,208]

The continuous insertion reaction was further applied to synthesize poly(phenoxy propylene sulfide) star polymers by the use of calixarenes-based macroinitiators. Four, eight and twelve arm star-shaped polysulfides were generated from the corresponding thioester calixarene derivatives by the insertion of the thiirane moiety into the thioester bond, which was catalyzed by TBAC. The control of the arm-length was straightforward done by means of monomer to macroinitiator ratio (**Figure 4.37)**.[209,210] In addition, the refractive index values of the synthesized star-polymers were investigated. This parameter increased with increasing number and length of the arms as well as with decreasing core size and hence with increasing sulfur content.[209,210]

This reaction principle was used to synthesize cyclic polysulfides via ring-expansion polymerization. Phenoxy propylene sulfide were inserted into a cyclic thiourethane (**Figure 4.38**).[211]

In contrast to the polysulfide of the linear initiators, the polymers with the cyclic starter exhibited at higher monomer to initiator ratios a weak shoulder in the SEC analysis. However, for polymers with molecular masses higher than 7000 g·mol^{-1} the molecular weight control was challenging.[211]

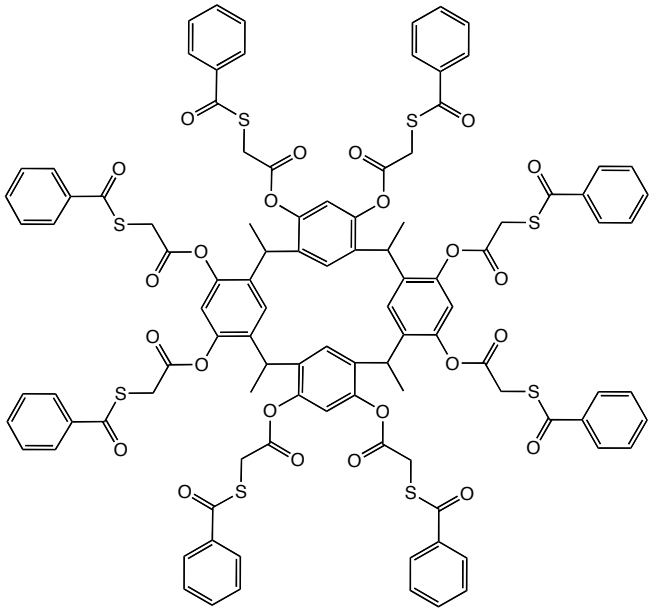

Figure 4.37: Calixarene-based macroinitiator with 8 thioester substituents.[209,210]

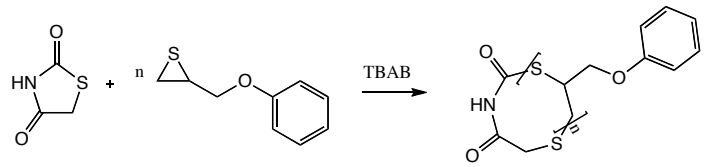

Figure 4.38: Synthesis of cyclic polysulfide via ring-expansion polymerization.[211]

In a further investigation, a cyclic dithioester (**Figure 4.39**) was used as initiator for phenoxy propylene sulfide.[130,212]

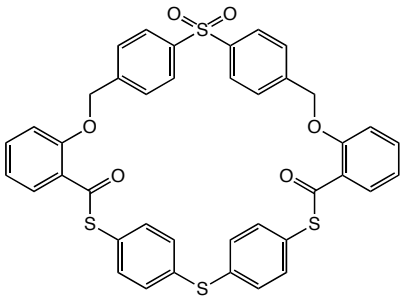

Figure 4.39: Cyclic dithioester as initiator for ring-expansion polymerization.[130,212]

The polydispersity of these polymers increased rapidly after about 90% monomer conversion due to ring-crossover reactions between thioester macrocycles.[130] This reaction was also detected for moieties with two inserted thiiranes[212] or for the initiator[213] itself. The value between the monomer insertion reaction and the thermodynamically controlled side-reaction was influenced by temperature and concentration of the catalyst.[130] The covalent thioester bond was dynamic under catalysis with quaternary onium salts, which was proven by two different linear dithioesters (**Figure 4.40**).[213]

The same reaction took place between thioester containing macrocycles and resulted in larger cycles, which led to high polydispersity indices by the reaction products in SEC.[130,212]

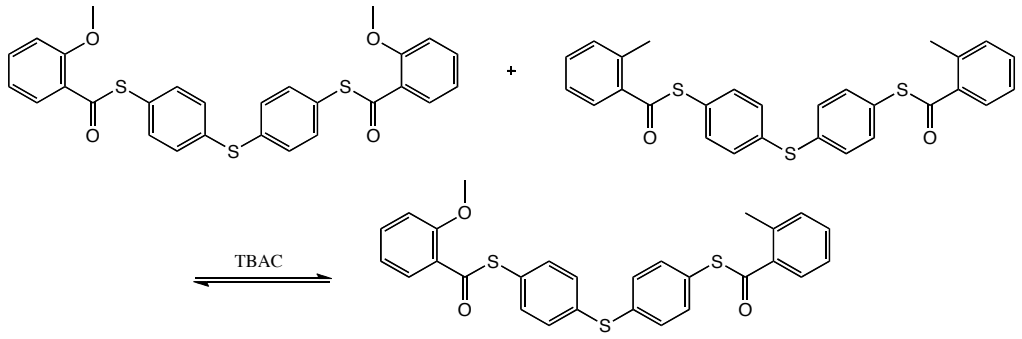

Figure 4.40: Prove of the dynamic covalent thioester bond.[213]

The insertion reaction with 2-(*tert*-butoxymethyl)thiirane and 3-butoxypropylene sulfide as well as propylene sulfide, as mentioned before, gave unsatisfactory results, for example low yields.[130,202,208]
In contrast to these findings, the polymerization of a different ether substituted thiirane, methoxypropylene sulfide, was accomplished under ionic catalysis.[200]
Furthermore, the polymerization of allyloxymethylthiirane was described with different ionic initiator systems. Anionic polymerization was successfully provided with lithium ethane thiolate. In contrast, the reaction with ethyllithium evidenced no polymer formation. These results suggest a significant difference in the chemical reactivity of the allyloxy group and the episulfide ring towards alkyllithium. The authors concluded a faster reaction of the ethyllithium with the allyloxy function, which might involve the formation of hydrogen and a stabilized allylcarbanion.[201] The cationic polymerization initiated with boron trifluoride etherate yielded exclusively the 1,3-polymer, even at higher temperatures.[203]
In 1964, Whistler and Seib introduced the ring-opening polymerization of a sugar episulfide to gain a polysulfide with sugar molecules along the polymer backbone (**Figure 4.41**). Boron trifuoride was used as cationic catalyst and the formed polymer showed a broad molecular weight distribution. At higher temperature and higher monomer concentrations, the formation of an insoluble polymer through a crosslinking reaction increased. However, at moderate temperature the amount of the side-product was rather low.[214]

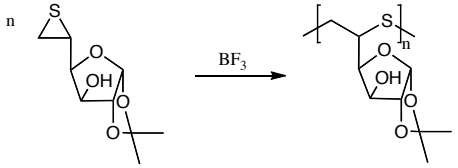

Figure 4.41: Polymerization of the sugar episulfides.[214]

Beside the already mentioned investigation of 2-(hydroxyl)thiirane, Bonnans-Plaisance and Levesque studied its sulfur analog 2-(mercapto)thiirane. In contrast to the hydroxyl thiirane, in the polymerization of mercaptoepisulfide with a dithiobenzoate the chain transfer of the thiol function and the living end-group of the polymer was dominant. The homopolymerization of mercaptothiirane was enabled in DMF, but a broad polydispersity as well as a decreased polymerization rate occurred. Furthermore, the post-polymerization modification of the free thiol functionality along the polymer backbone either with acetyl chloride, 1-methoxy-2-methyl-1-trimethyl-siloxypropene or methyl iodide led in high percentage or exclusively to crosslinked polymers, due to dialkyl sulfide formation of two thiol groups. Solely, the alkylation with benzyl chloride was successfully affected. The polymerization of protected mercaptothiirane, for example (benzylthio)methylthiirane, was successfully achieved and exhibited high polymerization rate, because the

chain transfer was suppressed.[181,182] In a follow-up study, the synthesis and polymerization of a methyl(2,3-epithiopropylthio) ethanoate was introduced. Use of mono- or dithiobenzoates as initiators enabled the polymerization of the thiirane without the attack of the carboxylate function. Cleavage of the ester groups along the polymer backbone via saponification rapidly led to polyacids (**Figure 4.42**).[215]

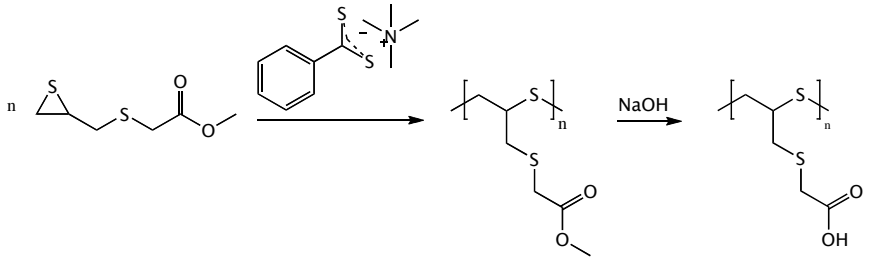

Figure 4.42: Polymerization of methyl(2,3-epithiopropylthio) ethanoate and saponification.[215]

Bonnans-Plaisance et al. further described the use of an episulfide with a polyether side-chain as macromonomers. A short PEG chain with a different number of repeating units with up to seven and a methoxy end-group was bond to the thiirane via either an ester connection or an ether linkage. In addition, bis-macromonomers with three or four ethylene glycol units were used for the investigation of hydrogels.[216] In a follow-up study, the synthesis of the macromonomers was enlarged to sixteen monomer units and a methoxy end-group in the polyether side-chain. Besides the homopolymers of these monomers, copolymers consisting of the macromonomer and propylene sulfide as well as macromonomers with different PEG chain lengths were synthesized. The resulting copolymers exhibited a comb-like structure and an amphiphilic behavior with a low critical micelle concentration. They were enabled to act as surfactants and the surface tension of the synthesized materials was investigated in more detail, which was lowered for all homopolymers. Although copolymers with propylene sulfide hold a larger hydrophobic polymer backbone, the surface tension of these materials did not show a significant change. In contrast, copolymers with longer alkyloxy chains as end-group of the PEG side-chain decreased the surface tension significantly. **Figure 4.43** shows the explored copolymers.[217]

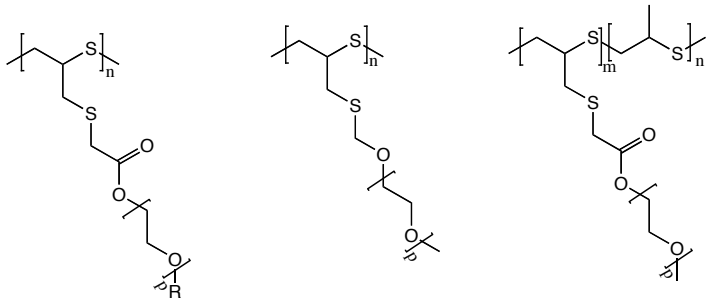

p = 4, 7, 16 R = CH_3

p = 10 R = $C_{12}H_{25}$, $C_{18}H_{37}$

p = 20 R = $C_{16}H_{33}$

p = 3, 4

p = 7, 16

Figure 4.43: Synthesized polysulfide copolymers with PEG side-chains.[216,217]

In addition, the hydrolysis of these comb-like copolymers was explored under different conditions. These structures exhibit either a monothioacetal or an ester function. Solely under strong acidic conditions the monothioacetal was cleaved to result in copolymers with various thiol functionalities (**Figure 4.44**). The use

of a buffered solution led to cleavage of the ester function in basic and acidic media, resulting in the polyacid (compare to **Figure 4.42**).[218]

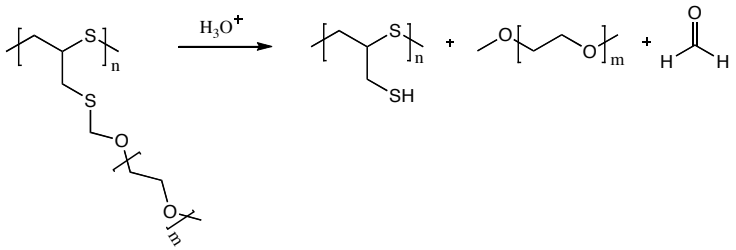

Figure 4.44: Synthesized polysulfide copolymers with PEG side-chains.[218]

4.1.5.4 Polysulfides with liquid crystalline side-chains

In 1993, the first synthesis for polysulfides with biphenyl groups was published. Two different thiiranes with biphenyl groups were synthesized and polymerized via ring-opening mechanism catalyzed by dithiobenzoate (**Figure 4.45**). The substituted episulfides were synthesized from 2-(mercapto)thiirane and the corresponding biphenyl bromide derivative.[219]

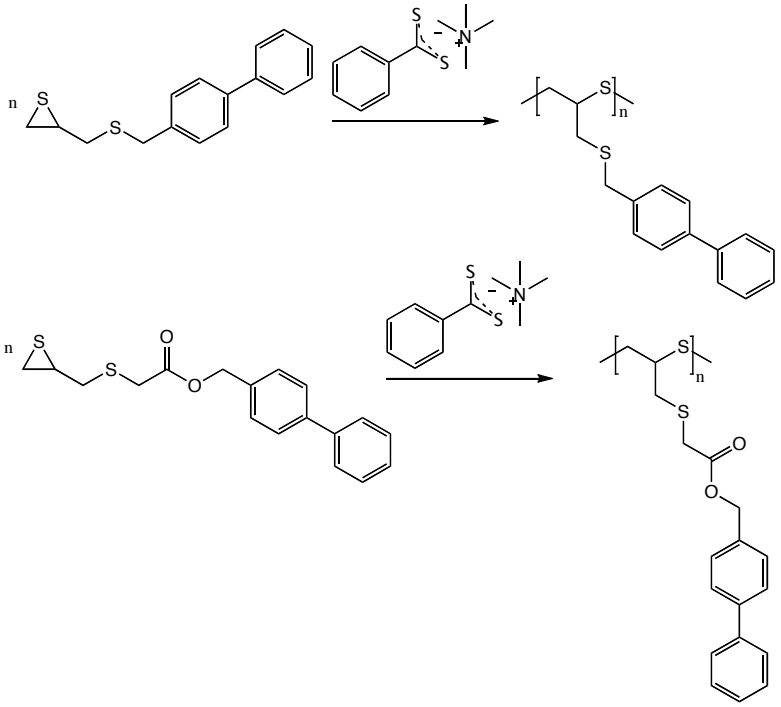

Figure 4.45: Synthesized polysulfide with biphenyl side-chains.[219]

Unsubstituted molecules such as biphenyl showed rarely liquid crystalline behavior, hence the structure of the side-chain was varied. Liquid crystalline polysulfides with different biphenyl and 4-alkoxybiphenyl side-chains were successfully synthesized, although long and flexible spacer groups such as oxyethylene between the polythioether backbone and the mesogene were necessary. The obtained materials built highly ordered smectic mesophases shown by polarized optical microscope. In **Figure 4.46** is one polymer shown as an example.[220] In addition, the characteristics of these liquid crystalline polymers were further investigated.[221]

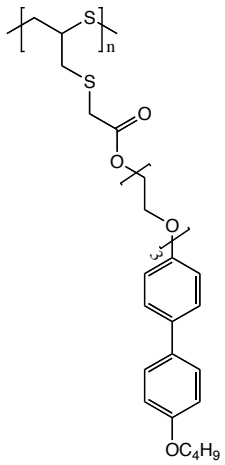

Figure 4.46: Synthesized polysulfide with 4-alkoxybiphenyl side-chains, which exhibited liquid crystalline behavior.[220]

Furthermore, low molecular mass alkoxy stilbene units were attached to a thiirane to result in enantiotropic liquid crystalline polymers after ring-opening polymerization (**Figure 4.47**).[222]

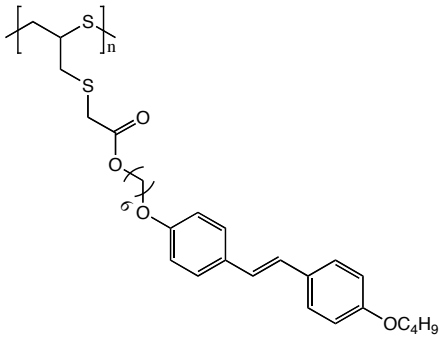

Figure 4.47: Synthesized polysulfide with 4-alkoxy stilbene side-chains, which exhibited liquid crystalline behavior.[222]

In a more recent work, the synthesis of a polyepichlorohydrin-based liquid-crystalline polymer was presented. This approach used a different preparation method, chloromethylthiirane was polymerized under cationic catalysis of boron trifluoride etherate and 4-methoxyazobenzene derivative as mesogene was attached to the polymer backbone in a post-polymerization modification (**Figure 4.48**). These liquid crystalline copolymers exhibited a nematic phase.[204]

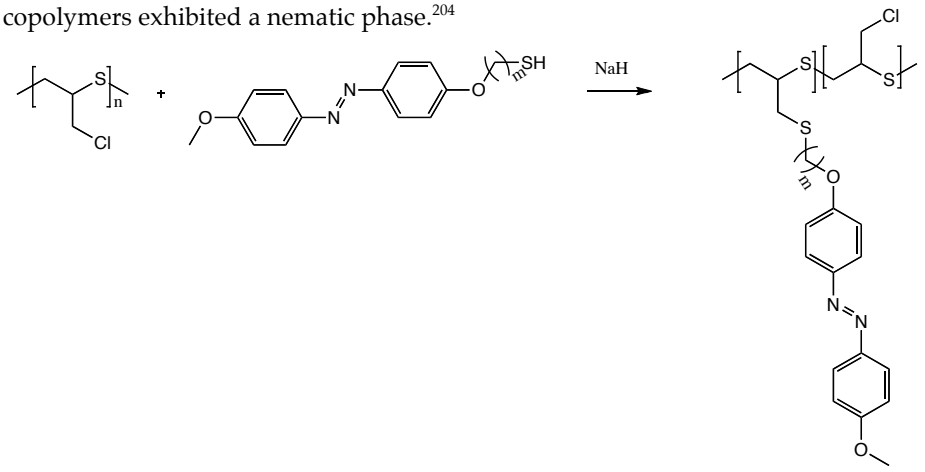

Figure 4.48: Polyepichlorohydrin-based liquid-crystalline polymer. [204]

4.2 Motivation for the work carried out in this thesis

The aim of this project was the use of several polyglycerol-based macroinitiators for the anionic ring-opening polymerization of ethylene sulfide and propylene sulfide. This concept is based on two publications of our group, showing the use of hyperbranched polyglycerol as a macroinitiator for ethylene oxide and glycolide. These "grafting-from" approaches led to multi-arm star polymers with interesting properties, which were different from the properties of their linear homologs.[223,224]

This thesis aims at extending the portfolio of polysulfides regarding various novel and complex polymer-architectures. To this end, various polyglycerol-based polyether homo- or copolymers were converted into initiators for episulfides. The structures of the macroinitiators were based on linear polyglycerol (*lin*PG) and hyperbranched polyglycerol (*hb*PG), poly(ethylene glycol)-poly(allyl glycidyl ether) (PEG-PAGE) as well as poly(allyl glycidyl ether)-poly(ethylene glycol)-poly(allyl glycidyl ether) (PAGE-PEG-PAGE). The formed macroinitiators exhibited between seven and thirty-six initiation groups for thiirane polymerization and the architecture of the synthesized copolymers ranged from star-shaped over brush-like to comb-like and pom-pom structures. Thus, a library of defined graft copolymers with ethylene sulfide and propylene sulfide homopolymers as well as random copolymers with different molecular weights and numbers of side-chains were synthesized. An additional target was the synthesis of tailored poly(ethylene sulfide) containing copolymer moieties, which are soluble in common organic solvents and well processible.

The structure of the obtained materials has been characterized via IR- as well as NMR-spectroscopy and SEC, furthermore, the thermal behavior was analyzed with DSC-measurements and the different architectures were compared among each other. In addition, the corresponding linear polysulfides have been synthesized as a comparison and benzyl thioacetate acted as initiator.

In a second step, the synthesized polysulfides are attached to the surfaces of gold nanoparticles and bare gold substrates. The surface of the coated gold supports has been analyzed with AFM and the wettability was measured with a contact angle goniometer. The absorption of the polymer-coated gold nanoparticles was characterized via UV-vis spectroscopy.

4.3 Synthesis of different polyglycerol-based thioacetates

Common polymerization of episulfides requires a thiolate to initiate the reaction. Hence, the polyglycerol-based copolymers were converted into multifunctional macroinitiators with terminal thioacetate groups as protected thiols. The use of protected thiols was described in literature and was chosen to avoid impurities of disulfides in the polymerization. Disulfides were not capable of initiating the thiirane polymerization, which changed the calculated monomer to initiator ratio and thus the targeted molecular weights of the products. Furthermore, disulfides led to undesired side-reactions such as end-capping and chain-transfer reactions of the growing polymer backbone, which resulted in a product mixture of polymers with different lengths and terminal groups, as mentioned before (compare **Figure 4.8**).[126]

The synthesis of the macroinitiators was based on the protocol introduced by the Tirelli group. The hydroxyl functions of the linear and hyperbranched PGs were converted into allyl groups with allyl bromide in a two-step protocol. Subsequently, the allyl groups were reacted with thioacetic acid in a thiol-ene reaction catalyzed by AIBN (**Figure 4.49a**,**b**).[128]

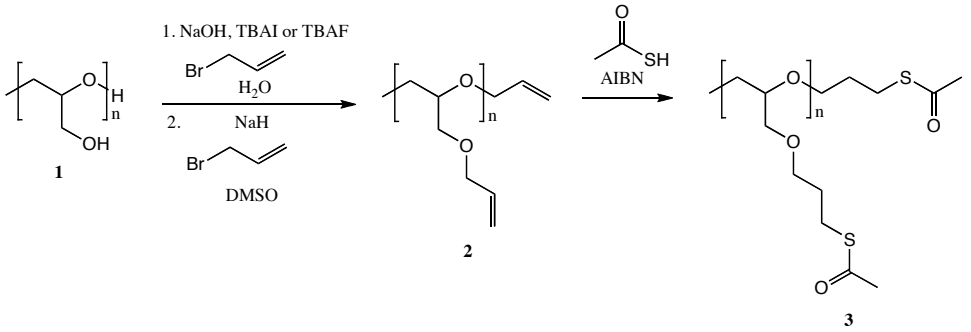

Figure 4.49a: Transformation of *lin*PG into a macroinitiator for episulfides.

The crucial point of this synthesis was the complete conversion of hydroxyl groups into allyl groups. This was enabled in two reaction steps. The first step was the reaction of the polyether polyol moieties (**1**, **4**) and allyl bromide under basic conditions in water supported by a phase-transfer catalyst.[225] The achieved conversion amounted to 50-75% of the hydroxyl groups in the phase transfer catalysis. In the second step, the use of dimsyl sodium as a strong base enabled complete allylation of the polyglycerol.[238] Complete conversion of the hydroxyl groups was confirmed via IR-spectroscopy. Subsequently, the allyl groups were reacted with thioacetate in an AIBN catalyzed thiol-ene reaction in THF.[128]

Several linear and hyperbranched polyglycerols with different molecular weights and thus different number of hydroxyl functionalities were converted to polyglycerol thioacetates (**3**, **6**) by using the shown strategy. Various polyglycerol-based macroinitiators for anionic polymerization of episulfides with a different number of initiating groups were obtained. The post-polymerization modification was successful, which was controlled with IR- and NMR-spectroscopy. The synthesized macroinitiators were further analyzed via SEC, and the results are summarized in **Table 4.1**.

In total, four different *lin*PGs were transformed into macroinitiators with nine, seventeen, eighteen and thirty-six initiating groups as well as four *hb*PG samples to moieties with seven, nine, eighteen and twenty-two terminal thioacetate groups. The hyperbranched macroinitiator **Hb 3** and **Hb 4** were based on the same precursor molecule, while only 82% of the allyl groups of **Hb 3** were converted to thioacetates functionalities and it exhibited eighteen instead of twenty-two initiating groups. The polydispersity indices of the received macroinitiators ranged from 1.09 to 1.58. The PDIs of the hyperbranched polymers were slightly higher compared to the linear samples, except for macroinitiator **Li 4**.

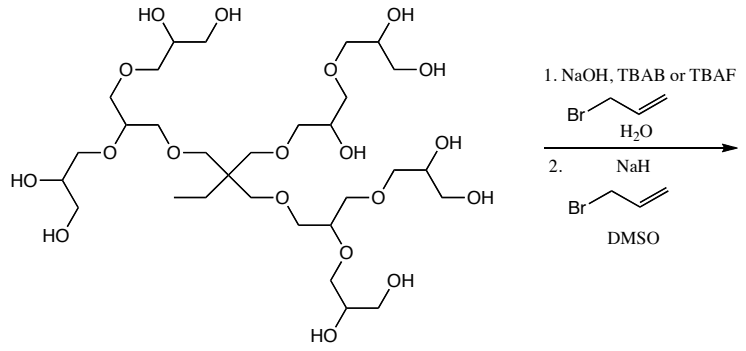

4

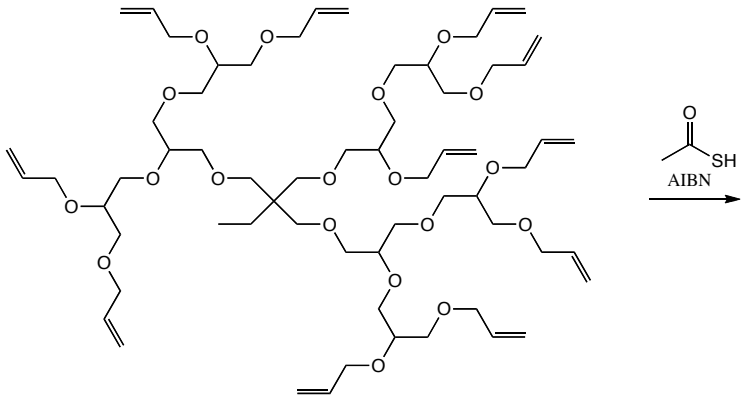

5

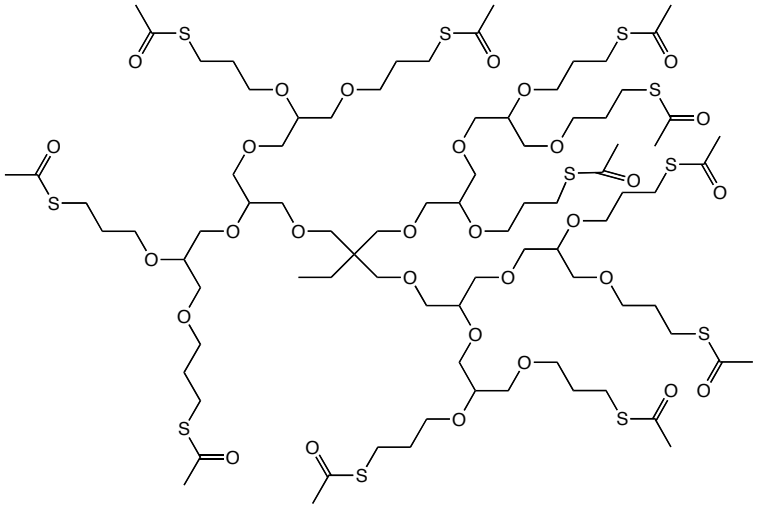

6

Figure 4.49b: Transformation of *hb*PG into a macroinitiator for episulfides.

Table 4.1: Summary of the synthesized polyglycerol-based macroinitiators.

	Precursor		Macroinitiator			
	Architecture	$\overline{M_n}$ (^{1}H NMR) [g·mol^{-1}]	Thioacetates per molecule	$\overline{M_n}$ (^{1}H NMR) [g·mol^{-1}]	$\overline{M_n}$ (SEC)* [g·mol^{-1}]	PDI (SEC)*
Li 1	*lin*	700	9	1750	1950	1.20
Li 2	*lin*	1300	17	3250	1500	1.23
Li 3	*lin*	1350	18	3450	4400	1.09
Li 4	*lin*	2700	36	6900	3400	1.58
Hb 1	*hb*	750	7	1700	900	1.49
Hb 2	*hb*	800	9	1850	1500	1.31
Hb 3**	*hb*	2650	18	5400	3600	1.43
Hb 4	*hb*	2650	22	5600	4400	1.28

*SEC: eluent: THF; polystyrene standard calibration; **82% of the allyl groups were converted into thioacetate groups

The use of poly(ethylene glycol)-poly(allyl glycidyl ether) di- and triblock-copolymers enabled the thiol-ene reaction immediately (**Figure 4.50a**,**b**).

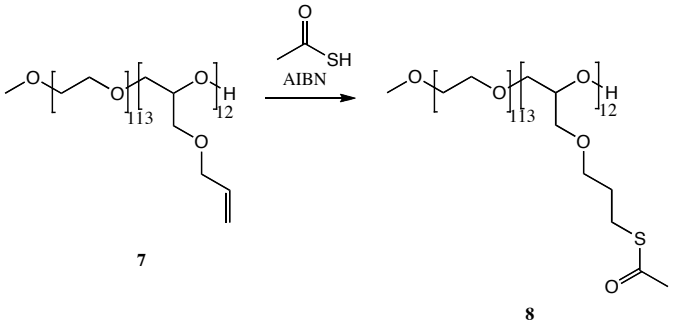

Figure 4.50a: Transformation of a PEG-PAGE block-copolymer into a macroinitiator for episulfides.

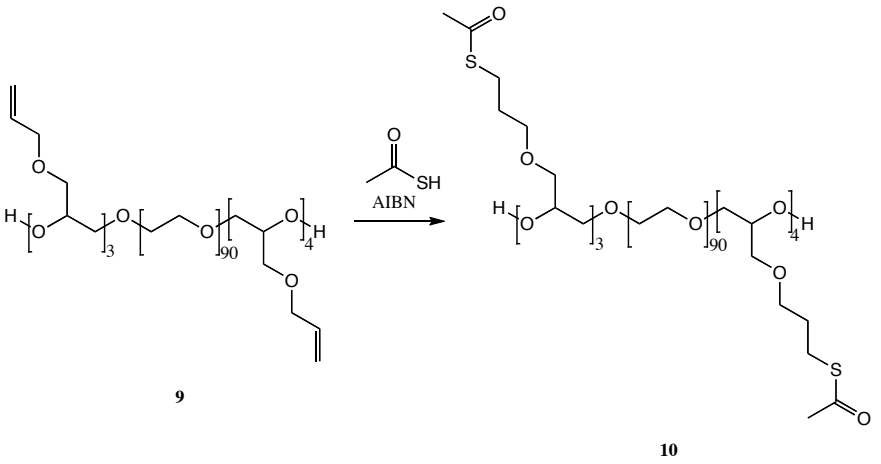

Figure 4.50b: Transformation of a PAGE-PEG-PAGE triblock-copolymer into a macroinitiator for episulfides.

The thiol-ene reaction of the PEG-PAGE copolymers was conducted similarly to the polyglycerol samples. This PEG-PAGE block-copolymer (**7**) exhibited after conversion twelve thioacetate groups, the PEG block contained 113 monomer units and thus a molecular weight of 5000 g·mol^{-1}. The PAGE-PEG-PAGE triblock-copolymer (**9**) consisted of seven initiating groups on average, of which three and four thioacetates, respectively, were at each terminal end of the PEG block, which implied ninety monomer units and thus a molecular weight of 4000 g·mol^{-1}. Its PDI was narrow, i.e., below 1.10 in both cases. The results are summarized in **Table 4.2**.

Table 4.2: Summary of the synthesized PEG-PAGE-based macroinitiators.

	Precursor		**Macroinitiator**			
	Architecture	$\overline{M_n}$ (SEC) [g·mol^{-1}]	Thioacetates per molecule	$\overline{M_n}$ (^{1}H NMR) [g·mol^{-1}]	$\overline{M_n}$ (SEC)* [g·mol^{-1}]	PDI (SEC)*
PEG I	diblock	6000	12	7300	6300	1.06
PEG II	triblock	4000	7	5300	4700	1.09

*SEC: eluent: DMF; PEG standard calibration

4.3.1 Synthesis of different polyglycerol-based thiols

In addition, the mentioned post-polymerization modification of the polyethers might be used as an alternative to convert hydroxyl functions into thiol groups of different polyether moieties. This method was already described for several substances, for example for PEG, as mentioned before.[153,226,227] The thioacetates are cleavable under basic conditions and the resulting thiolates were protonated under acidic conditions afterwards. Thus the direct and full thiolation of hyperbranched and linear polyglycerol was enabled in four steps. The use of PAGE did not effect the allylation of *lin*PG and the generation of multiple thiol functionalities along the polymer backbone was achievable in two steps. Thiolation of poly(ethylene glycol)-poly(allyl glycidyl ether) di- and triblock-copolymers was possible in two steps.

Table 4.3: Summary of the synthesized polythiols.

	Precursor			**Polythiol**	
	Polythioacetate	$\overline{M_n}$ (SEC)* [g·mol^{-1}]	PDI (SEC)*	$\overline{M_n}$ (SEC)** [g·mol^{-1}]	PDI (SEC)**
Hb 2-SH	Hb 2	1200	1.53	1600	2.60
Hb 4-SH	Hb 4	4400	1.28	3900	2.50
Li 3-SH	Li 3	4400	1.09	4500	2.20
Li 4-SH	Li 4	3400	1.58	6000	4.75
PEG I-SH	PEG I	6300	1.06	6600	1.19
PEG II-SH	PEG II	4700	1.09	4700	1.10

*SEC: PEG: eluent: DMF; PEG standard calibration; PG: eluent: THF; polystyrene standard calibration

**SEC: eluent: DMF; PEG standard calibration

Cleavage of the different synthesized polythioacetates was conducted as proof of principle experiment, and the results are summarized in **Table 4.3**. The successful synthesis of the different polythiols was proven via a reaction that was specific for thiols,[228] and in addition with NMR-spectroscopy. The obtained materials were also analyzed with SEC, showing rather broad polydispersity for the PG-based polymers. The chromatograms exhibited bimolecular distributions due to the intermolecular formation of disulfide bonds under air contact. In contrast, the SEC of the converted PEG-PAGE-based copolymers showed only a slight peak broadening. Apparently the PEG block prevented rapid dimerization to disulfides. However, during the characterization the exposure to air was unavoidable.

For the thiolation of hyperbranched polyglycerol different approaches were described in literature. The Haag group introduced a protocol that requires first the conversion of the terminal hydroxyl functions of the *hb*PG into amine groups. Subsequently these amine groups were reacted with 3-(tritylthio)propionic acid, 2-iminothiolane or acetyl-thiopropionic acid, respectively. In all cases thiol groups were generated at the terminal position and 2-iminothiolane was described to afford the best results. However, these techniques yielded internal amides or imidamides, respectively. In total, this synthetic approach needed four or five steps, respectively, and it should be noted, that only 20% of the hydroxyl groups of the PG were converted in this study.[229] In a second publication, *hb*PG was reacted with 3-mercaptopropanic acid to gain thiol functionalities. In one reaction step 65% of the hydroxyl groups of the precursor were converted and an ester function was formed.[230] Different copolymer structures with a PEG backbone and thiol groups have been also known. However, the thiol functionalities were bond similarly via ester or amide linkers to the polymer.[231]

The named linker groups such as ester, amide and imidamide might interfere in a subsequent reaction or application and furthermore, thiols tend to oxidize to disulfides upon exposure to air. The novel protocol introduced in this thesis to synthesize different polyglycerol-based macroinitiators, might represent an alternative to generate thiol functionalities via transformation of polyether moieties. This approach implied the benefit of full conversion of the hydroxyl functions to thiol groups and the cleavage might be realized immediately before use under inert gas to avoid disulfide formation.

4.4 Polyglycerol-based polysulfides

The synthesized linear and hyperbranched polyglycerol-based macroinitiators were used to obtain novel polysulfide topologies with different architectures, with different episulfides, variable number of side-chains and various block lengths. The use of *lin*PG-based macroinitiators led to polymer brushes and the *hb*PG-based starters were used to generate star-shaped graft polymers (**Figure 4.51**).

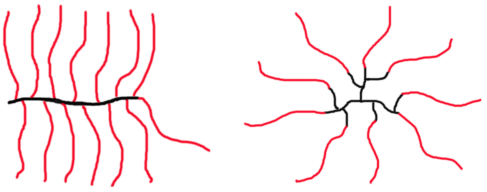

Figure 4.51: Scheme of PG-polysulfide copolymers with different architectures (red = polysulfide; black = PG) (left: brush copolymers from *lin*PG; right: star copolymers with *hb*PG core).

4.4.1 Polyglycerol-based poly(propylene sulfide)

Anionic ring-opening polymerization of propylene sulfide with polyglycerol-based macroinitiators was conducted under the conditions of the improved protocol of the Tirelli group.[128] The thioacetates (**3**, **6**) were cleaved *in-situ* with sodium methoxide solution, and the polymerization was conducted in THF under argon atmosphere with tributylphosphine (TBP) as a reduction agent to avoid disulfide formation during the polymerization. After the polymerization of propylene sulfide, the reaction mixture was buffered with acetic acid as well as DBU. Subsequently, ethyl bromoacetate as an end-capping reagent was introduced to obtain polyglycerol-poly(propylene sulfide) copolymers (**11**, **12**). **Figures 4.52a** and **b** show the polymerization of propylene sulfide with linear and hyperbranched PG-based macroinitiators.

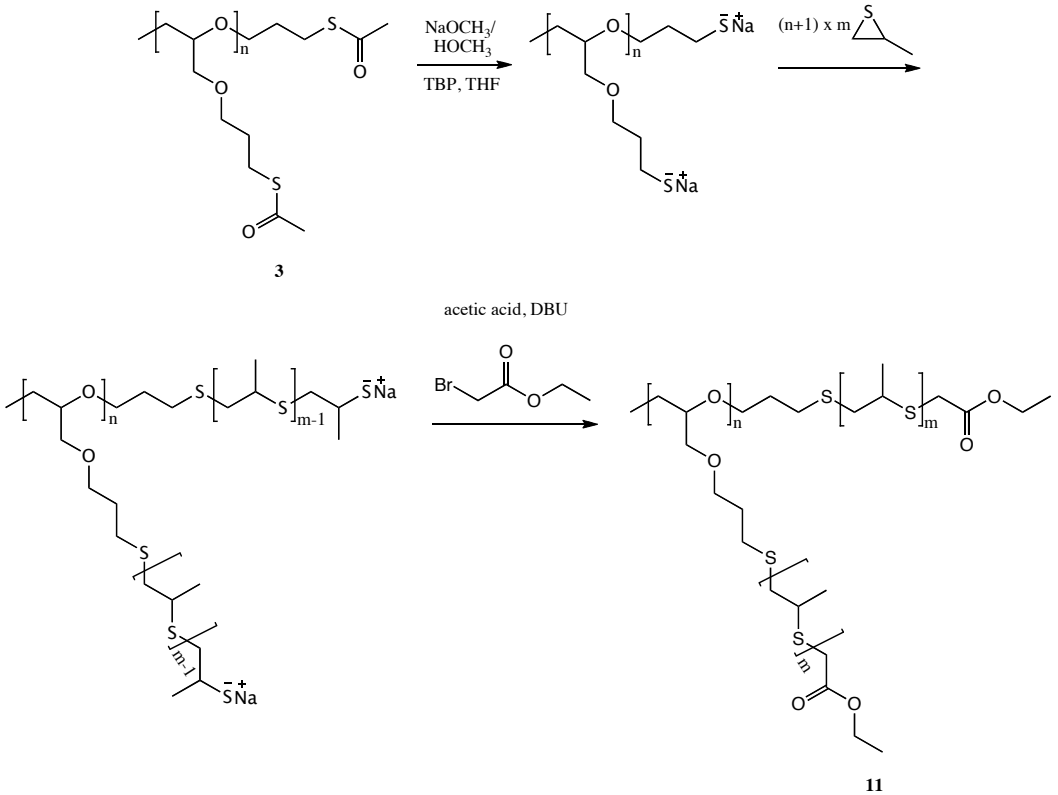

Figure 4.52a: Polymerization of PS with *lin*PG-based macroinitiator to polymer-brushes.

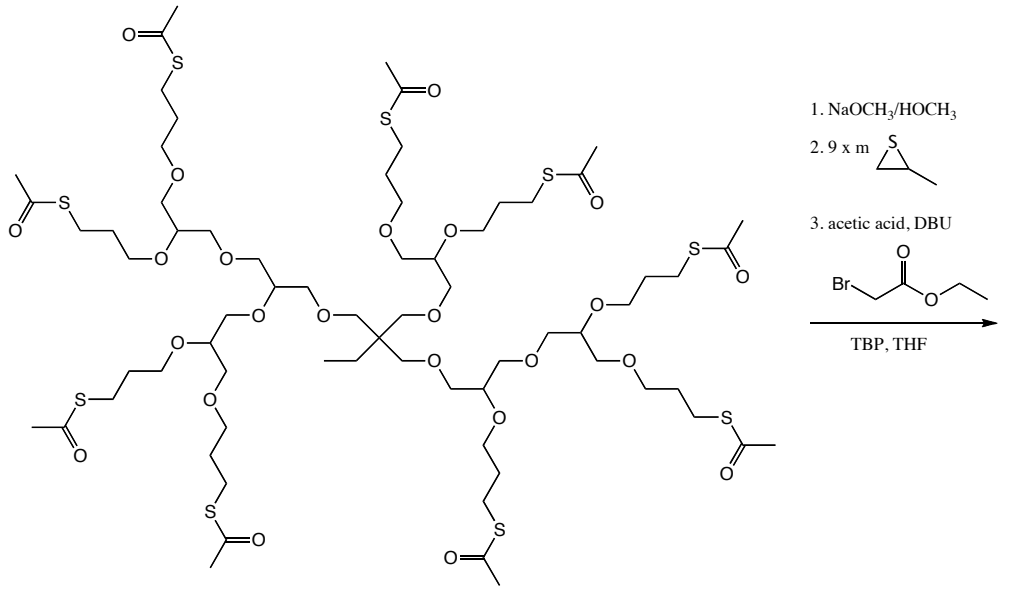

6

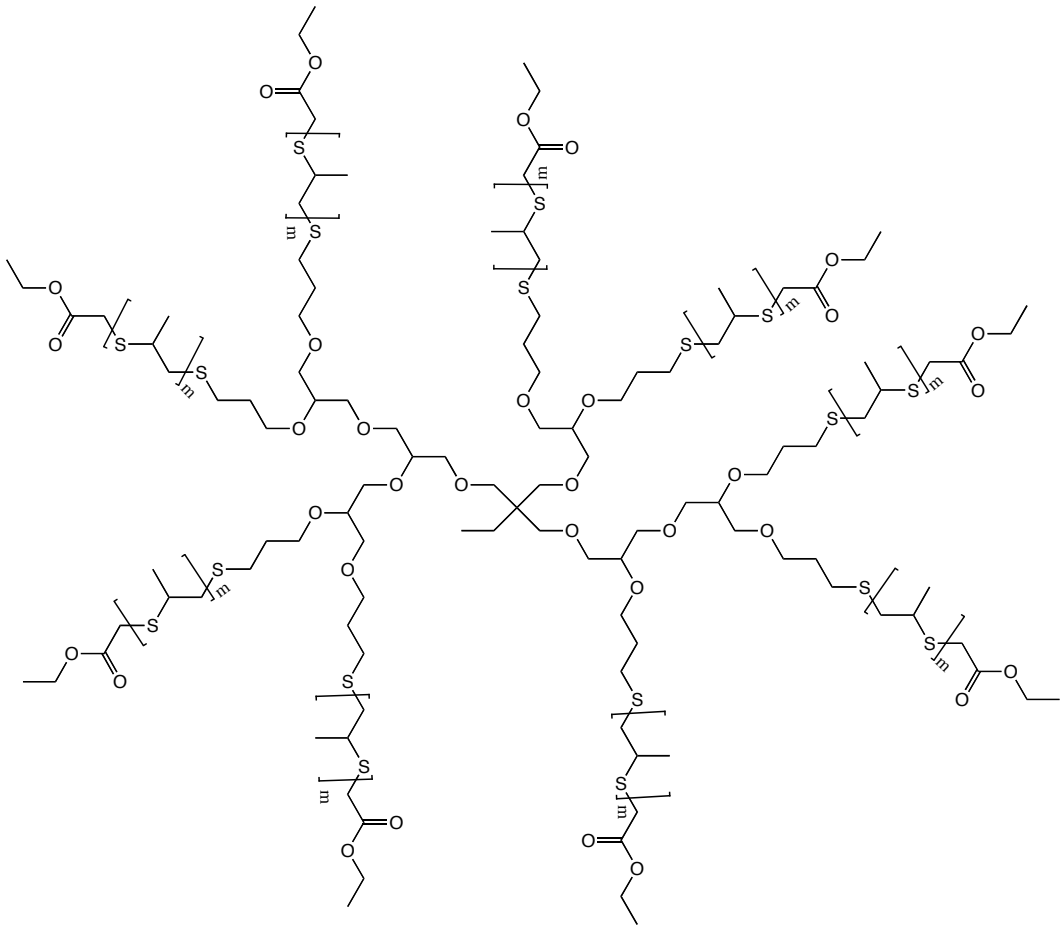

12

Figure 4.52b: Polymerization of PS with *hb*PG-based macroinitiator to star polymers.

Several PG-based macroinitiators were used and the degree of polymerization (DP) was varied from ten over twenty and thirty to forty per initiating group. The SEC traces of macroinitiator **Hb 1** and the corresponding graft polymers are shown in **Figure 4.53** as an example. The obtained copolymers exhibited a low molecular weight by-product, which was formed in all polymerizations. Formation of the side-product was independent of the architecture and the number of initiating groups of the used macroinitiator. While in case of a macroinitiator with higher molecular weight such as **Li 4**, the low molecular side-product was smaller than macroinitiator in SEC (**Figure 4.54**). The amount of the side-product increased with increasing DP and thus an increasing monomer to initiator ratio.

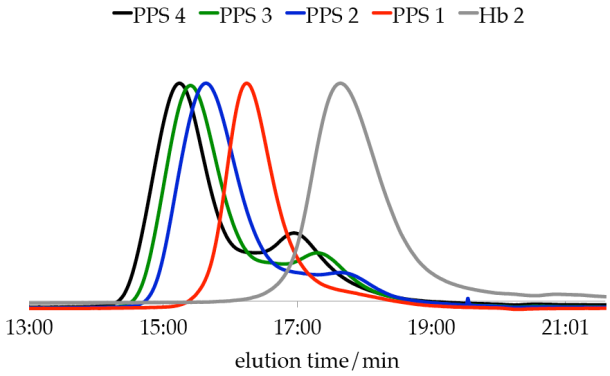

Figure 4.53: SEC traces (eluent: THF; polystyrene standard calibration) of macroinitiator **Hb 2** and corresponding PG-PPS graft copolymers **PPS 1-4** (DP 10-40 per thioacetate).

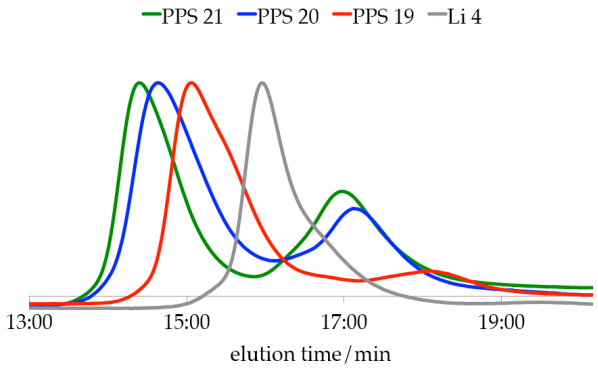

Figure 4.54: SEC traces (eluent: THF; polystyrene standard calibration) of macroinitiator **Li 4** and corresponding PG-PPS graft copolymers **PPS 19-21** (DP 10-30 per thioacetate).

Due to the undesired second mode, different reaction conditions were investigated to optimize the polymerization and to obtain a product with monomodal distribution. The results of several graft-copolymerizations of propylene sulfide under different conditions are summarized in **Table 4.4**. The weight percentages of the targeted copolymer and the low molecular by-product were analyzed via Gaussian fits of the peak areas of the SEC traces, which is shown in **Figure 4.55** as an example.

These results were used to evaluate the different reaction conditions. The described method led to 30-50 percentage of the low molecular side-product. Variation of the temperature did not improve the distribution of the polymerization product, neither lower temperature (0 °C) nor higher temperature (45 °C). In further approaches the influence of the reduction agent was investigated. The addition of water, which was essential for the reductive effect of TBP, did not improve the polymerization.

Table 4.4: Summary of the synthesized polyglycerol-poly(propylene sulfide) copolymers.[a]

	Macroinitiator	Theoretical DP (per thioacetate)	$\overline{DP_n}$ (^{1}H NMR)	End-capping yield (^{1}H NMR) [mol%]	Peak 1			Peak 2	
					Amount* [%wt.]	$\overline{M_n}$ (SEC)** [g·mol^{-1}]	$\overline{DP_n}$	Amount* [%wt.]	$\overline{M_n}$ (SEC)** [g·mol^{-1}]
PPS 1	Hb 2	9 x 10	9 x 11	100	69	5100	9 x 6	31	-
PPS 2	Hb 2	9 x 20	9 x 21	76	67	10500	9 x 14	33	1600
PPS 3	Hb 2	9 x 30	9 x 30	79	62	15300	9 x 21	38	2500
PPS 4	Hb 2	9 x 40	9 x 38	81	61	18600	9 x 26	39	3000
PPS 5	Hb 2[b]	9 x 30	9 x 30	74	60	13000	9 x 18	38	2350
PPS 6	Hb 2[b]	9 x 40	9 x 41	64	55	18100	9 x 26	45	3000
PPS 7	Hb 2[e]	9 x 30	9 x 38	81	74	17100	9 x 24	26	2600
PPS 8	Hb 3	22 x 10	22 x 10	73	65	11850	22 x 7	35	2400
PPS 9	Hb 3	22 x 20	22 x 16	66	56	14900	22 x 9	44	2250
PPS 10	Hb 3	22 x 30	22 x 20	65	60	18900	22 x 12	40	2200
PPS 11	Hb 3[g]	22 x 30	22 x 25	72	57	21300	22 x 14	25	2900
PPS 12	Li 1	9 x 30	9 x 38	65	60	19000	9 x 26	40	2750
PPS 13	Li 1[c]	9 x 30	9 x 11	90	56	5300	9 x 6	44	-
PPS 14	Li 1[c,o]	9 x 30	9 x 18	64	60	11600	9 x 15	40	1600
PPS 15	Li 1[j]	9 x 30	=	=	=	=	=	=	=
PPS 16	Li 1[k]	9 x 30	9 x 29	64	59	15100	9 x 20	41	1650
PPS 17	Li 1[n]	9 x 30	9 x 27	72	58	18100	9 x 25	42	2500
PPS 18	Li 1[k,n]	9 x 30	9 x 34	51	55	19300	9 x 27	45	3400
PPS 19	Li 4	36 x 10	36 x 12	87	60	16500	36 x 4	40	1600
PPS 20	Li 4	36 x 20	36 x 27	79	51	29800	36 x 9	49	3250
PPS 21	Li 4	36 x 30	36 x 30	74	50	37500	36 x 12	50	3500
PPS 22	Li 4[d]	36 x 30	36 x 36	62	38	34000	36 x 11	62	3300
PPS 23	Li 4[m]	36 x 30	36 x 26	58	50	34000	36 x 11	50	3700
PPS 24	Li 4[g,o]	36 x 30	36 x 37	38	32	34300	36 x 11	68	3100
PPS 25	Li 4[f,r]	36 x 30	36 x 42	44	39	37700	36 x 12	58	3700
PPS 26	Li 4[g,r]	36 x 30	36 x 21	58	36	30300	36 x 9	64	2500
PPS 27	Li 4[g,p]	36 x 30	36 x 32	73	38	42300	36 x 14	62	3800
PPS 28	Li 4[h,q]	36 x 30	36 x 39	77	41	40700	36 x 13	59	3000
PPS 29	Li 4[i,o]	36 x 30	36 x 49	92	41	50600	36 x 17	59	5550
PPS 30	Li 4[l]	36 x 30	36 x 37	100	40	36000	36 x 12	60	3300

*peak area calculated via a Gaussian fit of the SEC trace; **SEC: eluent: THF; polystyrene standard calibration

[a] Unless otherwise indicated, the polymerizations were carried out with TBP (5-fold molar excess in comparison to thioacetates), sodium methoxide added all before the polymerization, room temperature, 45 minutes reaction time.

[b] T = 45 °C.

[c] T = 0 °C.

[d] different bottle of TBP.

[e] Reducing agent: $NaBH_4$.

[f] 30% sodium methoxide solution was added before polymerization

[g] 30% sodium methoxide solution was added before polymerization and 70% afterwards.

[h] 15% sodium methoxide solution was added before polymerization and 85% afterwards.

[i] 50% sodium methoxide solution was added.
before polymerization and 50% afterwards.

[j] H_2O (5-fold molar excess in comparison with TBP) added before polymerization.

[k] H_2O (same molar ratio than TBP) added before polymerization.

[l] Sodium methoxide (1,5-fold molar excess in comparison to thioacetates).

[m] 50% more solvent.

[n] THF distillated before use (NaK-alloy).

[o] reaction time: 3 hours.

[p] reaction time: 6 hours.

[q] reaction time: 16 hours.

[r] reaction time: 18 hours.

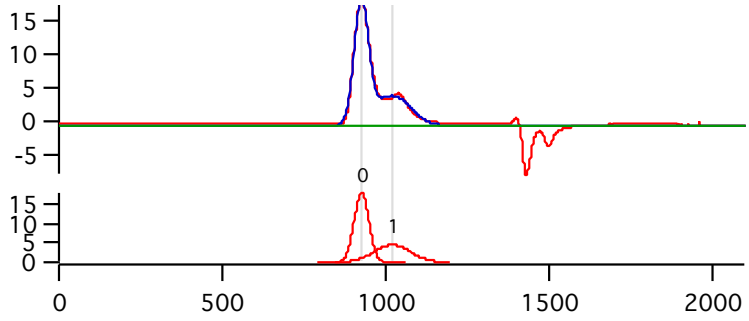

Figure 4.55: Exemplary Gaussian fit on the SEC trace to determine the peak area and hence the amount of the by-product.

Furthermore, a different TBP batch and a stronger reduction agent such as sodium borohydride were used, but neither of them influenced the reaction course positively to minimize the undesired mode. Hence, the by-product is most probably not caused by disulfide formation.

The used PG-based macroinitiators exhibited a large number of active polymer chains in close proximity, which might lead to interferences. Hence the number of living centers was reduced, by partial cleavage of the thioacetate groups. The thioacetate moieties were present in equilibrium with thiolates, which are the active species of the polymerization. A consistent polymerization among all initiating groups was postulated, although longer reaction times were required due to a decreased number of growing polymer chains at the same time. These conditions were achieved by reducing the amount of added sodium methoxide solutions and thus a partially cleavage of the thioacetates. Different approaches were conducted, thereby 15% to 50% of the sodium methoxide solution was added at the beginning of the polymerization and the remaining thioacetates were cleaved after the polymerization to ensure complete termination with ethyl bromoacetate. Under these conditions the side-product was preferentially formed and the peak area of the low molecular weight compound amounted between 58 and 64%. In addition, the use of 50% excess of sodium methoxide solution, a less concentrated reaction mixture as well as THF, distilled from sodium-potassium alloy, did not show any improvement. The side-product weighted in these cases between 40 and 60%.

Furthermore, the addition of propylene sulfide in small portions or by a slow monomer addition protocol via a syringe pump to reduce the local monomer concentration failed as well as the use of shorter polymerization times.

It should be noted, that the side-product was exclusively formed in polymerizations with polyglycerol-based macroinitiators. In comparison a set of linear PPS homopolymers (**PPS 31**-**34**) was synthesized with benzyl thioacetate (BT), a common initiator for propylene sulfide.[126] In this case homopolymerization was successfully conducted, and the results are shown in **Table 4.5**.

The obtained linear homopolymers of propylene sulfide were monomodal, with molecular weight distributions below 1.25. The DPs were analyzed via ^{1}H NMR spectroscopy and were in good agreement with the theoretical values. The reaction with the end-capping reagent was nearly quantitative and achieved at least 94mol% in case of the homopolymers.

In summary, the polymerization with the original recipe of the Tirelli group gave the best results for the PG-based macroinitiators, however an undesired side-product was formed. None of the modified polymerization conditions improved the obtained product compositions.

Table 4.5: Summary of the synthesized linear poly(propylene sulfide) homopolymers.

	Initiator	Theo. DP (per thioacetate)	$\overline{DP_n}$ (^{1}H NMR)	End-capping yield (^{1}H NMR) [mol%]	Theoretical $\overline{M_n}$ [g·mol^{-1}]	$\overline{M_n}$ (^{1}H NMR) [g·mol^{-1}]	$\overline{M_n}$ (SEC)* [g·mol^{-1}]	PDI (SEC)*
PPS 31	BT	10	12	94	1100	950	780	1.22
PPS 32	BT	20	20	100	1700	1700	1400	1.18
PPS 33	BT	30	31	100	2500	2400	2000	1.22
PPS 34	BT	40	40	100	3200	3200	2700	1.25

*SEC: eluent: THF; polystyrene standard calibration

Subsequently, options for purification of the synthesized copolymers were investigated. Neither the fractionating precipitation with different solvent mixtures of methanol and dichloromethane nor dialysis with dialysis tubings of several pore sizes enabled the extraction of the low molecular weight by-product from the targeted PG-PPS copolymers. Purification of the polyglycerol-based PPS graft polymers was only successful by machine-aided preparative SEC in chloroform. As an example the SEC traces of the samples **PPS 1-4** after purification are shown in **Figure 4.56**. The results of the purified copolymers are summarized in **Table 4.6**. The drawback of the purification via recycling preparative HPLC was that only 50 mg of the copolymer could be injected and purified per run.

Table 4.6: Summary of the purified polyglycerol-poly(propylene sulfide) copolymers.

	Macroinitiator	Theo. DP (per thioacetate)	$\overline{DP_n}$ (^{1}H NMR)	End-capping yield (^{1}H NMR) [mol%]	Theoretical $\overline{M_n}$ [g·mol^{-1}]	$\overline{M_n}$ (^{1}H NMR) [g·mol^{-1}]	$\overline{M_n}$ (SEC)* [g·mol^{-1}]	PDI (SEC)*
PPS 1	Hb 2	9 x 10	9 x 11	100	8900	9600	7000	1.20
PPS 2	Hb 2	9 x 20	9 x 18	73	15600	14300	15000	1.13
PPS 3	Hb 2	9 x 30	9 x 25	82	22300	18900	19500	1.14
PPS 4	Hb 2	9 x 40	9 x 32	64	28900	23600	23500	1.11
PPS 10	Hb 3	22 x 30	22 x 25	71	56200	47100	30000	1.18
PPS 19	Li 4	36 x 10	36 x 10	89	35200	35200	23000	1.12
PPS 20	Li 4	36 x 20	36 x 17	66	61900	53800	32000	1.22
PPS 21	Li 4	36 x 30	36 x 20	80	88500	61800	45000	1.12

*SEC: eluent: THF; polystyrene standard calibration

After chromatography-based purification, the copolymers showed monomodal distributions with a polydispersity index below 1.25 and in most cases below 1.20. The synthesized copolymers were obtained as highly viscous liquids with a good solubility in THF, chloroform and dichloromethane, but they were insoluble in methanol. The degree of polymerization was determined by ^{1}H NMR via ratio of the CH_2-groups of the macroinitiator (-O-CH_2-**CH_2**-CH_2-S-, the signal is highlighted in yellow) and the signals of the

PPS backbone (the signals are highlighted in green and purple). In **Figure 4.57** the ^{1}H NMR of **PPS 19** is shown as an example. The targeted DPs were achieved in case of the copolymers with ten monomer-repeating units per thioacetate groups. The higher homologs were of somewhat lower molecular weight than expected. Clearly, with increasing DP and increasing number of initiating groups the difference of the targeted DP and obtained DP increased. Hence, the strongest difference was detected for **PPS 21**, which was based on the linear polyglycerol macroinitiator with thirty-six initiating groups and a theoretical degree of polymerization of thirty. The obtained copolymer was 33% smaller than calculated. The residual propylene sulfide units were incorporated into the by-product. Its amount also increased with increasing monomer concentration in the polymerization mixture.

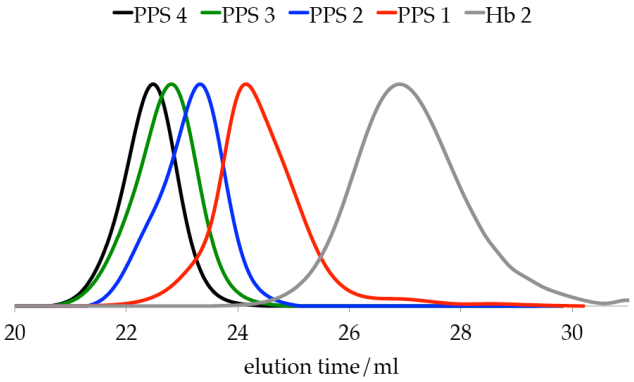

Figure 4.56: SEC traces (eluent: THF; polystyrene standard calibration) of macroinitiator **Hb 2** and corresponding purified PG-PPS graft copolymers **PPS 1-4** (DP 10-40 per thioacetate).

The peak area ratio in the ^{1}H NMR spectrum of the signal of methylene groups of the PG-based macroinitiator (-O-CH_2-**CH_2**-CH_2-S-; highlighted in yellow) and the methylene groups of the termination reagent (-S-**CH_2**-COO-, highlighted in brown) was used to calculate the end-capping efficiency. The achieved end-capping yield was in the range of 64 to 100mol%. The incomplete termination reaction was caused by the formed by-product, which reacted also with ethyl bromoacetate.

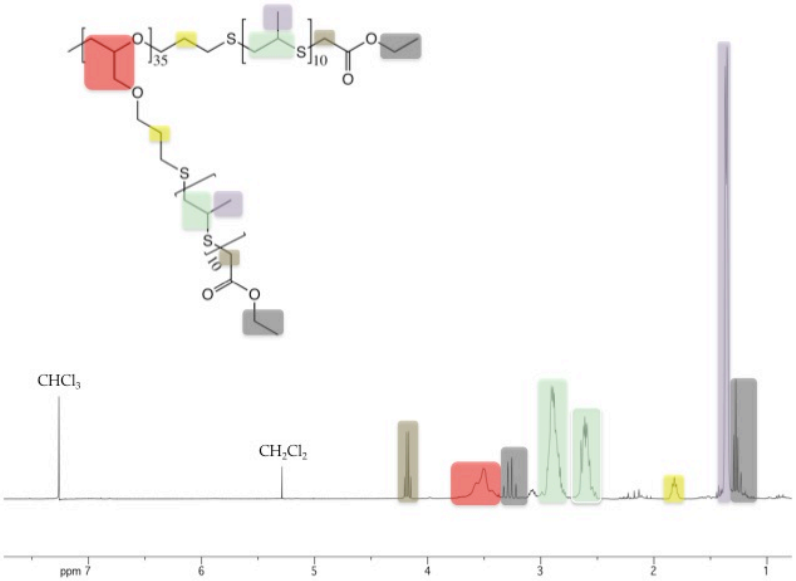

Figure 4.57: ^{1}H NMR spectrum of **PPS 19** (400 MHz, $CDCl_3$) and peak assignment of the copolymer structure.

The structure of the novel copolymers was also investigated via ^{13}C NMR spectroscopy. The spectrum of **PPS 19** is illustrated in **Figure 4.58**. All signals were visible and were assigned both in ^{1}H and ^{13}C NMR except for two methylene groups of the propylene linkers between the PG core and the PPS shell (-O-**CH_2**-CH_2-**CH_2**-S-). The CH_2-groups next to the oxygen atoms were situated in a similar chemical environment as the methylene groups of the polyglycerol and consequently these methylene groups exhibited a similar chemical shift in ^{1}H and ^{13}C NMR. The identical behavior was present in case of the methylene groups next to the sulfur atoms. These were comparable to the methylene groups of the poly(propylene sulfide) backbone and hence, the signals were not separated from the PPS signals in NMR.

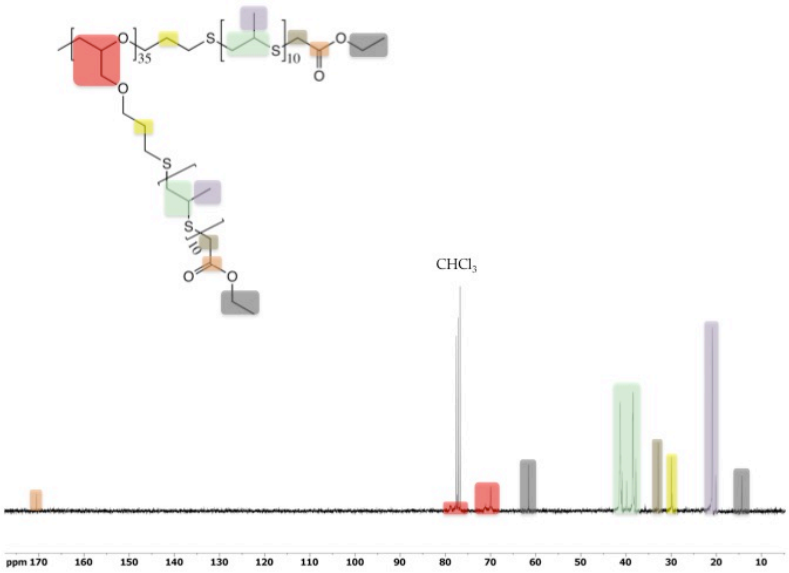

Figure 4.58: ^{13}C NMR spectrum of **PPS 19** (75.5 MHz, $CDCl_3$) and peak assignment of the copolymer structure.

The thermal behavior of the synthesized polymers was investigated with differential scanning calorimetry (DSC). The obtained calorimetric glass transition temperatures are summarized in **Table 4.7**. As an example the DSC traces of the macroinitiator **Hb 2** and the polyglycerol-poly(propylene sulfide) star polymers are shown in **Figure 4.59**. The glass transition temperature of the *hb*PG-based macroinitiator was detected at -58 °C. The obtained glass transition temperatures of the copolymers with different architectures were compared to the values of the linear homopolymers, which were described in literature.[120] Glass transition temperatures of the star- and brush-shaped PPS-copolymers did not show such a strong dependency on the molecular mass, as expected from the linear homopolymers. However, if the molecular weight of the PPS per chain in the graft polymers was considered, the value corresponded rather well to the glass transition temperatures described by Nicol et al.[120] The T_g of a homopolymer with 900 g·mol^{-1} was detected at -54 °C and was slightly lower than the value detected for copolymers with 750 g·mol^{-1} and 800 g·mol^{-1} at -50 °C. The T_g of the copolymers with 1350 g·mol^{-1} up to 1850 g·mol^{-1} was detected at -46 °C or -47 °C and thus was similar to the homopolymers with 1600 g·mol^{-1} and -47 °C. Hence, the T_gs were adjusted with increasing molecular weight of the homopolymers and the graft-copolymers per chain. It was shown that the multi-arm copolymers exhibited a different thermal behavior compared to PPS homopolymers, as expected. Entirely, the comparison of one polysulfide chain of the graft-copolymers with the homopolymers showed similar T_g values.

Table 4.7: Summary of the thermal behavior of the purified polyglycerol-poly(propylene sulfide) copolymers.

	Macroinitiator	$\overline{DP_n}$ (^{1}H NMR)	Theoretical $\overline{M_n}$ [g·mol^{-1}]	$\overline{M_n}$ (^{1}H NMR) [g·mol^{-1}]	$\overline{M_n}$ PPS per chain (^{1}H NMR) [g·mol^{-1}]	T_g (DSC)* [°C]
Hb 2	-	-	-	-	-	-58
PPS 1	Hb 2	9 x 11	8900	9600	9 x 800	- 50
PPS 2	Hb 2	9 x 18	15600	14300	9 x 1350	- 48
PPS 3	Hb 2	9 x 25	22300	18900	9 x 1850	- 47
PPS 4	Hb 2	9 x 32	28900	23600	9 x 2350	- 47
PPS 10	Hb 3	22 x 25	56200	47100	22 x 1850	-46
PPS 19	Li 4	36 x 10	35200	35200	36 x 750	- 50
PPS 20	Li 4	36 x 17	61900	53800	36 x 1250	- 48
PPS 21	Li 4	36 x 20	88500	61800	36 x 1500	- 46

*DSC: temperature range: -100 °C – 50 °C with 10° C·min^{-1}

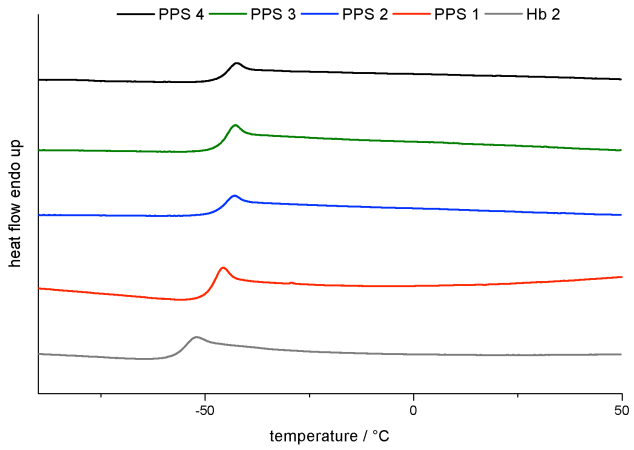

Figure 4.59: DSC traces (-100 °C – 50 °C with 10 °C·min^{-1}) of macroinitiator **Hb 2** and corresponding purified PG-PPS graft copolymers **PPS 1-4** (DP 10-40 per thioacetate).

Recycling preparative HPLC was also used to separate the low molecular weight compound, which was formed in the graft-polymerization of PPS onto linear and hyperbranched polyglycerol macroinitiators (compare to **Figures 4.53** and **4.54**). The ^{1}H NMR spectrum of the low molecular weight compound is shown in **Figure 4.60**. Beside the signals of the end-capped poly(propylene sulfide), two signals at 5.8 ppm and 5.1 ppm were observed (highlighted in blue). The detected peak pattern is characteristic for an allyl group. The proposed side-reaction is shown in **Figure 4.61**. Sodium methoxide solution was capable of deprotonating the methyl group of the propylene sulfide, which subsequently underwent a rearrangement to a thiolate with an allyl group. These thiolates acted as initiator for propylene sulfide to result in a PPS homopolymer (**13**). This reaction was also observed by Boileau and Sigwalt during their approach to use a living

poly(ethylene glycol) as initiator for polysulfides. As mentioned before, the targeted copolymers were not formed, but instead poly(propylene sulfide) homopolymer with an unsaturated end-group.[134]
The corresponding side-reaction was also described for propylene oxide and the formation of poly(propylene oxide) with an allyl ether end-group.[232,233] In case of propylene oxide this side-reaction is avoidable when using larger counterions, such as cesium and at lower temperatures, such as room temperature. Apparently this concept did not work for polymerizations of propylene sulfide, because the side-reaction still occurred with lower temperature like 0°C or with potassium as a counterion.

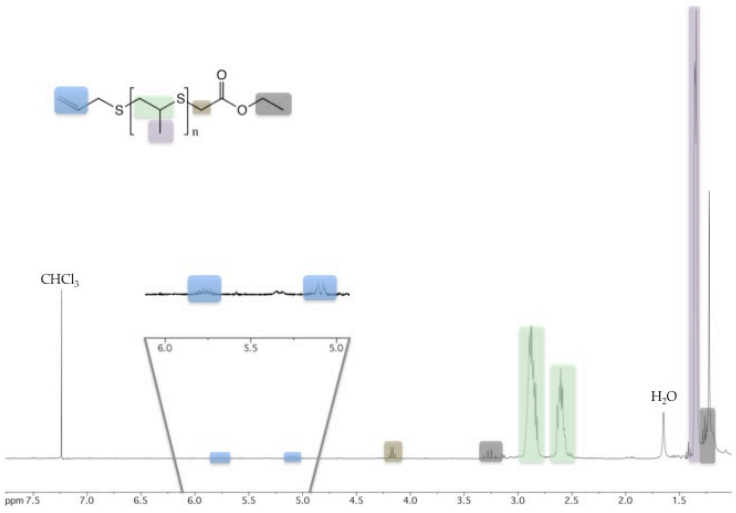

Figure 4.60: ^{1}H NMR spectrum of low molecular weight side-product (400 MHz, $CDCl_3$) and peak assignment of the homopolymer.

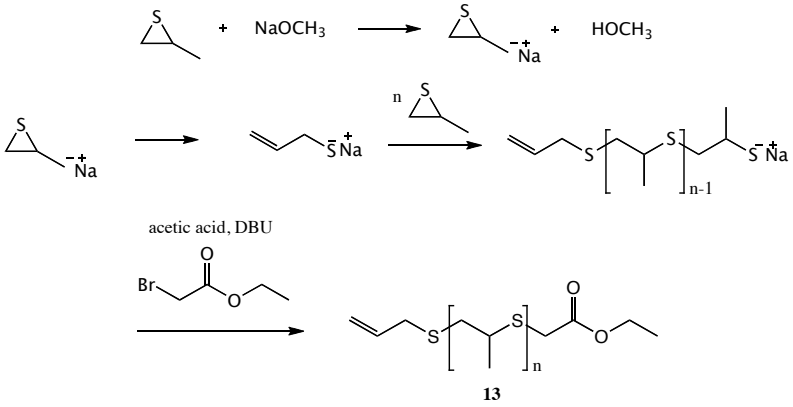

Figure 4.61: Proposed side-reaction.

To obtain additional evidence for the proposed side-reaction, the polymerization was carried out under common conditions with sodium methoxide solution, except no additional initiator was added. The SEC trace of the obtained product is illustrated in **Figure 4.62**.
The ^{1}H NMR was congruent to the one in **Figure 4.60**, which was measured for the side-product of the graft-polymerization with PG-based macroinitiators. The SEC trace and the obtained NMR spectrum demonstrate that the polymerization of propylene sulfide was affected without the addition of initiator.

Polymerization with the PG-based macroinitiators was investigated in more detail to manifest the low molecular weight by-product was formed in an identical reaction. The PS-graft-copolymerization with **Hb 2** and a degree of polymerization of thirty per thioacetate was realized under common conditions and end-capped after five, ten, fifteen and twenty minutes, respectively. As indicated by the SEC-traces of these approaches, the side-product was already detectable after five minutes (**Figure 4.63**). The amount of side-product as well as the molecular weight increased with increasing time, as expected.

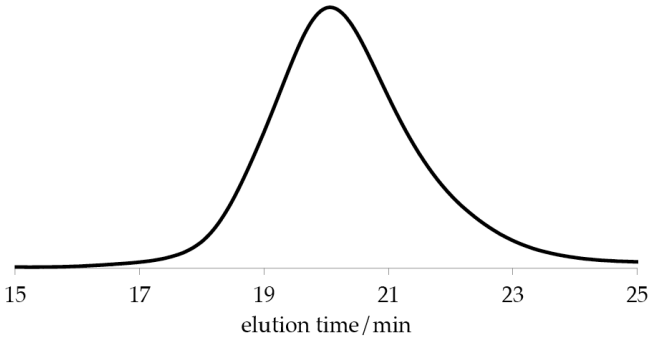

Figure 4.62: SEC-trace (eluent: THF; polystyrene standard calibration) of the obtained polymer, without an initiator.

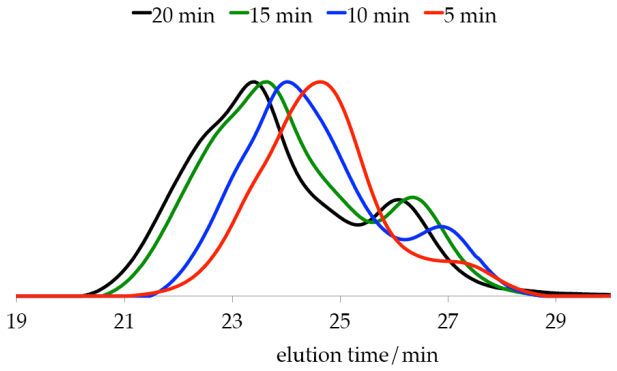

Figure 4.63: SEC-traces (eluent: THF; polystyrene standard calibration) of a kinetic experiment with **Hb 2** (the polymerization was terminated after different times).

To gather further support for the proposed side-reaction, the polymerization was run in a NMR-tube and followed online by ^{1}H NMR. **Figure 5.64** shows four spectra of the online NMR kinetic experiment. The polyglycerol-based macroinitiator **Hb** 2 was dissolved in 0.7 ml THF-d_8 and the mixture was degassed by five cycles of freeze-pump-thaw. 1.05 equiv (per thioacetate) sodium methoxide solution in deuterated methanol was added. After five to ten minutes propylene sulfide was added, and after shaking the NMR-tube, every minute a spectrum with four scans was recorded. After fifty minutes reaction time a spectrum with thirty-two scans was measured. The spectrum on the top was conducted after ten minutes, the second after thirty minutes, the third after fifty minutes and the one on the bottom was recorded with thirty-two scans after the NMR kinetic. The peaks of the monomer decreased and the peaks of the polymer backbone increased, as targeted. In the spectrum ten minutes after monomer addition the proton signals of the unsaturated end-group of deprotonated and rearranged propylene sulfide were already present. These peaks were also observable in the spectrum with thirty-two scans after the kinetic. These results emphasize that the proposed side-reaction took place in graft-polymerizations of propylene sulfide with polyglycerol-based macroinitiators.

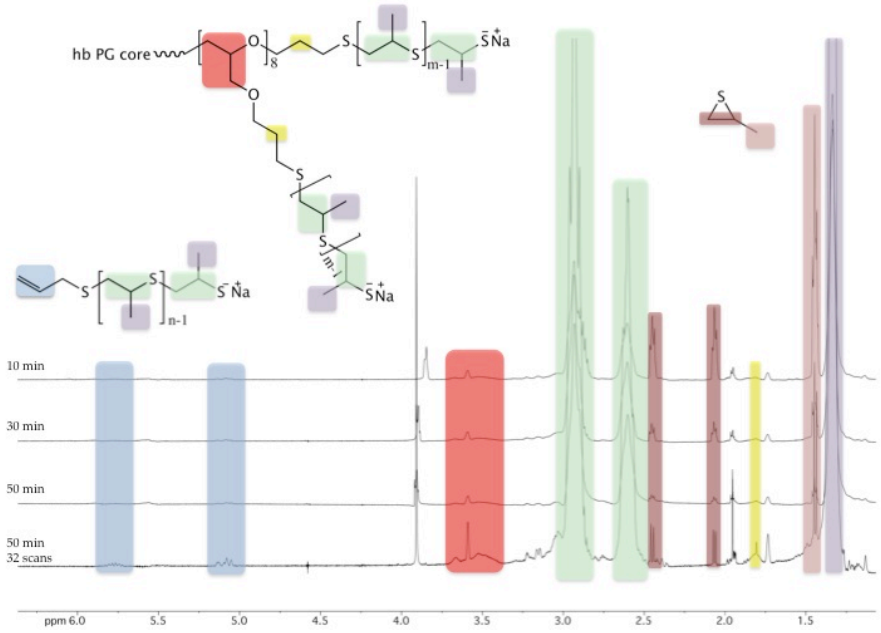

Figure 4.64: Online ^{1}H NMR experiment of the polymerization of PS with PG-based macroinitiator (400 MHz, $CDCl_3$).

4.4.2 Polyglycerol-based poly(ethylene sulfide)

Linear and hyperbranched polyglycerol-based macroinitiators with a different number of thioacetate groups were used to initiate the anionic ring-opening polymerization of ethylene sulfide to obtain soluble copolymers. In case of ethylene sulfide the observed side-reaction should not occur.

This concept is based on an approach of Wolf et al., in which the use of *hb*PG as macroinitiator for short polyglycolide arms enabled the formation of soluble star-shaped copolymers. The analog linear copolymers as well as the homopolymer of polyglycolide were insoluble in common organic solvents due to the well-known high degree of crystallization of polyglycolide.[224]

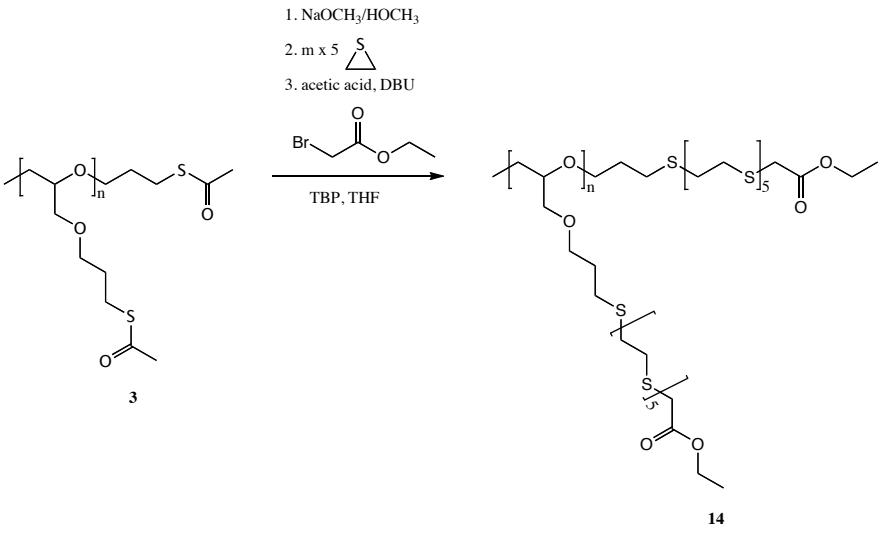

Figure 4.65a: Polymerization of ES with *lin*PG-based macroinitiator to polymer-brushes.

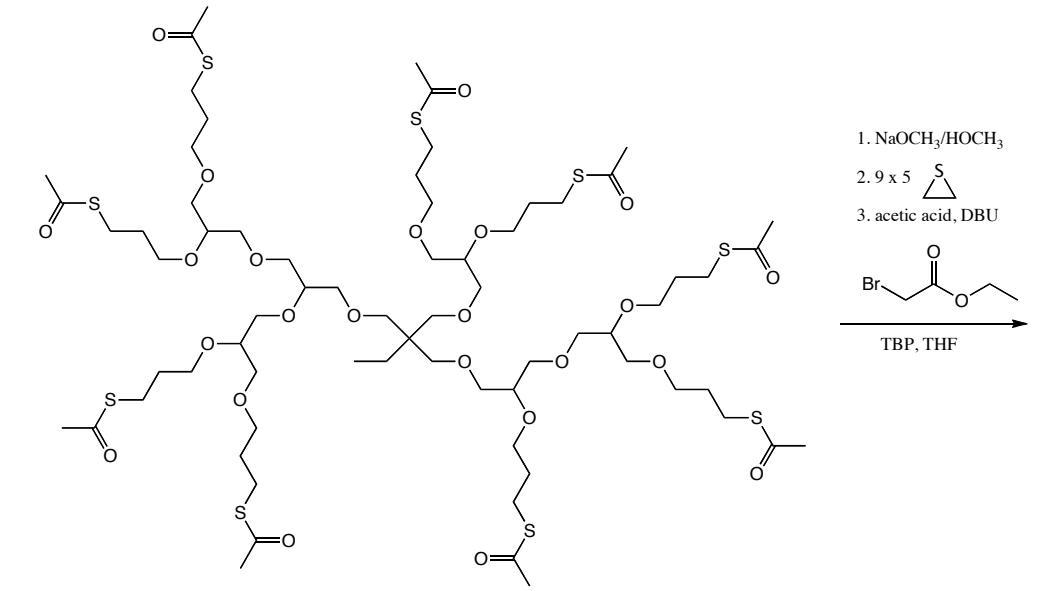

6

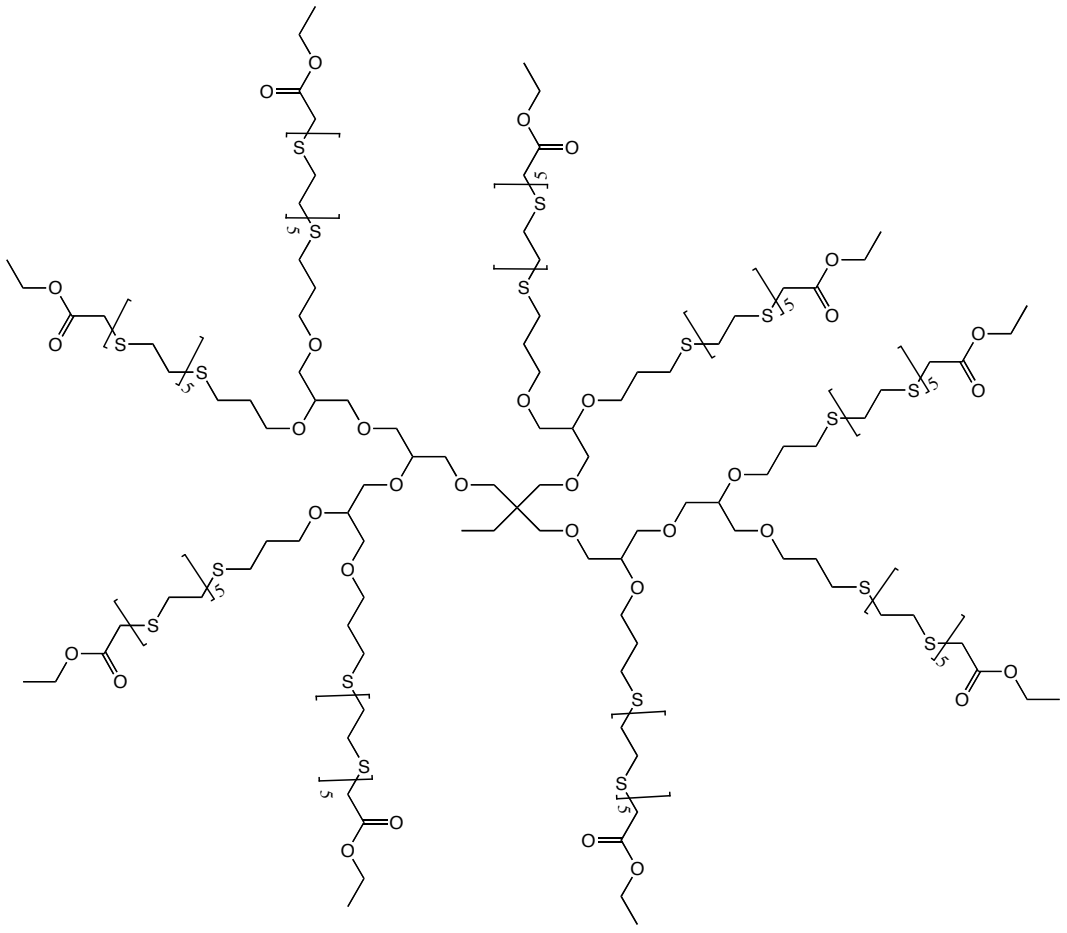

15

Figure 4.65b: Polymerization of ES with *hb*PG-based macroinitiator to star polymers.

Graft-copolymerization of five ethylene sulfide units per initiating group was conducted under the same conditions as described for propylene sulfide and ethyl bromoacetate was also used as termination agent. The copolymer synthesis with *hb*PG- and *lin*PG-based macroinitiators is illustrated in **Figures 4.65a** and **b** and the results of the graft-polymerization are summarized in **Table 4.8**. The synthesis was successful with four different initiators, but the copolymers were not completely soluble in common organic solvents. SEC measurements were neither in DMF nor in THF or chloroform (TCM) enabled, even after oxidation with hydrogen peroxide the compounds did not solubilize in DMF. The approach to obtain good soluble PES copolymer structures by the use of a large linear or hyperbranched macroinitiator with short polysulfide arms failed.

Table 4.8: Summary of the synthesized polyglycerol-poly(ethylene sulfide) copolymers.

	Macroinitiator	**Theoretical DP** (per thioacetate)	$\overline{DP_n}$ (^{1}H NMR)	**End-capping yield** (^{1}H NMR) [mol%]	**Theoretical** $\overline{M_n}$ [g·mol^{-1}]	$\overline{M_n}$ (^{1}H NMR) [g·mol^{-1}]	$\overline{M_n}$ (SEC)* [g·mol^{-1}]
PES 1	Hb 2	9 x 5	9 x 4	64	4950	4400	-
PES 2	Hb 4	22 x 5	22 x 4	65	13200	11900	-
PES 3	Li 2	17 x 5	17 x 4	81	9100	8100	-
PES 4	Li 4	36 x 5	-	-	18000	-	-

*SEC: eluent: DMF, THF or TCM

However, NMR spectroscopy was conducted with deuterated chloroform in suspension, except **PES 4** was entirely insoluble and in the NMR spectrum no signal was observed.
The NMR spectrum of **PES 1** is shown in **Figure 4.66** as example.

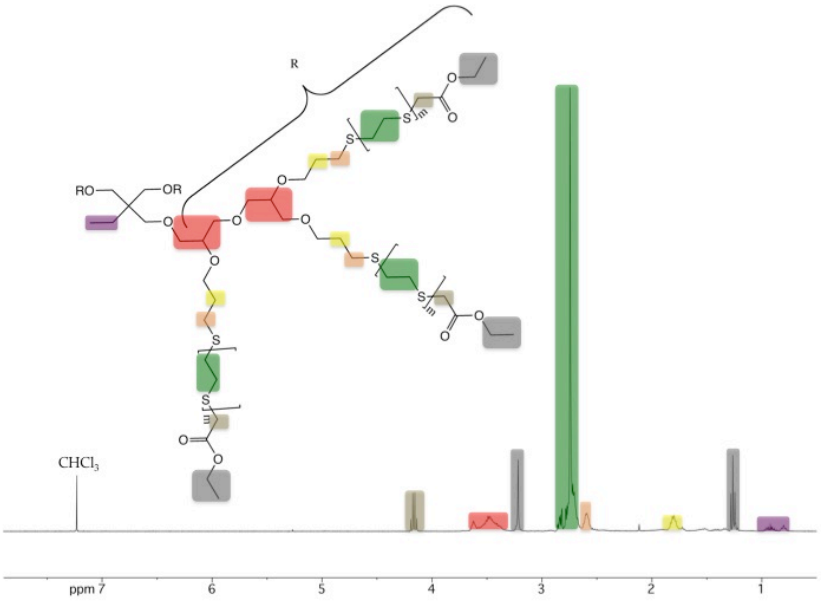

Figure 4.66: ^{1}H NMR spectrum of **PES 1** (400 MHz, $CDCl_3$) and peak assignment of the copolymer structure.

The achieved DPs and the end-capping yields were calculated via NMR spectroscopy, similar to the PG-PPS copolymer, by the signal ratios of the methylene groups of the initiators (-O-CH_2-**CH_2**-CH_2-S-) and the NMR signals of the polymer backbone ([-**CH_2**-**CH_2**-S-]$_n$) or the methylene group of the end-capping agent (-S-**CH_2**-COO-), respectively. The by NMR obtained DPs were slightly lower as targeted. This might be caused by the incomplete solubility of the measured copolymers. Moieties with lower DPs were better soluble and with increasing DP the solubility decreased. Hence, the calculated DPs might be underestimated.

Additionally, the thermal behavior of the synthesized block-copolymers was investigated via DSC. The obtained values are shown in **Table 4.9**. A glass transition temperature was solely for **PES 2** with the larger hyperbranched macroinitiator detected at -46 °C. In all DSC traces of the copolymer samples appeared a melting point (T_m) of the poly(ethylene sulfide) block. The highest melting point with 123 °C was measured for **PES 4** with the *lin*PG-based brush copolymer with thirty-six PES-chains. The melting points of the star-shaped copolymer with nine PES arms as well as the brush-like sample with seventeen polysulfide chains were comparable with 105 °C and 106 °C, respectively.

Table 4.9: Summary of the thermal behavior of the synthesized polyglycerol-poly(ethylene sulfide) copolymers.

	Macroinitiator	$\overline{DP_n}$ (^{1}H NMR)	**Theoretical** $\overline{M_n}$ [g·mol^{-1}]	$\overline{M_n}$ (^{1}H NMR) [g·mol^{-1}]	$\overline{M_n}$ PES per chain (^{1}H NMR) [g·mol^{-1}]	**T_g** (DSC)* [°C]	**T_m** (DSC)* [°C]
PES 1	Hb 2	9 x 4	4950	4400	9 x 240	-	105
PES 2	Hb 4	22 x 4	13200	11900	22 x 240	-46	96
PES 3	Li 2	17 x 4	9100	8100	17 x 240	-	106
PES 4	Li 4	36 x 5**	18000	-	36 x 300**	-	123

*DSC: temperature range: -95 °C - 250 °C with 10 °C·min^{-1}; **theoretical DP

Copolymer **PES 2** exhibited the lowest melting temperature with 96 °C, although this block-copolymer had more PES arms as the smaller star-shaped homolog **PES 1**. The hyperbranched polyglycerol core exhibited still a T_g, as mentioned before, and furthermore, it clearly affected the thermal characteristics of the PES shell and lowered its melting behavior.

In summary, a significant influence of the different architecture and number of initiating groups was observed in DSC in contrast to the different PG-PPS block-copolymer samples. Particularly a large hyperbranched polyglycerol-based macroinitiator impinged on the thermal behavior of the copolymers.

4.4.3 Polyglycerol-based random polysulfides

In a further approach, the synthesized polyglycerol-based macroinitiators were used for the random polymerization of propylene sulfide and ethylene sulfide. The random copolymerization of the episulfides should prevent the crystallization of the synthesized copolymers and enable the synthesis of soluble polysulfides. The synthesis was conducted under the same conditions as the graft-copolymerizations described before, except both monomers were added at the same time. The synthesis of brush-like and star-shaped random polysulfides is shown in **Figures 4.67a** and **b**. This procedure was attempted to synthesize a library of polysulfides with different architectures and monomer contents. The DP of propylene sulfide was varied in each case between ten and forty and the DP of ethylene sulfide was enhanced from five over ten to fifteen. The results of the synthesized star-shaped polysulfides with macroinitiator **Hb 1** are shown in **Table 4.10** and results of the synthesized copolymer brushes with macroinitiator **Li 3** are shown in **Table 4.11**.

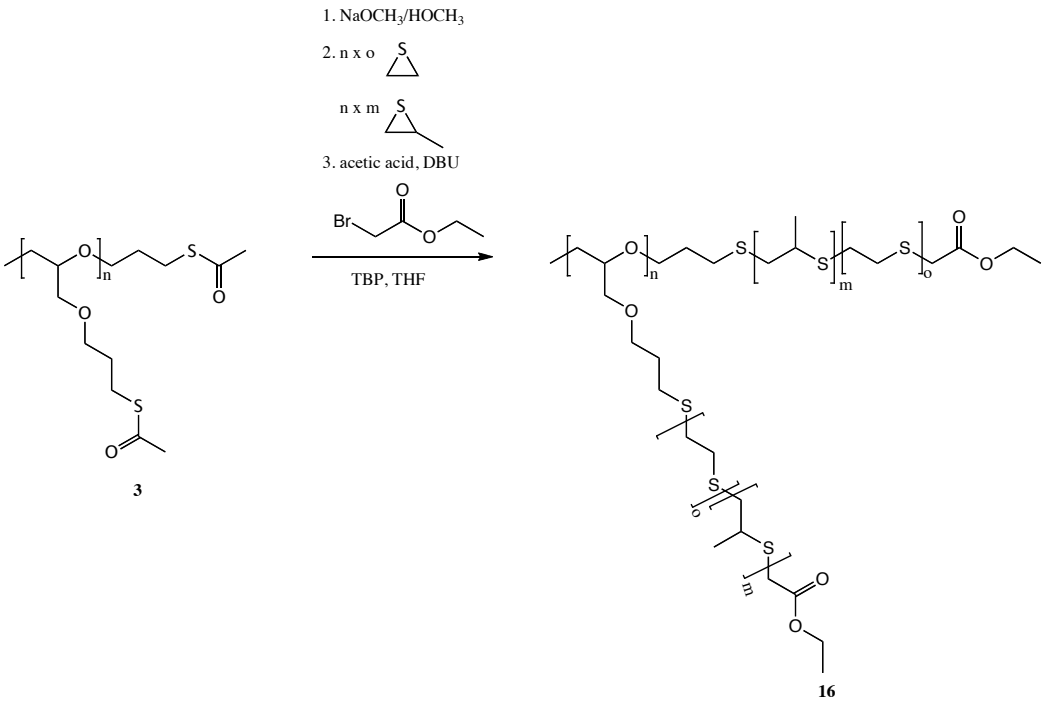

Figure 4.67a: Random polymerization of ES and PS with *lin*PG-based macroinitiator to polymer-brushes.

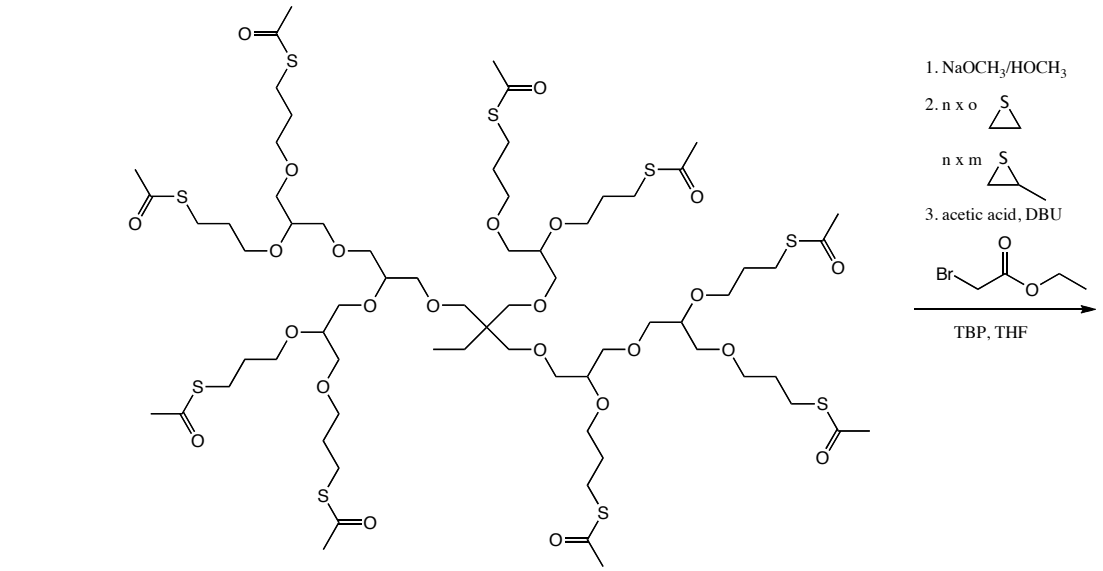

6

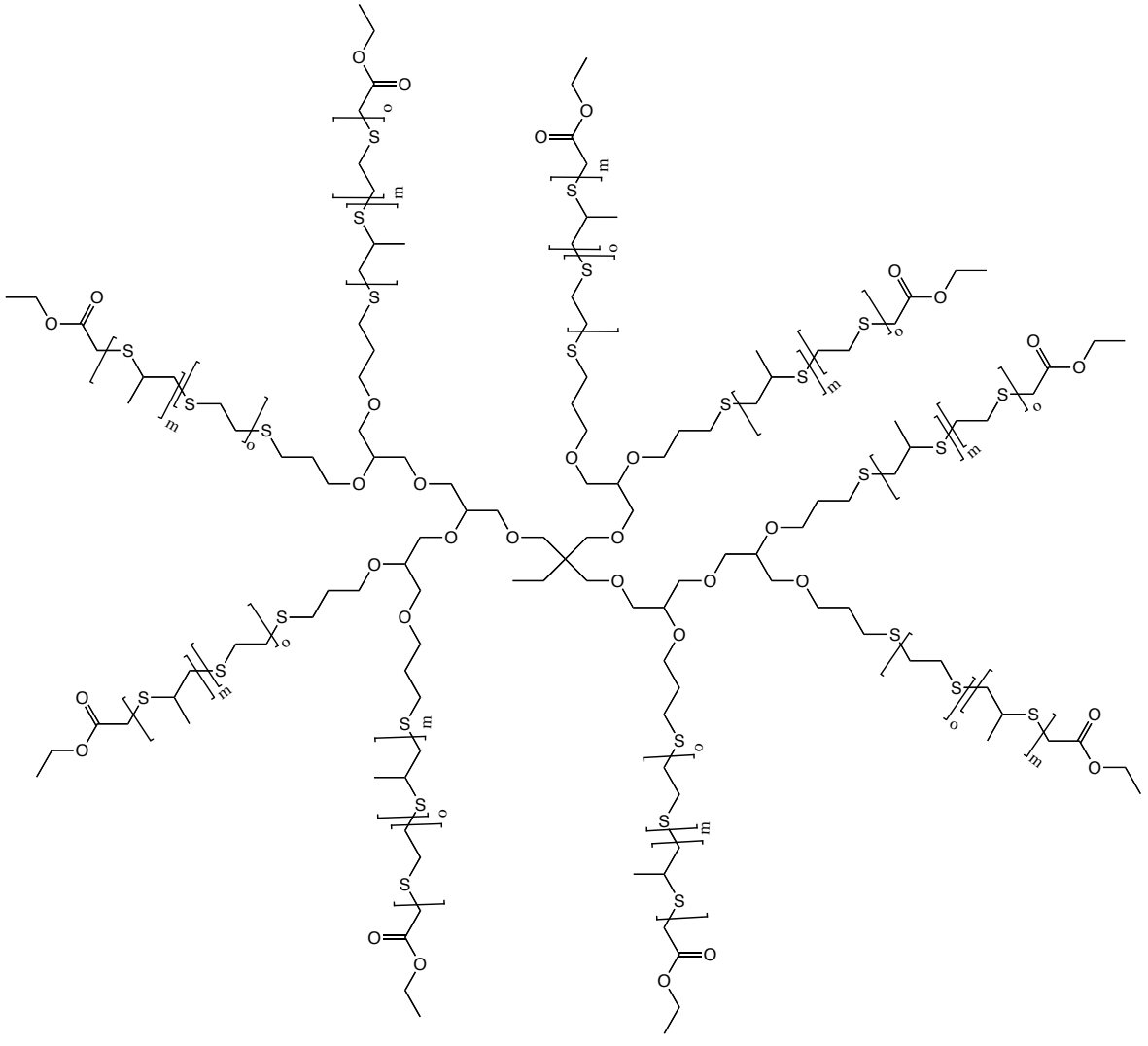

17

Figure 4.67b: Random polymerization of ES and PS with *hb*PG-based macroinitiator to star polymers.

Table 4.10: Summary of the polyglycerol-poly(propylene sulfide)-poly(ethylene sulfide) random star copolymers (macroinitiator: **Hb 1**).

	Theo. DP PS (per thioacetate)	**Theo. DP ES** (per thioacetate)	$\overline{DP_n}$ **PS** (^{1}H NMR)	$\overline{DP_n}$ **ES** (^{1}H NMR)	**Theo. content ES*** [wt%]	**Content ES*** (^{1}H NMR) [wt%]	$\overline{M_n}$ (^{1}H NMR) [g·mol^{-1}]	$\overline{M_n}$ (SEC)** [g·mol^{-1}]	PDI (SEC)**
P(PS-ES) 1	7 x 10	7 x 5	7 x 11	7 x 7	29	34	9400	6500	1.56
P(PS-ES) 2	7 x 20	7 x 5	7 x 17	7 x 5	17	19	12900	9600	1.46
P(PS-ES) 3	7 x 30	7 x 5	7 x 21	7 x 5	12	16	15000	10100	1.48
P(PS-ES) 4	7 x 40	7 x 5	7 x 30	7 x 5	9	13	19700	12600	1.58
P(PS-ES) 5	7 x 10	7 x 10	7 x 10	7 x 12	45	49	12200	6900	1.65
P(PS-ES) 6	7 x 20	7 x 10	7 x 16	7 x 10	29	34	14500	9000	1.64
P(PS-ES) 7	7 x 30	7 x 10	7 x 23	7 x 10	21	26	18100	9800	1.67
P(PS-ES) 8	7 x 40	7 x 10	7 x 35	7 x 11	17	20	24800	10400	1.86
P(PS-ES) 9	7 x 10	7 x 15	7 x 7	7 x 10	55	54	9800	6500	1.69
P(PS-ES) 10	7 x 20	7 x 15	7 x 16	7 x 13	38	40	15800	8200	1.75
P(PS-ES) 11	7 x 30	7 x 15	7 x 22	7 x 11	29	29	18000	10800	1.69
P(PS-ES) 12	7 x 40	7 x 15	7 x 22	7 x 10	23	27	17600	10100	1.79
P(PS-ES) 13	7 x 10	7 x 20	-	-	62	-	-	-	-

*content ES of the polysulfide content; **SEC: eluent: TCM; polystyrene standard calibration

Table 4.11: Summary of the polyglycerol-poly(propylene sulfide)-poly(ethylene sulfide) random brush copolymers (macroinitiator: **Li 3**).

	Theo. DP PS (per thioacetate)	**Theo. DP ES** (per thioacetate)	$\overline{DP_n}$ **PS** (^{1}H NMR)	$\overline{DP_n}$ **ES** (^{1}H NMR)	**Theo. content ES*** [wt%]	**Content ES*** (^{1}H NMR) [wt%]	$\overline{M_n}$ (^{1}H NMR) [g·mol^{-1}]	$\overline{M_n}$ (SEC)** [g·mol^{-1}]	PDI (SEC)**
P(PS-ES) 14	18 x 10	18 x 5	18 x 9	18 x 6	29	35	22700	8200	2.09
P(PS-ES) 15	18 x 20	18 x 5	18 x 20	18 x 6	17	20	37400	9300	2.26
P(PS-ES) 16	18 x 30	18 x 5	18 x 23	18 x 6	12	17	41400	10900	2.15
P(PS-ES) 17	18 x 40	18 x 5	18 x 26	18 x 5	9	13	44300	8300	2.77
P(PS-ES) 18	18 x 10	18 x 10	18 x 10	18 x 10	45	47	29400	7400	2.40
P(PS-ES) 19	18 x 20	18 x 10	18 x 17	18 x 11	29	32	37700	10300	2.15
P(PS-ES) 20	18 x 30	18 x 10	18 x 25	18 x 10	21	24	48400	10300	2.40
P(PS-ES) 21	18 x 40	18 x 10	18 x 29	18 x 10	17	22	53800	6100	3.74
P(PS-ES) 22	18 x 10	18 x 15	18 x 11	18 x 15	55	53	35100	5700	2.87
P(PS-ES) 23	18 x 20	18 x 15	18 x 17	18 x 15	38	42	43200	9700	2.29
P(PS-ES) 24	18 x 30	18 x 15	18 x 25	18 x 15	29	34	54900	9300	2.65
P(PS-ES) 25	18 x 40	18 x 15	18 x 31	18 x 14	23	27	60800	11100	2.61

*content ES of the polysulfide content; **SEC: eluent: TCM; polystyrene standard calibration

Random graft-copolymerization of ethylene sulfide and propylene sulfide was successfully conducted with *lin*PG- and *hb*PG-based macroinitiators. The targeted ES content ranged between 9 and 62 wt%, however, the synthesized compounds contained 13 to 54wt% ES. Interestingly, the obtained ES content of the corresponding star-shaped and brush-like copolymers was in most cases similar and exhibited at most 2wt% difference. The ES content calculated by NMR spectroscopy was often slightly higher than targeted (2-6wt%). This result might be caused by the higher reactivity of ethylene sulfide compared to propylene sulfide, which was also described in literature by several authors[140,190] as mentioned in the introduction of chapter 4. Copolymers with ES content up to 55wt% were soluble in common organic solvents such as dichloromethane, chloroform and THF. The star-shaped polysulfide **P(PS-ES) 13** with a theoretical ES content of 62wt% did not solubilize in chloroform and the characterization of this sample was not possible via SEC and NMR spectroscopy. The proton NMR spectrum of **P(PS-ES) 18** is shown in **Figure 4.68** as an example. The DPs of ethylene sulfide and propylene sulfide were determined via the ratio of the CH_2-groups

of the macroinitiator (highlighted in yellow) and the signal of the PES polymer backbone (highlighted in dark green) as well as the signals of the protons of the PPS backbone (highlighted in purple and light green), respectively. The achieved end-capping yield was again calculated by the ration of the methylene groups of the macroinitiator and the methylene groups of the end-capping reagent (highlighted in brown).

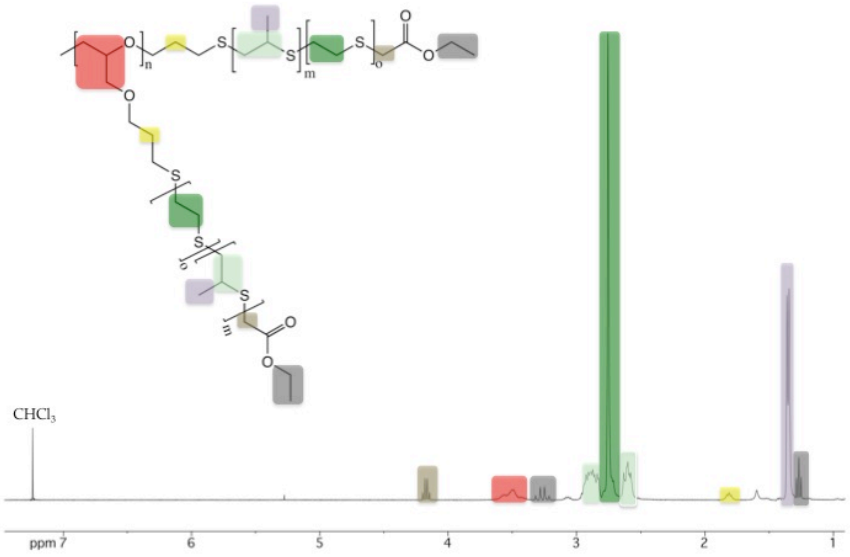

Figure 4.68: ^{1}H NMR spectrum of **P(PS-ES) 18** (400 MHz, $CDCl_3$) and peak assignment of the copolymer structure.

In **Figure 4.69** is the carbon NMR spectrum and the peak assignment of copolymer **P(PS-ES) 1** shown.

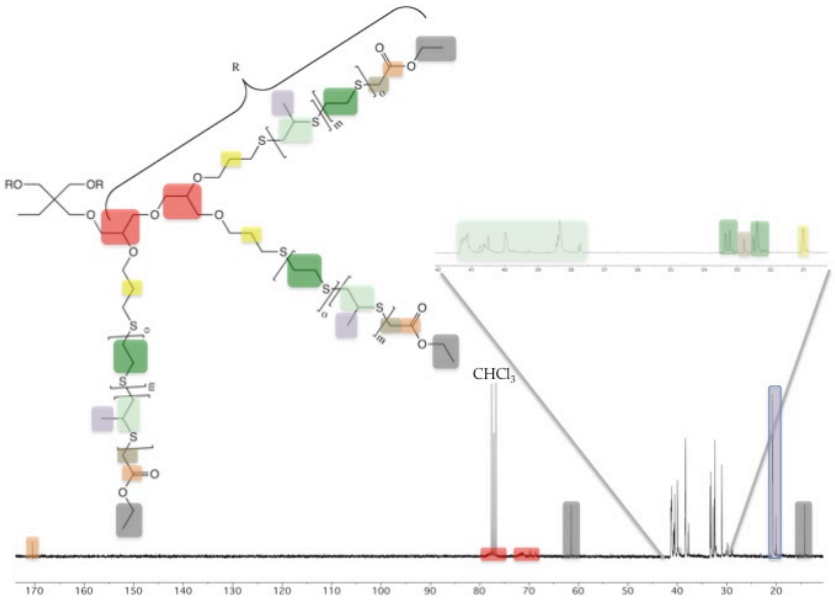

Figure 4.69: ^{13}C NMR spectrum of **P(PS-ES) 1** (75.5 MHz, $CDCl_3$) and peak assignment of the copolymer structure.

The appearance of the copolymers changed with increasing ES content. This was also optically observable, the viscous materials became with increasing ES content more crystalline. In **Figure 4.70** the photographs of the star-shaped copolymers with different polysulfide contents are illustrated.

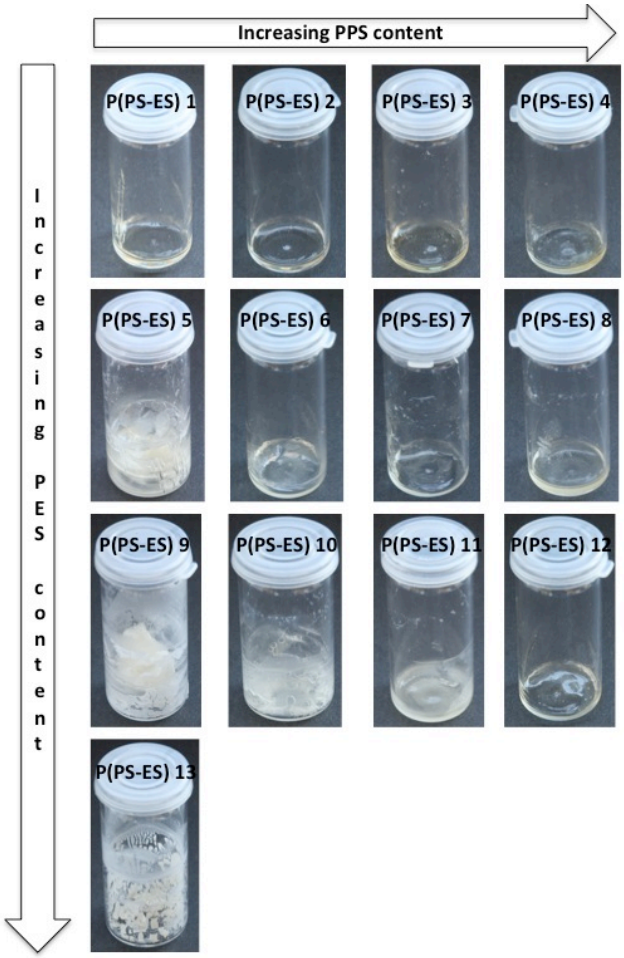

Figure 4.70: Photographs of the random star-shaped polysulfides (**P(PS-ES) 1**-**13**).

The obtained end-capping yield of the synthesized copolymers was in most cases above 80mol% and often higher than 90mol%. The polydispersity index was for all synthesized copolymers rather high. Star-shaped copolymers (**P(PS-ES) 1**-**13**), which were based on the hyperbranched initiator with seven thioacetates, exhibited moderate PDIs with 1.46 to 1.86. The molecular weight distribution of the brush copolymers (**P(PS-ES) 14**-**25**) initiated by **Li 3** was higher with 2.09 to 2.87, the copolymer **P(PS-ES) 20** with a PDI of 3.74 was an exemption. The PDIs increased in most cases with increasing DPs of ethylene sulfide and propylene sulfide. SEC traces of the star-shaped copolymers **P(PS-ES) 1**-**4** are illustrated in **Figure 4.71** and the SEC traces of the brush-like polysulfides **P(PS-ES) 14**-**17** are shown in **Figure 4.72**. The broad distribution might be caused by a faster incorporation of ethylene sulfide and thus, kind of partial crystallization of the growing polymer chain might occur, which might slow down the reaction kinetic and resulted in a broader distribution. A second reason for the broad molecular weight distribution might be the side-reaction, which also occurred in the polymerization of propylene sulfide. SEC traces of the copolymers based on the linear macroinitiator exhibited a low molecular weight compound, which confirmed the side-reaction caused by the deprotonation of propylene sulfide and the subsequent rearrangement.

Linear random copolymers of ethylene sulfide and propylene sulfide were synthesized as comparison. Benzyl thioacetate (BT) was used as initiator. **Table 4.12** summarizes the results. The linear copolymers (**P(PS-ES) 26**-**37**) were well distributed with PDIs below 1.31, which indicated again the broadening of the molecular weight distribution, exclusively emerged in the polymerizations with PG-based macroinitiators. The achieved content of ES of the linear copolymers was also higher than targeted with 12-53wt%, similar to the results of copolymers initiated with the macroinitiators **Hb 1** and **Li 3**. The termination efficiency amounted for all linear random copolymers over 90mol%.

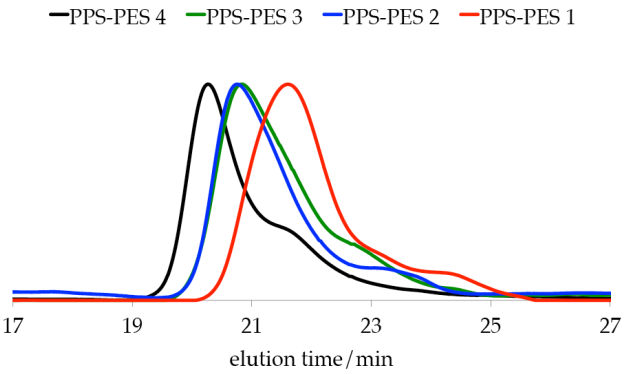

Figure 4.71: SEC-traces (eluent: TCM; polystyrene standard calibration) of the PG-PPS-PPS random graft copolymers **P(PS-ES) 1**-**4**.

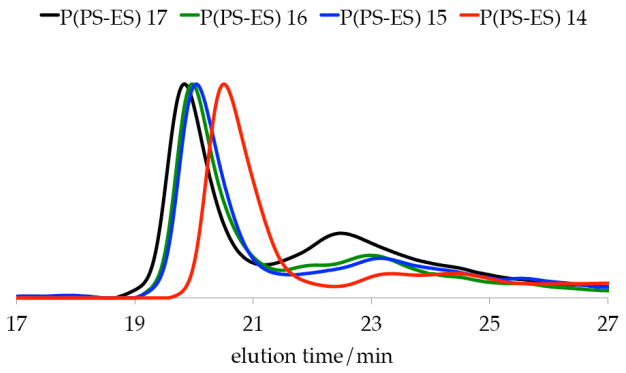

Figure 4.72: SEC-traces (eluent: TCM; polystyrene standard calibration) of the PG-PPS-PPS random graft copolymers **P(PS-ES) 14**-**17**.

As mentioned before, ethylene sulfide is known to be more reactive in anionic ring-opening polymerization compared to propylene sulfide. This might lead to not completely random copolymers, and the incorporation of the episulfide monomers might follow a gradient. The incorporation of ethylene sulfide might be favored at first and subsequently more propylene sulfides might react with the growing polymer chains. The synthesized copolymers were analyzed via ^{13}C NMR spectroscopy in more detail by evaluation of the diads and triads. The diads and triads of polysulfide copolymers were already described, for example, by Corno et al.[140,141,191] and further NMR investigation together with *ab initio* molecular orbital calculations were done by Sasanuma.[234]

In addition, the synthesis of poly(ethylene sulfide)-poly(propylene sulfide) block-copolymers should be used as comparison to except the formation of block-copolymers during the random copolymerization. The synthesis of soluble star-shaped block-copolymers with the *hb*PG-based macroinitiator **Hb 1** failed, even

with long PPS blocks and short PES blocks. The miscarriage was independent of the order of the added episulfides monomer.

Table 4.12: Summary of the linear random poly(propylene sulfide-ethylene sulfide) copolymers (initiator: **BT**).

	Theo. DP PS	**Theo. DP ES**	$\overline{DP_n}$ **PS** (^{1}H NMR)	$\overline{DP_n}$ **ES** (^{1}H NMR)	**Theo. content ES*** [wt%]	**Content ES*** (^{1}H NMR) [wt%]	$\overline{M_n}$ (^{1}H NMR) [g·mol^{-1}]	$\overline{M_n}$ (SEC)** [g·mol^{-1}]	PDI (SEC)**
P(PS-ES) 26	10	5	10	6	29	33	1300	1200	1.17
P(PS-ES) 27	20	5	18	6	17	21	1900	1900	1.16
P(PS-ES) 28	30	5	25	6	12	16	2400	2500	1.16
P(PS-ES) 29	40	5	31	5	9	12	1800	3200	1.27
P(PS-ES) 30	10	10	11	11	45	45	1700	1600	1.19
P(PS-ES) 31	20	10	19	7	29	23	2000	2100	1.15
P(PS-ES) 32	30	10	25	9	21	23	2600	2800	1.22
P(PS-ES) 33	40	10	34	13	17	24	3500	2900	1.27
P(PS-ES) 34	10	15	13	18	55	53	2300	1800	1.21
P(PS-ES) 35	20	15	25	20	38	39	3300	3000	1.24
P(PS-ES) 36	30	15	29	20	29	36	3600	3500	1.19
P(PS-ES) 37	40	15	40	16	23	24	4100	4000	1.31

*content ES of the polysulfide content; **SEC: eluent: TCM; polystyrene standard calibration

The synthesis of linear PPS-PES as well as PES-PPS block-copolymers was conducted with benzyl thioacetate as initiator. The block-copolymerization was conducted under the common conditions, except the second episulfides monomer was added after the polymerization of the first monomer. The results are summarized in **Table 4.13**. The synthesis of two sets of different linear block-copolymers was successfully conducted. The molecular weight distributions were rather narrow with PDIs below 1.50 and in most cases below 1.30. PES-PPS block-copolymers exhibited slightly higher PDIs. The calculated end-capping efficiency of the linear polysulfide copolymers was for the synthesized copolymers higher than 85mol%. The sequence of the monomer addition did not cause a difference in end-capping efficiency.

A comparison of a random copolymer and a block-copolymer by ^{13}C NMR spectra is shown in **Figure 4.73**. The diads and triads were assigned according to the literature[140,141,191] although the peaks were slightly

shifted and further split up due to higher resolution of the NMR equipment and a different deuterated solvent.

Table 4.13: Summary of the synthesized linear poly(propylene sulfide-*b*-ethylene sulfide) and poly(ethylene sulfide-*b*-propylene sulfide) copolymers (initiator: **BT**).

	Theo. DP **PS**	Theo. DP **ES**	$\overline{DP_n}$ **PS** (^{1}H NMR)	$\overline{DP_n}$ **ES** (^{1}H NMR)	$\overline{M_n}$ (^{1}H NMR) [g·mol^{-1}]	$\overline{M_n}$ (SEC)* [g·mol^{-1}]	PDI (SEC)*
PPS-PES 1	10	5	11	7	1400	1500	1.14
PPS-PES 2	20	5	22	7	2300	2200	1.21
PPS-PES 3	30	5	33	7	3100	3300	1.19
PPS-PES 4	40	5	37	7	3400	3900	1.28
PES-PPS 1	10	5	13	5	1500	1200	1.27
PES-PPS 2	20	5	23	5	2200	1800	1.23
PES-PPS 3	30	5	34	5	3000	2600	1.26
PES-PPS 4	40	5	42	7	3700	2800	1.46

*SEC: eluent: TCM; polystyrene standard calibration

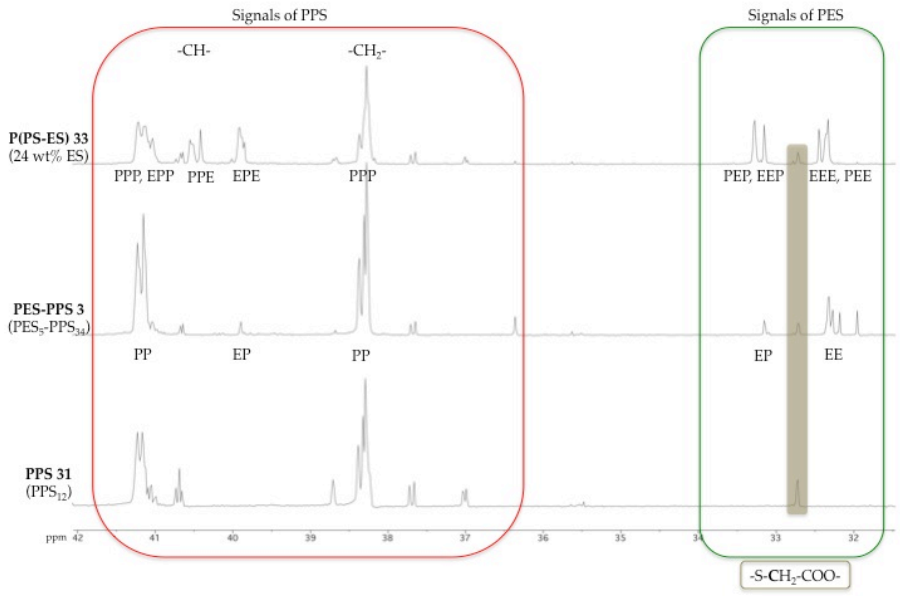

Figure 4.73: ^{13}C NMR spectra sections of different linear polysulfides **PPS 31, PES-PPS 3 and P(PS-ES) 33** (75.5 MHz, $CDCl_3$) from 31-42 ppm and assignment of the diads and triads.

In literature, the ^{13}C NMR (25.14 MHz, C_6D_6) signal of the methylene carbon of a poly(propylene sulfide) homopolymer was described as a singlet at 39.0 ppm and the methine carbon exhibited two peaks between 41 and 42 ppm, caused by the tacticity.[191] The carbon peaks of the PPS homopolymer **PPS 31**, initiated by benzyl thioacetate and terminated with ethyl bromoacetate, exhibited several split ups

(**Figure 4.73**, spectrum on the bottom). Beside the higher frequency of the NMR equipment, these findings might be caused by the influence of the initiator and end-capping reagent. The linear block-copolymer (**Figure 4.73**, spectrum in the middle) was used to assign the diads according to the named literature and the random copolymer for the assignment of the triads (**Figure 4.73**, spectrum on the top). The block-copolymer and the random copolymer showed significant differences in the peak splitting of the carbon atoms in NMR spectroscopy. Obviously, the random copolymer did not lead to block-like structures despite the higher reactivity of ethylene sulfide compared to propylene sulfide.

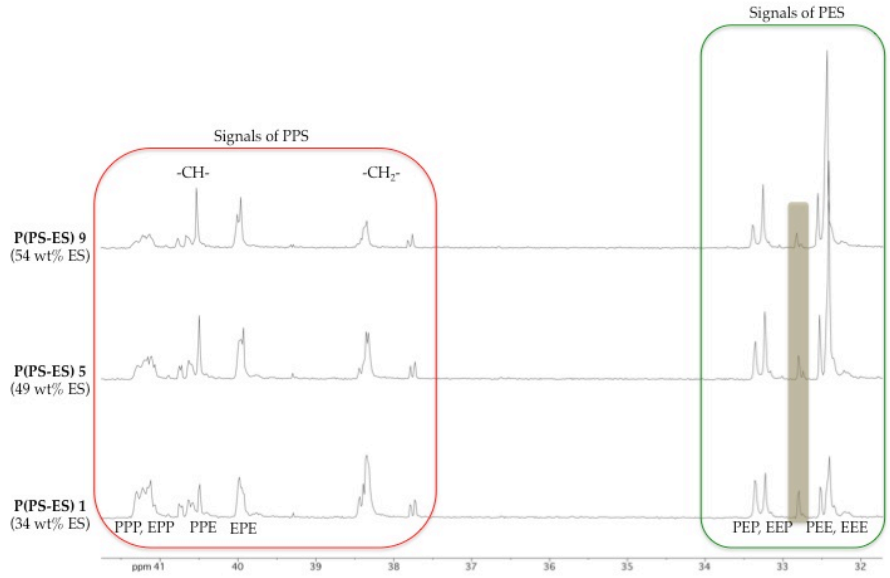

Figure 4.74: ^{13}C NMR spectra of **P(PS-ES) 1, 5 and 9** (75.5 MHz, $CDCl_3$) from 32-41 ppm and assignment of the triads.

In **Figure 4.74** the triads of three different star-shaped random copolymers **P(PS-ES) 1, 5 and 9** with increasing ES content are illustrated. The triads were assigned according to the literature and the information obtained by the NMR analysis of the different linear polysulfides. Apparently, the signal intensity of the poly(propylene sulfide) decreased and the signal of the poly(ethylene sulfide) increased with increasing ES content, as expected. Different signals were investigated in more detail, the triad signals of the PPP and the EPP series decreased with increasing ES content and the triads of PPE and EPE increased. The signals of the PES exhibited a similar behavior. The intensity of the PEP triad decreased with increasing ES content and the EEP as well as the PEE triad slightly increased, as expected, and the intensity of the EEE triad increased significantly.

The molecular weight distribution of the synthesized polysulfides was reduced via recycling preparative HPLC in chloroform. This was shown for **P(PS-ES) 8** as an example. The used copolymer exhibited the highest PDI of the star-shaped polysulfides with 1.86. SEC traces before purification and afterwards are shown in **Figure 4.75**. Its PDI was lowered to 1.29 after purification. The ES content was calculated via proton NMR spectroscopy and did not change significantly. The ES content before recycling preparative HPLC averaged 20% and afterwards 19%.

In summary, the triad analysis as well as the slightly decreasing ES content after separation of the low molecular compounds via recycling preparative HPLC indicated a tenuous gradient incorporation of the ethylene sulfide during the random copolymerization of episulfides. In addition, the solubility of the

random copolymers in contrast to the insoluble block-copolymers from the macroinitiator **Hb 1** confirmed the nearly random structure of the synthesized compounds.

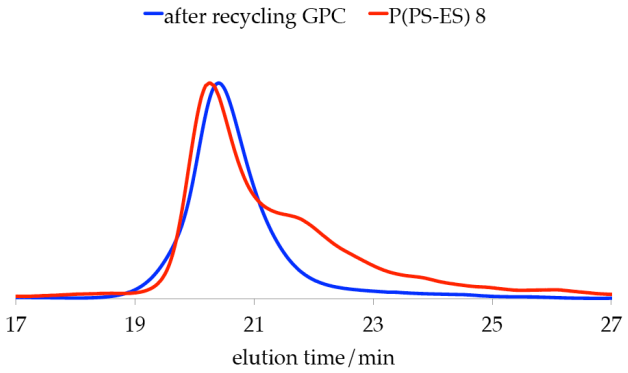

Figure 4.75: SEC-traces (eluent: TCM; polystyrene standard calibration) of **P(PS-ES) 8** before and after recycling preparative HPLC.

The thermal behavior of the synthesized random copolymers initiated by PG-based macroinitiators was exemplarily analyzed via DSC. The results are summarized in **Table 4.14**.

Table 4.14: Summary of the thermal behavior of the synthesized random polyglycerol-poly(ethylene sulfide)-poly(propylene sulfide) copolymers.

	Macro-initiator	Content ES* (^{1}H NMR) [wt%]	$\overline{M_n}$ (^{1}H NMR) [g·mol^{-1}]	$\overline{M_n}$ PES per chain (^{1}H NMR) [g·mol^{-1}]	$\overline{M_n}$ PPS per chain (^{1}H NMR) [g·mol^{-1}]	$\overline{M_n}$ PPS-PES per chain (^{1}H NMR) [g·mol^{-1}]	T_m (DSC)** [°C]	T_g (DSC)** [°C]
P(PS-ES) 1	Hb 1	34	9400	7 x 400	7 x 800	7 x 1200	-	-49
P(PS-ES) 5	Hb 1	49	12200	7 x 700	7 x 700	7 x 1400	-	-50
P(PS-ES) 9	Hb 1	54	9800	7 x 600	7 x 500	7 x 1100	-	-51
P(PS-ES) 14	Li 3	35	22700	18 x 400	18 x 700	18 x 1100	-	-53
P(PS-ES) 22	Li 3	53	35100	18 x 900	18 x 800	18 x 1700	-	-50

*content ES of the polysulfide content; **DSC: temperature range: -95 °C – 250 °C with 10 °C·min^{-1}

DSC traces of the synthesized polyglycerol-poly(ethylene sulfide)-poly(propylene sulfide) copolymers did not show a melting temperature of a PES block, which emphasized also the random structure of the polysulfides. For block-copolymer structures consisting of poly(ethylene sulfide) a melting point of the crystalline PES block would be expected. The glass transition temperatures of the PG-based polysulfide copolymers were similar to them from the PG-based poly(propylene sulfide) copolymers. In case of the star copolymers the T_g seemed to depend only on the length of the PPS arms. The measured values were similar to those of the *hb*PG-PPS and decreased with decreasing molecular weight of the PPS content. The

copolymer brush **P(PS-ES) 22** exhibited a similar value. For **P(PS-ES) 14** a surprisingly low T_g was detected at -53 °C, which might be caused by the error margin of the measurement. The results demonstrated that the content of ES did not influence the thermal behavior of polyglycerol-poly(ethylene sulfide)-poly(propylene sulfide) copolymers significantly.

4.5 Poly(ethylene glycol)-poly(allyl glycidyl ether)-based polysulfides

The synthesized poly(ethylene glycol)-poly(allyl glycidyl ether)-based macroinitiator **PEG I** was used to obtain polysulfides with one PEG chain. The copolymer structures were varied according to different episulfides and various block lengths. The use of PEG-PAGE-based macroinitiators led to comb-like polymers (**Figure 4.76**), which were similar to the brush copolymer with an additional PEG chain.

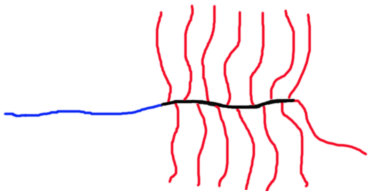

Figure 4.76: Scheme of PEG-PAGE-based polysulfide copolymers with comb-like architecture (red = polysulfide; black = PAGE; blue = PEG).

4.5.1 PEG-PAGE-based poly(propylene sulfide)

The thioacetate functionalized diblock-copolymer was used as macroinitiator for the anionic ring-opening polymerization of propylene sulfide **(Figure 4.77)**.

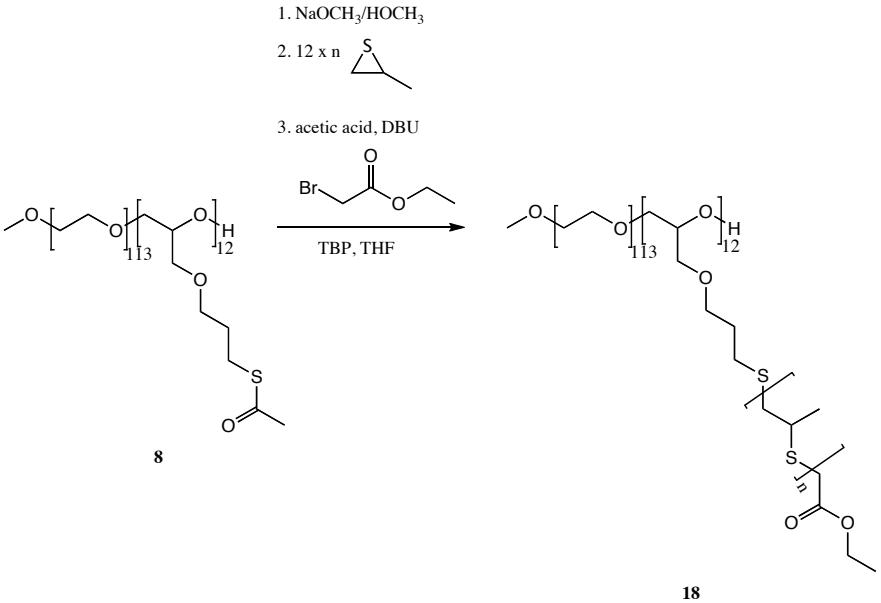

Figure 4.77: Polymerization of PS with PEG-PAGE-based macroinitiator to comb-like copolymers.

The graft-polymerization of propylene sulfide was carried out under the common conditions as described for the polyglycerol-based macroinitiators in chapter 4.4.1. The degree of polymerization was varied in the range of ten to forty per thioacetate group of the macroinitiator. The results of the synthesized comb copolymers consisting of poly(propylene sulfide) are summarized in **Table 4.15**. Graft-copolymerization of propylene sulfide was successfully conducted with a PEG-containing diblock-copolymer as macroinitiator.

The PEG chain of the copolymers influenced the physical properties. Unlike the copolymers with the PG-based macroinitiators, the polysulfide copolymers with a DP of ten or twenty were soluble in methanol, but insoluble in cold diethyl ether. In contrast to this, the comb-like copolymers with DP of thirty and forty were soluble in diethyl ether and insoluble in methanol, as expected for polysulfides. The influence of the PEG chain was also visually observable. The photographs of the four different PPS copolymers are shown in **Figure 4.78**. Copolymer **PPS 35** with nine monomer units per initiating groups was solid and with increasing propylene sulfide content the material properties were shifted over wax-like to highly viscous.

Table 4.15: Summary of the synthesized poly(ethylene glycol)-poly(allyl glycidyl ether)-poly(propylene sulfide) copolymers.

	Macroinitiator	Theo. DP (per thioacetate)	$\overline{DP_n}$ (^{1}H NMR)	End-capping yield (^{1}H NMR) [mol%]	Theoretical $\overline{M_n}$ [g·mol^{-1}]	$\overline{M_n}$ (^{1}H NMR) [g·mol^{-1}]	$\overline{M_n}$ (SEC)* [g·mol^{-1}]	PDI (SEC)*
PPS 35	PEG I	12 x 10	12 x 9	100	16700	15800	7700	1.13
PPS 36	PEG I	12 x 20	12 x 14	85	25600	20300	13000	1.10
PPS 37	PEG I	12 x 30	12 x 20	85	34500	25600	15800	1.22
PPS 38	PEG I	12 x 40	12 x 31	100	43400	35400	21500	1.22

*SEC: eluent: DMF; PEG standard calibration

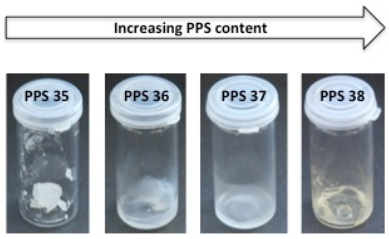

Figure 4.78: Photographs of the comb-like poly(propylene sulfide) copolymers (**PPS 35-38**).

The obtained copolymers **PPS 35-38** exhibited monomodal and narrow molecular weight distributions with PDIs below 1.25. SEC traces in DMF of the macroinitiator and the graft copolymers are illustrated in **Figure 4.79**.

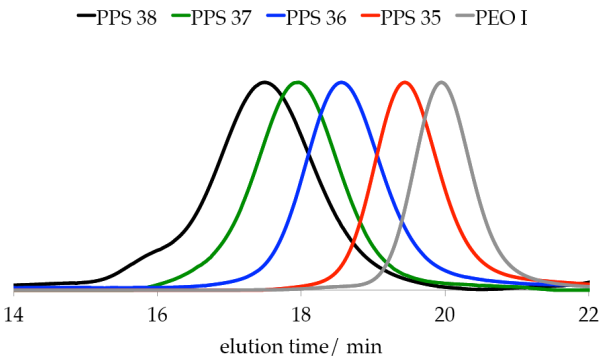

Figure 4.79: SEC traces (eluent: DMF; poly(ethylene glycol) standard calibration) of macroinitiator **PEG I** and corresponding PEG-PAGE-PPS graft copolymers **PPS 35-38** (DP 10-40 per thioacetate).

The side-reaction, which was observed for the polymerizations of propylene sulfide and led to low molecular weight side-products and thus a broader PDI, did not occur with the PEG-PAGE-based macroinitiator. The PEG chain might reduce the electrostatic repulsion of the growing copolymer with a high number of thiolates in close proximity. In addition, the low percentage of peroxidation of a commercially available PEG, which was used as skeletal structure of the macroinitiator, might suppress the deprotonation of the propylene sulfide, which constituted the initial step of the by-product formation.
The degree of polymerization of the obtained copolymers was calculated via ^{1}H NMR spectroscopy, similar to the PG-based polysulfide. The ratio of the peak areas of the methylene groups of the macroinitiators (-O-CH_2-**CH_2**-CH_2-S-; highlighted in yellow) and the peak area of the poly(propylene sulfide) signals ([-**CH_2**-**CH**(**CH_3**)-S-]$_n$; highlighted in green). The end-capping efficiency was determined analog via the signal of the methylene groups of the macroinitiator (-O-CH_2-**CH_2**-CH_2-S-) and the signal of the methylene groups of the ethyl acetate end-groups (-S-**CH_2**-COO-; highlighted in brown). In **Figure 4.80** the NMR spectrum of **PPS 36** is shown as an example. The calculated DPs were slightly lower than targeted. The obtained end-capping efficiency was for all comb-like copolymers higher than 85mol% and often quantitative.

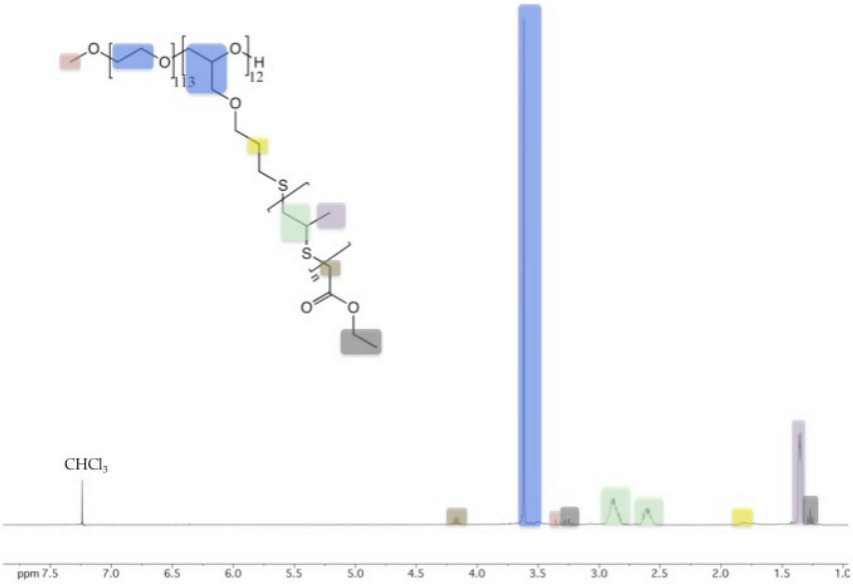

Figure 4.80: ^{1}H NMR spectrum of **PPS 36** (400 MHz, $CDCl_3$) and peak assignment of the copolymer structure.

Additionally, the comb-like PEG-PAGE-based poly(propylene sulfide) compounds were investigated by ^{13}C NMR spectroscopy. The ^{13}C spectrum of **PPS 35** and the peak assignment is illustrated in **Figure 4.81**.
The thermal behavior of copolymer **PPS 35** was analyzed by DSC.

Table 4.16: Summary of the thermal behavior of the PEG-PAGE-based poly(propylene sulfide) copolymer.

	Macroinitiator	$\overline{DP_n}$ (^{1}H NMR)	**Theoretical** $\overline{M_n}$ [g·mol^{-1}]	$\overline{M_n}$ (^{1}H NMR) [g·mol^{-1}]	$\overline{M_n}$ PPS per chain (^{1}H NMR) [g·mol^{-1}]	T_g (DSC)* [°C]	T_m (DSC)* [°C]
PPS 35	PEG I	12 x 9	16700	15800	12 x 700	-49	49

*DSC: temperature range: -95 °C – 220 °C with 10 °C·min^{-1}

The DSC trace is shown in **Figure 4.82** and the results are summarized in **Table 4.16**. The sample exhibited a glass transition temperature of the poly(propylene sulfide) arms at -49 °C and a melting point of the poly(ethylene glycol) block at 49 °C. The value of the T_g was comparable to them of the brush-like and star-shaped copolymers initiated by PG-based macroinitiator with a similar PPS arm lengths. The assumption that the macroinitiator and the architecture of the copolymer did not influence the thermal behavior of the poly(propylene sulfide), which seemed solely influenced by the length of one polysulfide arms, was confirmed by the analyzed copolymer comb with an addition PEG chain. In contrast to this, the polysulfide chains influenced the melting point of the PEG chain of the macroinitiator. The T_m of a corresponding PEG-PAGE block-copolymer was described to be at 57 °C.[235] The T_m of the PEG chain of the copolymer was significantly lowered.

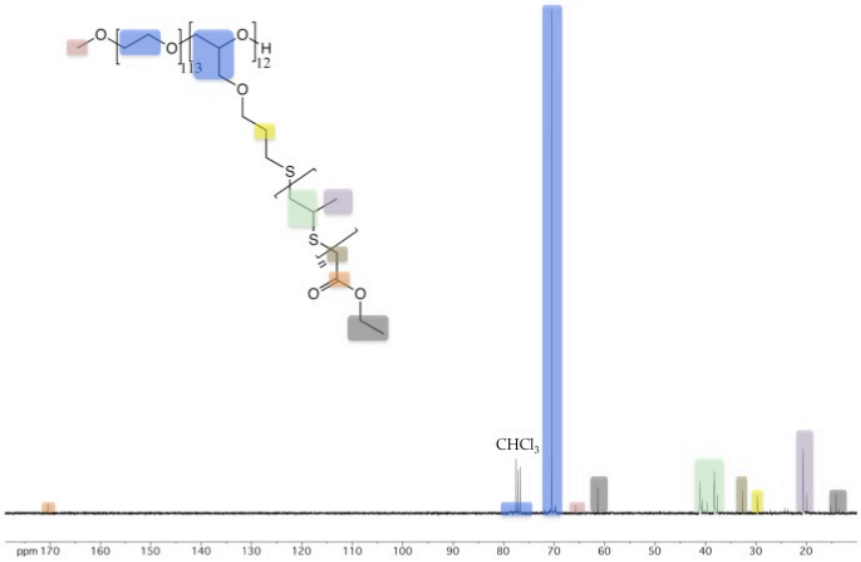

Figure 4.81: ^{13}C NMR spectrum of **PPS 35** (75.5 MHz, $CDCl_3$) and peak assignment of the copolymer structure.

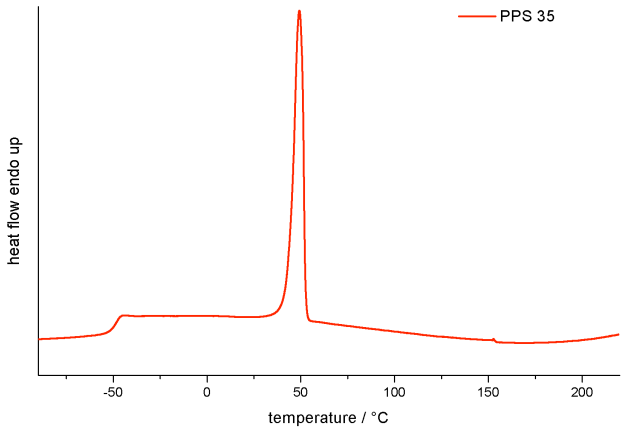

Figure 4.82: DSC trace (-100 °C – 220 °C with 10 °C·min^{-1}) of the PEG-PAGE-PPS graft copolymer **PPS 35** (DP 9 per thioactete).

4.5.2 PEG-PAGE-based poly(ethylene sulfide)

The PEG-PAGE-based macroinitiator was also used to initiate the anionic ring-opening polymerization of ethylene sulfide. This macroinitiator held an additional PEG-chain, which might be enabled to provide the synthesis of soluble PES containing copolymers by the concept of a large number of short PES arms. The polymerization was conducted in analogy to them with the PG-based macroinitiators in chapter 4.4.2. The reaction is illustrated in **Figure 4.83**.

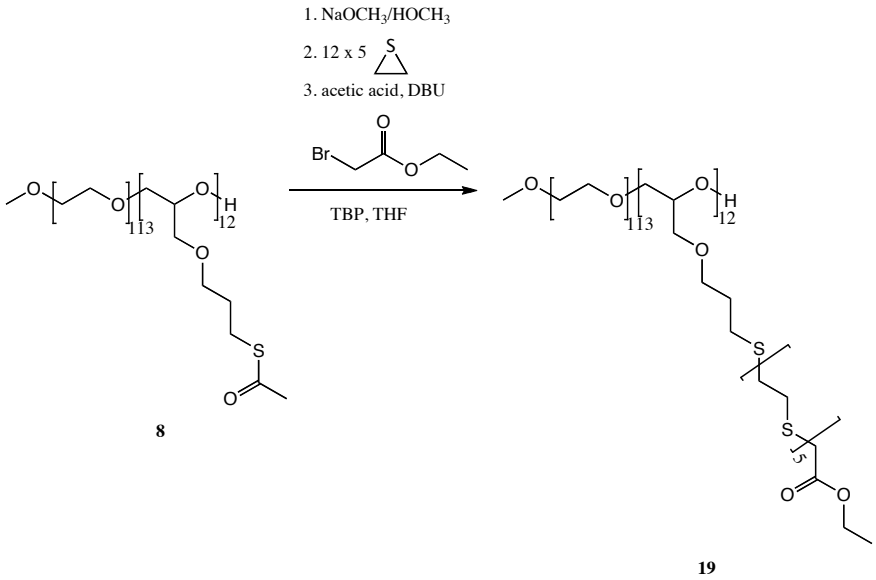

Figure 4.83: Polymerization of ES with PEG-PAGE-based macroinitiator to comb-like copolymers.

The result of the synthesis of copolymer **19** is shown in **Table 4.17**.

Table 4.17: Summary of the synthesized poly(ethylene glycol)-poly(allyl glycidyl ether)-poly(ethylene sulfide) copolymers.

	Macroinitiator	Theoretical DP (per thioacetate)	$\overline{DP_n}$ (^{1}H NMR)	End-capping yield (^{1}H NMR) [mol%]	Theoretical $\overline{M_n}$ [g·mol^{-1}]	$\overline{M_n}$ (^{1}H NMR) [g·mol^{-1}]	$\overline{M_n}$ (SEC)* [g·mol^{-1}]
PES 5	PEG I	12 x 5	12 x 5	97	11400	11400	-

*SEC: eluent: DMF; PEG standard calibration

Despite the PEG-chain, the concept of the synthesis of well soluble PES containing polymers failed also with the PEG-PAGE-based macroinitiator. Analysis via SEC was not possible, while the measurement of a proton NMR of the copolymer suspension was feasible. The NMR spectrum of **PES 5** is shown in **Figure 4.84**. The spectrum was used to calculate the DP and end-capping efficiency of the synthesized copolymer by the common strategy by the peak ratio of the CH_2-groups of the macroinitiator (-O-CH_2-**CH_2**-CH_2-S-) as well as the peak of the polymer backbone ([-**CH_2**-**CH_2**-S-]$_n$) and the CH_2-groups of the end-capping reagent (-S-**CH_2**-COO-), respectively. The targeted DP of five per initiating group was accomplished and the end-capping reaction with ethyl bromoacetate was nearly quantitative with 97mol%.

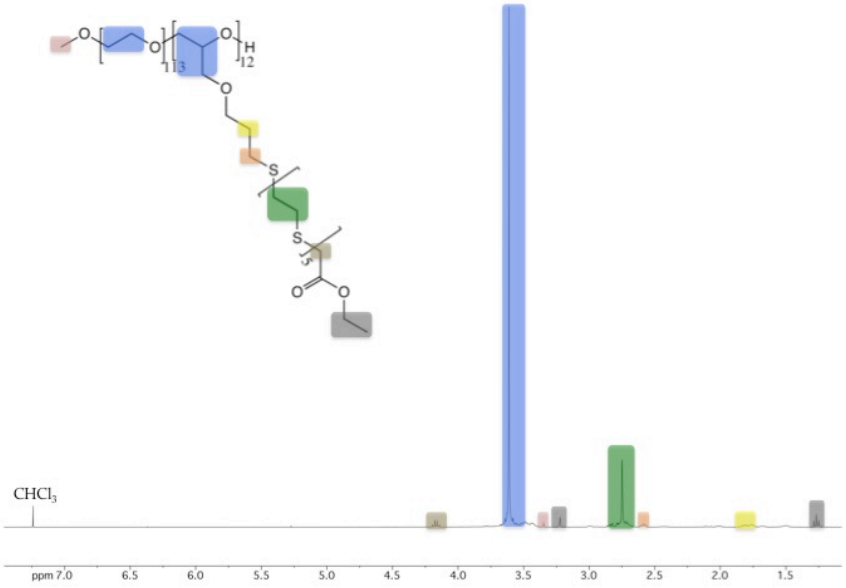

Figure 4.84: ^{1}H NMR spectrum of **PES 5** (400 MHz, $CDCl_3$) and peak assignment of the copolymer structure.

In addition, DSC was used to analyze the thermal behavior of the copolymer PES 5. The results are summarized in **Table 4.18**.

Table 4.18: Summary of the thermal behavior of the PEG-PAGE-based poly(ethylene sulfide) copolymer.

	Macroinitiator	$\overline{DP_n}$ (^{1}H NMR)	**Theoretical** $\overline{M_n}$ [g·mol^{-1}]	$\overline{M_n}$ (^{1}H NMR) [g·mol^{-1}]	$\overline{M_n}$ PPS per chain (^{1}H NMR) [g·mol^{-1}]	T_m^{PEG} (DSC)* [°C]	T_m^{PES} (DSC)* [°C]
PES 5	PEG I	12 x 5	11400	11400	300	47	103

*DSC: temperature range: -95 °C – 200 °C with 10 °C·min^{-1}

In comparison to the poly(propylene sulfide) analog of **PES 5**, the melting point of the PEG chain was again slightly lowered to 47 °C. The melting point of the PES arms was detected at 103 °C. Polyglycerol-based poly(ethylene sulfide) copolymers were significantly influenced by the architecture of the copolymers. The architecture of this comb-like copolymer was comparable to the copolymer brushes initiated by the *lin*PG-based macroinitiator. The value of **PES 5** with 103 °C matched to the values detected for the brush copolymers **PES 3** and **PES 4**. These PES-copolymers exhibited a linear trend of an increasing melting temperature with an increasing number of PES arms (**Figure 4.85**).

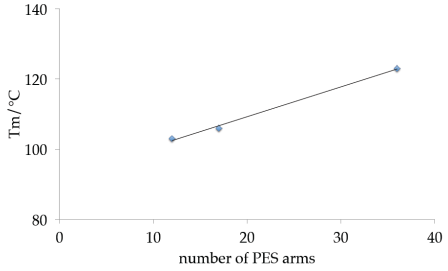

Figure 4.85: Melting temperature versus number of PES arms for **PES 3**-**5**.

4.5.3 PEG-PAGE-based random polysulfides

The macroinitiator **PEG I** was also used as initiator for the random copolymerization of ethylene sulfide and propylene sulfide. The anionic ring-opening polymerization was carried out under the common conditions as described before in chapter 4.4.3. **Figure 4.86** shows the conducted synthesis.

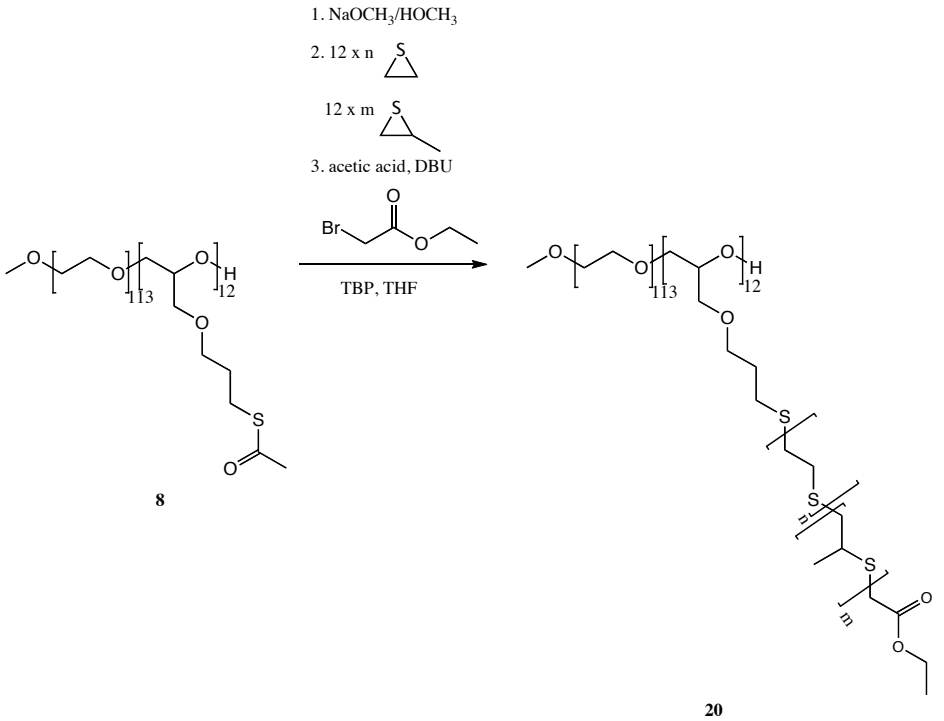

Figure 4.86: Random polymerization of ES and PS with PEG-PAGE-based macroinitiator to comb-like polymers.

The DP of propylene sulfide per initiating group was varied in the range of ten to forty and the DP of ethylene sulfide per thioacetate was modified in each case from five over ten to fifteen, which corresponds to an ethylene sulfide content between 9 and 55wt%. Random copolymerization of ethylene sulfide and propylene sulfide initiated by the PEG-PAGE-based macroinitiator was successful. The results of the synthesized random copolymers are summarized in **Table 4.19**. In summary, the polymers were slightly smaller than targeted. A similar trend was also observed for the corresponding copolymers with the polyglycerol-based macroinitiators as well as in case of the analog poly(propylene sulfide) copolymers. However, the obtained ES content was with 11 to 57wt% again up to 5wt% higher than targeted, due to the higher reactivity of ethylene sulfide.

The PDIs of the copolymers with low DPs of ethylene sulfide and propylene sulfide, such as the copolymers **P(PS-ES) 38-40, 42**, **43 and 46** were rather low with below 1.50. Although with increasing DP of the two episulfides monomers the molecular weight distribution increased. The already described side-reaction was observed and a low molecular compound occurred in SEC. As an example the SEC traces of the random copolymers **P(PS-ES) 38-41** in DMF are shown in **Figure 4.87**. The molecular weight distribution was narrow up to a DP of thirty for propylene sulfide. In contrast, for a DP of forty for PS a low molecular weight by-product was formed.

Different contents of the monomers influenced the physical properties as expected. The synthesized copolymers with a DP of five for ES per initiating group were with increasing PPS content first wax-like and later highly viscous, in analogy to the poly(propylene sulfide) comb copolymers. However, with increasing

ES content the copolymers were more solid and crystalline. In **Figure 4.88** are the photographs of the different random polysulfides illustrated.

Table 4.19: Summary of the PEG-PAGE-based poly(propylene sulfide)-poly(ethylene sulfide) random comb copolymers (macroinitiator: **PEG I**).

	Theo. DP PS (per thioacetate)	**Theo. DP ES** (per thioacetate)	$\overline{DP_n}$ **PS** (^{1}H NMR)	$\overline{DP_n}$ **ES** (^{1}H NMR)	**Theo. content ES*** [wt%]	**Content ES*** (^{1}H NMR) [wt%]	$\overline{M_n}$ (^{1}H NMR) [g·mol^{-1}]	$\overline{M_n}$ (SEC)** [g·mol^{-1}]	PDI (SEC)**
P(PS-ES) 38	12 x 10	12 x 5	12 x 8	12 x 5	29	34	18500	10300	1.20
P(PS-ES) 39	12 x 20	12 x 5	12 x 14	12 x 4	17	19	23200	13400	1.16
P(PS-ES) 40	12 x 30	12 x 5	12 x 19	12 x 4	12	15	27600	17300	1.16
P(PS-ES) 41	12 x 40	12 x 5	12 x 27	12 x 4	9	11	34700	10800	1.94
P(PS-ES) 42	12 x 10	12 x 10	12 x 7	12 x 8	45	48	19800	8100	1.46
P(PS-ES) 43	12 x 20	12 x 10	12 x 15	12 x 9	29	33	27700	11300	1.42
P(PS-ES) 44	12 x 30	12 x 10	12 x 22	12 x 8	21	23	33200	10000	1.87
P(PS-ES) 45	12 x 40	12 x 10	12 x 29	12 x 8	17	18	39400	11700	1.94
P(PS-ES) 46	12 x 10	12 x 15	12 x 6	12 x 10	55	57	20400	13600	1.14
P(PS-ES) 47	12 x 20	12 x 15	12 x 14	12 x 12	38	41	28900	10400	1.65
P(PS-ES) 48	12 x 30	12 x 15	12 x 22	12 x 12	29	31	36100	9800	1.99
P(PS-ES) 49	12 x 40	12 x 15	12 x 25	12 x 9	23	23	36600	10000	2.60

*content ES of the polysulfide content; **SEC: eluent: DMF; PEG standard calibration

The end-capping efficiency was calculated via ^{1}H NMR spectroscopy, as demonstrated before via the peak ratio of the methylene groups of the macroinitiator (-O-CH_2-**CH_2**-CH_2-S-) and the peaks of the methylene group of the terminating reagent (-S-**CH_2**-COO-). In most cases the end-capping efficiency of the copolymers were higher than 85mol% and were often higher than 90mol%.

The DPs of ethylene sulfide and propylene sulfide were also determined by NMR spectroscopy via the peak ratios of the CH_2-groups of the macroinitiator (-O-CH_2-**CH_2**-CH_2-S-) and the signals of the polymer backbone for propylene sulfide ([-**CH_2**-**CH**(**CH_3**)-S-]$_n$) as well as for ethylene sulfide ([-**CH_2**-**CH_2**-S-]$_n$). **Figure 4.89** shows the ^{1}H NMR of **P(PS-ES) 38** as an example.

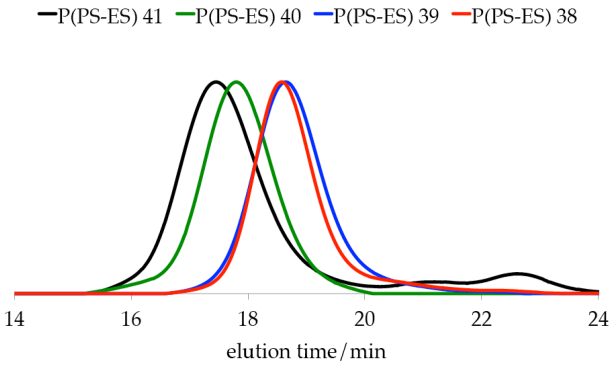

Figure 4.87: SEC traces (eluent: DMF; poly(ethylene glycol) standard calibration) of the PEG-PAGE-PPS random graft copolymers **P(PS-ES) 38-41**.

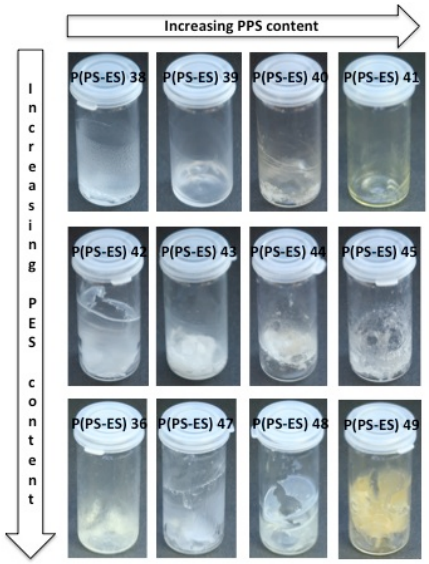

Figure 4.88: Photographs of the random comb-like polysulfides (**P(PS-ES) 38-49**).

^{13}C NMR spectroscopy was used to prove the random or rather random structure of the poly(ethylene sulfide)-poly(propylene sulfide) copolymers initiated by the macroinitiator **PEG I**, which was based on a PEG-PAGE diblock-copolymer. The ^{13}C NMR spectrum of **P(PS-ES) 38** is illustrated in **Figure 4.90a**. The signals of the methylene and methine carbon atoms of propylene sulfide from 37-42 ppm as well as the carbon signals of the ethylene sulfide backbone from 32-34 ppm are shown in **Figure 4.90b** in more detail. The different triads were assigned according to the polyglycerol-based random polysulfides in chapter 4.4.3 and the in literature described results of linear random polysulfide copolymers.[140,141,191] The splitting of the different signals of both episulfide monomers supported the random or rather random structure of comb-like copolymer compounds. It was presumably a rather random structure due to the higher reactivity of the ethylene sulfide and hence, a slight gradient in the incorporation of the two monomers might occure, which led first to ES richer and later to PS richer regions in the copolymer structure.

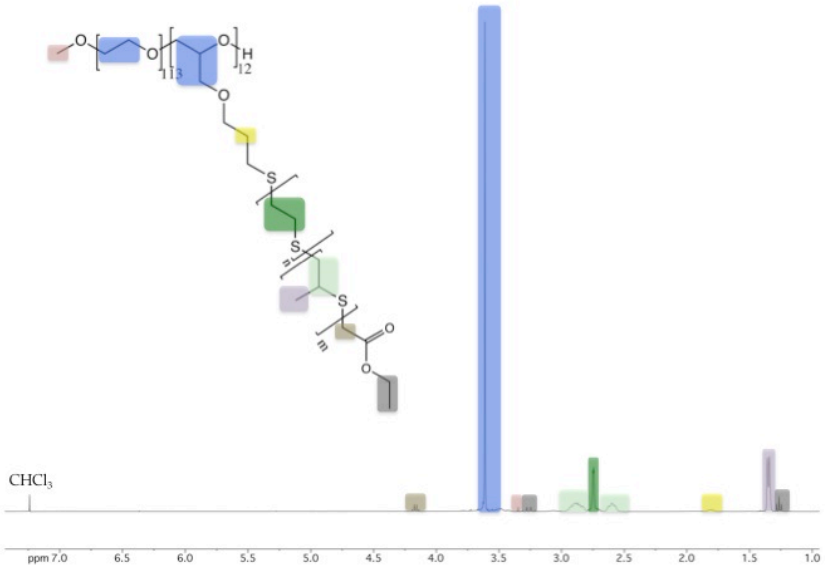

Figure 4.89: ^{1}H NMR spectrum of **P(PS-ES) 38** (400 MHz, $CDCl_3$) and peak assignment of the copolymer structure.

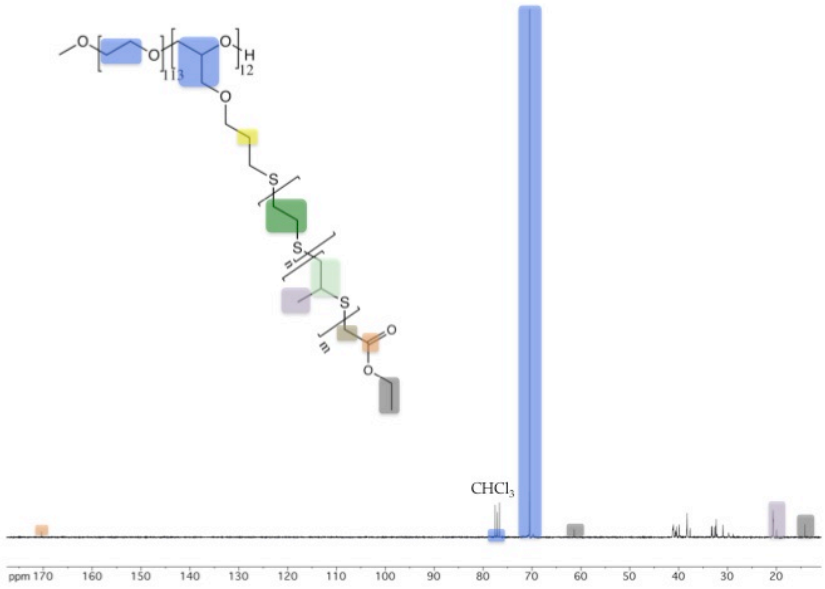

Figure 4.90a: ^{13}C NMR spectrum of **P(PS-ES) 38** (75.5 MHz, $CDCl_3$) and peak assignment of the copolymer structure.

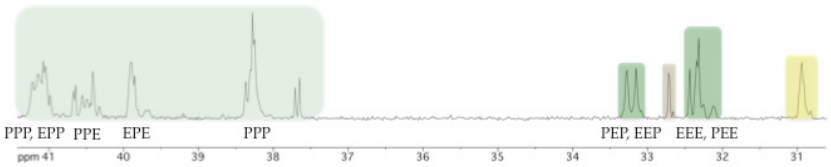

Figure 4.90b: ^{13}C NMR spectrum sections of **P(PS-ES) 38** (75.5 MHz, $CDCl_3$) from 31-42 ppm and assignment of the triads.

The thermal behavior of the synthesized random copolymers was investigated by DSC measurements and the results are summarized in **Table 4.20**.

Table 4.20: Summary of the thermal behavior of the PEG-PAGE-based random polysulfide copolymer.

	Macro-initiator	**Content ES*** (^{1}H NMR) [wt%]	$\overline{M_n}$ (^{1}H NMR) [g·mol^{-1}]	$\overline{M_n}$ PES per chain (^{1}H NMR) [g·mol^{-1}]	$\overline{M_n}$ PPS per chain (^{1}H NMR) [g·mol^{-1}]	$\overline{M_n}$ PPS-PES per chain (^{1}H NMR) [g·mol^{-1}]	**T_g** (DSC)* [°C]	**T_m** (DSC)* [°C]
P(PS-ES) 38	PEG I	34	18500	300	600	900	-50	48
P(PS-ES) 42	PEG I	48	19800	500	500	1000	-48	48
P(PS-ES) 46	PEG I	57	20400	600	450	1050	-48	42

*DSC: temperature range: -95 °C – 200 °C with 10 °C·min^{-1}

The analyzed random copolymer with one PEG chain and a comb-like structure exhibited a glass transition temperature of the polysulfide arms and a melting point of the PEG chain. A T_g of the polysulfide chains was detected at -50 °C and -48 °C, respectively. These results suggested again that the T_g of the copolymers was only influenced by the poly(propylene sulfide) content. Similar results were observed in case of the polyglycerol-based star-shaped and brush-like random polysulfide copolymers. The melting temperature of the PEG chains of the samples **P(PS-ES) 38** and **42** with 34wt% and 48wt% ES content was detected at 48 °C. This value was comparable to the T_ms measured for the poly(ethylene sulfide) copolymers (chapter 4.5.2) and the poly(propylene sulfide) copolymers (chapter 4.5.1). The copolymer sample **P(PS-ES) 46** exhibited a surprising low T_m of the PEG chain with 42 °C.

4.6 Poly(allyl glycidyl ether)-poly(ethylene glycol)-poly(allyl glycidyl ether)-based polysulfides

The synthesized poly(allyl glycidyl ether)-poly(ethylene glycol)-poly(allyl glycidyl ether)-based macroinitiator **PEG II** was used to obtain polysulfides with one PEG chain in the middle, between several polysulfide arms. Its copolymer structures were varied according to different episulfides and various block lengths. The use of PAGE-PEG-PAGE-based macroinitiators led to pom-pom copolymers (**Figure 4.91**).

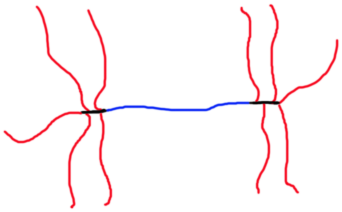

Figure 4.91: Scheme of PAGE-PEG-PAGE-based polysulfide copolymers with pom-pom-like architecture (red = polysulfide; black = PAGE; blue = PEG).

4.6.1 PAGE-PEG-PAGE-based poly(propylene sulfide)

The thioacetate functionalized triblock-copolymer consisting of PAGE and PEG was used as macroinitiator for the anionic ring-opening polymerization of propylene sulfide. The conducted synthesis is illustrated in **Figure 4.92**.

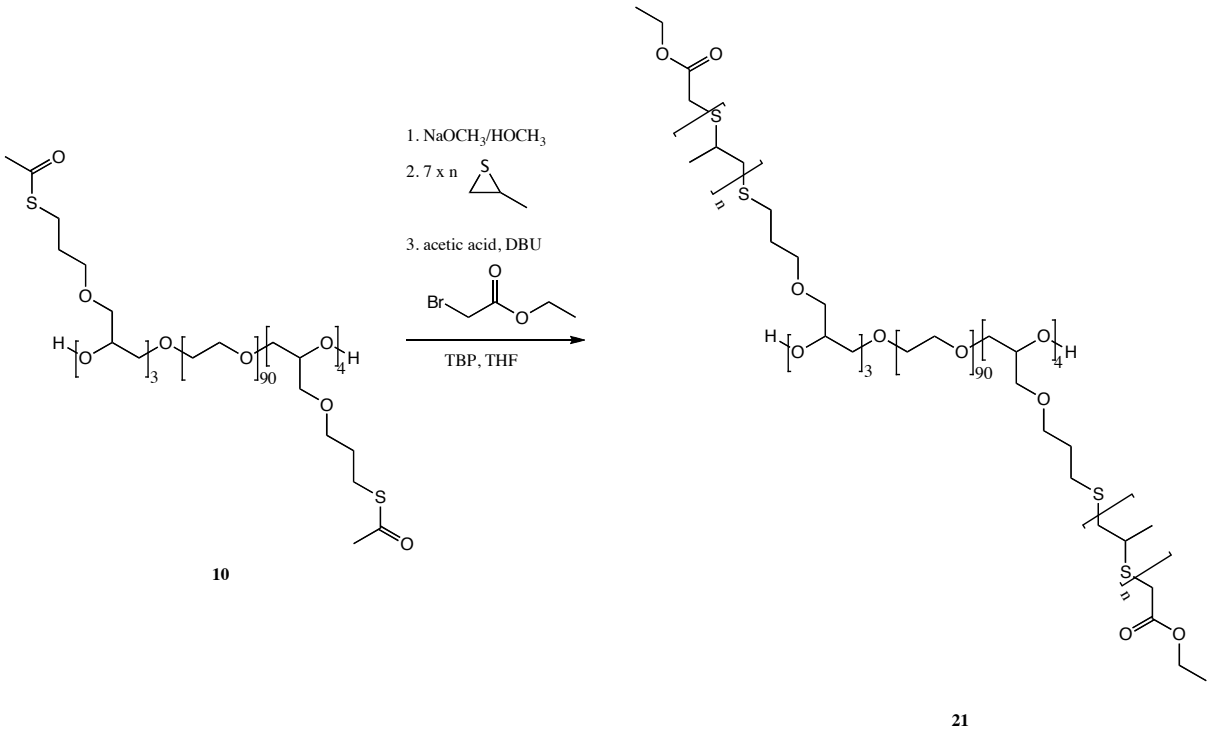

Figure 4.92: Polymerization of PS with PAGE-PEG-PAGE-based macroinitiator to pom-pom-like copolymers.

The polymerization was conducted under the same conditions as described for polysulfides initiated by linear and hyperbranched polyglycerol-based macroinitiators (chapter 4.5.1) as well as PEG-PAGE-based macroinitiator (chapter 4.5.1). The synthesis of pom-pom-like polysulfide was successful. The results of the PAGE-PEG-PAGE-based poly(propylene sulfide) copolymers are summarized in **Table 4.21**. The DP of propylene sulfide was varied from ten to forty per initiating group.

Table 4.21: Summary of the synthesized poly(allyl glycidyl ether)-poly(ethylene glycol)-poly(allyl glycidyl ether)-poly(propylene sulfide) copolymers.

	Macroinitiator	Theo. DP (per thioacetate)	$\overline{DP_n}$ (^{1}H NMR)	End-capping yield (^{1}H NMR) [mol%]	Theoretical $\overline{M_n}$ [g·mol^{-1}]	$\overline{M_n}$ (^{1}H NMR) [g·mol^{-1}]	$\overline{M_n}$ (SEC)* [g·mol^{-1}]	PDI (SEC)*
PPS 39	PEG II	7 x 10	7 x 10	100	10800	10800	7700	1.12
PPS 40	PEG II	7 x 20	7 x 19	91	16000	15500	11700	1.26
PPS 41	PEG II	7 x 30	7 x 31	89	21200	21700	13100	1.17
PPS 42	PEG II	7 x 40	7 x 37	100	26400	24800	15400	1.19

*SEC: eluent: DMF; PEG standard calibration

The physical properties of the obtained copolymers were similar to them of the comb-like copolymers with one PEG chain. With increasing propylene sulfide content the state of matter of the copolymers was shifted from solid over wax-like to highly viscous. This behavior is illustrated with photographs in **Figure 4.93**. Copolymers with propylene sulfide DPs of ten or twenty per thioacetate group of the macroinitiator were soluble in methanol and insoluble in cold diethyl ether. The copolymers **PPS 39** and **40** were both insoluble in methanol and cold diethyl ether.

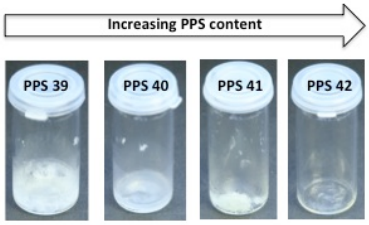

Figure 4.93: Photographs of the pom-pom-like poly(propylene sulfide) copolymers (**PPS 39-42**).

The synthesized poly(propylene sulfide) graft-copolymers exhibited monomolecular and narrow molecular weight distributions with PDIs below 1.30. SEC traces of the macroinitiator **PEG II** and the four different pom-pom-like copolymers with poly(propylene sulfide) **PPS 39-42** is shown in **Figure 4.94**.

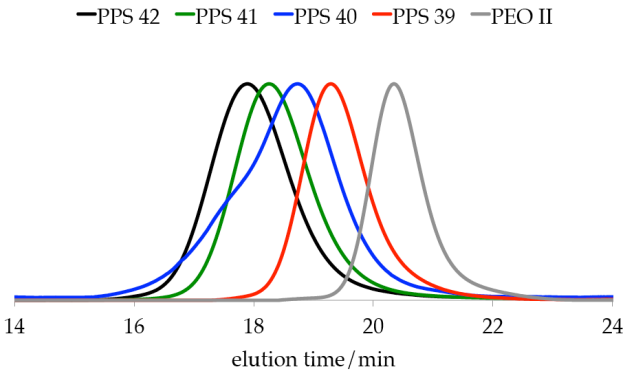

Figure 4.94: SEC traces (eluent: DMF; poly(ethylene glycol) standard calibration) of macroinitiator **PEG II** and corresponding PAGE-PEG-PAGE-PPS graft copolymers **PPS 39-42** (DP 10-40 per thioacetate).

Formation of the homopolymer as side-reaction due to the deprotonation and rearrangement of propylene sulfide did not occur in case of **PEG II**. This result supported the observation of the propylene sulfide polymerization with the PEG-PAGE-based macroinitiator **PEG I** that the PEG chain of the macroinitiator suppressed the formation of the low molecular weight by-product.

The achieved DP as well as the end-capping efficiency was again determined via proton NMR spectroscopy. As an example the ^{1}H NMR spectrum of **PPS 42** is shown in **Figure 4.95**.

The DP of propylene sulfide per initiating group was analyzed by the ratio of the peak areas of the PEG backbone of the macroinitiator ([-**CH$_2$**-**CH$_2$**-O-]$_n$); highlighted in blue) and the peak area of the poly(propylene sulfide) signals ([-**CH$_2$**-**CH**(**CH$_3$**)-S-]$_n$; highlighted in green). The achieved DPs per thioacetate group were almost as targeted, except **PPS 42** was with 37 monomer units slightly smaller than targeted. The end-capping efficiency was determined analog via signal of the PEG backbone of the macroinitiator ([-**CH$_2$**-**CH$_2$**-O-]$_n$) and the signal of the methylene groups of the ethyl acetate end-groups (-S-**CH$_2$**-COO-; highlighted in brown). The calculated termination of the active end-groups amounted for all copolymers more than 89 mol% and was often quantitative.

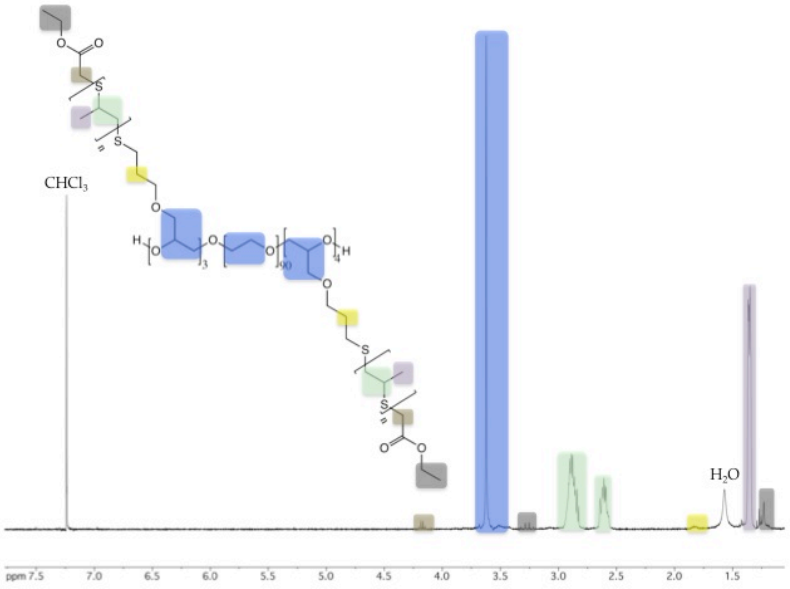

Figure 4.95: ^{1}H NMR spectrum of **PPS 42** (400 MHz, $CDCl_3$) and peak assignment of the copolymer structure.

In addition, the pom-pom-like PPS copolymers based on a PAGE-PEG-PAGE macroinitiator were analyzed by ^{13}C NMR spectroscopy. In **Figure 4.96** the ^{13}C NMR spectrum of **PPS 39** and the peak assignment is illustrated.

DSC was used to analyze the thermal behavior of **PPS 39**. In **Table 4.22** these results are summarized. The copolymer sample **PPS 39** with ten monomer repeating units per initiating groups exhibited a glass transition temperature at -49 °C and a melting temperature at 40 °C in DSC. As expected, the T_g of the poly(propylene sulfide) arms was similar to the values detected for star-shaped polysulfides as well as the comb- and brush-like PPS copolymers with molecular weights of 700 to 800 g·mol^{-1}. The melting point of the PEG chain was with 40 °C significant lower than for the PPS copolymers initiated by the PEG-PAGE-based macroinitiator. On the one hand, the shorter PEG chain in case of macroinitiator PEG II with a molecular weight of 4000 g·mol^{-1} compared to 5000 g·mol^{-1} of **PEG I** might explain this result. Additionally, **PEG II** was based on a triblock-copolymer of PAGE and poly(propylene sulfide) and the PEG chain was modified on

both sides. Although the number of repeating units was with seven units smaller compared to the PEG-PAGE diblock-copolymer with twelve monomer units in case of **PEG I**.

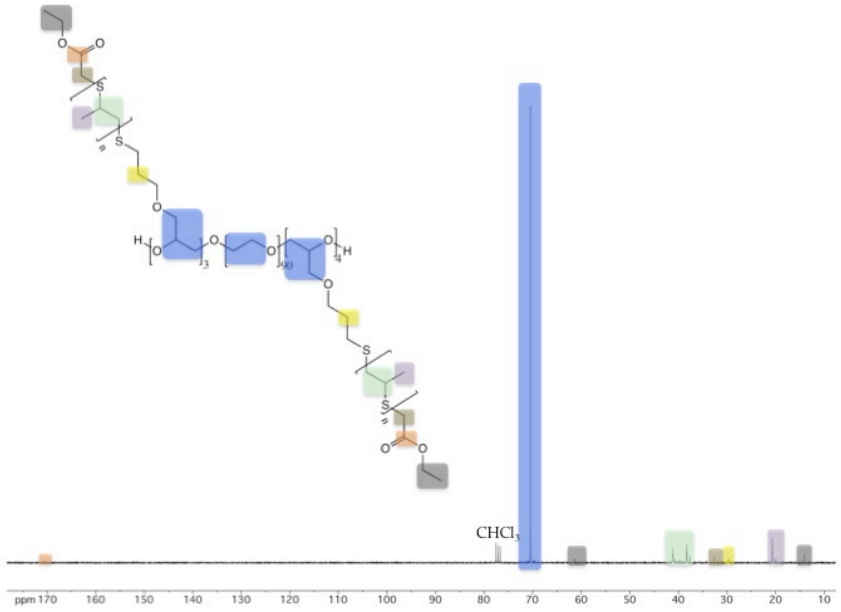

Figure 4.96: ^{13}C NMR spectrum of **PPS 39** (75.5 MHz, $CDCl_3$) and peak assignment of the copolymer structure.

Table 4.22: Summary of the thermal behavior of the PAGE-PEG-PAGE-based poly(propylene sulfide) copolymer.

	Macroinitiator	$\overline{DP_n}$ (^{1}H NMR)	**Theoretical** $\overline{M_n}$ [g·mol^{-1}]	$\overline{M_n}$ (^{1}H NMR) [g·mol^{-1}]	$\overline{M_n}$ PPS per chain (^{1}H NMR) [g·mol^{-1}]	T_g (DSC)* [°C]	T_m (DSC)* [°C]
PPS 39	PEG II	7 x 10	10800	10800	7 x 800	-49	40

*DSC: temperature range: -95 °C – 220 °C with 10 °C·min^{-1}

4.6.2 PAGE-PEG-PAGE-based poly(ethylene sulfide)

The thioacetate functionalized triblock-copolymer PAGE-PEG-PAGE was used as macroinitiator to synthesize soluble poly(ethylene sulfide) containing copolymer structures. The synthesis was conducted under the common conditions as described before. Synthesis of pom-pom-like copolymers with the PAGE-PEG-PAGE-based macroinitiator **PEG II** is shown in **Figure 4.97**.

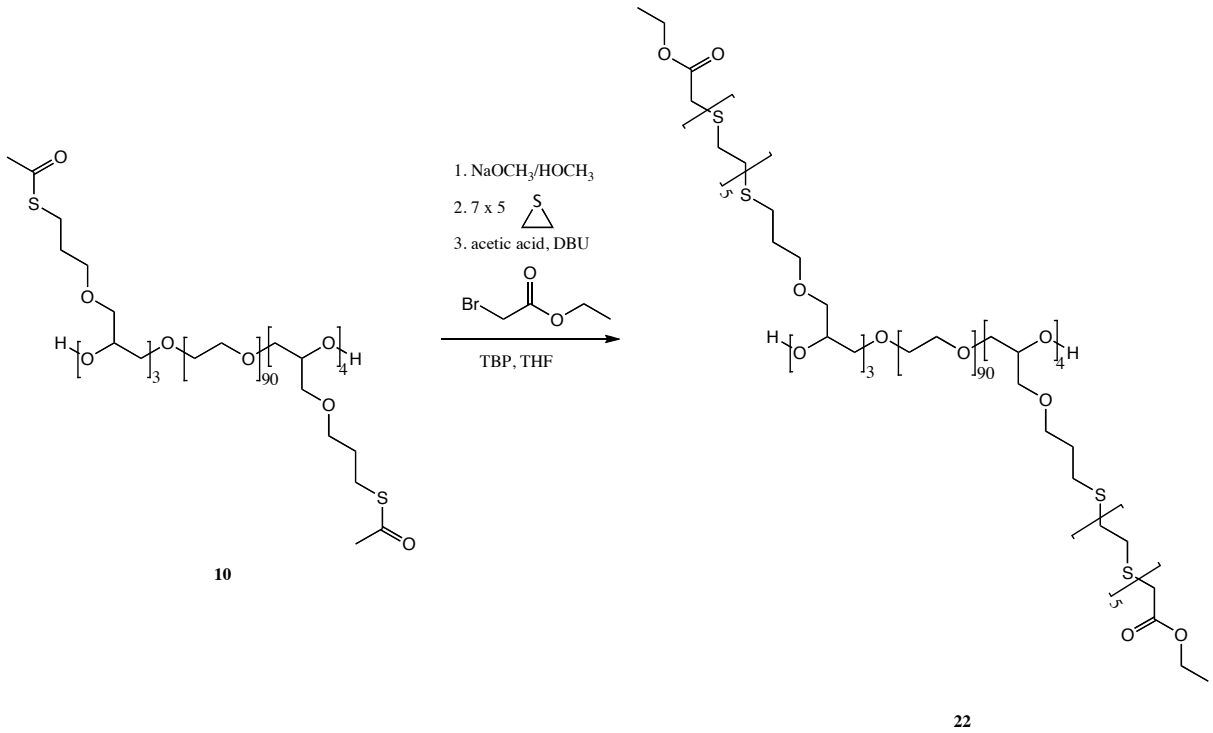

Figure 4.97: Polymerization of ES with PAGE-PEG-PAGE-based macroinitiator to pom-pom-like copolymers.

The results of the graft-polymerization of ethylene sulfide are summarized in Table **4.23**. The concept of the synthesis of soluble poly(ethylene sulfide) containing copolymers by the use of a macroinitiator with multiple initiating groups and short PES chains was successful with the macroinitiator **PEG II**. The obtained copolymer was soluble in chloroform as well as dichloromethane and a complete characterization was enabled.

Table 4.23: Summary of the synthesized poly(allyl glycidyl ether)-poly(ethylene glycol)-poly(allyl glycidyl ether)-poly(ethylene sulfide) copolymers.

	Macroinitiator	Theo. DP (per thioacetate)	$\overline{DP_n}$ (^{1}H NMR)	End-capping yield (^{1}H NMR) [mol%]	Theoretical $\overline{M_n}$ [g·mol^{-1}]	$\overline{M_n}$ (^{1}H NMR) [g·mol^{-1}]	$\overline{M_n}$ (SEC)* [g·mol^{-1}]	PDI (SEC)*
PPS 39	PEG II	7 x 5	7 x 5	100	7700	7700	5700	1.09

*SEC: eluent: DMF; PEG standard calibration

The molecular weight distribution was monomolecular and narrow with a PDI of 1.09. The SEC trace of **PES 6** in DMF is illustrated in **Figure 4.98**.

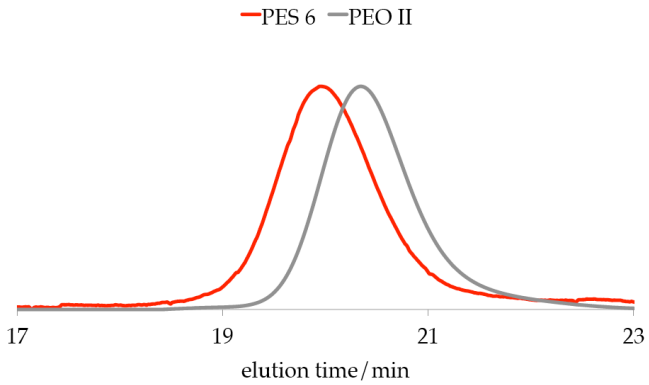

Figure 4.98: SEC traces (eluent: DMF; poly(ethylene glycol) standard calibration) of macroinitiator **PEG II** and corresponding PAGE-PEG-PAGE-PES graft copolymers **PES 6** (DP 5 per thioacetate).

The end-capping efficiency was also calculated via proton NMR spectroscopy by the use of the signal ratio of the PEG backbone ([-**CH$_2$**-**CH$_2$**-O-]$_n$) of the macroinitiator and the signals of the end-capping reagent (-S-**CH$_2$**-COO-). The living end-groups of the synthesized copolymer were quantitatively terminated. The targeted DP of ethylene sulfide of five per thioacetate was accomplished. The DP of ethylene sulfide was also determined via the ratio of the signal of the PEG backbone ([-**CH$_2$**-**CH$_2$**-O-]$_n$) of the macroinitiator and the signal of the polymer backbone ([-**CH$_2$**-**CH$_2$**-S-]$_n$). **Figure 4.99** illustrates the ^{1}H NMR of **PES 6**.

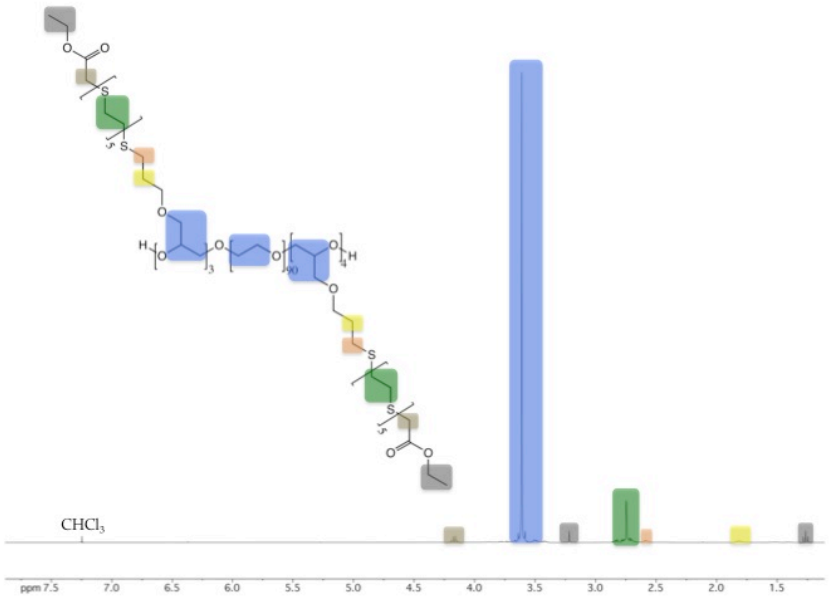

Figure 4.99: ^{1}H NMR spectrum of **PES 6** (400 MHz, $CDCl_3$) and peak assignment of the copolymer structure.

The structure of the pom-pom-like poly(ethylene sulfide) copolymer was investigated via ^{13}C NMR spectroscopy and the ^{13}C NMR spectrum of **PES 6** is shown in **Figure 4.100**.

Thermal properties of the pom-pom-like poly(ethylene sulfide) copolymer was investigated via DSC measurements. The DSC results are summarized in **Table 4.24**. The copolymer exhibited two different melting temperatures, as expected. The melting temperature of the PEG chain was detected at 37 °C and was slightly lowered compared to the PPS analog. The same behavior was also observed for the PPS and PES comb-like copolymers initiated by the macroinitiator **PEG I**.

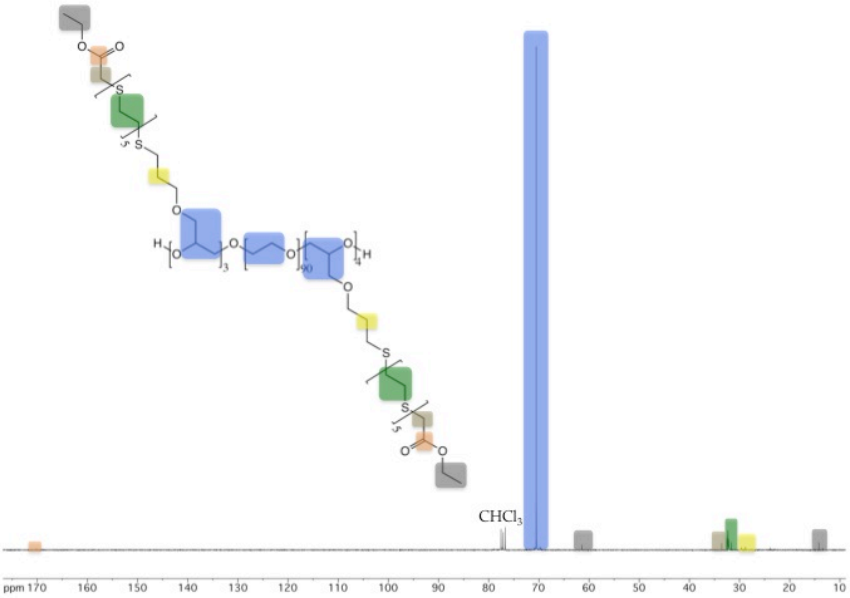

Figure 4.100: ^{13}C NMR spectrum of **PES 6** (75.5 MHz, $CDCl_3$) and peak assignment of the copolymer structure.

Table 4.24: Summary of the thermal behavior of the PAGE-PEG-PAGE-based poly(ethylene sulfide) copolymer.

	Macroinitiator	$\overline{DP_n}$ (^{1}H NMR)	**Theoretical** $\overline{M_n}$ [g·mol^{-1}]	$\overline{M_n}$ (^{1}H NMR) [g·mol^{-1}]	$\overline{M_n}$ PPS per chain (^{1}H NMR) [g·mol^{-1}]	$\mathbf{T_m}^{\mathbf{PEG}}$ (DSC)* [°C]	$\mathbf{T_m}^{\mathbf{PES}}$ (DSC)* [°C]
PES 6	PEG II	7 x 5	7700	7700	300	37	111

*DSC: temperature range: -95 °C – 200 °C with 10 °C·min^{-1}

The melting temperature of the PES chains was detected at 111 °C. Hence, it was slightly higher than the T_m of the star-shaped poly(ethylene sulfide) copolymers and in the region of the comb- and brush-like copolymers. The architecture of the pom-pom-like copolymers might be also described as a "double brush" and thus it is related to the architecture of the comb-like copolymers.

4.6.3 PAGE-PEG-PAGE-based random polysulfides

The synthesized macroinitiator **PEG II** was also used as macroinitiator for the random anionic ring-opening ethylene sulfide and propylene sulfide. The polymerization was carried out under the common conditions as described for the polyglycerol-based macroinitiators as well as for the PEG-PAGE-based macroinitiator. The conducted synthesis is illustrated in **Figure 4.101**.

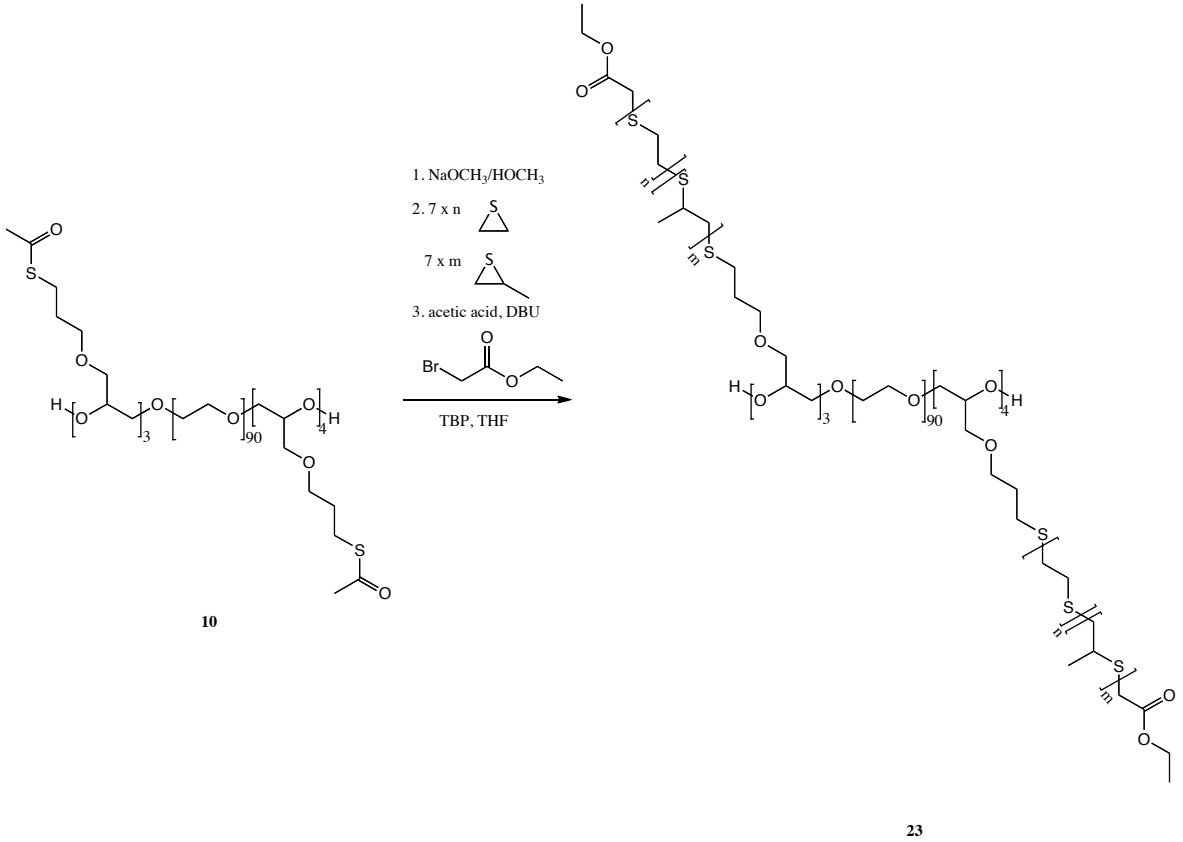

Figure 4.101: Random polymerization of ES and PS with PAGE-PEG-PAGE-based macroinitiator to pom-pom-like polymers.

The DP of both episulfide monomers per thioacetate group was varied. The number of propylene sulfide repeating units was increased in the range from ten over twenty and thirty to forty, and for each copolymer the DP of ethylene sulfide was changed from five over ten to fifteen. The targeted ES content of the copolymers amounted between 9 and 55wt%. The results of the random copolymerization are summarized in **Table 4.25**.

The copolymers with higher DPs of ethylene sulfide and propylene sulfide again exhibited a broader distribution due to formation of polysulfide homopolymers as low molecular side-product. The PDI was for most random copolymers below 1.70. SEC traces of the samples **P(PS-ES) 54**-**57** are shown in **Figure 4.102**.

Formation of the homopolymer was also detected for copolymers initiated with the polyglycerol-based macroinitiators as well as the random polymers with higher DPs of the episulfides monomers initiated by the PEG-PAGE-based macroinitiator **PEG I**. For all polysulfide copolymers, independent of the macroinitiator and the architecture, the amount of the side-product increased with increasing DP of the episulfide monomers.

Table 4.25: Summary of the PEG-PAGE-based poly(propylene sulfide)-poly(ethylene sulfide) random comb copolymers (macroinitiator: **PEG I**).

	Theo. DP PS (per thioacetate)	**Theo. DP ES** (per thioacetate)	$\overline{DP_n}$ **PS** (^{1}H NMR)	$\overline{DP_n}$ **ES** (^{1}H NMR)	**Theo. content ES*** [wt%]	**Content ES*** (^{1}H NMR) [wt%]	$\overline{M_n}$ (^{1}H NMR) [g·mol^{-1}]	$\overline{M_n}$ (SEC)** [g·mol^{-1}]	PDI (SEC)**
P(PS-ES) 50	7 x 10	7 x 5	7 x 10	7 x 6	29	33	13400	8100	1.22
P(PS-ES) 51	7 x 20	7 x 5	7 x 18	7 x 6	17	21	17500	10400	1.18
P(PS-ES) 52	7 x 30	7 x 5	7 x 26	7 x 5	12	13	21200	11400	1.39
P(PS-ES) 53	7 x 40	7 x 5	7 x 35	7 x 6	9	12	26300	14200	1.27
P(PS-ES) 54	7 x 10	7 x 10	7 x 10	7 x 11	45	47	15500	7500	1.35
P(PS-ES) 55	7 x 20	7 x 10	7 x 18	7 x 10	29	31	19200	9400	1.38
P(PS-ES) 56	7 x 30	7 x 10	7 x 26	7 x 10	21	24	23300	10800	1.40
P(PS-ES) 57	7 x 40	7 x 10	7 x 35	7 x 10	17	19	28000	10900	1.55
P(PS-ES) 58	7 x 10	7 x 15	7 x 10	7 x 16	55	56	17600	6000	1.71
P(PS-ES) 59	7 x 20	7 x 15	7 x 20	7 x 15	38	38	22300	8900	1.58
P(PS-ES) 60	7 x 30	7 x 15	7 x 28	7 x 15	29	30	26500	9400	1.68
P(PS-ES) 61	7 x 40	7 x 15	7 x 37	7 x 16	23	26	31600	11400	1.62

*content ES of the polysulfide content; **SEC: eluent: DMF; PEG standard calibration

The DP of the two monomers was again calculated via ^{1}H NMR spectroscopy. The ^{1}H NMR spectrum of **P(PS-ES) 54** is illustrated in **Figure 4.103**. The signal ratio of the PEG polymer backbone ([-**CH$_2$**-**CH$_2$**-O-]$_n$; highlighted in blue) as well as of the PES polymer backbone ([-**CH$_2$**-**CH$_2$**-S-]$_n$; highlighted in dark green) and the propylene sulfide polymer backbone ([-**CH$_2$**-**CH**(**CH$_3$**)-S-]$_n$; highlighted in light green) was used. The determined DPs of propylene sulfide were in most cases slightly lower than targeted. The calculated DPs of ethylene sulfide were for most copolymers slightly higher than targeted. Hence, the ES content of the pom-pom polysulfide copolymers was with 12wt% to 56wt% higher than requested. The same result also appeared in case of the random copolymers initiated by the polyglycerol-based macroinitiators and the PEG-PAGE-based comb-like polysulfides.

The end-capping efficiency was determined by ^{1}H NMR spectroscopy using the signal ratio of the PEG polymer backbone ([-**CH$_2$**-**CH$_2$**-O-]$_n$) and the methylene groups of the end-capping reagent. The calculated

end-capping efficiency was for all random copolymer higher than 75mol% and in most cases even quantitative.

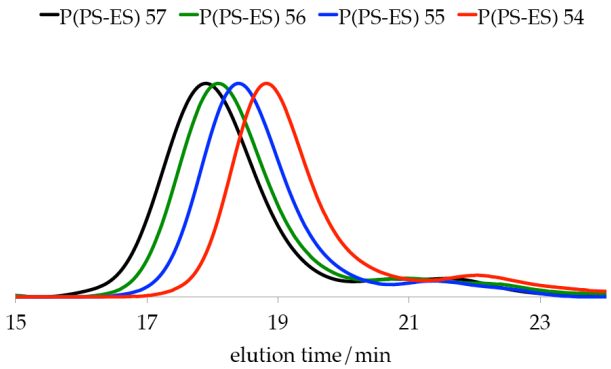

Figure 4.102: SEC traces (eluent: DMF; poly(ethylene glycol) standard calibration) of macroinitiator **PEG II** and corresponding PAGE-PEG-PAGE-PES graft copolymers **P(PS-ES) 54-57**.

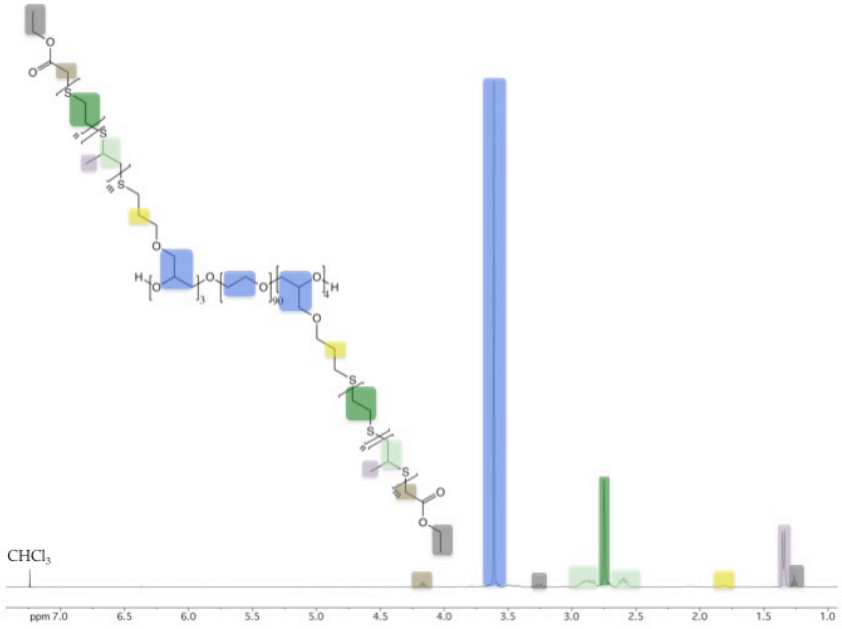

Figure 4.103: ^{1}H NMR spectrum of **P(PS-ES) 54** (400 MHz, $CDCl_3$) and peak assignment of the copolymer structure.

The physical behavior changed also in case of the pom-pom-like random sulfides, as expected. The behavior was similar to those of the comb-like copolymers initiated by the PEG-PAGE-based macroinitiator. The samples with five ethylene sulfide units per thioacetate changed with increasing propylene sulfide content from solid over wax-like to highly viscous. An increasing ethylene sulfide content led to solid materials, although the sample **P(PS-ES) 61** was still wax-like (**Figure 4.104**). All synthesized copolymers were insoluble in cold diethyl ether and with increasing ES content also insoluble in methanol.

The copolymer structure was also analyzed by ^{13}C NMR spectroscopy. **Figure 4.105a** shows the ^{13}C NMR of **P(PS-ES) 50** as an example.

Additionally, ^{13}C NMR spectroscopy was used to prove the random or nearly random structure of the synthesized moieties. The signals of the methylene and methine carbon atoms of propylene sulfide from

37-42 ppm as well as the signals of the carbon atoms of the ethylene sulfide backbone from 32-34 ppm are shown in **Figure 4.105b** in more detail. These signals were compared to the signals of the poly(ethylene sulfide) copolymer as well as to the poly(ethylene sulfide) copolymer. The different triads of the random copolymer were assigned according to the polyglycerol-based random polysulfides in chapter 4.4.3, the PEG-PAGE-based random polysulfides in chapter 4.5.3 and the already mentioned literature.[140,141,191]

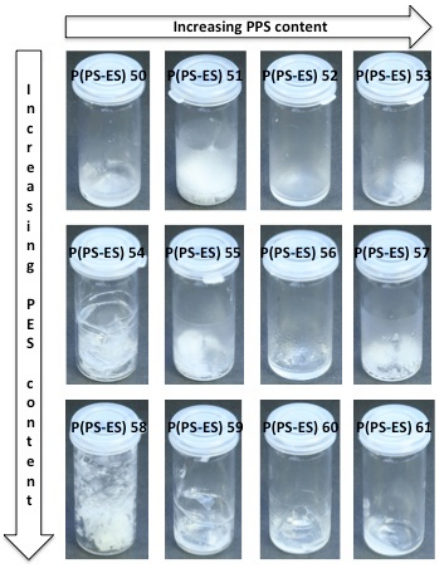

Figure 4.104: Photographs of the random comb-like polysulfides (**P(PS-ES) 50**-**61**).

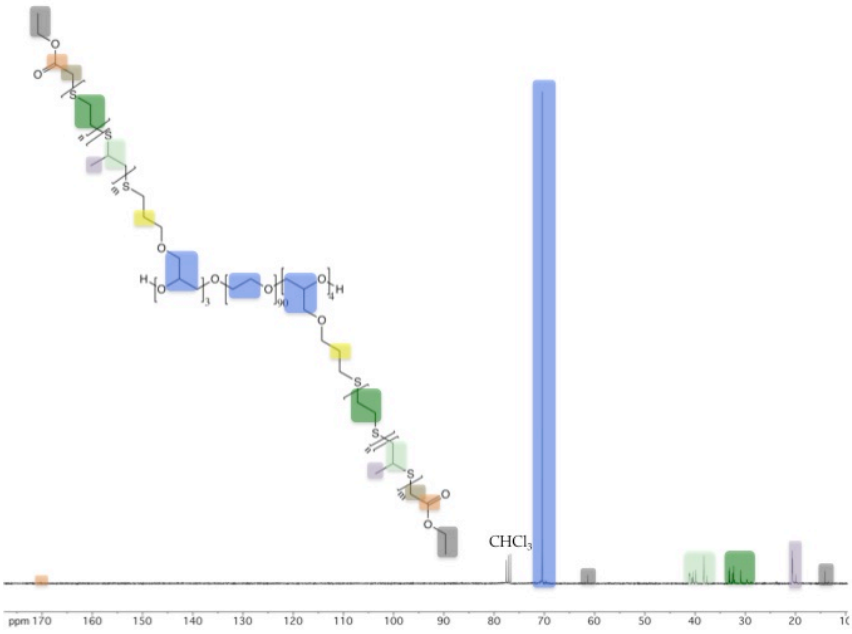

Figure 4.105a: ^{13}C NMR spectrum of **P(PS-ES) 50** (75.5 MHz, $CDCl_3$) and peak assignment of the copolymer structure.

The comparison of the two episulfide copolymers and the random episulfide copolymers supported also the random or nearly random structure of the synthesized copolymers. A peak splitting of the different carbon signals, which was caused by a random incorporation, was clearly observed. The signal of the carbon of the

methylene groups of the macroinitiator (-O-CH_2-**CH_2**-CH_2-S-) was for the different copolymers also slightly shifted as shown in **Figure 4.105b**.

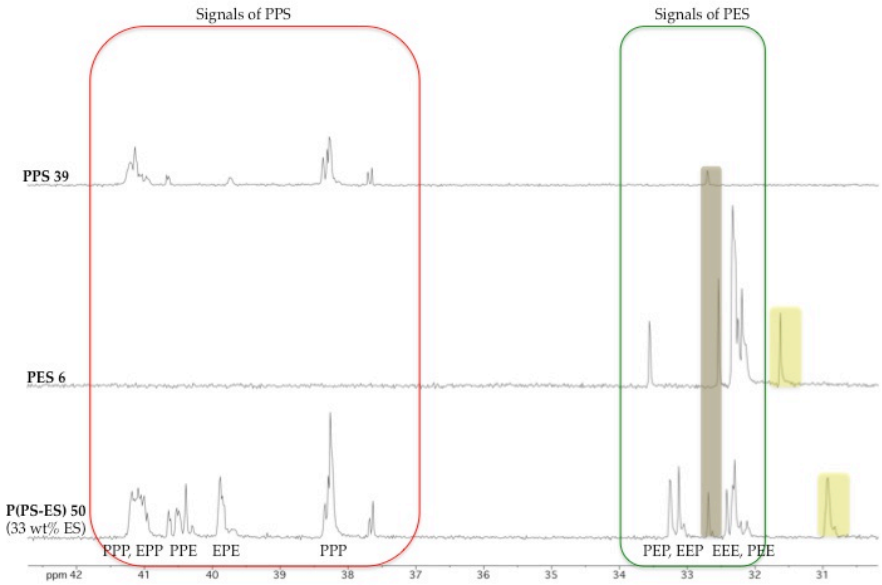

Figure 4.105b: ^{13}C NMR spectrum sections of **P(PS-ES) 50**, **PES 6** and **PPS 39** (75.5 MHz, $CDCl_3$) from 30-43 ppm and assignment of the triads.

DSC was used to analyze the thermal characteristics of the pom-pom-like copolymers. The results are shown in **Table 4.26**.

Table 4.26: Summary of the thermal behavior of the PAGE-PEG-PAGE-based random polysulfide copolymer.

	Macro-initiator	**Content ES*** (^{1}H NMR) [wt%]	$\overline{M_n}$ (^{1}H NMR) [g·mol^{-1}]	$\overline{M_n}$ PES per chain (^{1}H NMR) [g·mo750l^{-1}]	$\overline{M_n}$ PPS per chain (^{1}H NMR) [g·mol^{-1}]	$\overline{M_n}$ PPS-PES per chain (^{1}H NMR) [g·mol^{-1}]	**T_g** (DSC)** [°C]	**T_m** (DSC)** [°C]
P(PS-ES) 50	PEG II	33	13400	350	750	1100	-49	39
P(PS-ES) 58	PEG II	56	17600	950	750	1700	-50	27

*DSC: temperature range: -95 °C – 200 °C with 10 °C·min^{-1}

The analyzed random copolymers with one PEG chain between the polysulfide chains and thus, a pom-pom-like structure exhibited a glass transition temperature of the polysulfide arms and a melting point of the PEG chain. The T_g of the polysulfide chains was detected at -50 °C and -49 °C, respectively. These results suggested again that the T_g of the copolymers was only influenced by the length of a single poly(propylene sulfide) chain. Similar results were observed in case of the synthesized star-shaped, brush-like as well as comb-like random polysulfide copolymers. The melting temperature of the copolymer **P(PS-ES) 50** was detected at 39 °C and was comparable to the values determined for the pom-pom-like copolymers of ethylene sulfide and propylene sulfide. The T_m of the PEG chain of the copolymer sample **P(PS-ES) 58** was surprisingly low with 27 °C. The same behavior was also observed for the random episulfide copolymers

initiated by the macroinitiator **PEG I**, which is based on the diblock-copolymer of PEG and PAGE. These results indicated a significant lowering of the melting point of the random copolymers if the ethylene sulfide content was higher than 50wt%.

4.7 Surface attachment of the synthesized polysulfides

The synthesized poly(thioether) moieties were used to adsorb to gold surfaces and two main strategies were pursued. The first strategy involved the exchange of stabilizers of gold nanoparticles in aqueous solution and the characterization via UV-vis spectroscopy. The second strategy used the adsorption of sulfur-containing polymers onto bare gold substrates. Coated gold supports were subsequently analyzed via static water angle goniometry and AFM measurements.

4.7.1 Gold nanoparticles

Gold nanoparticles (Au NPs) were synthesized by the method introduced by Turkevitch[41] and further developed by Frens.[42] Au NPs with a size of about 20 nm were produced by the reduction of aqueous chloroaurate solution with trisodium citrate.[72] Au NPs capped with polysulfides were synthesized by the exchange of the citrate stabilizers on the surface of nanoparticles. A solution of the sulfur-containing polymers in dichloromethane or toluene was layered by the Au NPs solution in water and the mixture was shaken for one hour. The water phase as well as the organic solution was subsequently analyzed by UV-vis spectroscopy. **Figure 4.106** illustrates the adsorption spectrum of the synthesized Au NPs. The adsorption maximum of the intensive red nanoparticle solution was detected at 518.5 nm in water. As a comparison the AuNPs were extracted with pure dichloromethane (DCM) and toluene (TOL), respectively, to except any influence by the solvent. The results are shown in **Figure 4.107**.

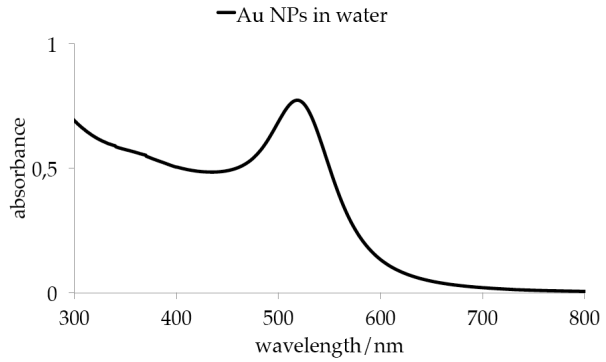

Figure 4.106: UV-vis spectrum of the aqueous Au NPs solution.

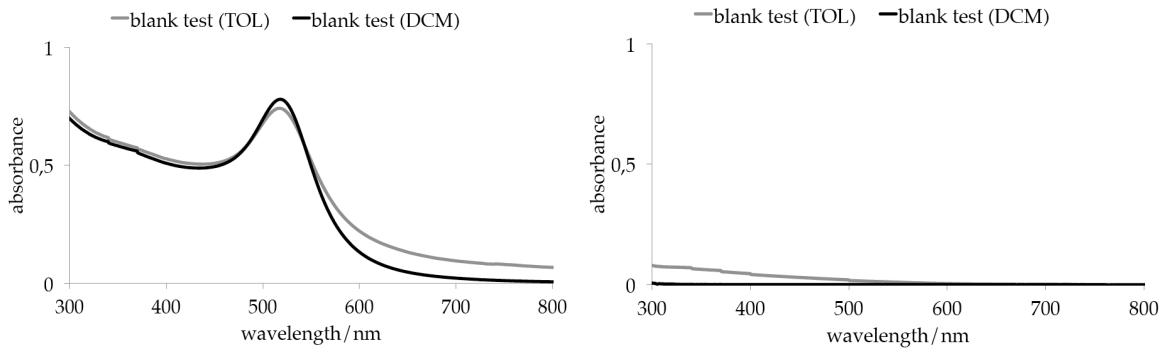

Figure 4.107: UV-vis spectra of the blank tests (left: aqueous phase; right: organic phase).

In **Figure 4.108** photographs of a typical adsorption reaction with a polymer and the blank sample are shown. The appearance of the blank sample with pure dichloromethane did not change. The red-colored Au NPs remained in the water phase, as already shown by UV-vis spectroscopy (**Figure 4.107**). After extraction with a sulfur-containing polymer solution, the intensive red Au NPs were removed from the aqueous solution.

Figure 4.108: Photographs of the Au NP extraction (left: blank sample with pure dichloromethane; right: polymer solution in dichloromethane).

The adsorption of the aqueous solution was nearly congruent to the bare Au NPs solution with 518 nm and the organic phases exhibited almost no absorbance. These results proved that the solvents did not bear any influence on the adsorption of the extracted Au NPs. The observed behavior was solely triggered by the synthesized polysulfide copolymers. In the following, the results of the different polysulfides are summarized according to their architecture. The linear polysulfides were also analyzed as comparison. When the copolymers with ten repeating units of propylene sulfide per thioacetate and forty units per thioacetate of one polysulfide set were enabled to extract the Au NPs of the aqueous solution, it was assumed that the copolymers in between with a DP of twenty and thirty were also abled to extract the nanoparticles.

4.7.1.1 Linear polysulfides

The results of the adsorption of linear polysulfides initiated by benzyl thioacetate (chapter 4.4) onto Au NPs are summarized in **Table 4.27**. The polymers were solubilized in dichloromethane and extracted with aqueous Au NP solution.

All linear copolymers were enabled to extract the Au NPs of the aqueous solution, except the PPS homopolymers **PPS 31** and **32** with less than twenty propylene sulfide repeating units as well as the block-copolymer **PPS-PES 4**. This result was unexpected, since the block-copolymer **PES-PPS 4** with the inverse sequence was enabled to extract the Au NPs. The sequence of the block-copolymer in combination with the block lengths might be crucial for the linker exchange on the surface of the Au NPs. The polymer backbone of the PPS homopolymers with less than twenty repeating units might be to short to ensure the particle extraction.

However, in most cases the polysulfide-capped nanoparticles were not soluble in dichloromethane and they were separated between the water and the organic phase or on the surface of the glass vial. Only the Au NPs stabilized with block-copolymers **PPS-PES 1** and **PES-PPS 1** resulted in an intensive red dichloromethane solution and an adsorption maximum of 521 and 532 nm, respectively. The random copolymer **P(PS-ES) 30** exhibited only a weak adsorption band. UV-vis spectra of the aqueous phase as well as the organic phase of the linear polysulfide block-copolymers **PPS-PES 1**-**4** are illustrated as an example in **Figure 4.109**. In this set of polysulfides the extraction of the Au NPs failed for one block-copolymer (**PPS-PES 4**), as already mentioned. In addition, with copolymer (**PPS-PES 1**) soluble polysulfide nanoparticles were obtained, as described before, and an adsorption maximum appeared. In all organic polymer solutions a continuous drift in different characteristics was observed.

The extraction behavior of the linear polysulfides appeared to be influenced by the sequence and the length of the poly(thioether) backbone.

Table 4.27: Summary of the UV-vis spectroscopy data of the linear polysulfide copolymer (dichloromethane).

	Initiator	Architecture	Polymer	Monomers (DP per thioacetate) (^{1}H NMR)	Content ES* (^{1}H NMR) [wt%]	λ_{max} (H_2O) [nm]	λ_{max} (DCM) [nm]
PPS 31	BT	linear	PPS	PS (1 x 12)	0	518	-
PPS 32	BT	linear	PPS	PS (1 x 20)	0	518	-
PPS 33	BT	linear	PPS	PS (1 x 31)	0	-	-
PPS 34	BT	linear	PPS	PS (1 x 40)	0	-	-
PPS-PES 1	BT	linear	block-copolymer	PS (1 x 11); ES (1 x 7)	34	-	521
PPS-PES 2	BT	linear	block-copolymer	PS (1 x 22); ES (1 x 7)	21	-	-
PPS-PES 3	BT	linear	block-copolymer	PS (1 x 33); ES (1 x 7)	15	-	-
PPS-PES 4	BT	linear	block-copolymer	PS (1 x 37); ES (1 x 7)	13	519	-
PES-PPS 1	BT	linear	block-copolymer	ES (1 x 5); PS (1 x 13)	24	-	532
PES-PPS 4	BT	linear	block-copolymer	ES (1 x 5); PS (1 x 42)	9	-	-
P(PS-ES) 26	BT	linear	random copolymer	PS (1 x 10); ES (1 x 6)	33	-	-
P(PS-ES) 29	BT	linear	random copolymer	PS (1 x 31); ES (1 x 5)	12	-	-
P(PS-ES) 30	BT	linear	random copolymer	PS (1 x 11); ES (1 x 11)	45	527**	-
P(PS-ES) 33	BT	linear	random copolymer	PS (1 x 34); ES (1 x 13)	24	-	-
P(PS-ES) 34	BT	linear	random copolymer	PS (1 x 13); ES (1 x 18)	53	-	-
P(PS-ES) 37	BT	linear	random copolymer	PS (1 x 40); ES (1 x 16)	24	-	-

*content ES of the polysulfide content; **weak absorption band

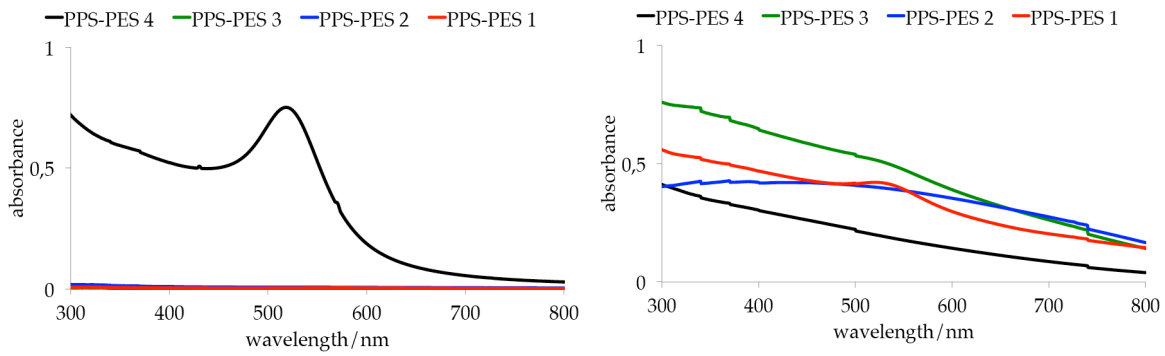

Figure 4.109: UV-vis spectra of the extraction with **PPS-PES 1-4** (left: aqueous phase; right: organic phase).

In a further experiment, the extraction of the Au NPs was conducted with polymer solutions in toluene. The results of these extraction experiments are summarized in **Table 4.28**. The polymers were solubilized in toluene and the extraction was conducted under the same conditions as in dichloromethane.

Table 4.28: Summary of the UV-vis spectroscopy data of the linear polysulfide copolymer (toluene).

	Initiator	**Architecture**	**Polymer**	**Monomers** (DP per thioacetate) (^{1}H NMR)	**Content ES*** (^{1}H NMR) [wt%]	λ_{max} (H_2O) [nm]	λ_{max} (TOL) [nm]
PPS 31	BT	linear	PPS	PS (1 x 12)	0	518	-
PPS 32	BT	linear	PPS	PS (1 x 20)	0	519	-
PPS 33	BT	linear	PPS	PS (1 x 31)	0	-	531**
PPS 34	BT	linear	PPS	PS (1 x 40)	0	-	-
PPS-PES 1	BT	linear	block-copolymer	PS (1 x 11); ES (1 x 7)	34	544**	-
PPS-PES 2	BT	linear	block-copolymer	PS (1 x 22); ES (1 x 7)	21	-	-
PPS-PES 3	BT	linear	block-copolymer	PS (1 x 33); ES (1 x 7)	15	-	533**
PPS-PES 4	BT	linear	block-copolymer	PS (1 x 37); ES (1 x 7)	13	520	-
PES-PPS 1	BT	linear	block-copolymer	ES (1 x 5); PS (1 x 13)	24	-	-
PES-PPS 4	BT	linear	block-copolymer	ES (1 x 5); PS (1 x 42)	9	-	533**
P(PS-ES) 26	BT	linear	random copolymer	PS (1 x 10); ES (1 x 6)	33	-	-
P(PS-ES) 29	BT	linear	random copolymer	PS (1 x 31); ES (1 x 5)	12	-	-
P(PS-ES) 30	BT	linear	random copolymer	PS (1 x 11); ES (1 x 11)	45	-	-
P(PS-ES) 33	BT	linear	random copolymer	PS (1 x 34); ES (1 x 13)	24	-	-
P(PS-ES) 34	BT	linear	random copolymer	PS (1 x 13); ES (1 x 18)	53	522**	-
P(PS-ES) 37	BT	linear	random copolymer	PS (1 x 40); ES (1 x 16)	24	547**	-

*content ES of the polysulfide content; **weak absorption band

The extraction efficiency of the polymer solutions in toluene was similar to this in dichloromethane, except that the block-copolymer **PPS-PES 1** and the random copolymers **P(PS-ES) 34** and **37** showed a weak adsorption band in aqueous solution. The bathochromic shift to longer adsorption wavelengths in the aqueous solution from 519 nm to 547 nm indicated an agglomeration of gold nanoparticles. Since the adsorption wavelength is depending on the size of the nanoparticles and larger Au NPs adsorb at larger wavelengths. Toluene enabled the solubilization of some polysulfide-capped nanoparticles. The Au NPs capped with longer polysulfide chains were soluble in toluene and indicated weak adsorption bands at 531 nm and 533 nm for the adsorbed polymers **PPS 33**, **PPS-PES 2** and **PES-PPS 4**. This bathochromic shift might be caused by the change of the stabilizers on the nanoparticle surface as well as the change of the solvent polarity from water to toluene. The solubilization of Au NPs stabilized with linear random polysulfides failed also in toluene.

In summary, the use of toluene and dichloromethane enabled the synthesis of Au NPs stabilized with different linear poly(ethylene sulfide)-poly(propylene sulfide) block-copolymers as well as poly(propylene sulfide) homopolymers. Nanoparticles capped with shorter polymer chains were rather soluble in dichloromethane and Au NPs with longer polymer chains were more soluble in toluene.

4.7.1.2 Star-shaped polysulfides

The synthesized star-shaped polysulfides were also used to exchange the citrate stabilizers on the surface of Au NPs. Ligand exchange was conducted under the same conditions as described for linear polysulfides. The results of the extraction with star-shaped polysulfide solutions in dichloromethane are summarized in **Table 4.29**.

Table 4.29: Summary of the UV-vis spectroscopy data of the star-shaped polysulfide copolymer (dichloromethane).

	Initiator	**Architecture**	**Polymer**	**Monomers** (DP per thioacetate) (^{1}H NMR)	**Content ES*** (^{1}H NMR) [wt%]	λ_{max} (H_2O) [nm]	λ_{max} (DCM) [nm]
PPS 1	Hb 2	star-shaped	PPS	PS (9 x 11)	0	-	-
PPS 4	Hb 2	star-shaped	PPS	PS (9 x 32)	0	-	-
P(PS-ES) 1	Hb 1	star-shaped	random copolymer	PS (7 x 11); ES (7 x 7)	34	-	-
P(PS-ES) 2	Hb 1	star-shaped	random copolymer	PS (7 x 17); ES (7 x 5)	19	-	-
P(PS-ES) 3	Hb 1	star-shaped	random copolymer	PS (7 x 21); ES (7 x 5)	16	518	-
P(PS-ES) 4	Hb 1	star-shaped	random copolymer	PS (7 x 30); ES (7 x 5)	13	519	-
P(PS-ES) 5	Hb 1	star-shaped	random copolymer	PS (7 x 10); ES (7 x 12)	49	-	-
P(PS-ES) 6	Hb 1	star-shaped	random copolymer	PS (7 x 16); ES (7 x 10)	34	-	-
P(PS-ES) 7	Hb 1	star-shaped	random copolymer	PS (7 x 23); ES (7 x 10)	26	-	-
P(PS-ES) 8	Hb 1	star-shaped	random copolymer	PS (7 x 35); ES (7 x 11)	20	518	-
P(PS-ES) 9	Hb 1	star-shaped	random copolymer	PS (7 x 7); ES (1 x 10)	54	-	-
P(PS-ES) 10	Hb 1	star-shaped	random copolymer	PS (7 x 16); ES (1 x 13)	40	-	-
P(PS-ES) 11	Hb 1	star-shaped	random copolymer	PS (7 x 22); ES (1 x 11)	29	-	-
P(PS-ES) 12	Hb 1	star-shaped	random copolymer	PS (7 x 22); ES (1 x 10)	27	518	-

*content ES of the polysulfide content; **weak absorption band

The extraction behavior of the star-shaped polysulfides was similar to the linear polysulfide, except the short poly(propylene sulfide) homopolymers were also enabled to transfer the AuNPs from the aqueous solution. Compared to the linear PPS homopolymers, which hold only one polysulfide chain, the star-shaped poly(propylene sulfide) samples have a network of polythioether chains, and the coating of the nanoparticles was easier obtained, as expected. Random copolymers with a DP of propylene sulfide of forty were again not able to extract the Au NPs from the water phase. The long polysulfide chains might be to hydrophobic to facilitate the exchange of the citrates linker of the Au NPs in aqueous solution.

The successfully capped Au NPs were not soluble in dichloromethane and toluene was used as organic solvent to extract the Au NPs from the aqueous solution. **Table 4.30** illustrates the results. The transfer behavior of the Au NPs of the aqueous solution was identical to the extraction with polysulfides solutions in dichloromethane. However, the solubilization of several polymer-coated nanoparticles was enabled in toluene. Au NPs covered with short and medium polysulfide moieties exhibited an adsorption band in the organic phase. The absorption maxima were again shifted to larger wavelengths, which suggested either a slight agglomeration of Au NPs in the polysulfide network, which might be caused by the close proximity of several Au NPs inside the polymer braid. A further explanation of the bathorchromic shift might be the change of the chemical surrounding of the nanoparticles.

Table 4.30: Summary of the UV-vis spectroscopy data of the star-shaped polysulfide copolymer (toluene).

	Initiator	**Architecture**	**Polymer**	**Monomers** (DP per thioacetate) (^{1}H NMR)	**Content ES*** (^{1}H NMR) [wt%]	λ_{max} (H_2O) [nm]	λ_{max} (TOL) [nm]
PPS 1	Hb 2	star-shaped	PPS	PS (9 x 11)	0	-	534
PPS 4	Hb 2	star-shaped	PPS	PS (9 x 32)	0	-	-
P(PS-ES) 1	Hb 1	star-shaped	random copolymer	PS (7 x 11); ES (7 x 7)	34	-	-
P(PS-ES) 2	Hb 1	star-shaped	random copolymer	PS (7 x 17); ES (7 x 5)	19	-	535**
P(PS-ES) 3	Hb 1	star-shaped	random copolymer	PS (7 x 21); ES (7 x 5)	16	519	-
P(PS-ES) 4	Hb 1	star-shaped	random copolymer	PS (7 x 30); ES (7 x 5)	13	519	-
P(PS-ES) 5	Hb 1	star-shaped	random copolymer	PS (7 x 10); ES (7 x 12)	49	-	534
P(PS-ES) 6	Hb 1	star-shaped	random copolymer	PS (7 x 16); ES (7 x 10)	34	-	537**
P(PS-ES) 7	Hb 1	star-shaped	random copolymer	PS (7 x 23); ES (7 x 10)	26	-	-
P(PS-ES) 8	Hb 1	star-shaped	random copolymer	PS (7 x 35); ES (7 x 11)	20	520	-
P(PS-ES) 9	Hb 1	star-shaped	random copolymer	PS (7 x 7); ES (1 x 10)	54	-	-
P(PS-ES) 10	Hb 1	star-shaped	random copolymer	PS (7 x 16); ES (1 x 13)	40	-	533**
P(PS-ES) 11	Hb 1	star-shaped	random copolymer	PS (7 x 22); ES (1 x 11)	29	-	548**
P(PS-ES) 12	Hb 1	star-shaped	random copolymer	PS (7 x 22); ES (1 x 10)	27	521	-

*content ES of the polysulfide content; **weak absorption band

4.7.1.3 Brush-like polysulfides

The synthesized random polysulfide copolymers were also investigated regarding the extraction of Au NPs of aqueous solutions by exchange of the citrate groups at the surface of the nanoparticles. Extractions were done both with polymer solution in dichloromethane and toluene. The results of the different extractions are shown in **Table 4.31** and **Table 4.32**.

The Au NPs were successfully removed from the aqueous solution by the extraction with the polymer solution in dichloromethane as well as in toluene. The random polysulfide brushes coated the nanoparticles effectively, but the capped Au NPs did not dissolve in dichloromethane. They were located between the

organic and the aqueous phase or deposited on the surface of the glass vial, as observed before. In contrast, several polysulfide-shielded nanoparticles were soluble in toluene and exhibited a weak adsorption band with an adsorption maximum at 531 nm or 533 nm, respectively. The adsorption maximum of Au NPs was slightly shifted bathochromic, which indicated again an agglomeration of nanoparticles or was induced by the change of the stabilizers of the nanoparticles or the changed solvent polarity. Toluene appeared to solubilize Au NPs coated with ten units of propylene sulfide repeating units per initiating group and different contents of ethylene sulfide.

Table 4.31: Summary of the UV-vis spectroscopy data of the brush-like random polysulfide copolymer (dichloromethane).

	Initiator	**Architecture**	**Polymer**	**Monomers** (DP per thioacetate) (^{1}H NMR)	**Content ES*** (^{1}H NMR) [wt%]	λ_{max} (H_2O) [nm]	λ_{max} (DCM) [nm]
P(PS-ES) 14	Li 3	brush-like	random copolymer	PS (18 x 9); ES (18 x 6)	35	-	-
P(PS-ES) 17	Li 3	brush-like	random copolymer	PS (18 x 26); ES (18 x 5)	13	-	-
P(PS-ES) 18	Li 3	brush-like	random copolymer	PS (18 x 10); ES (18 x 10)	47	-	-
P(PS-ES) 21	Li 3	brush-like	random copolymer	PS (18 x 10); ES (18 x 29)	22	-	-
P(PS-ES) 22	Li 3	brush-like	random copolymer	PS (18 x 11); ES (18 x 15)	53	-	-
P(PS-ES) 25	Li 3	brush-like	random copolymer	PS (18 x 31); ES (18 x 14)	27	-	-

*content ES of the polysulfide content; **weak absorption band

Table 4.32: Summary of the UV-vis spectroscopy data of the brush-like random polysulfide copolymer (toluene).

	Initiator	**Architecture**	**Polymer**	**Monomers** (DP per thioacetate) (^{1}H NMR)	**Content ES*** (^{1}H NMR) [wt%]	λ_{max} (H_2O) [nm]	λ_{max} (TOL) [nm]
P(PS-ES) 14	Li 3	brush-like	random copolymer	PS (18 x 9); ES (18 x 6)	35	-	533
P(PS-ES) 17	Li 3	brush-like	random copolymer	PS (18 x 26); ES (18 x 5)	13	-	-
P(PS-ES) 18	Li 3	brush-like	random copolymer	PS (18 x 10); ES (18 x 10)	47	-	-
P(PS-ES) 21	Li 3	brush-like	random copolymer	PS (18 x 10); ES (18 x 29)	22	-	-
P(PS-ES) 22	Li 3	brush-like	random copolymer	PS (18 x 11); ES (18 x 15)	53	-	531**
P(PS-ES) 25	Li 3	brush-like	random copolymer	PS (18 x 31); ES (18 x 14)	27	-	-

*content ES of the polysulfide content; **weak absorption band

4.7.1.4 Comb-like polysulfides

The organic solution of the synthesized comb-like polysulfides with an additional PEG chain were also extracted with aqueous Au NPs solution and subsequently analyzed via UV-vis spectroscopy. Dichloromethane was used as solvent for the preparation of polysulfide solution and the extraction was

conducted as described before. Extraction with the toluene solutions of the polysulfides failed due to the formation of an emulsion during the extraction and hence, the segregation of the organic and aqueous phase was inhibited. The additional PEG chain of the copolymers, which exhibited good solubility in water, might cause this.

The results of the extraction of the aqueous Au NPs solution with the polysulfide solutions in dichloromethane are summarized in **Table 4.33**. Extraction of the Au NPs from aqueous solution was merely successfully enabled for short comb-like polysulfides with a DP of ten for propylene sulfide per initiating group and various contents of ethylene sulfide.

Table 4.33: Summary of the UV-vis spectroscopy data of the comb-like polysulfide copolymer (dichloromethane).

	Initiator	**Archi-tecture**	**Polymer**	**Monomers** (DP per thioacetate) (^{1}H NMR)	**Content ES*** (^{1}H NMR) [wt%]	λ_{max} (H_2O) [nm]	λ_{max} (DCM) [nm]
PPS 35	PEG I	comb-like	PPS	PS (12 x 9)	0	-	519
PPS 36	PEG I	comb-like	PPS	PS (12 x 14)	0	519	-
PPS 37	PEG I	comb-like	PPS	PS (12 x 20)	0	518	-
PPS 38	PEG I	comb-like	PPS	PS (12 x 31)	0	513	-
P(PS-ES) 38	PEG I	comb-like	random copolymer	PS (12 x 8); ES (12 x 5)	34	-	528
P(PS-ES) 39	PEG I	comb-like	random copolymer	PS (12 x 14); ES (12 x 4)	19	-	-
P(PS-ES) 40	PEG I	comb-like	random copolymer	PS (12 x 19); ES (12 x 4)	15	518	-
P(PS-ES) 41	PEG I	comb-like	random copolymer	PS (12 x 27); ES (12 x 4)	11	519	-
P(PS-ES) 42	PEG I	comb-like	random copolymer	PS (12 x 7); ES (12 x 8)	48	-	530
P(PS-ES) 43	PEG I	comb-like	random copolymer	PS (12 x 15); ES (12 x 9)	33	-	522
P(PS-ES) 44	PEG I	comb-like	random copolymer	PS (12 x 22); ES (12 x 8)	23	518	-
P(PS-ES) 45	PEG I	comb-like	random copolymer	PS (12 x 29); ES (12 x 8)	18	518	-
P(PS-ES) 46	PEG I	comb-like	random copolymer	PS (12 x 6); ES (12 x 10)	57	-	522
P(PS-ES) 47	PEG I	comb-like	random copolymer	PS (12 x 14); ES (12 x 12)	41	518	-
P(PS-ES) 48	PEG I	comb-like	random copolymer	PS (12 x 22); ES (12 x 12)	31	518	-
P(PS-ES) 49	PEG I	comb-like	random copolymer	PS (12 x 25); ES (12 x 9)	23	518	-

*content ES of the polysulfide content; **weak absorption band

In most cases the polysulfide-capped Au NPs were soluble in dichloromethane and an adsorption maxima for the poly(propylene sulfide) copolymer **PPS 35** as well as for the random polysulfides **P(PS-ES) 38**, **42**, **43** and **46** was detected. The PEG chain of the comb-like polysulfide moieties seemed to improve the solubility of polymer-shielded Au NPs in dichloromethane. In most cases the adsorption maxima were not shifted significantly compared to the pure Au NPs solution, hence the comb-like polysulfides suppressed almost the aggregation of Au NPs and the exchange of the stabilizers did not change the absorption behavior.

4.7.1.5 Pom-pom-like polysulfides

Extraction of Au NPs from aqueous solution was also tested by the use of the synthesized pom-pom-like polysulfides. The polysulfides were solubilized in dichloromethane and the extraction was done under the common conditions as described before. The use of sulfur-containing polymer solutions in toluene for the ligand exchange at the nanoparticle surface failed due to the formation of an emulsion. The same behavior was also observed in case of the comb-like polysulfides and was caused by the PEG chain of these copolymers.

The results of the extraction of the aqueous nanoparticles with pom-pom-like polysulfides in dichloromethane solutions are summarized in **Table 4.34**.

Table 4.34: Summary of the UV-vis spectroscopy data of the pom-pom-like polysulfide copolymer (dichloromethane).

	Initiator	**Archi-tecture**	**Polymer**	**Monomers** (DP per thioacetate) (^{1}H NMR)	**Content ES*** (^{1}H NMR) [wt%]	λ_{max} (H_2O) [nm]	λ_{max} (DCM) [nm]
PPS 39	PEG II	pom-pom	PPS	PS (7 x 10)	0	-	-
PPS 40	PEG II	pom-pom	PPS	PS (7 x 19)	0	519	-
PPS 41	PEG II	pom-pom	PPS	PS (7 x 31)	0	519	-
PPS 42	PEG II	pom-pom	PPS	PS (7 x 37)	0	518	-
P(PS-ES) 50	PEG II	pom-pom	random copolymer	PS (7 x 10); ES (7 x 6)	33	-	-
P(PS-ES) 53	PEG II	pom-pom	random copolymer	PS (7 x 35); ES (7 x 6)	12	-	-
P(PS-ES) 54	PEG II	pom-pom	random copolymer	PS (7 x 10); ES (7 x 11)	47	-	-
P(PS-ES) 57	PEG II	pom-pom	random copolymer	PS (7 x 35); ES (7 x 10)	19	-	-
P(PS-ES) 58	PEG II	pom-pom	random copolymer	PS (7 x 10); ES (1 x 16)	56	-	-
P(PS-ES) 61	PEG II	pom-pom	random copolymer	PS (7 x 37); ES (1 x 16)	26	-	-

*content ES of the polysulfide content; **weak absorption band

Poly(propylene sulfide) graft copolymers with more than ten propylene sulfide repeating units per chain were not capable of transferring the gold nanoparticles from the water phase and the obtained adsorption maxima of the aqueous solutions were comparable to the pure nanoparticle solution. Similar results were also achieved with the comb-copolymers, which were based on the macroinitiator **PEG I**. But in contrast to the comb-copolymers, all tested random polysulfides with a pom-pom-like architecture, which were initiated by macroinitiator **PEG II**, adsorbed on the Au NPs and removed them from the aqueous solution. However, none of these polymer-capped nanoparticles were soluble in dichloromethane. It was presumed that the pom-pom-like polysulfides developed a huge polymer network, which might connected by the Au NPs as coupling points.

In summary, the observed extraction efficiency depended closely on the architecture of the used polysulfide as well as on the composition of the copolymers, the sequence of the block-copolymers and the length of polymer backbone.

4.7.2 Gold substrates

A variety of the synthesized different polysulfides with various architectures were used to coat bare gold substrates. Gold supports were dipped into polymer solution in dichloromethane for a certain time. A scheme of the coating procedure is illustrated in **Figure 4.110**.

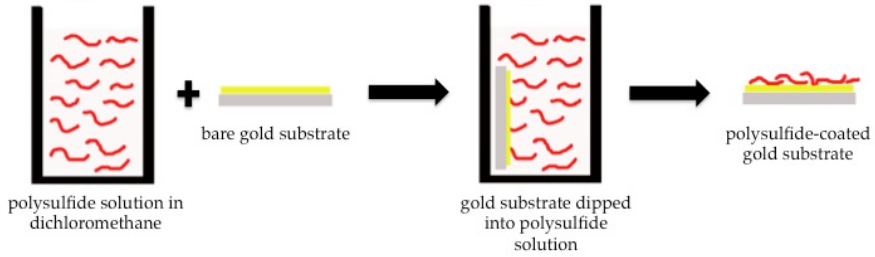

Figure 4.110: Scheme of the coating process (not drawn to scale).

The substrates were rinsed numerous times with dichloromethane to remove all unbounded substances from the gold surface. Subsequently, the wettability as well as topography of the surface of the polysulfide-coated substrates was investigated via contact angle goniometer and AFM.

4.7.2.1 Wettability

Wettability of the polysulfide-coated gold substrates was investigated via static contact angle measurement of a water droplet. Förch et al. defined the contact angle as angle at which a liquid or vapor meets a solid. This is shown by a scheme in **Figure 4.111**.[236]

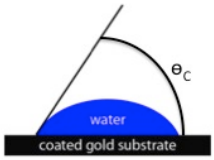

Figure 4.111: Scheme of the contact angle.[236]

The wettability of a surface depends on the surface tension or the energy of the interface. A hydrophilic surface, for example, led to a completely spread out of a water droplet on the surface due to strong attraction. In this case a small contact angle is detected. In contrast, a hydrophobic surface exhibited contact angles exceeding 90 °. Surfaces with larger contact angles than 150 ° are called superhydrophobic. Water droplets rest on these surfaces without a significant wetting.[236]

The results of the static contact angle measurement of a water droplet on a copolymer-coated surface are summarized for the polyglycerol-based polysulfides in **Table 4.35**.

The error margin was in the range of ± 3 ° and was slightly higher than the reported values of ± 2 ° by Engquist et al,[237] who used a similar equipment. A bare TSG substrate was equally processed as the polymer-coated substrates, except it was dipped in pure dichloromethane instead of in a polysulfide solution in dichloromethane. The contact angle of this sample was measured as a comparison and was detected at about 88 °. All investigated polysulfide-covered substrates exhibited smaller contact angles, than the TSG comparison and the surfaces of the copolymer-coated supports were more hydrophilic as the pure gold surface. In case of poly(propylene sulfide) graft-polymers the contact angle decreased with increasing DP of propylene sulfide per initiating groups. The number as well as the architecture of the adsorbed polymers influenced the contact angle significantly. Linear polyglycerol-based poly(propylene sulfide) graft-

copolymers with a brush-like architecture and thirty-six PPS arms were noteworthy more hydrophobic with a contact angle of 82 ° for **PPS 19**. Compared to this, star-shaped poly(propylene sulfide) block-copolymers, initiated by a small hyperbranched polyglycerol, with nine polysulfide arms exhibited a contact angle of 73 °. Different brush-like polysulfides indicated that the contact angle increased also with the number of polysulfide arms. Surfaces coated with a polysulfide with thirty-six polysulfide chains were notably more hydrophobic than those coated with polysulfides with only eighteen polysulfide arms of the same architecture.

Table 4.35: Summary of the static contact angles of the polyglycerol-based polysulfides-coated gold substrates.

	Initiator	**Archi-tecture**	**Polymer**	**Monomers** (DP per thioacetate) (^{1}H NMR)	**Content ES*** (^{1}H NMR) [wt%]	**Static contact angle** (H_2O) [°]
bare gold**	-	-	-	-	-	88 ± 2
PPS 1	Hb 2	star-shaped	PPS	PS (9 x 11)	0	73 ± 1
PPS 2	Hb 2	star-shaped	PPS	PS (9 x 18)	0	79 ± 2
PPS 3	Hb 2	star-shaped	PPS	PS (9 x 25)	0	83 ± 2
P(PS-ES) 1	Hb 1	star-shaped	random copolymer	PS (7 x 11); ES (7 x 7)	34	80 ± 1
P(PS-ES) 5	Hb 1	star-shaped	random copolymer	PS (7 x 10); ES (7 x 12)	49	73 ± 1
P(PS-ES) 9	Hb 1	star-shaped	random copolymer	PS (7 x 7); ES (7 x 10)	54	78 ± 2
PPS 19	Li 4	brush-like	PPS	PS (36 x 10)	0	82 ± 2
PPS 21	Li 4	brush-like	PPS	PS (36 x 20)	0	85 ± 2
P(PS-ES) 14	Li 3	brush-like	random copolymer	PS (18 x 9); ES (18 x 6)	35	71 ± 2
P(PS-ES) 18	Li 3	brush-like	random copolymer	PS (18 x 10); ES (18 x 10)	47	68 ± 3
P(PS-ES) 22	Li 3	brush-like	random copolymer	PS (18 x 11); ES (18 x 15)	53	76 ± 3

*content ES of the polysulfide content; **reference (equally processed)

For the random copolymer-coated substrates of both architectures no clear trend was observed. First the contact angle decreased with increasing ethylene sulfide content as well as a constant propylene sulfide content and with further increasing ethylene sulfide content the contact angle increased again. The change of the contact angles might also be caused through different surface layers. The static contact angle of a water droplet was definitely influenced, when the polyglycerol-based macroinitiator was located on the top of the coated layer.

In summary, the architecture and the number of polysulfide arms as well as the composition of the polysulfide chains of the polyglycerol-based graft copolymers influenced the static contact angle of a water droplet significantly, as expected.

The results of the contact angle measurements of several PEG-containing polysulfides are shown in **Table 4.36**.

Table 4.36: Summary of the static contact angles of the PEG-PAGE-based polysulfide-coated gold substrates.

	Initiator	**Architecture**	**Polymer**	**Monomers** (DP per thioacetate) (^{1}H NMR)	**Content ES*** (^{1}H NMR) [wt%]	**Static contact angle** (H_2O) [°]
PPS 35	PEG I	comb-like	PPS	PS (12 x 9)	0	76 ± 3
P(PS-ES) 38	PEG I	comb-like	random copolymer	PS (12 x 8); ES (12 x 5)	34	74 ± 3
P(PS-ES) 42	PEG I	comb-like	random copolymer	PS (12 x 7); ES (12 x 8)	48	67 ± 3
P(PS-ES) 46	PEG I	comb-like	random copolymer	PS (12 x 6); ES (12 x 10)	57	64 ± 2
PPS 39	PEG II	pom-pom-like	PPS	PS (7 x 10)	0	56 ± 3
P(PS-ES) 50	PEG II	pom-pom-like	random copolymer	PS (7 x 10); ES (7 x 6)	33	60 ± 2
P(PS-ES) 54	PEG II	pom-pom-like	random copolymer	PS (7 x 10); ES (7 x 11)	47	70 ± 3
P(PS-ES) 58	PEG II	pom-pom-like	random copolymer	PS (7 x 10); ES (7 x 16)	56	67 ± 3

*content ES of the polysulfide content

The gold substrates coated with polysulfides, which held an additional PEG-chain, were more hydrophilic compared to the corresponding polyglycerol-based polysulfide without an PEG-chain, as expected for copolymers with a hydrophilic block, such as PEG. For surfaces coated with the comb-like polysulfides the static contact angle of a water droplet continuous decreased for increasing ethylene sulfide content from 76 ° to 64 °. Polysulfide arms, which stuck to the gold surface, might cause the increase in hydrophobicity of these capped surfaces and the PEG chains were present on the top of the coated substrate. The poly(propylene sulfide) graft-copolymer **PPS 39** with a pom-pom-like architecture exhibited the lowest measured contact angle with about 56 °. Random copolymers with a pom-pom-like structure did not show a clear trend concerning to the static contact angle. The contact angle first increased with increasing ethylene sulfide content and later decreased with further increasing ethylene sulfide content. The inconsistent contact angle alteration might be caused be the pom-pom-like architecture, in which the PEG-chain acted as linker between the polysulfide arms which could either be present on the top of the surface or covered between the polysulfide chains.

4.7.2.2 Atomic Force Microscope (AFM)

The template stripped gold (TSG) method[238] was used to produce flat gold surfaces, which were subsequently coated with different polysulfides. The change of the static contact angle of a water droplet of the investigated substrates indicated a successful adsorption of the synthesized polysulfides (chapter 4.7.2.1). The surface topographies of polysulfide-coated gold substrates were subsequently analyzed via AFM. The aim of this study was the investigation of a potential influence of the different architecture as well as an impact of the monomer composition of the used adsorbents on the surface topography.

A TSG substrate was used as blank test. It was dipped in pure dichloromethane instead of a polymer solution to exclude any effect on the surface topography by the solvent and the dipping process. The AFM height images of some polysulfide-coated gold substrates as well as the blank test are illustrated in **Figure 4.112**.

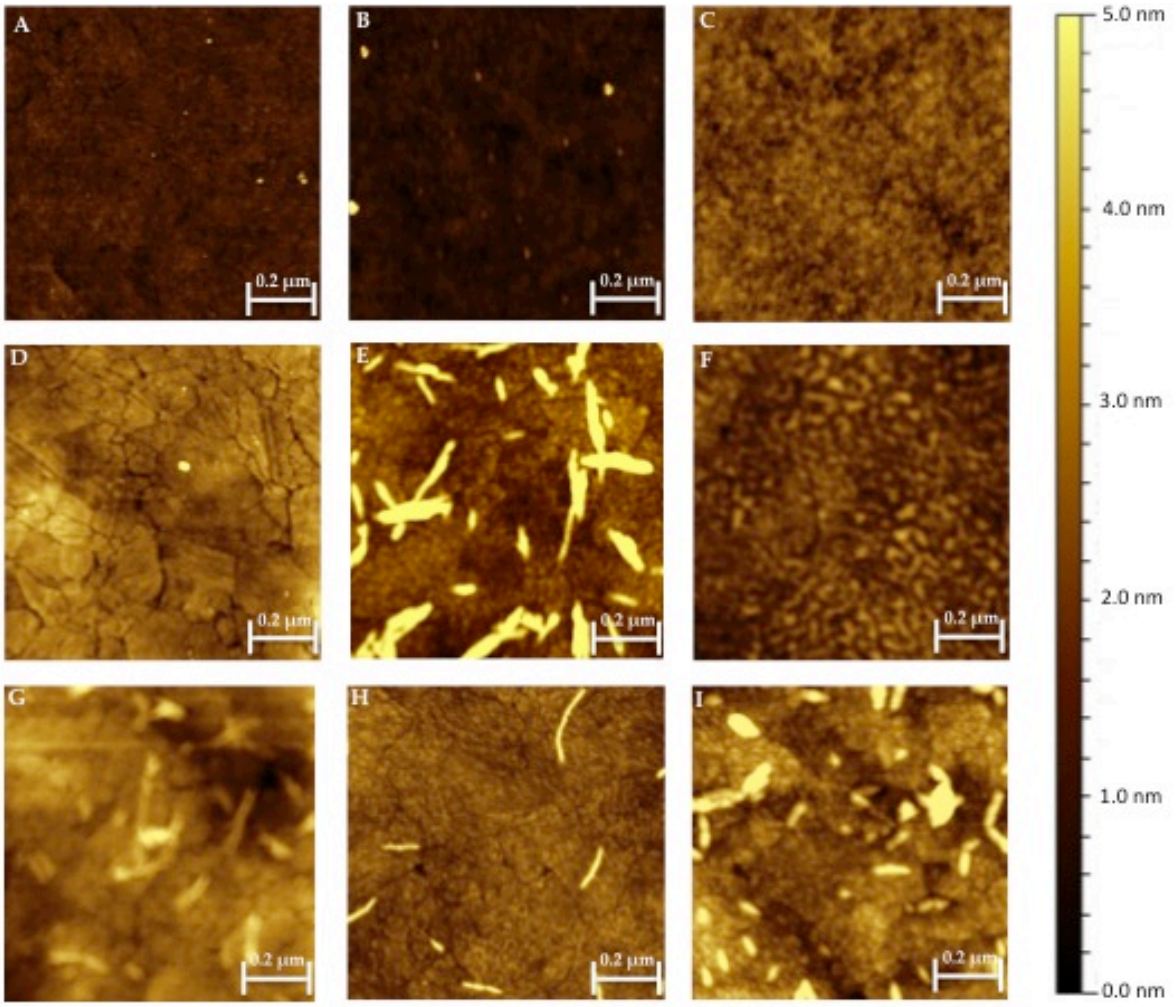

Figure 4.112: AFM height images of different coated gold substrates recorded in tapping mode; (A = TSG; B = **PPS 1** (star-shaped); C = **PPS 2** (star-shaped); D = **P(PS-ES) 5** [49wt% ES] (star-shaped); E = **P(PS-ES) 9** [54wt% ES] (star-shaped); F = **P(PS-ES) 14** [35wt% ES] (brush-like); G = **P(PS-ES) 22** [53wt% ES] (brush-like); H = **P(PS-ES) 34** [53wt% ES] (comb-like); I = **P(PS-ES) 58** [56wt% ES] (pom-pom-like)).

The illustrated AFM images constitute a variety of the measured AFM pictures. **Figure 4.112 A** shows the TSG substrate as comparison. The topography of the blank test was rather flat with a typical structuring. **Figure 4.113** shows the characteristic topography more clearly. **Figures 4.112 B**-**D** were obtained from the sample coated with star-shaped PPS with a DP of ten and twenty as well as the star-shaped random polysulfide with 49wt% ES, respectively. Image **4.112 F** was recorded by scanning the gold surface, which was previously dipped in a dichloromethane solution of the brush-like random copolymer **P(PS-ES) 14** with a ethylene sulfide content of 35wt%. The illustrated height images were representative for most polysulfide-coated gold substrates. The detected surface topography of these modified samples was not significantly different to the topography of the TSG. However, the adsorption of the random copolymers with the highest ES content with about 55wt% led to distinctive difference of the surface. These polymers led to worm-like structures on the gold surface (**Figures 4.112 E, G**-**I**). The length and the width of the aggregates on the surface depended on the used polymer architecture of the adsorbents.

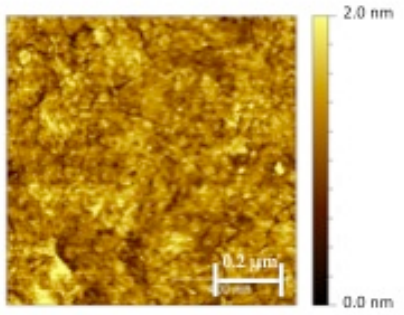

Figure 4.113: AFM height images of TSG black test.

The random star copolymer **P(PS-ES) 9** exhibited mostly rather long and broad worm-like structures. In **Figures 4.114** two profiles of the height image of this sample are shown. The worm-like structures were between 4 and 6 nm high, between 4 and 14 nm broad and 7 and 30 nm long.

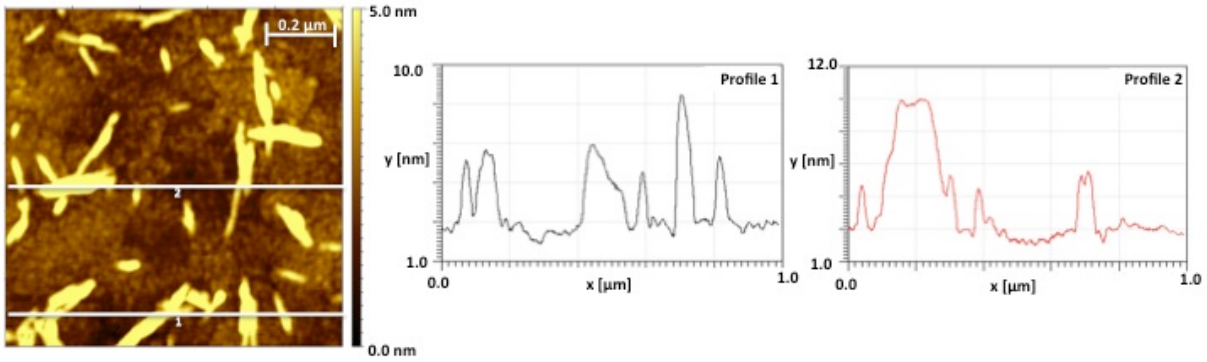

Figure 4.114: Profiles of the AFM height image of **P(PS-ES) 9** [54wt% ES] (star-shaped)-coated gold substrate.

In contrast, the tube-shaped objects on the surface coated with the comb-like polysulfide **P(PS-ES) 34** seem significantly narrower and the surface was less covered. Two profiles of the height image are shown in **Figures 4.115**. The height of these worm-like structures was rather uniform with 3 to 4 nm. The width of these objects was similar with 4 to 5 nm and the length varied between 5 and 30 nm.

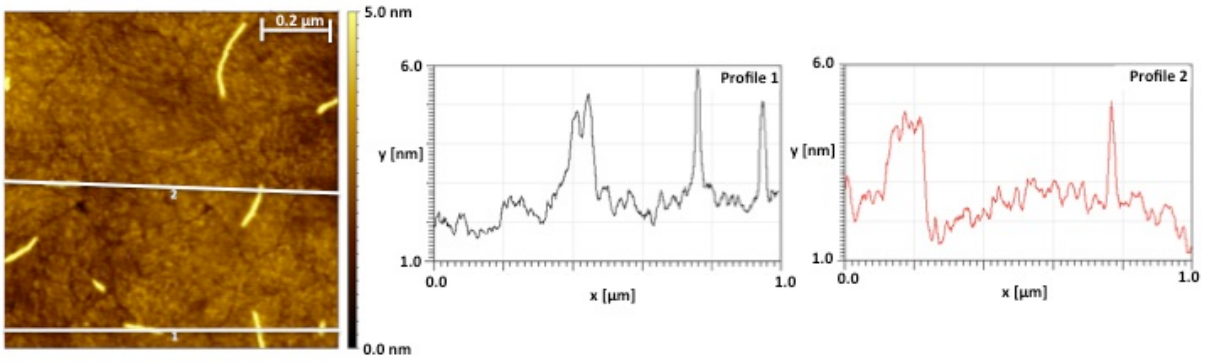

Figure 4.115: Profiles of the AFM height image of **P(PS-ES) 34** [53wt% ES] (comb-like)-coated gold substrate.

The surface patterning might resulted by aggregation of the polysulfides due to the high content of ethylene sulfide, which led to less solubility in dichloromethane.

In addition, the AFM height images were used to determine the root mean square (RMS) roughness of the surfaces. The RMS roughness describes the standard deviation of the surface height and is a common parameter to characterize the roughness of a surface.[240] This value was used to determine whether there was no polymer adsorbed on the surface or if the polysulfides recreated the typical structure of the TSG. This behavior is illustrated by a scheme in **Figure 4.116**.

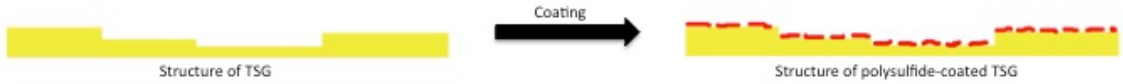

Figure 4.116: Scheme of the recreation of TSG structure by the adsorbed polysulfide (shown in red) (not drawn to scale).

The obtained RMS values of the polysulfide-coated TSG templates are summarized in **Table 4.37**. The RMS roughness of processed TSG as comparison over an area of 1 x 1 μm^2 was about 0.3 nm. The obtained value was comparable to the RMS roughness for TSG described in literature with 0.2-0.8 nm.[238,245] The roughness of the gold substrates coated with the different PPS polymers was detected in the range of 0.4 to 0.7 nm. The obtained values were slightly higher than the RMS roughness of the TSG reference, however in most cases the values were in the range of the measurement error. Coating with the brush-like **PPS 19** and **21** with thirty-six polysulfides arms as well as larger star-shaped **PPS 10** samples with twenty-two PPS chains led to RMS values of 0.6 and 0.7, respectively. Likewise the substrates modified with the star-shaped **PPS 1** and **2**, comb-like **PPS 35** and pom-pom-like **PPS 39** with seven to twelve polysulfide arms exhibited comparable roughness. Hence, the architecture, the degree of polymerization of propylene sulfide as well as the presence of a PEG chain did not bear a significant influence on the surface roughness. Solely, a higher number of PPS arms with twenty-two and thirty-six, respectively, led to a slight increase of the RMS roughness beyond the margin of error.

For the random polysulfide copolymers a nearly homogenous trend was observed. The surface roughness increased with increasing ethylene sulfide content for most polymer samples. The surface roughness of the substrates coated with random copolymers with 33-35wt% was calculated to be about 0.6 nm, independent of the architecture of the polymer. Similar RMS values were observed for the surface shielded with the star-copolymer and the comb-copolymer with 48 and 49wt% ES content. The surface roughness of these samples was slightly higher than the surface roughness of the TSG comparison. In contrast to this, the obtained surface roughness of the pom-pom copolymers as well as of the brush copolymers with a similar ethylene sulfide content was approximately 1.8 nm and 1.9 nm, respectively. For most polymer architectures, the highest RMS roughness was observed for the random copolymers with an ES content of 53-57wt%, as expected from the topography of the height images. The roughness of the surfaces coated with copolymers with PEG content was less harsh than the one without a PEG chain. The surface of the gold substrate coated with the comb-like random polysulfide **P(PS-ES) 46** was not completely covered with narrow worm-like aggregates and exhibited a RMS value of about 0.8 nm. The RMS value of the gold substrate shielded with the pom-pom-like copolymer was rougher with about 1.2 nm. The surface covered with larger worm-like aggregates exhibited a RMS roughness of circa 1.6 nm. Brush-like copolymers with thirty-six polysulfide arms exhibited the highest RMS values with approximately 2.6 nm. A similar trend was also observed for the samples coated with PPS polymers with a higher number of polysulfide arms.

Table 4.37: Summary of the RMS roughness of the polysulfides-coated gold substrates.

	Initiator	**Architecture**	**Polymer**	**Monomers** (DP per thioacetate) (^{1}H NMR)	**Content ES*** (^{1}H NMR) [wt%]	**RMS roughness** (1 x 1 µm^2) [nm]
bare gold**	-	-	-	-	-	0.3 ± 0.1
PPS 1	Hb 2	star-shaped	PPS	PS (9 x 11)	0	0.5 ± 0.2
PPS 2	Hb 2	star-shaped	PPS	PS (9 x 18)	0	0.4 ± 0.1
PPS 10	Hb 3	star-shaped	PPS	PS (22 x 25)	0	0.7 ± 0.2
P(PS-ES) 5	Hb 1	star-shaped	random copolymer	PS (7 x 10); ES (7 x 12)	49	0.5 ± 0.1
P(PS-ES) 9	Hb 1	star-shaped	random copolymer	PS (7 x 7); ES (7 x 10)	54	1.6 ± 0.2
PPS 19	Li 4	brush-like	PPS	PS (36 x 10)	0	0.7 ± 0.2
PPS 21	Li 4	brush-like	PPS	PS (36 x 20)	0	0.6 ± 0.0
P(PS-ES) 14	Li 3	brush-like	random copolymer	PS (18 x 9); ES (18 x 6)	35	0.6 ± 0.1
P(PS-ES) 18	Li 3	brush-like	random copolymer	PS (18 x 10); ES (18 x 10)	47	1.9 ± 0.6
P(PS-ES) 22	Li 3	brush-like	random copolymer	PS (18 x 11); ES (18 x 15)	53	2.6 ± 0.8
PPS 35	PEG I	comb-like	PPS	PS (12 x 9)	0	0.4 ± 0.1
P(PS-ES) 38	PEG I	comb-like	random copolymer	PS (12 x 8); ES (12 x 5)	34	0.6 ± 0.2
P(PS-ES) 42	PEG I	comb-like	random copolymer	PS (12 x 7); ES (12 x 8)	48	0.5 ± 0.1
P(PS-ES) 46	PEG I	comb-like	random copolymer	PS (12 x 6); ES (12 x 10)	57	0.8 ± 0.3
PPS 39	PEG II	pom-pom-like	PPS	PS (7 x 10)	0	0.4 ± 0.1
P(PS-ES) 50	PEG II	pom-pom-like	random copolymer	PS (7 x 10); ES (7 x 6)	33	0.6 ± 0.2
P(PS-ES) 54	PEG II	pom-pom-like	random copolymer	PS (7 x 10); ES (7 x 11)	47	1.8 ± 0.5
P(PS-ES) 58	PEG II	pom-pom-like	random copolymer	PS (7 x 10); ES (7 x 16)	56	1.2 ± 0.3

*content ES of the polysulfide content; **reference (equally processed)

In some cases, the gold surfaces were not completely or homogenously coated with polysulfide, which was reflected in larger error values with up to 0.8 nm. The highest error with 0.8 nm was calculated for the substrate coated with **P(PS-ES) 22**, although this was also the surface with the highest RMS value with 2.6 nm.

In summary, the change of the static contact angle of a water droplet as well as the slightly higher RMS roughness compared to the TSG comparison suggested a successful surface coverage of gold substrates with polysulfides. Most polysulfides recreated the surface topography of TSG. The only exceptions were the random copolymers with ES content higher than 50wt%, which exhibited worm-like aggregates on the gold surface. Solubility effects of the copolymers with such a high ethylene sulfide content caused these results.

4.7.2.2.1 Second coating with gold nanoparticles

Additionally, a further experiment was explored to prove the polysulfide coating of gold substrates and to study a potential influence by the different architectures. The synthesized copolymers were adsorbed onto flat bare gold supports under the conditions described before in chapter 4.7.2.2. Subsequently, the polysulfide-coated substrates were dipped into an aqueous gold nanoparticle solution for one hour and the surface topography was also analyzed via AFM. Gold nanoparticles were enabled to adsorb onto the polythioether modified supports, because not all of the numerous sulfur atoms of the polysulfide backbones were in contact with the gold surface. A bare gold substrate was used as a comparison and was also dipped into the nanoparticle solution to exclude the adsorption of Au NPs to the surface by physisorption. The obtained AFM height images are illustrated in **Figure 4.117**.

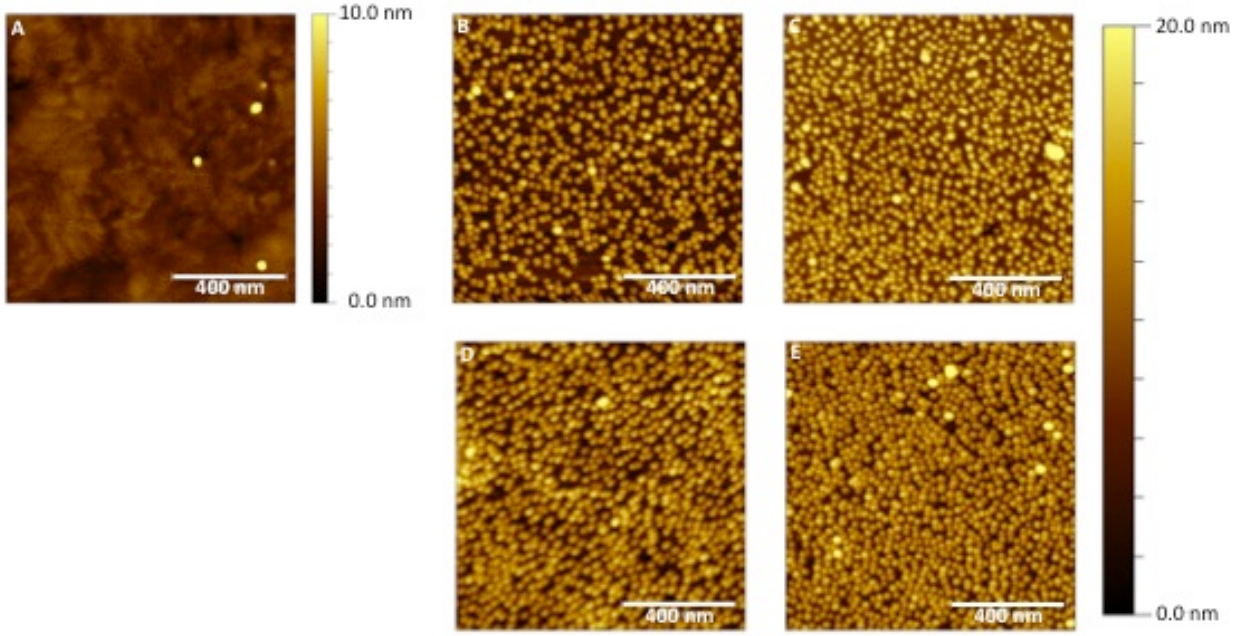

Figure 4.117: AFM height images of different Au NP-coated gold substrates recorded in tapping mode; (A = blind sample; B = **P(PS-ES) 9** [54wt% ES] (star-shaped); C = **P(PS-ES) 22** [53wt% ES] (brush-like); D = **P(PS-ES) 38** [53wt% ES] (comb-like); E = **P(PS-ES) 58** [56wt% ES] (pom-pom-like)).

The TSG sample as comparison exhibited merely a few adsorbed gold nanoparticles on the surface (**Figure 4.117 A**). In comparison, the surface of the polysulfide-coated gold supports was closely covered with Au NPs. Hence, the second adsorption of 20 nm sized Au NPs onto polysulfide-capped gold substrates was successful as proven by the AFM measurements. The nanoparticles on the surface were equally sized until a few examples of larger aggregates. Au NPs were spaced out evenly at the polysulfide-covered substrate and no significant influence regarding the surface patterning was observed.

In all analyzed samples the surface of the substrates was completely covered. However, in case of the star-shaped random copolymer (**Figure 4.117 B**) the nanoparticles seemed to be less dense packed on the surface compared to the corresponding brush-like (**Figure 4.117 C**), comb-like (**Figure 4.117 D**) and the pom-pom-like polysulfide (**Figure 4.117 E**) random copolymers.

In addition, the profiles of the nanoparticle-coated star-shaped copolymer samples and the comb-copolymer samples are shown in **Figure 4.118** and in **Figure 4.119**, respectively. Since the surface coverage of these two polysulfides without Au NPs was significant different (**Figures 4.112, 4.114, 4.115**). The surface coated with

the comb-like **P(PS-ES) 38** was not completely covered and the detected aggregates were narrower compared to surface shielded with **P(PS-ES) 9**, as mentioned before. The observed worm-like aggregates on the surface of the coated substrates did not influence the patterning of Au NPs on the surface. The surface appeared for both samples equally covered with Au NPs without differences in altitude, which might be caused by the worm-like aggregates (compare to **Figure 4.112, 4.114, 4.115)**.

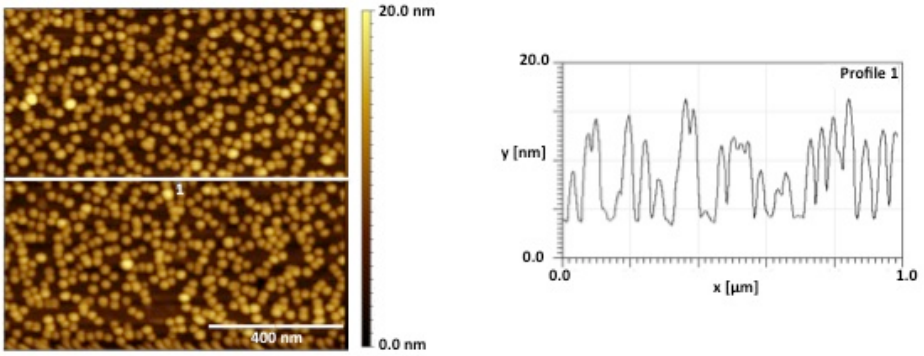

Figure 4.118: Profiles of the AFM height image of Au NP-coated gold substrate modified with **P(PS-ES) 9** (star-shaped).

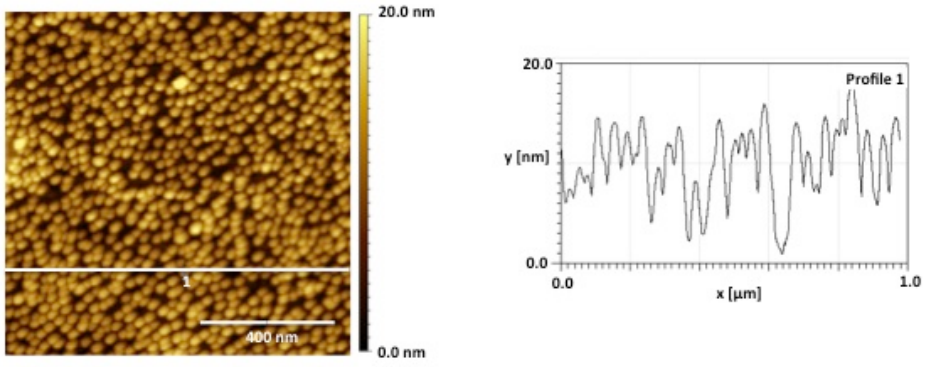

Figure 4.119: Profiles of the AFM height image of Au NP-coated gold substrate modified with **P(PS-ES) 38** (comb-like).

In summary, a second adsorption of Au NPs onto gold substrates modified with polysulfide was accomplished. The architecture of the used random polysulfides did not show a significant influence on the patterning of adsorbed Au NPs with a size of 20 nm. Furthermore, neither the number of polysulfides arms nor PEG chain weighted the patterning of Au NPs on the surface of polysulfide-modified gold substrates.

4.8 Summary and conclusion

Conversion of linear and hyperbranched polyglycerol as well as different PEG-PAGE di-and triblock-copolymers to moieties with multiple terminal thioacetate groups was successfully affected. A two-step protocol was used to ensure the full conversion of all hydroxyl functionalities of the polyglycerol into allyl groups. Subsequently, the per-allylated species were transformed via a thiole-ene reaction with thioacetic acid and AIBN to terminal thioacetate groups. These thioacetates were polymers with protected terminal mercaptans. The conducted syntheses were on one hand an alternative synthetic route to introduce terminal thiol functionalities to polyether polyol species and on the other hand, the synthesized polymers were used as macroinitiators for the anionic ring opening polymerization of different episulfide monomers. The use of linear and hyperbranched polyglycerol-based macroinitiators for episulfides facilitated the synthesis of both brush-like and star-shaped polysulfides. Variation of the molecular weight and hence, the number of terminal groups of the skeletal polymer enabled the synthesis of poly(thioether) moieties with a different number of arms. The range of the polysulfide architectures was extended to comb-like and pom-pom-like structures with an additional PEG chain by the use of PEG-PAGE- as well as PAGE-PEG-PAGE-based macroinitiators.

The named macroinitiators with a different number of thioacetates were used to obtain a library of different polysulfides with various architectures and numbers of arms. First of all, a set of poly(propylene sulfide) graft polymers were successfully synthesized by the initiation with the obtained macroinitiators. The DP was in all cases varied from ten to forty per thioacetate group of the macroinitiator. Different poly(propylene sulfide) graft-copolymers were completely characterized via ^{1}H and ^{13}C NMR- as well as IR-spectroscopy and additionally by DSC and SEC measurements. The obtained results were compared among each other. Furthermore, benzyl thioacetate as a common initiator for polysulfides was used to synthesize linear polysulfides as comparison.

In case of the polyglycerol-based macroinitiators a side-reaction was observed, which was neither monitored in the polymerizations with the PEG-containing macroinitiators nor with benzyl thioacetate. The side-reaction was analyzed via kinetics in SEC as well as online ^{1}H NMR spectroscopy. Propylene sulfide was deprotonated and a subsequent rearrangement to an allyl thiolate, which was enabled to act as initiator for propylene sulfide and a PPS homopolymer was formed. The amount of side-product increased with increasing DP and increasing monomer content. The low molecular by-product was prosperously removed by purification with recycling preparative HPLC and star-shaped as well as brush-like copolymers with low molecular weight dispersities below 1.22 were obtained. PEG-PAGE di- and triblock-copolymers-based macroinitiators provided directly, without further purification, monomodal and narrow distributions with PDIs in SEC below 1.26. The linear comparison yielded also monomodal and narrow polysulfides with PDIs below 1.25.

Glass transition temperatures of the copolymers were compared to the values described in literature.[120] The detected T_gs of the graft copolymers with various architectures were lower than expected for poly(propylene sulfide)s with such a high molecular weight. However, the consideration of only one PPS arm provided values, which were comparable to them of the homopolymers with similar molecular weight. The values of the homopolymer with ten repeating units were slightly lower, hence with increasing molecular weight the values of the homopolymer and the corresponding polysulfide arms of the copolymers were equalized. This behavior was independent of the architecture and number of polysulfide arms of the graft copolymers. A separate T_g of the polyglycerol-based core was not detected. The melting temperature of the macroinitiators with a PEG chains was slightly influenced by the polysulfide shell. The T_m was lowered in comparison to

pure PEG-PAGE block-copolymers.[235] Compared to the PEG-PAGE-based macroinitiator, the T_m of the PEG block of the PAGE-PEG-PAGE was more significantly influenced.

Furthermore, the syntheses of soluble poly(ethylene sulfide) copolymers were tested by the concept of macroinitiators with multiple initiating groups and a small number of episulfide repeating units per thioacetate. The synthesis of soluble graft copolymers was only successful in cases of the pom-pom-like copolymers initiated by the PAGE-PEG-PAGE-based macroinitiator. In this case, the seven polysulfide arms were spatially parted by a PEG chain. Both the PEG block in the middle and the small number of polysulfide chains had a positive influence regarding the solubility. The use of further macroinitiators led to partially soluble copolymers. The analysis of the copolymers suspensions was capable via NMR-spectroscopy, but the investigation by SEC failed. The copolymer initiated by the linear polyglycerol-based macroinitiator with thirty-six thioacetates was an exception, this copolymer was completely insoluble in common organic solvents. DSC was used for the analysis of the thermal characteristics. The copolymers with different architectures did not exhibit a uniform behavior. The comb-like copolymer was comparable to the brush-like copolymers, the only distinction was the PEG chain. For this copolymers the melting temperature of the poly(ethylene sulfide) arms linearly increased with increasing number of polysulfide arms. The T_m values of the polysulfide chains in case of the small star-shaped as well as the pom-pom-like copolymer were comparable to them of the graft copolymer brushes and combs. Again no T_g of the polyglycerol cores was detected and the melting temperature of the PEG blocks was similar to the values measured for the poly(propylene sulfide) copolymers. A significant influence was observed for a large hyperbranched polyglycerol core. For this sample the T_g of the macroinitiator was detected and the T_m of the poly(ethylene sulfide) shell was significantly lowered.

Synthesis of soluble poly(ethylene sulfide)-containing copolymers with several architectures was successfully achieved by random copolymerization of ethylene sulfide and propylene sulfide. The synthesized episulfide graft copolymers were investigated via NMR and IR spectroscopy as well as by DSC and SEC.

Homopolymerization of propylene sulfide as side-reaction after proton abstraction was observed for all macroinitiators, although in less distinctive manner. The linear random copolymers initiated by benzyl thioacetate constituted an exception. The obtained copolymers were monomodal with narrow molecular weight distributions below 1.31. For the macroinitiators, which contained a PEG block, the formation of the by-product was not observed for low episulfides DPs. However, with increasing monomer contents the side-reaction took also place in case of the PEG-PAGE di- and triblock-copolymer-based macroinitiators. The PEG-chain was not able to reduce the electrostatic repulsion of the large number of charged moieties in close proximity for higher episulfides concentrations or to suppress the deprotonation of propylene sulfide by the present peroxidation.

The best results were achieved in case of the pom-pom-like copolymers. The molecular weight distribution of the copolymers with low DPs of the thiiranes was narrow with PDIs below 1.40. The comb-like random copolymers were also narrow distributed with PDIs below 1.42 for low episulfides concentrations, but with increasing monomer contents the side-reaction was observed more markedly. The copolymer with the highest ethylene sulfide exhibited the broadest distribution with 1.71. The achieved PDI of the star-shaped random copolymers in SEC ranged between 1.46 and 1.79. In contrast, the copolymer brushes showed significant broader distributions with PDIs above two. By the use of recycling preparative HPLC the molecular weight distributions could by lowered, which was shown for one star-shaped random copolymer. The calculated ethylene sulfide content was almost constant and was merely reduced around 1wt%.

^{13}C NMR spectroscopy was used to investigate the random copolymerization of the thiirane monomers. The observed peak splitting was compared to the results described in literature.[140,141,191,234] The triads were assigned according to the mentioned publications, although the measured spectra exhibited a higher resolution, because the spectra were measured with higher frequency. The triads clearly negated the presence of block-like structures, although the EEE triad increased more significantly than expected for random copolymers. These results, the higher reactivity of ethylene sulfide compared to propylene sulfide and the slight decrease of the ethylene sulfide content after recycling preparative HPLC suggested the existence of random copolymers, but the monomers were incorporated with a slight gradient. In the beginning of the polymerization slightly more ethylene sulfide was incorporated and at the end of the polysulfide arms the propylene sulfide content was enriched. DSC measurements supported these results, because no melting point of propylene sulfide was detected, as expected for copolymers with a random structure. The glass transition temperature seemed only to be influenced by the propylene sulfide content of a single polysulfide arm. The melting temperature of the PEG chain of the pom-pom-like and comb-like copolymers exhibited for low ethylene sulfide contents comparable values for propylene sulfide and ethylene sulfide graft copolymers. However, for ethylene sulfide contents over 50wt% the T_m of the PEG block was significantly lowered.

In addition, the synthesis of soluble poly(ethylene sulfide)-poly(propylene sulfide) block-copolymers with various architectures were only in case of benzyl thioacetate successfully conducted. The synthesis of star-shaped block-copolymers failed even for low ethylene sulfide contents.

Different copolymers with multiple thioether functionalities were used to adsorb on gold surfaces. An aqueous gold nanoparticle solution was extracted with organic polymer solutions to exchange the citrate linkers on the particle surface with the copolymer and to transfer them from the aqueous phase into the organic phase. The extraction efficiency depended on the architecture of the copolymers as well as on the monomer content and chain length. The linear poly(propylene sulfide) samples with lower DP were not capable of transferring the Au NPs from the aqueous solution. It seemed that the copolymer chain was not long enough to cover the nanoparticles completely. Random copolymers as well as graft-copolymers with different architectures with longer polymer chain length facilitated the removal of Au NPs of the aqueous phase. In many cases the polysulfide-coated nanoparticles were not soluble in the organic solvent and were separated between the two phases as well as on the surface of the used glass vials. This might be caused be the formation of large networks, which were connected via Au NPs. However, in several cases the polymers were soluble in dichloromethane or toluene, which depended on the size and the architecture of the used copolymer. Hence, the solubilization of the each polysulfide-shielded particles was tailored and might be feasible by further variation of the solvents.

The surface topography of gold substrates, which were modified by the adsorption of polysulfides, was investigated via static contact angle measurements as well as AFM measurements. The obtained static contact angles of a water droplet on the modified gold surface was in all cases significant different to the TSG reference. The RMS roughness was calculated from the AFM height images and was used to confirm a successful coating procedure. In general, the surface roughness was in all investigated cases higher compared to the bare gold support, but for a few polysulfides the RMS value was in the range of the error margin. However, in most cases the RMS increased with increasing ethylene sulfide content. The detected surface topology was in most cases similar to the characteristic topology of the TSG, except the samples coated with polysulfides with higher ethylene sulfide contents than 50wt% exhibited worm-like structures on the surface, which might be caused by aggregation phenomena due to the high ES content and hence,

solubility effects. The polysulfides with smaller ethylene sulfide contents led to a recreation of the TSG surface structure by the adsorbed polysulfides, independent of the architecture of the used polyether moiety. Additionally, polysulfide-shielded gold substrates were used to adsorb Au NPs from aqueous solution. The large number of thioether functionalities along the chains of the polysulfide moieties was not in contact with the gold surface and the adsorption of Au NPs was realized. The surface packing of the gold nanoparticles was in case of the star-shaped less dense compared to the comb-like, pom-pom-like and brush-like copolymers. However, neither a significant influence of the arrangement of the adsorbed Au NPs on the modified gold surface with polysulfide of different architectures nor an influence of the PEG block on the patterning was detected.

In summary, the synthesis of different polysulfides with several architectures and a various number of arms was successful. The molecular weight distribution as well as the thermal behavior was significantly influenced by the structure of the used polysulfide as well as their architecture, the number of arms and the chain length. Successful adsorption of the synthesized moiety onto gold surfaces was proven by the change of the static contact angle of a water droplet and the RMS roughness in comparison to TSG as well as by UV-vis spectroscopy after adsorption to the surface of aqueous gold nanoparticles.

4.9 Experimental

4.9.1 Materials

Hyperbranched polyglycerol, linear polyglycerol as well as the PEG-PAGE diblock and triblock-copolymers were synthesized according to literature reported methods.[235,241,242] The synthesis of benzyl thioacetate was also described before.[243] For the preparation of gold substrates the protocol for template-stripped gold was used.[238] The aqueous gold nanoparticle solution was obtained according to a described procedure.[72] The size of the gold nanoparticles were controlled by measurement of Z-average. All other chemicals were commercially available from Sigma-Aldrich UK or Germany, Acros or Fluka and used as received, unless otherwise noted. Colored allyl bromide was distilled at atmospheric pressure after adding three drops of limonene to destroy the impurities (bromine). THF was degassed via bubbling of argon through the solvent for one hour or by five cycles of freeze-pump-thaw. AIBN was recrystallized from methanol before used. The used deuterated solvents dimethyl sulfoxide-d_6 (99.8%) and chloroform-d (99.8%) were purchased from Cambridge Isotope Laboratories or Deutero GmbH. Tetrahydrofuran-d_8 (99.5%) and methanol-d_4 (99.8%) for the online ^{1}H NMR experiments were also purchased from Deutero GmbH. Sodium trideutero methoxide was prepared according to a described protocol.[244] All reactions were conducted under argon. The polymerizations were either carried out in the parallel reactor Carousel from Radleys or in a glass flask capped with a rubber septum. The analytical data are shown on the basis of one example per copolymer architecture.

4.9.2 General protocol of the macroinitiator synthesis

4.9.2.1 Polyglycerol ally ether (PAE)[225,239]

In a typical experiment, a mixture of polyglycerol and sodium hydroxide (5 equiv. per OH-group of the polymer) in water was stirred at room temperature. 0.1 equiv. (per OH-group) phase transfer catalyst (tetrabutylammonium fluoride trihydrate, tetrabutylammonium iodide or tetrabutylammonium bromide) and 5 equiv. (per OH-group) allyl bromide were added and the reaction mixture was stirred at room temperature for 4-5 days. After addition of cold brine the solution was extracted five times with dichloromethane. The organic solution was dried over anhydrous sodium sulfate, filtrated and the solvent was completely removed. The crude product was dissolved in dry dimethyl sulfoxide and added slowly to a solution of sodium hydride (2 equiv. per OH-group) in dry dimethyl sulfoxide. The solution was stirred at room temperature for 15 minutes. Then a solution of allyl bromide (3 equiv. per OH-group) in dry dimethyl sulfoxide was dropped to the mixture and stirred for 18 hours. After slow addition of ice to the reaction mixture, cold brine was added and extracted five times with dichloromethane. The organic solution was dried over anhydrous sodium sulfate, filtrated and the solvent was completely removed. The viscous oil was dissolved in dichloromethane and extracted five times with water. The organic phase was dried again, filtrated and the solvent was completely removed to yield a viscous oil.

Characterization:

Linear polyglycerol allyl ether:

FT-IR (on ATR crystal) [in cm^{-1}]: 3079, 2864, 1460, 1085, 995, 919. ^{1}H NMR (DMSO-d_6): δ (ppm) = 5.93-5.80 (m, CH_2=**CH**-CH_2-); 5.27-5.10 (m, **CH_2**=CH-CH_2-); 4.07-3.92 (m, CH_2=CH-**CH_2**-); 3.54-3.37 (broad, PG protons).

Hyperbranched polyglycerol allyl ether:

FT-IR (on ATR crystal) [in cm^{-1}]: 3079, 2865, 1459, 1086, 994, 920. ^{1}H NMR (300 MHz, DMSO-d_6): δ (ppm) = 5.91-5.79 (m, CH_2=**CH**-CH_2-); 5.26-5.20 (d, **CH_2**=CH-CH_2-(cis)); 5.14-5.07 (t, **CH_2**=CH-CH_2-(trans)); 4.06-3.91 (m, CH_2=CH-**CH_2**-); 3.59-3.38 (broad, PG protons); 1.34-1.24 (m, **CH_2**-CH_3 initiator); 0.83-0.74 (t, CH_2-**CH_3** initiator).

Table 4.37: Summary of the synthesized polyglycerol allyl ethers.

	Precursor			Polyglycerol ally ether (PAE)				
	Architecture	$\overline{M}_n$ (^{1}H NMR) [g·mol^{-1}]	Hydroxyl functions per molecule	$\overline{M}_n$ (^{1}H NMR) [g·mol^{-1}]	$\overline{M}_n$ (SEC)* [g·mol^{-1}]	PDI (SEC)*	Yield [%]	Conversion (^{1}H NMR & IR) [%]
^{l}PAE 1	*lin*	700	9	1050	1500	1.31	47	100
^{l}PAE 2	*lin*	1300	17	2000	1300	1.12	85	100
^{l}PAE 3	*lin*	1350	18	2100	3000	1.16	48	100
^{l}PAE 4	*lin*	2700	36	4150	5500	1.27	43	100
^{h}PAE 1	*hb*	750	7	1000	500	1.49	80	100
^{h}PAE 2	*hb*	800	9	1150	1100	1.31	87	100
^{h}PAE 3	*hb*	2650	22	4000	2500	1.22	84	100

*SEC: eluent: THF (polystyrene standard calibration) or DMF (PEG standard calibration)

4.9.2.2 Polyglycerol-based thioacetate[128]

The ally ether moiety was dissolved in THF and 0.1 equiv. (per allyl ether) AIBN and 4 equiv. (per allyl ether) thioacetic acid was added under stirring. The reaction mixture was degassed via freezing the mixture in liquid nitrogen, evacuating under high vacuum and filling the reaction vessel with argon after bringing back to room temperature. This procedure was repeated five times. The reaction was then heated to 60 °C for 3-5 days. Dowex resin 1x8 (further treated with 0.1 M aqueous sodium hydroxide solution and washed with 200 ml of methanol and 100 ml of THF) was introduced and stirred at room temperature for 2 hours. After filtration the solvent was completely removed and the crude product was dissolved in dichloromethane. This solution was extracted twice with 5% sodium bicarbonate solution and three times with water. The mixture was dried over anhydrous sodium sulfate, filtrated and the solvent was completely removed. In case of the polyglycerol cores, the viscous oil was extracted three times with cold hexane to yield a viscous yellow oil or dialyzed against chloroform for one day. PEG-PAGE di- and triblock-based thioacetates were twice precipitated in cold diethyl ether.

Table 4.38: Summary of the synthesized polyglycerol-based thioacetates.

	Precursor		Macroinitiator					
	Name	Polymer	Thioacetates per molecule	$\overline{M_n}$ (^{1}H NMR) [g·mol^{-1}]	$\overline{M_n}$ (SEC)* [g·mol^{-1}]	PDI (SEC)*	Yield [%]	Conversion (^{1}H NMR & IR) [%]
Li 1	^{l}PAE 1	*lin*PEA	9	1750	1850	1.20	69	100
Li 2	^{l}PAE 2	*lin*PEA	17	3250	1500	1.23	26	100
Li 3	^{l}PAE 3	*lin*PEA	18	3450	4400	1.09	49	100
Li 4	^{l}PAE 4	*lin*PEA	36	6900	3400	1.58	49	100
Hb 1	^{h}PAE 1	*hb*PEA	7	1700	900	1.49	80	100
Hb 2	^{h}PAE 2	*hb*PEA	9	1850	1500	1.31	63	100
Hb 3**	^{h}PAE 3	*hb*PEA	18	5400	3600	1.43	62	86
Hb 4	^{h}PAE 3	*hb*PEA	22	5600	4400	1.28	36	100
PEG I	-	PEG-PAGE	12	7300	6300	1.06	82	100
PEG II	-	PAGE-PEG-PAGE	7	5300	4700	1.09	79	100

*SEC: eluent: THF (polystyrene standard calibration) or DMF (PEG standard calibration);

**82% of the allyl groups were converted into thioacetate groups

Characterization:

Linear polyglycerol thioacetate:

FT-IR (on ATR crystal) [in cm^{-1}]: 2910, 2867, 1687, 1426, 1353, 1102, 952. ^{1}H NMR (300 MHz, DMSO-d_6): δ (ppm) = 3.57-3.39 (broad, PG protons); 2.88-2.83 (t, -**CH$_2$**-S-CO-CH$_3$); 2.31 (s, -S-CO-**CH$_3$**); 1.74-1.67 (m, -**CH$_2$**-CH$_2$-S-CO-CH$_3$).

Hyperbranched polyglycerol thioacetate:

FT-IR (on ATR crystal) [in cm^{-1}]: 2865, 1686, 1428, 1353, 1101, 953. ^{1}H NMR (300 MHz, DMSO-d_6): δ (ppm) = 3.55-3.37 (broad, PG protons); 2.89-2.83 (m, -**CH$_2$**-S-CO-CH$_3$); 2.31 (s, -S-CO-**CH$_3$**); 1.74-1.67 (m, **CH$_2$**-CH$_2$-S-CO-CH$_3$); 0.79 (t, CH$_2$-**CH$_3$** initiator).

Hb 3: FT-IR (on ATR crystal) [in cm^{-1}]: 2866, 1686, 1428, 1353, 1101, 943. ^{1}H NMR (300 MHz, DMSO-d_6): δ (ppm) = 5.90-5.80 (m, CH$_2$=**CH**-CH$_2$-); 5.27-5.19 (d, **CH$_2$**=CH-CH$_2$-(cis)); 5.14-5.06 (t, **CH$_2$**=CH-CH$_2$-(trans)); 4.07-3.92 (m, CH$_2$=CH-**CH$_2$**-); 3.55-3.39 (broad, PG protons); 2.89-2.84 (m, -**CH$_2$**-S-CO-CH$_3$); 2.30 (s, -S-CO-**CH$_3$**); 1.77-1.64 (m, -**CH$_2$**-CH$_2$-S-CO-CH$_3$); 0.79 (t, CH$_2$-**CH$_3$** initiator).

PEG-PAGE di- and triblock-based thioacetates:

PEG I: FT-IR (on ATR crystal) [in cm^{-1}]: 2881, 1689, 1466, 1341, 1101, 960. ^{1}H NMR (400 MHz, CHCl$_3$-*d*): δ (ppm) = 3.82-3.43 (broad, PEG chain); 3.38 (s; **CH$_3$**O-PEG-); 2.93 (t; -CH$_2$-**CH$_2$**-S-CO-CH$_3$); 2.33 (s, -S-CO-**CH$_3$**); 1.86-1.80 (m, -**CH$_2$**-CH$_2$-S-CO-CH$_3$).

PEG II: FT-IR (on ATR crystal) [in cm^{-1}]: 2881, 1689, 1466, 1342, 1101, 961. ^1H NMR (400 MHz, $CHCl_3$-*d*): δ (ppm) = 3.83-3.43 (broad, PEG chain); 2.95-2.92 (m; -CH_2-**CH_2**-S-CO-CH_3); 2.33 (s, -S-CO-**CH_3**); 1.86-1.79 (m, -**CH_2**-CH_2-S-CO-CH_3).

4.9.3 General polymerization protocol for propylene sulfide[128]

The reaction vessel was flushed with argon for 5 minutes and THF was degassed via bubbling argon through the solvent for 60 minutes or by freezing the mixture in liquid nitrogen, evacuating under high vacuum and filling the reaction vessel with argon after bringing back to room temperature for five times. 5 ml of the degassed THF was added to the reaction flask and the macroinitiator or benzyl thioacetate in 1 ml THF was added. Then a reducing agent in 1 ml THF and in total 1.05 equiv. sodium methoxide solution (per thioacetate) (0.5 M in methanol) in 1 ml THF was introduced. After five minutes 10, 20, 30 or 40 equiv. propylene sulfide (per thioacetate) in 1 ml degassed THF were added and the reaction mixture was stirred. The pH was adjusted using 1.1 equiv. (per thioacetate) of acetic acid in 1 ml THF and 1.15 equiv. (per thioacetate) DBU in 1 ml THF. 2 equiv. (per thioacetate) of ethyl bromoacetate in 1 ml THF was subsequently added and the reaction was stirred twenty hours at room temperature. The solvent was removed at the rotary evaporator, dissolved in dichloromethane and the solution was extracted three times with water. The organic phase was dried over anhydrous sodium sulfate, filtrated and the solvent was completely removed. The viscous oil was extracted three times with methanol and dried in vacuum. The PEG-PAGE di- and triblock-based thioacetates with DP 10 and 20 per thioacetate were an exception and were precipitated in cold diethyl ether for three times. Recycling preparative HPLC was used to purify some of the polyglycerol-based graft copolymers.

Characterization:

Linear polyglycerol-*graft*-poly(propylene sulfide):

Yield: 75-100% (before recycling preparative HPLC); end-capping efficiency: 66-89mol%; FT-IR (on ATR crystal) [in cm^{-1}]: 2959, 2921, 2865, 1731, 1449, 1372, 1266, 1224, 1173, 1102. ^1H NMR (400 MHz, $CDCl_3$-*d*): δ (ppm) = 4.24-4.15 (q, -OOC-**CH_2**-CH_3); 3.69-3.39 (broad, PG protons); 3.36-3.22 (q, -S-**CH_2**-COO-CH_2-CH_3); 2.94-2.83 (broad, diastereotopic **H** of -**CH_2**- PPS chain, -**CH**- PPS chain); 2.68-2.54 (broad, diastereotopic **H** of -**CH_2**- PPS chain); 1.88-1.76 (m, -O-CH_2-**CH_2**-CH_2-S-); 1.40-1.35 (broad, -**CH_3** PPS chain); 1.32-1.26 (t, -OOC-CH_2-**CH_3**). ^{13}C-NMR (75.5 MHz, $CDCl_3$-*d*): δ (ppm) = 170.54 (-**C**(O)O-CH_2-CH_3); 79.01-77.38 (PG core); 71.08-69.99 (PG core); 61.55 (-C(O)O-**CH_2**-CH_3); 41.43-39.86 (-**CH**- PPS chain); 38.54-37.81 (-**CH_2**- PPS chain); 32.88 (-S-**CH_2**-C(O)O); 29.96 (-CH_2-**CH_2**-CH_2-S-); 20.88 (-**CH_3** PPS chain); 14.33 (-OOC-CH_2-**CH_3**).

Hyperbranched polyglycerol-*graft*-poly(propylene sulfide):

Yield: 24-73% (before recycling preparative HPLC); end-capping efficiency: 64-100mol%; FT-IR (on ATR crystal) [in cm^{-1}]: 2958, 2920, 2864, 1731, 1448, 1372, 1266, 1223, 1173, 1102. ^1H NMR (400 MHz, $CDCl_3$-*d*): δ (ppm) = 4.21-4.15 (q, -OOC-**CH_2**-CH_3); 3.65-3.38 (broad, PG protons); 3.34-3.22 (q, -S-**CH_2**-COO-CH_2-CH_3); 2.92-2.83 (broad, diastereotopic **H** of -**CH_2**- PPS chain, -**CH**- PPS chain); 2.66-2.58 (broad, diastereotopic **H** of -**CH_2**- PPS chain); 1.87-1.78 (m, -O-CH_2-**CH_2**-CH_2-S-); 1.38-1.35 (broad, -**CH_3** PPS chain); 1.30-1.26 (t, -OOC-CH_2-**CH_3**).

Poly(ethylene glycol)-poly(allyl glycidyl ether)-*graft*-poly(propylene sulfide):
Yield: 71-100%; end-capping efficiency: 85-100mol%; FT-IR (on ATR crystal) [in cm^{-1}]: 2957, 2889, 1730, 1449, 1372, 1279, 1241, 1173, 1102. ^{1}H NMR (400 MHz, $CDCl_3$-*d*): δ (ppm) = 4.22-4.17 (q, -OOC-**CH_2**-CH_3); 3.78-3.58 (broad, PEG chain); 3.38 (s; **CH_3**O-PEG-); 3.34-3.24 (q, -S-**CH_2**-COO-CH_2-CH_3); 2.96-2.81 (broad, diastereotopic **H** of -**CH_2**- PPS chain, -**CH**- PPS chain); 2.66-2.56 (broad, diastereotopic **H** of -**CH_2**- PPS chain); 1.85-1.82 (m, -O-CH_2-**CH_2**-CH_2-S-); 1.39-1.37 (broad, -**CH_3** PPS chain); 1.31-1.25 (t, -OOC-CH_2-**CH_3**). ^{13}C-NMR (75.5 MHz, $CDCl_3$-*d*): δ (ppm) = 170.54 (-**C**(O)O-CH_2-CH_3); 78.85-76.87 (PAGE signals); 72.03-69.94 (PEG chain); 65.95 (**CH_3**O-PEG-); 61.53 (-C(O)O-**CH_2**-CH_3); 41.29-39.86 (-**CH**- PPS chain); 38.53-37.81 (-**CH_2**- PPS chain); 32.87 (-S-**CH_2**-C(O)O); 29.94 (-CH_2-**CH_2**-CH_2-S-); 20.87-20.12 (-**CH_3** PPS chain); 14.33 (-OOC-CH_2-**CH_3**).

Poly(allyl glycidyl ether)-poly(ethylene glycol)-poly(allyl glycidyl ether)-*graft*-poly(propylene sulfide):
Yield: 18-78%; end-capping efficiency: 89-100mol%; FT-IR (on ATR crystal) [in cm^{-1}]: 2884, 1730, 1451, 1372, 1279, 1224, 1173, 1102. ^{1}H NMR (400 MHz, $CDCl_3$-*d*): δ (ppm) = 4.21-4.16 (q, -OOC-**CH_2**-CH_3); 3.83-3.44 (broad, PEG chain); 3.33-3.23 (q, -S-**CH_2**-COO-CH_2-CH_3); 2.95-2.84 (broad, diastereotopic **H** of -**CH_2**- PPS chain, -**CH**- PPS chain); 2.65-2.58 (broad, diastereotopic **H** of -**CH_2**- PPS chain); 1.86-1.81 (m, -O-CH_2-**CH_2**-CH_2-S-); 1.38-1.36 (broad, -**CH_3** PPS chain); 1.30-1.27 (t, -OOC-CH_2-**CH_3**). ^{13}C-NMR (75.5 MHz, $CDCl_3$-*d*): δ (ppm) = 170.64 (-**C**(O)O-CH_2-CH_3); 72.17-70.00 (PEG chain); 61.64 (-C(O)O-**CH_2**-CH_3); 41.48-40.01 (-**CH**- PPS chain); 38.64-37.92 (-**CH_2**- PPS chain); 32.98 (-S-**CH_2**-C(O)O); 29.95 (-CH_2-**CH_2**-CH_2-S-); 20.96-20.26 (-**CH_3** PPS chain); 14.42 (-OOC-CH_2-**CH_3**).

Poly(propylene sulfide) as reference:
Yield: 33-100%; end-capping efficiency: 94-100mol%; FT-IR (on ATR crystal) [in cm^{-1}]: 2959, 2920, 1731, 1450, 1372, 1266, 1224, 1173, 1099. ^{1}H NMR (400 MHz, $CDCl_3$-*d*): δ (ppm) = 7.29-7.20 (m, **C_6H_5**-CH_2-S-); 4.19-4.13 (q, -OOC-**CH_2**-CH_3); 3.71 (s, C_6H_5-**CH_2**-S-); 3.31-3.20(q, -S-**CH_2**-COO-CH_2-CH_3); 2.93-2.77 (broad, diastereotopic **H** of -**CH_2**- PPS chain, -**CH**- PPS chain); 2.62-2.56 (broad, diastereotopic **H** of -**CH_2**- PPS chain); 1.35-1.30 (broad, -**CH_3** PPS chain); 1.27-1.24 (t, -OOC-CH_2-**CH_3**). ^{13}C-NMR (75.5 MHz, $CDCl_3$-*d*): δ (ppm) = 170.62 (-**C**(O)O-CH_2-CH_3); 138.53-127.34 (**C_6H_5**-CH_2-S-); 61.62 (-C(O)O-**CH_2**-CH_3); 42.31-40.38 (-**CH**- PPS chain); 38.95 (C_6H_5-**CH_2**-S-); 38.29-37.22 (-**CH_2**- PPS chain); 32.96 (-S-**CH_2**-C(O)O); 20.95-20.68 (-**CH_3** PPS chain); 14.40 (-OOC-CH_2-**CH_3**).

4.9.4 General polymerization protocol for ethylene sulfide

In a typical experiment the reaction vessel was evacuated three times under high vacuum and purged again with argon. THF was degassed by freezing the mixture in liquid nitrogen, evacuating under high vacuum and filling the reaction vessel with argon after bringing back to room temperature for five times. 5 ml of the degassed THF was added to the reaction flask and the macroinitiator in 1 ml THF was added. Then 5 equiv. (per thioacetate) TBP in 1 ml THF and in total 1.05 equiv. (per thioacetate) sodium methoxide solution (0.5 M in methanol) in 1 ml THF was introduced. After five minutes 5 equiv. (per thioacetate) ethylene sulfide in 1 ml degassed THF were added and the reaction mixture was stirred for 16 hours. The pH was adjusted using 1.1 equiv. (per thioacetate) of acetic acid in 1 ml THF and 1.15 equiv. (per thioacetate) DBU in 1 ml THF. 2 equiv. (per thioacetate) of ethyl bromoacetate in 1 ml THF was subsequently added and the reaction was stirred twenty hours at room temperature. The solvent was removed at the rotary evaporator, dissolved in

dichloromethane and the solution was extracted three times with water. The organic phase was dried over anhydrous sodium sulfate, filtrated and the solvent was completely removed. The viscous oil was extracted three times with methanol and dried in vacuum. The PEG-PAGE di- and triblock-based thioacetates were precipitated in cold diethyl ether for three times.

Characterization:

Linear polyglycerol-*graft*-poly(ethylene sulfide):

Yield: 18%; end-capping efficiency: 81mol%; FT-IR (on ATR crystal) [in cm^{-1}]: 2929, 1726, 1425, 1264, 1186, 1101. ^{1}H NMR (400 MHz, $CDCl_3$-*d*): δ (ppm) = 4.23-4.17 (q, -OOC-**CH_2**-CH_3); 3.62-3.49 (broad, PG protons); 3.25 (s, -S-**CH_2**-COO-CH_2-CH_3); 2.88-2.74 (broad, -**CH_2**- PES chain); 2.64-2.60 (m; -CH_2-**CH_2**-S-CO-CH_3); 1.88-1.83 (m, -O-CH_2-**CH_2**-CH_2-S-); 1.32-1.28 (t, -OOC-CH_2-**CH_3**)

Hyperbranched polyglycerol-*graft*-poly(ethylene sulfide):

Yield: 14-19%; end-capping efficiency: 64-65mol%; FT-IR (on ATR crystal) [in cm^{-1}]: 2930, 2860, 1739, 1425, 1365, 1267, 1186, 1104. ^{1}H NMR (400 MHz, $CDCl_3$-*d*): δ (ppm) = 4.22-4.17 (q, -OOC-**CH_2**-CH_3); 3.65-3.42 (broad, PG protons); 3.25 (s, -S-**CH_2**-COO-CH_2-CH_3); 2.87-2.71 (broad, -**CH_2**- PES chain); 1.86-1.81 (m, -O-CH_2-**CH_2**-CH_2-S-); 1.31-1.27 (t, -OOC-CH_2-**CH_3**).

Poly(ethylene glycol)-poly(allyl glycidyl ether)-*graft*-poly(ethylene sulfide):

Yield: 81%; end-capping efficiency: 97mol%; FT-IR (on ATR crystal) [in cm^{-1}]: 2875, 1731, 1466, 1426, 1342, 1279, 1241, 1186, 1101. ^{1}H NMR (400 MHz, $CDCl_3$-*d*): δ (ppm) = 4.22-4.16 (q, -OOC-**CH_2**-CH_3); 3.69-3.37 (broad, PEG chain); 3.37 (s; **CH_3**O-PEG-); 3.24 (s, -S-**CH_2**-COO-CH_2-CH_3); 2.88-2.70 (broad, -**CH_2**- PES chain); 2.62-2.59 (m; -CH_2-**CH_2**-S-CO-CH_3); 1.86-1.81 (m, -O-CH_2-**CH_2**-CH_2-S-); 1.31-1.27 (t,-OOC-CH_2-**CH_3**).

Poly(allyl glycidyl ether)-poly(ethylene glycol)-poly(allyl glycidyl ether)-*graft*-poly(ethylene sulfide):

Yield: 79%; end-capping efficiency: 100mol%; FT-IR (on ATR crystal) [in cm^{-1}]: 2880, 1466, 1359, 1280, 1241, 1101. ^{1}H NMR (400 MHz, $CDCl_3$-*d*): δ (ppm) = 4.21-4.16 (q, -OOC-**CH_2**-CH_3); 3.75-3.43 (broad, PEG chain); 3.23 (s, -S-**CH_2**-COO-CH_2-CH_3); 2.83-2.72 (broad, -**CH_2**- PES chain); 2.62-2.59 (m; -CH_2-**CH_2**-S-CO-CH_3); 1.85-1.80 (m, -O-CH_2-**CH_2**-CH_2-S-); 1.30-1.26 (t,-OOC-CH_2-**CH_3**). ^{13}C-NMR (75.5 MHz, $CDCl_3$-*d*): δ (ppm) = 170.20 (-**C**(O)O-CH_2-CH_3); 79.18-77.32 (PAGE signals) 72.62-69.35 (PEG chain); 61.43 (-C(O)O-**CH_2**-CH_3); 33.56 (-S-**CH_2**-C(O)O); 32.54-31.63 (-**CH_2**- PES chain); 29.64 (-CH_2-**CH_2**-CH_2-S-); 14.18 (-OOC-CH_2-**CH_3**).

4.9.5 General polymerization protocol for the random copolymerization

In a typical experiment the reaction vessel was evacuated three times under high vacuum and purged again with argon. THF was degassed by freezing the mixture in liquid nitrogen, evacuating under high vacuum and filling the reaction vessel with argon after bringing back to room temperature for five times. 5 ml of the degassed THF was added to the reaction flask and the macroinitiator or benzyl thioacetate in 1 ml THF was added. Then 5 equiv. (per thioacetate) TBP in 1 ml THF and in total 1.05 equiv. (per thioacetate) sodium methoxide solution (0.5 M in methanol) in 1 ml THF was introduced. After five minutes 5, 10 or 15 equiv. (per thioacetate) ethylene sulfide in 1 ml THF and 10, 20, 30 or 40 equiv. propylene sulfide in 1 ml THF were added and the reaction mixture was stirred for 16 hours. The pH was adjusted using 1.1 equiv. (per thioacetate) of acetic acid in 1 ml THF and 1.15 equiv. (per thioacetate) DBU in 1 ml THF. 2 equiv. (per

thioacetate) of ethyl bromoacetate in 1 ml THF was subsequently added and the reaction was stirred twenty hours at room temperature. The solvent was removed at the rotary evaporator, dissolved in dichloromethane and the solution was extracted three times with water. The organic phase was dried over anhydrous sodium sulfate, filtrated and the solvent was completely removed. The viscous oil was extracted three times with methanol and dried in vacuum. The PEG-PAGE di- and triblock-based thioacetates with DP 10 and 20 per thioacetate were an exception and were precipitated in cold diethyl ether for three times.

Characterization:

Linear polyglycerol-*graft*-poly(ethylene sulfide))-poly(propylene sulfide):

Yield: 28-94%; end-capping efficiency: 50-100mol%; FT-IR (on ATR crystal) [in cm^{-1}]: 2957, 2921, 2865, 1729, 1422, 1260, 1172, 1091. ^{1}H NMR (400 MHz, $CDCl_3$-*d*): δ (ppm) = 4.23-4.18 (q, -OOC-**CH_2**-CH_3); 3.67-3.46 (broad, PG protons); 3.35-3.25 (s, -S-**CH_2**-COO-CH_2-CH_3); 2.96-2.87 (broad, diastereotopic **H** of -**CH_2**- PPS chain, -**CH**- PPS chain); 2.82-2.75 (broad, -**CH_2**- PES chain); 2.66-2.61 (broad, diastereotopic **H** of -**CH_2**- PPS chain); 1.88-1.79 (m, -O-CH_2-**CH_2**-CH_2-S-); 1.40-1.38 (broad, -**CH_3** PPS chain); 1.32-1.29 (t, -OOC-CH_2-**CH_3**).

Hyperbranched polyglycerol-*graft*-poly(ethylene sulfide)-poly(propylene sulfide):

Yield: 50-81%; end-capping efficiency: 72-96mol%; FT-IR (on ATR crystal) [in cm^{-1}]: 2958, 2919, 2864, 1729, 1448, 1365, 1173, 1100. ^{1}H NMR (400 MHz, $CDCl_3$-*d*): δ (ppm) = 4.22-4.17 (q, -OOC-**CH_2**-CH_3); 3.66-3.44 (broad, PG protons); 3.34-3.23 (m, -S-**CH_2**-COO-CH_2-CH_3); 2.96-2.85 (broad, diastereotopic **H** of -**CH_2**- PPS chain, -**CH**- PPS chain); 2.80-2.73 (broad, -**CH_2**- PES chain); 2.65-2.66 (broad, diastereotopic **H** of -**CH_2**- PPS chain); 1.86-1.79 (m, -O-CH_2-**CH_2**-CH_2-S-); 1.38-1.37 (broad, -**CH_3** PPS chain); 1.31-1.27 (t, -OOC-CH_2-**CH_3**). ^{13}C-NMR (75.5 MHz, $CDCl_3$-*d*): δ (ppm) = 170.65 (-**C**(O)O-CH_2-CH_3); 72.22-68.15 (PG core); 61.66 (-C(O)O-**CH_2**-CH_3); 41.49-39.48 (-**CH**- PPS chain); 38.63-37.92 (-**CH_2**- PPS chain); 33.54-32.34 (-**CH_2**- PES chain); 32.99 (-S-**CH_2**-C(O)O); 31.21 (-CH_2-**CH_2**-CH_2-S-); 20.97-20.13 (-**CH_3** PPS chain); 14.44 (-OOC-CH_2-**CH_3**).

Poly(ethylene glycol)-poly(allyl glycidyl ether)-*graft*-poly(ethylene sulfide)-poly(propylene sulfide):

Yield: 29-100%; end-capping efficiency: 68-100mol%; FT-IR (on ATR crystal) [in cm^{-1}]: 2886, 1729, 1451, 1342, 1279, 1241, 1186, 1101.^{1}H NMR (400 MHz, $CDCl_3$-*d*): δ (ppm) = 4.22-4.17 (q, -OOC-**CH_2**-CH_3); 3.75-3.43 (broad, PEG chain); 3.37 (s; **CH_3**O-PEG-); 3.34-3.23 (m, -S-**CH_2**-COO-CH_2-CH_3); 2.98-2.85 (broad, diastereotopic **H** of -**CH_2**- PPS chain, -**CH**- PPS chain); 2.81-2.73 (broad, -**CH_2**- PES chain); 2.65-2.60 (broad, diastereotopic **H** of -**CH_2**- PPS chain); 1.87-1.81 (m, -O-CH_2-**CH_2**-CH_2-S-); 1.38-1.37 (broad, -**CH_3** PPS chain); 1.31-1.27 (t,-OOC-CH_2-**CH_3**). ^{13}C-NMR (75.5 MHz, $CDCl_3$-*d*): δ (ppm) = 170.43 (-**C**(O)O-CH_2-CH_3); 78.84-77.37 (PAGE signals); 70.93-69.83 (PEG chain); 61.44 (-C(O)O-**CH_2**-CH_3); 41.28-39.12 (-**CH**- PPS chain); 38.43-37.71 (-**CH_2**- PPS chain); 33.34-32.38 (-**CH_2**- PES chain); 32.78 (-S-**CH_2**-C(O)O); 31.00 (-CH_2-**CH_2**-CH_2-S-); 20.77-20.02 (-**CH_3** PPS chain); 14.22 (-OOC-CH_2-**CH_3**).

Poly(allyl glycidyl ether)-poly(ethylene glycol)-poly(allyl glycidyl ether)-*graft*-poly(ethylene sulfide)-poly(propylene sulfide):

Yield: 53-84%; end-capping efficiency: 76-100mol%; FT-IR (on ATR crystal) [in cm^{-1}]: 2885, 1729, 1451, 1342, 1279, 1101. ^{1}H NMR (400 MHz, $CDCl_3$-*d*): δ (ppm) = 4.22-4.17 (q, -OOC-**CH_2**-CH_3); 3.72-3.44 (broad, PEG chain); 3.34-3.24 (m, -S-**CH_2**-COO-CH_2-CH_3); 2.96-2.85 (broad, diastereotopic **H** of -**CH_2**- PPS chain, -**CH**- PPS chain); 2.78-2.73 (broad, -**CH_2**- PES chain); 2.64-2.60 (broad, diastereotopic **H** of -**CH_2**- PPS chain); 1.87-1.82

(m, -O-CH_2-**CH_2**-CH_2-S-); 1.38-1.37 (broad, -**CH_3** PPS chain); 1.31-1.27 (t,-OOC-CH_2-**CH_3**). ^{13}C-NMR (75.5 MHz, $CDCl_3$-*d*): δ (ppm) = 170.42 (-**C**(O)O-CH_2-CH_3); 78.51-77.43 (PAGE signals); 71.95-69.80 (PEG chain); 61.42 (-C(O)O-**CH_2**-CH_3); 41.24-39.91 (-**CH**- PPS chain); 38.40-37.69 (-**CH_2**- PPS chain); 33.31-32.18 (-**CH_2**- PES chain); 32.75 (-S-**CH_2**-C(O)O); 30.99 (-CH_2-**CH_2**-CH_2-S-); 20.75-20.01 (-**CH_3** PPS chain); 14.21 (-OOC-CH_2-**CH_3**).

Poly(ethylene sulfide)-poly(propylene sulfide) as reference:

Yield: 28-89%; end-capping efficiency: 90-100mol%; FT-IR (on ATR crystal) [in cm^{-1}]: 2957, 2921, 2866, 1729, 1425, 1371, 1267, 1174, 1098. ^{1}H NMR (400 MHz, $CDCl_3$-*d*): δ (ppm) = 7.32-7.24 (m, **C_6H_5**-CH_2-S-); 4.22-4.16 (q, -OOC-**CH_2**-CH_3); 3.75-3.74 (d, C_6H_5-**CH_2**-S-); 3.34-3.23 (q, -S-**CH_2**-COO-CH_2-CH_3); 2.97-2.83 (broad, diastereotopic **H** of -**CH_2**- PPS chain, -**CH**- PPS chain); 2.77-2.75 (broad, -**CH_2**- PES chain); 2.69-2.57 (broad, diastereotopic **H** of -**CH_2**- PPS chain); 1.38-1.31 (broad, -**CH_3** PPS chain); 1.31-1.27 (t, -OOC-CH_2-**CH_3**). ^{13}C-NMR (75.5 MHz, $CDCl_3$-*d*): δ (ppm) = 170.41 (-**C**(O)O-CH_2-CH_3); 138.15-127.13 (**C_6H_5**-CH_2-S-); 61.41 (-C(O)O-**CH_2**-CH_3); 41.25-39.89 (-**CH**- PPS chain); 38.73 (C_6H_5-**CH_2**-S-); 38.40-37.04 (-**CH_2**- PPS chain); 33.31-30.99 (-**CH_2**- PES chain); 32.76 (-S-**CH_2**-C(O)O); 20.75-20.01 (-**CH_3** PPS chain); 14.21 (-OOC-CH_2-**CH_3**).

4.9.6 General polymerization protocol for the block-copolymerization

In a typical experiment the reaction vessel was evacuated three times under high vacuum and purged again with argon. THF was degassed by freezing the mixture in liquid nitrogen, evacuating under high vacuum and filling the reaction vessel with argon after bringing back to room temperature for five times. 5 ml of the degassed THF was added to the reaction flask and benzyl thioacetate in 1 ml THF was added. Then 5 equiv. TBP in 1 ml THF and 1.05 equiv. sodium methoxide solution (0.5 M in methanol) in 1 ml THF was introduced. After five minutes 5 equiv. ethylene sulfide or 10, 20, 30 or 40 equiv. propylene sulfide in 1 ml THF was added and after 45 minutes 10, 20, 30 or 40 equiv. propylene sulfide or 5 equiv. ethylene sulfide, respectively, in 1 ml THF were added and the reaction mixture was stirred for 45 minutes. The pH was adjusted using 1.1 equiv. of acetic acid in 1 ml THF and 1.15 equiv. DBU in 1 ml THF. 2 equiv. of ethyl bromoacetate in 1 ml THF was subsequently added and the reaction was stirred twenty hours at room temperature. The solvent was removed at the rotary evaporator, dissolved in dichloromethane and the solution was extracted three times with water. The organic phase was dried over anhydrous sodium sulfate, filtrated and the solvent was completely removed. The viscous oil was extracted three times with methanol and dried in vacuum.

Characterization:

Poly(ethylene sulfide)-*block*-poly(propylene sulfide) as reference:

Yield: 50-80%; end-capping efficiency: 72-100mol%; FT-IR (on ATR crystal) [in cm^{-1}]: 2958, 2922, 2865, 1729, 1426, 1372, 1264, 1173, 1097. ^{1}H NMR (400 MHz, $CDCl_3$-*d*): δ (ppm) = 7.32-7.24 (m, **C_6H_5**-CH_2-S-); 4.22-4.16 (q, -OOC-**CH_2**-CH_3); 3.75 (s, C_6H_5-**CH_2**-S-); 3.34-3.23 (q, -S-**CH_2**-COO-CH_2-CH_3); 2.94-2.81 (broad, diastereotopic **H** of -**CH_2**- PPS chain, -**CH**- PPS chain); 2.77-2.75 (broad, -**CH_2**- PES chain); 2.69-2.59 (broad, diastereotopic **H** of -**CH_2**- PPS chain); 1.38-1.36 (broad, -**CH_3** PPS chain); 1.30-1.27 (t, -OOC-CH_2-**CH_3**). ^{13}C-NMR (75.5 MHz, $CDCl_3$-*d*): δ (ppm) = 170.42 (-**C**(O)O-CH_2-CH_3); 128.86-127.18 (**C_6H_5**-CH_2-S-); 61.43 (-C(O)O-**CH_2**-CH_3); 41.27-39.94 (-**CH**- PPS chain); 38.41-37.69 (-**CH_2**- PPS chain); 36.41 (C_6H_5-**CH_2**-S-); 33.20-31.33 (-**CH_2**- PES chain); 32.76 (-S-**CH_2**-C(O)O); 20.76-20.03 (-**CH_3** PPS chain); 14.23 (-OOC-CH_2-**CH_3**).

4.9.7 General protocol for the adsorption of polysulfides onto gold

4.9.7.1 Adsorption of polysulfides onto Au NPs

5 ml of the aqueous gold particle solution was extracted with 5 ml polysulfide solution (1 $mg \cdot ml^{-1}$ in dichloromethane or toluene) via shaking at a frequency of 500 min^{-1} at room temperature for 60 minutes. Immediately after this time the water phases as well as the organic phases were characterized using a UV-vis spectrometer.

4.9.7.2 Adsorption of polysulfides onto bare gold substrates

A bare template-stripped gold substrate was dipped in polysulfide solution (1 $mg \cdot ml^{-1}$) in dichloromethane at room temperature for 15 minutes to 20 hours. The substrates were rinsed 10 times with dichloromethane, dried under argon stream and stored under argon atmosphere until the AFM and static contact angle measurements.

4.9.7.3 Adsorption of Au NPs onto polysulfides-modified bare gold substrates

The polysulfides were adsorbed onto bare gold substrates as described before. Subsequently, the polymer-coated gold substrates were immersed into aqueous gold nanoparticle solution at room temperature for 60 minutes. The substrates were rinsed 10 times with distilled water, dried under argon stream and stored under argon atmosphere until the AFM measurements.

4.9.8 General polymerization protocol for online NMR experiments

The macroinitiator was dissolved in 0.7 ml THF-d_8 in a common NMR sealed with a rubber septum and the solution was degased by five cycles of freeze-pump-thaw. 1.05 equiv. (per thioacetate) sodium trideutero methoxide (0.5 M in methanol-d_4) was added and 30 equiv. (per thioacetate) propylene sulfide was introduced after five minutes under argon atmosphere. The reaction mixture was homogenized by shaking the NMR tube. Subsequently, every minute a NMR spectrum with four scans was recorded for 45-60 minutes and following a spectrum with thirty-two scans was recorded.

4.10 References

(87) Vo, C. D.; Kilcher, G.; Tirelli, N.; *Macromolecular Rapid Communications* **2009**, *30*, 299.
(88) Sander, M.; *Chemical Reviews* **1966**, *66*, 297.
(89) Delépine, M.; *Comptes rendus hebdomadaires des séances de l´Académie des sciences* **1920**, *171*, 36.
(90) Tarbell, D. S.; Harnish, D. P.; *Chemical Reviews* **1951**, *49*, 1.
(91) Delépine, M.; Eschenbrenner, S.; *Bulletin de la Société Chimique de France* **1923**, *33*, 703.
(92) Delépine, M.; *Bulletin de la Société Chimique de France* **1920**, *27*, 740.
(93) Boileau, S.; Coste, J.; Raynal, J.; Sigwalt, P.; *Comptes rendus hebdomadaires des séances de l´Académie des sciences* **1962**, *254*, 2774.
(94) Gobran, R. H.; Larsen, R.; *Journal of Polymer Science Part C: Polymer Letters* **1970**, *31*, 77.
(95) Gobran, R. H.; *Encyclopedia of Polymer Science and Technology* **1969**, *10*, 324.
(96) Catsiff, E. H.; Gillis, M. N.; *Journal of Polymer Science Part A: Polymer Chemistry* **1970**, *9*, 1271.
(97) Catsiff, E. H.; *Journal of Applied Polymer Science* **1971**, *15*, 1641.
(98) Gillis, M. N; Catsiff, E. H.; Gobran, R. H.; *Journal of Polymer Science Part A: Polymer Chemistry* **1971**, *9*, 1293.
(99) Moss, B.; Dorset, D. L.; *Journal of Macromolecular Science: Physics* **1983**, *B22(1)*, 69.
(100) Bhaumik, D.; Mark, J. E.; *Macromolecules* **1981**, *14*, 162.
(101) Welsh, W. J.; Mark, J. E.; Riande, E.; *Polymer Journal* **1980**, *12*, 467.
(102) Riande, E.; Guzmán, J.; *Macromolecules* **1981**, *14*, 1234.
(103) Sasanuma, Y.; Ohta, H.; Touma, I.; Matoba, H.; Hayashi, Y.; Kaito, A.; *Macromolecules* **2002**, *35*, 3748.
(104) Oyama, T.; Naka, K.; Chujo, Y.; *Macromolecules* **1999**, *32*, 5240.
(105) Aeiyach, S.; Dubois, J.-E.; Lacaze, P.-C.; *Journal of Electroanalytical Chemistry* **1986**, *207*, 117.
(106) Delépine, M.; Jaffeux, P.; *Comptes rendus hebdomadaires des séances de l´Académie des sciences* **1921**, *172*, 158.
(107) Marvel, C. S.; Weil, E. D.; *Journal of the American Chemical Society* **1954**, *76*, 61.
(108) Boileau, S.; Sigwalt, P.; *Comptes rendus hebdomadaires des séances de l´Académie des sciences* **1961**, *252*, 882.
(109) Boileau, S.; Champetier, G.; Sigwalt, P.; *Die Makromolekulare Chemie* **1963**, *69*, 180.
(110) Hemery, P.; Boileau, S.; Sigwalt, P.; *European Polymer Journal* **1971**, *7*, 1581.
(111) Hemery, P.; Boileau, S.; Sigwalt, P.; *Journal of Polymer Science: Polymer Letters Editions* **1975**, *13*, 49.
(112) Nicco, A.; Boucheron, B.; *European Polymer Journal* **1970**, *6*, 1477.
(113) Guerin, P.; Boileau, S.; Subira, F.; Sigwalt, P.; *European Polymer Journal* **1980**, *16*, 121.
(114) Sigwalt, P.; *Pure and Applied Chemistry* **1976**, *48*, 257.
(115) Tsuruta, T.; *Journal of Polymer Science Part D: Macromolecular Reviews* **1972**, *6*, 179.
(116) Furukawa, J.; Kawabata, N.; Kato, A.; *Journal of Polymer Science Part C: Polymer Letters* **1967**, *5*, 1073.
(117) Sigwalt, P.; *International Journal of Sulfur Chemistry* **1972**, *C 7*, 83.
(118) Dumas, P.; Sigwalt, P.; *Charality* **1991**, *3*, 484.
(119) Sasanuma, Y.; Hayashi, Y.; Matoba, H.; Touma, I.; Ohta, H.; Sawanobori, M.; Kaito, A.; *Macromolecules* **2002**, *35*, 8216.
(120) Nicol, E.; Nicolai, T.; Durand, D.; *Macromolecules* **1999**, *32*, 7530.
(121) Hirano, T.; Akutsu, S.; Tsuruta, T.; *Journal of Macromolecular Science, Part A: Pure and Applied Chemistry* **1969**, *2*, 315.
(122) Lambert, J. L.; Van Ooteghem, D.; Goethals, E. J.; *Journal of Polymer Science Part A: Polymer Chemistry* **1971**, *9*, 3055.
(123) Nicol, E.; Bonnans-Plaisance, C.; Levesque, G.; *Macromolecules* **1999**, *32*, 4485.
(124) Nicol, E.; Bonnans-Plaisance, C.; Dony, P.; Levesque, G.; *Macromolecular Chemistry and Physics* **2001**, *202*, 2843.
(125) Suzuki, A.; Nagai, D.; Ochiai, B.; Endo, T.; *Macromolecules* **2004**, *37*, 8823.
(126) Kilcher, G.; Wang, L.; Tirelli, N.; *Journal of Polymer Science Part A: Polymer Chemistry* **2008**, *46*, 2233.
(127) Wang, L.; Kilcher, G.; Tirelli, N.; *Macromolecular Chemistry and Physics* **2009**, *210*, 447.
(128) Wang, L.; Kilcher, G.; Tirelli, N.; *Macromolecular Bioscience* **2007**, *7*, 987.
(129) Wang, L.; Hu, P.; Tirelli, N.; *Polymer* **2009**, *50*, 2863.
(130) Kilcher, G.; Wang, L.; Duckham, C.; Tirelli, N.; *Macromolecules* **2007**, *40*, 5141.
(131) Aida, T.; Kawaguchi, K.; Inoue, S.; *Macromolecules* **1990**, *23*, 3887.

(132) Schuetz, J.-H.; Vana, P.; *Macromolecular Chemistry and Physics* **2011**, *212*, 1263.
(133) Kudo, H.; Sato, K.; Nishikubo, T.; *Macromolecules* **2010**, *43*, 9655.
(134) Boileau, S.; Sigwalt, P.; *Die Makromolekulare Chemie* **1973**, *171*, 11.
(135) Kim, J.; Kim, S. S.; Kim, K. H.; Jin, Y. H.; Mong, S. M.; Hwang, S. S.; Cho, B.-G.; Shin, D. Y.; Im, S. S.; *Polymer* **2004**, *45*, 3527.
(136) Nevin, R. S.; Pearce, E. M.; *Journal of Polymer Science Part C: Polymer Letters* **1965**, *3*, 487.
(137) Cooper, W.; Hale, P. T.; Walker, J. S.; *Polymer* **1974**, *15*, 175.
(138) Eaves, D. E.; Strokes, A.; *European Polymer Journal* **1975**, *11*, 215.
(139) Roggero, A.; Mazzei, A.; Bruzzone, M.; Cernia, E.; *Advances in Chemistry Series* **1975**, *142*, 330.
(140) Roggero, A.; Zotteri, L.; Proni, A.; Gandini, A.; Mazzei, A.; *European Polymer Journal* **1976**, *12*, 837.
(141) Corno, C.; Roggero, A.; *European Polymer Journal* **1976**, *12*, 159.
(142) Corno, C.; Roggero, A.; Salvatori, T.; Mazzei, A.; *European Polymer Journal* **1977**, *13*, 77.
(143) De Chirico, A.; Zotteri, L.; *European Polymer Journal* **1975**, *11*, 487.
(144) Sorta, E.; De Chirico, A.; *Polymer* **1976**, *17*, 348.
(145) Kobayashi, S.; Iwata, S.; Kim, H. J.; Shoda, S.; *Macromolecules* **1996**, *29*, 486.
(146) Sasanuma, Y.; Asai, S.; Kumagai, R.; *Macromolecules* **2007**, *40*, 3488.
(147) Sasanuma, Y.; Kumagai, R.; *Macromolecules* **2007**, *40*, 7393.
(148) Löwig, C.; Weidmann, S.; *Poggendorff´s Annalen* **1839**, *49*, 123.
(149) Meyer, V.; *Berichte der deutschen chemischen Gesellschaft* **1886**, *19*, 3259.
(150) Sundarrajan, S.; Ganesh, K.; Srinivasan, K. S. V.; *Polymer* **2003**, *44*, 61.
(151) Zhang, T.; Litt, M. H.; Rogers, C. E.; *Journal of Polymer Science Part A: Polymer Chemistry* **1994**, *32*, 1323.
(152) Bonnans-Plaisance, C.; Jean, M.; Lux, F.; *European Polymer Journal* **2003**, *39*, 863.
(153) Napoli, A.; Tirelli, N.; Kilcher, G.; Hubbell, J. A.; *Macromolecules* **2001**, *34*, 8913.
(154) Cerritelli, S.; Fontana, A.; Velluto, D.; Adrian, M.; Dubochet, J.; De Maria, P.; Hubbell, J. A.; *Macromolecules* **2005**, *38*, 7845.
(155) Cerritelli, S.; O´Neil, C. P.; Velluto, D.; Fontana, A.; Adrian, M.; Dubochet, J.; Hubbell, J. A.; *Langmuir* **2009**, *25*, 11328.
(156) Cerritelli, S.; Velluto, D.; Hubbell, J. A.; Fontana, A.; *Journal of Polymer Science Part A: Polymer Chemistry* **2008**, *46*, 2477.
(157) Napoli, A.; Tirelli, N.; Wehrli, E.; Hubbell, J. A.; *Langmuir* **2002**, *18*, 8324.
(158) Hu, P.; Tirelli, N.; *Bioconjugate Chemistry* **2012**, *23*, 438.
(159) Hu, P.; Tirelli, N.; *Reactive & Functional Polymers* **2011**, *71*, 303.
(160) Yu, S. S.; Scherer, R. L.; Ortega, R. A.; Bell, C. S.; O´Neil, C. P.; Hubbell, J. A.; Giorgio, T. D.; *Journal of Nanobiotechnology* **2011**, *9*, 7.
(161) Segura, T.; Hubbell, J. A.; *Bioconjugate Chemistry* **2007**, *18*, 736.
(162) O´Neil, C. P.; Suzuki, T.; Demurtas, D.; Finka, A.; Hubbell, J. A.; *Langmuir* **2009**, *25*, 9025.
(163) Velluto, D.; Demurtas, D.; Hubbell, J. A.; *Molecular Pharmaceutics* **2008**, *5*, 632.
(164) O´Neil, C. P.; van der Vlies, A. J.; Velluto, D.; Wandrey, C.; Demurtas, D.; Dubochet, J.; Hubbell, J. A.; *Journal of Controlled Release* **2009**, *137*, 146.
(165) Cerritelli, S.; Velluto, D.; Hubbell, J. A.; *Biomacromolecules* **2007**, *8*, 1966.
(166) Velluto, D.; Thomas, S. N.; Simeoni, E.; Schwartz, M. A.; Hubbell, J. A.; *Biomaterials* **2011**, *32*, 9839.
(167) Di Meo, E. M.; Di Crescenzo, A.; Velluto, D.; O´Neil, C. P.; Demurtas, D.; Hubbell, J. A.; Fontana, A.;*Macromolecules* **2010**, *43*, 3429.
(168) Bearinger, J. P.; Terrettaz, S.; Michel, R.; Tirelli, N.; Vogel, H.; Textor, M.; Hubbell, J. A.; *Nature Materials* **2003**, *2*, 259.
(169) Feller, L. M.; Cerritelli, S.; Textor, M.; Hubbell, J. A.; Tosatti, S. G. P.; *Macromolecules* **2005**, *38*, 10503.
(170) Feller, L.; Bearinger, J. P.; Wu, L.; Hubbell, J. A.; Tosatti, S.; *Surface Science* **2008**, *602*, 2305.
(171) Bearinger, J. P.; Stone, G.; Hiddessen, A. L.; Dugan, L. C.; Wu, L.; Hailey, P.; Conway, J. W.; Kuenzler, T.; Feller, L.; Cerritelli, S.; Hubbell, J. A.; *Langmuir* **2009**, *25*, 1238.
(172) Tang, C.; Feller, L.; Rossbach, P.; Keller, B.; Vörös, J.; Tosatti, S.; Textor, M.; *Surface Science* **2006**, *600*, 1510.
(173) Watanabe, Y.; Aida, T.; Inoue, S.; *Macromolecules* **1990**, *23*, 2612.
(174) Watanabe, Y.; Aida, T.; Inoue, S.; *Macromolecules* **1991**, *24*, 3970.
(175) Boileau, S.; Sigwalt, P.; *Comptes rendus hebdomadaires des séances de l´Académie des sciences* **1965**, *261*, 132.

(176) Morton, M.; Kammereck, R. F.; Fetters, L. J.; *British Polymer Journal* **1971**, *3*, 120.
(177) Morton, M.; Kammereck, R. F.; Fetters, L. J.; *Macromolecules* **1971**, *4*, 11.
(178) Domb, A.; Avny, Y.; *Journal of Applied Polymer Science* **1984**, *29*, 2517.
(179) Boileau, S., Sigwalt, P.; *Die Makromolekulare Chemie* **1970**, *131*, 8.
(180) Bonnans-Plaisance, C.; Levesque, G.; *Macromolecules* **1989**, *22*, 2020.
(181) Bonnans-Plaisance, C.; Levesque, G.; *Polymer* **1991**, *32*, 1318.
(182) Bonnans-Plaisance, C.; Guerin, P.; Levesque, G.; *Polymer* **1995**, *36*, 201.
(183) Nagai, A.; Koike, N.; Kudo, H.; Nishikubo, T.; *Macromolecules* **2007**, *40*, 8129.
(184) Morinaga, H.; Ochiai, B.; Mori, H.; Endo, T.; *Journal of Polymer Science Part A: Polymer Chemistry* **2006**, *44*, 3778.
(185) Nakano, K.; Tatsumi, G.; Nozaki, K.; *Journal of the American Chemical Society* **2007**, *129*, 15116.
(186) Lautenschlaeger, F.; Zeeman, P.; *Journal of Polymer Science: Polymer Chemistry Edition* **1972**, *10*, 3519
(187) Lautenschlaeger, F.; *Journal of Macromolecular Science: Pure and Applied Chemistry* **1972**, *A6*, 1089.
(188) MacKillop, D. A.; *Journal of Polymer Science Part C: Polymer Letters* **1970**, *8*, 199.
(189) Amerik, Y. B.; Shirokova, L. A.; Toltchinsky, I. M.; Krentsel, B. A.; *Die Makromolekulare Chemie* **1984**, *185*, 899.
(190) Shirokova, L. A.; Amerik, Yu. B.; Sleptsova, S. A.; *Vysokomolekulyarnye Soedineniya, Seriya B: Kratkie Soobshcheniya* (*Polymer Science, Series B. Polymer Chemsitry*) **1992**, *34*, 71.
(191) Corno, C.; Roggero, A.; Salvatori, T.; *European Polymer Journal* **1974**, *10*, 525.
(192) Il'ina, D. E.; Borisova, N. A.; Krentsel, B. A.; Davydov, B. E.; *Vysokomolekulyarnye Soedineniya, Seriya B: Kratkie Soobshcheniya* **1968**, *10*, 236.
(193) Rehor, A.; Tirelli, N.; Hubbell, J. A.; *Macromolecules* **2002**, *35*, 8688.
(194) Rehor, A.; Hubbell, J. A.; Tirelli, N.; *Langmuir* **2005**, *21*, 411.
(195) Reddy, S. T.; Rehor, A.; Schmoekel, H. G.; Hubbell, J. A.; Schwartz, M. A.; *Journal of Controlled Release* **2006**, *112*, 26.
(196) Rehor, A.; Schmoekel, H.; Tirelli, N.; Hubbell, J. A.; *Biomaterials* **2008**, *29*, 1958.
(197) Khutoryanskiy, V. V.; Tirelli, N.; *Pure and Applied Chemistry* **2008**, *80*, 1703.
(198) Allen, B. L.; Johnson, J. D.; Walker, J. P.; *ASC Nano* **2011**, *5*, 5263.
(199) Vandenberg, E. J.; *Journal of Polymer Science Part A: Polymer Chemistry* **1972**, *10*, 329.
(200) Spassky, N.; Dumas, P.; Sepulchre, M.; Sigwalt, P.; *Journal of Polymer Science: Polymer Symposia* **1975**, *52*, 327.
(201) Morton, M.; Kammereck, R. F.; Fetters, L. J.; *British Polymer Journal* **1971**, *3*, 120.
(202) Kameyama, A.; Shimotsuma, K.; Nishikubo, T.; *Macromolecular Rapid Communications* **1994**, *15*, 335.
(203) Lautenschläger, F.; Schnecko, H.; *Journal of Polymer Science Part A: Polymer Chemistry* **1970**, *8*, 2579.
(204) Bonnans-Plaisance, C.; Levesque, G.; *Die Makromolekulare Chemie* **1986**, *187*, 2841.
(205) He, C.; Zhang, C.; Zhang, O.; *Polymer International* **2009**, *58*, 1071.
(206) Hirata, M.; Ochiai, B.; Endo, T.; *Journal of Polymer Science Part A: Polymer Chemistry* **2010**, 4*8*, 525.
(207) Hirata, M.; Abe, Y.; Ochiai, B.; Endo, T.; *Journal of Polymer Science Part A: Polymer Chemistry* **2010**, 4*8*, 4385.
(208) Kameyama, A.; Masahiro, K.; Nishikubo, T.; *Tetrahedron Letters* **1994**, *35*, 4571.
(209) Kudo, H.; Inoue, H.; Nishikubo, T.; Anada, T.; *Polymer Journal* **2006**, *38*, 289.
(210) Kudo, H.; Inoue, H.; Nishikubo, T.; Inagaki, T.; Nishikubo, T.; *Macromolecules* **2009**, *42*, 1051.
(211) Kudo, H.; Sato, M.; Wakai, R.; Iwamoto, T.; Nishikubo, T.; *Macromolecules* **2008**, *41*, 521.
(212) Kudo, H.; Makino, S.; Kameyama, A.; Nishikubo, T.; *Macromolecules* **2005**, *38*, 5964.
(213) Kudo, H.; Makino, S.; Nishikubo, T.; *Journal of Polymer Science Part A: Polymer Chemistry* **2007**, 4*5*, 680.
(214) Whistler, R. L.; Seib, P. A.; *Journal of Polymer Science Part A: Polymer Chemistry* **1964**, 2, 2595.
(215) Bonnans-Plaisance, C.; Courric, S.; Levesque, G.; *Polymer Bulletin* **1992**, *28*, 489.
(216) Bonnans-Plaisance, C.; Rétif, P.; Levesque, G.; *Polymer Bulletin* **1995**, *34*, 141.
(217) Bonnans-Plaisance, C.; Nakache, Ph.; Rétif, P.; *Colloid & Polymer Science* **1998**, *276*, 297.
(218) Bonnans-Plaisance, C.; Rétif, P.; *Reactive & Functional Polymers* **1999**, *39*, 9-18.
(219) Bonnans-Plaisance, C.; Levesque, G.; Pomepui, B.; *Polymer* **1993**, *34*, 2003.
(220) Bonnans-Plaisance, C.; Corvazier, L.; *Polymer* **1997**, *38*, 3843.
(221) Bonnans-Plaisance, C.; Corvazier, L.; Zhao, Y.; *Polymer Bulletin* **1998**, *40*, 569.
(222) Bonnans-Plaisance, C.; Corvazier, L.; Emery, J.; Nicol, E.; *Polymer Bulletin* **1998**, *41*, 525.
(223) Doycheva, M.; Berger-Nicoletti, E.; Wurm, F.; Frey, H.; *Macromolecular Chemistry and Physics* **2010**, *211*, 35.

(224) Wolf, F. K.; Fischer, A. M.; Frey, H.; *Beilstein Journal of Organic Chemistry* **2010**, *6*, 67.
(225) Wyszogrodzka, M.; Möws, K.; Kamlage, S.; Wodzinska, J.; Plietker, B.; Haag, R.; *European Journal of Organic Chemistry* **2008**, *1*, 53.
(226) Thompson, M. S.; Vadala, T. P.; Vadala, M. L.; Lin, Y.; Riffle, J. S.; *Polymer* **2008**, *49*, 345.
(227) Fairbanks, B. D.; Singh, S. P.; Bowman, C. N.; Anseth, K. S.; *Macromolecules* **2011**, *44*, 2444.
(228) *Organikum 22. Auflage* (Becker, H. G. O. et al.) *Wiley-VCH Verlag GmbH & Co. KGaA*, Weinheim, Deutschland, Kapitel 1.2.11.2, 696.
(229) Calderón, M.; Graeser, R.; Kratz, F.; Haag, R.; *Bioorganic & Medicinal Chemistry Letters* **2009**, *19*, 3725.
(230) Wan, D.; Li, Z.; Huang, J.; *Journal of Polymer Science Part A: Polymer Chemistry* **2005**, 43, 5458.
(231) Li, Z.; Chau, Y.; *Bioconjugate Chemsitry* **2009**, *20*, 780.
(232) Steiner, E. C.; Pelletier, R. R.; Trucks, R. O.; *Journal of the American Chemical Society* **1964**, *86*, 4678.
(233) Yu, G.-E.; Heatley, F.; Booth, C.; Blease, T. G.; *Journal of Polymer Science Part A: Polymer Chemistry* **1994**, 32, 1131.
(234) Sasanuma, Y.; *Annual Reports on NMR Spectroscopy* **2003**, *49*, 213.
(235) Obermeier, B.; Frey, H.; *Bioconjugate Chemistry* **2011**, *22*, 436.
(236) *Surface Design: Applications in Bioscience and Nanotechnology* (Förch, R.; Schönherr, H.; Jenkins, A. T. A.) *Wiley-VCH Verlag GmbH & Co. KGaA*, Weinheim, Deutschland, 471.)
(237) Engquist, I.; Lundström, I.; Liedberg, B.; *Journal of Physical Chemistry* **1995**, *99*, 12257.
(238) Naumann, R.; Schiller, S. M.; Griess, F.; Grohe, B.; Hartmann, K. B.; Kärcher, I.; Köper, I.; Lübben, J.; Vasilev, K.; Knoll, W.; *Langmuir* **2003**, *19*, 5435-5443.
(239) Luo, J.; Pardin, C.; Zhu, Z. Z.; Lubell, W. D.; *Journal of Combinatorial Chemistry* **2007,** *9*, 582.
(240) Gadelmawla, E. S.; Koura, M. M.; Maksoud, T. M. A.; Elewa, I. M.; Soliman, H. H.; *Journal of Materials Processing Technology* **2002**, *123*, 133.
(241) Sunder, A.; Hanselmann, R.; Frey, H.; Mülhaupt, R.; *Macromolecules* **1999**, *32*, 4240.
(242) Taton, D.; Le Borgne, A.; Sepulchre, M.; Spassky, N.; *Macromolecular Chemistry and Physics* **1994**, *195*, 139.
(243) Zheng, T.; Burkhart, M.; Richardson, D. E.; *Tetrahedron Letters* **1999**, *40*, 603.
(244) Brahmbhatt, K. G.; Ahmed, N.; Singh, I. P.; Bhutani, K. K.; *Tetrahedron Letters* **2009**, *50*, 5501.
(245) Medalia, O.; Englander, J.; Guckenberger, R.; Sperling, J.; *Ultramicroscopy* **2002**, *90*, 103.

Chapter 5

Modified Lipoic Acid as an Initiator for ROP

5.1 Introduction[246-350]

Thiols, disulfides and sulfides are common linkers to fix polymers onto metal surfaces, as mentioned in chapter 3. α-lipoic acid carries a disulfide functionality and is often applied for that purpose. In the following, typical characteristics and application of α-lipoic acid are introduced.

5.1.1 α-Lipoic Acid (LA)[246-298]

α-Lipoic acid (LA), also known as thioctic acid or 1,2-dithiolane-3-pentanoic acid is a light yellow powder with a melting point of 60-62 °C and it is soluble in alcohols and chlorinated organic solvents, such as dichloromethane and chloroform.[246] Its structure is shown in **Figure 5.1**. The asterisked carbon atom carries four different substituents and thus α-lipoic acid possesses a chiral center.[247]

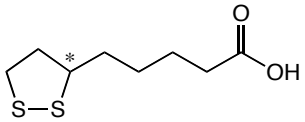

Figure 5.1: Structure of α-lipoic acid.

R-LA is a natural product, which occurs in plants, animals and humans.[248] In 1950, it was first isolated from liver by Lester J. Reed et al.[249] Endogenous LA synthesis is obtained *de novo* from actinic acid (a fatty acid) and cysteine as the sulfur source in the liver.[247] However, it can also be adsorbed from nutriment.[248]

LA is known as a cofactor of the mitochondrial dehydrogenase enzyme complex, which catalyzes the pyruvate dehydrogenase reaction. It is attached to a lysine of the enzyme via an amide bond between the amine of the amino acid and the carboxylic function of LA. Thus it is called lipoamide. LA serves in the acetyl transfer reaction and houses the acetyl group from pyruvate. The disulfide bond acts as oxidation agent of this reaction and lipoamide is reduced to acetyl lipoamide. In the next step, the acetyl group is transferred to Coenzyme A and Acetyl-CoA is formed, simultaneously dihydrolipoamide is developed from acetyl lipoamide. The last step of the catalytic cycle is the regeneration of the lipoamide via oxidation of dihydrolipoamide by the prosthetic FAD (flavin adenine dinucleotide)-group of the enzyme, which is subsequently oxidized via NAD^+ (nicotinamide adenine dinucleotide). In **Figure 5.2** the reaction cycle of the pyruvate dehydrogenase complex is schematically illustrated.[247,248,250,361]

In addition, LA can be used for metal chelation. Free iron and copper ions are redox active and might induce oxidative damage by generation of highly potential free radicals.[247,251] It was shown, that LA was enabled to avoid accumulation of iron and copper ions in animal models.[247,252] The reduced form of LA, dihydrolipoic acid (DHLA) prevented heavy metal poisoning by mercury and cadmium exposure. DHLA, for example, was described to chelate mercury and this complex exhibited an increased excretion.[248] Furthermore, it has been tested and is still in the research focus as medication for different diseases. The following citations are only a few examples. LA might by a potential drug for Alzheimer´s disease, which is characterized by chronic inflammatory processes or it can act as anti-inflammatory antioxidants and further more as modulator of redox sensitive signaling.[253]

In 2008, various benefits of LA on diabetes were summarized in a review. On one hand, LA might prevent diabetes by forestalling the beta cell destruction and on the other hand, it might enhance the glucose uptake.[247] Additionally, Halıcı et al. observed a positive effect in Japanese quails upon heat stress by the dietary supplement with LA.[254]

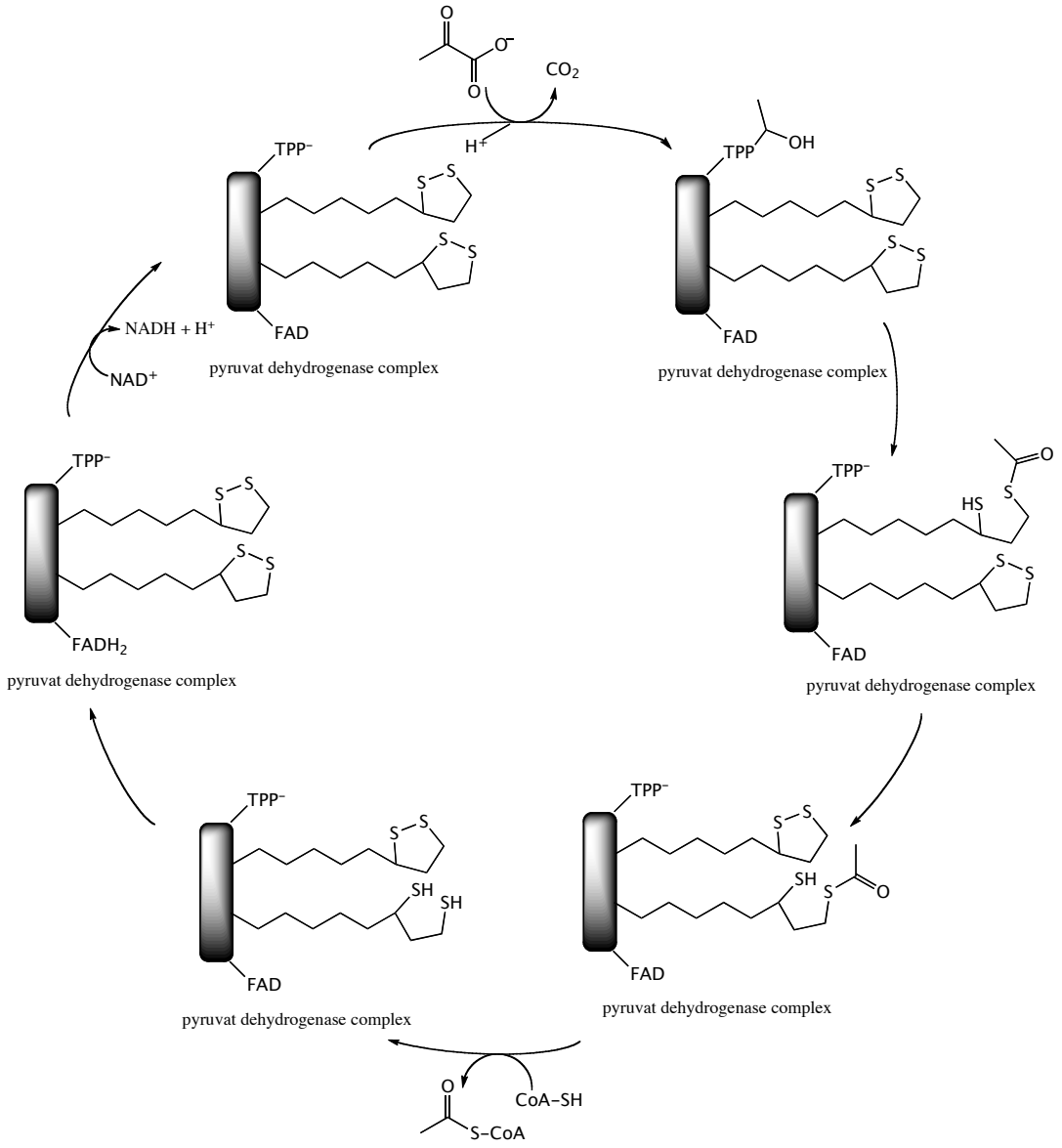

Figure 5.2: Schematic reaction cycle of the pyruvate dehydrogenase cycle.[247,248,250,361]

Sodium zinc histidine dithiooctanamide (**Figure 5.3**), an amide derivative of LA with histidine and zinc, showed in *in vitro* and *in vivo* studies a therapeutic potential against various human renal ischemia-reperfusion, which occurs frequently after renal transplantations and similar clinical settings.[255]

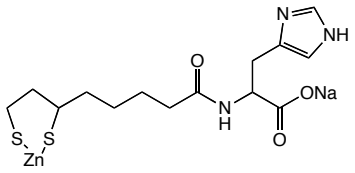

Figure 5.3: Structure of sodium zinc histidine dithiooctanamide.[255]

Zheng et al. demonstrated the use of lipoic acid-modified low molecular weight poly(ethylene imine) (PEI) as potential carriers for therapeutic gene delivery. Hydrophobic modification of the polymer led to well-

defined structures with almost no cytotoxicity even at high polymer concentrations. The modified PEI constituted a potential solution of the challenging problem of DNA condensation and release. The used polymer exhibited good DNA condensation ability with enhanced stability and the carriage as well as the release of the DNA into the cell nuclei, which was triggered by the reversible reduction of the LA side chain.[256]

In 2010, a totally recyclable solid phase supported reducing agent consisting of LA was introduced. PEG Aminomethyl-ChemMatrix® was used as solid phase, which was enabled to swell in aqueous media as well as in organic solvents. LA was linked to the support via an amide functionality. Subsequently, the LA derivative was reduced to its dihydrolipoic form, which acted as reducing agent for highly sensitive disulfide compounds to from the corresponding thiols. Thereby, the dihydrolipoic derivative was re-oxidized to the LA derivative with a disulfide bond. In this straightforward process the reducing agent could be recycled by reduction and acted again as a reducing agent.[257]

LA was also described as a monomer, which could be polymerized. Already in 1956, Thomas and Reed introduced the thermal polymerization of LA to a sticky and colorless product. The polymerization is shown in **Figure 5.4**. The depolymerization of poly(α-lipoic acid) to LA occurred in the presence of dilute sodium hydroxide solution. This reaction was slow at room temperature, but the reaction rate increased with increasing temperature.[258]

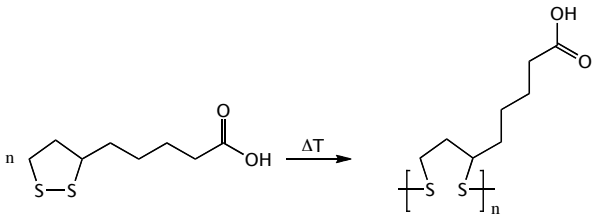

Figure 5.4: Thermal polymerization of α-lipoic acid.[258]

A further publication focused on the polymerization as well as on the photodecomposition of poly(α-lipoic acid).[259]

In a more recent work, the copolymerization of LA and 1,2-dithiane was described. The authors concluded the existence of a polycatenane structure consisting of cyclic polymers.[260] In a following work, the same group investigated the influence of zinc acetate on the network formation of these interlocked copolymers.[261]

LA was also used to functionalize gold nanoparticles (Au NPs) by the exchange of citrate linker on the nanoparticle surface. The SAM packing density increased by the addition of sodium chloride solution and the stability of the Au NPs also increased.[262]

5.1.1.1 <u>α-lipoic acid (LA) as linker group</u>[263-298]

α-lipoic acid and its derivatives are widely used linker to attach various compounds to metal surfaces as shown in the following.

Tappura et al. synthesized a library of different lipoic acid derivatives for the formation of self-assembled molecular thin films for the recognition of morphine. Hence, LA was reacted with various amines. The obtained amide variety ranged from a different number of hydroxyl functionalities, over different amines and carboxylates to structures with aromatic and aliphatic substituents. Some examples are illustrated in **Figure 5.5**. Those synthesized moieties were fixed to gold layers via the disulfide motif of the LA and further

investigated. SPR was used to study dissociation and association of morphine and the formed molecular thin films.[263]

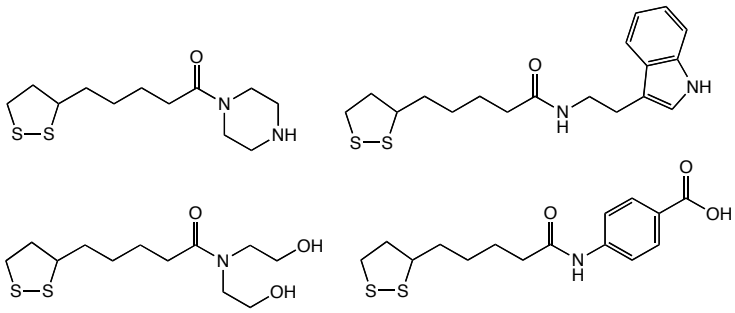

Figure 5.5: Some examples of the synthesized lipoic acid derivatives by Alberts et al.[263]

In a further approach, six different carbohydrates were attached to LA via a short linker and the protein and cell resistance of these materials were tested using a quartz microbalance. The obtained results exhibited a significant influence of the structure of the attached carbohydrate on the capability to reduce adsorption of Hella cells and human serum. In comparison to the other synthesized carbohydrate derivatives, the lipoic galactose moiety (**Figure 5.6**) showed the highest resistance against nonspecific binding. Additionally, a mixture of lipoic galactose and BSA (bovine serum albumin) exhibited resistant-ability, which was comparable to the best known systems for reduction of nonspecific adsorption.[264]

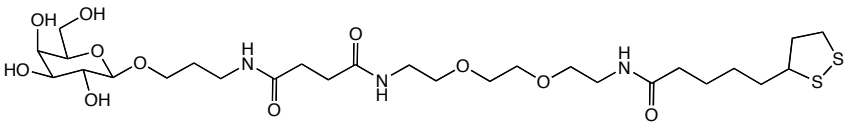

Figure 5.6: Structure of the lipoic galactose moiety.[264]

In 2005, a novel method to measure the packing densities of self-assembled thiolipid monolayers was introduced. Di-phytanyl-sn-glycerol was attached to LA via a tetraethylene glycol linker. Its structure is shown in **Figure 5.7**. The obtained thiolipid was used to form a self-assembled monolayer on the surface of a gold electrode. Subsequently the charge density on a covered gold electrode was measured by a new method, which relied on chronocoulometry.[265]

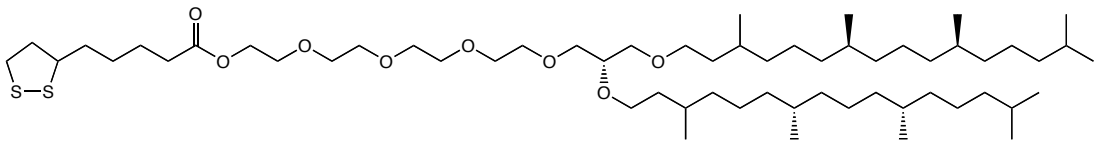

Figure 5.7: Structure of the thiolipid moiety.[265]

In a further investigation, a hydroquinone-caged biotin was linked via a tri(ethylene glycol) ester to LA to synthesize a bioactive biotin surface. A mixed SAM of tri(ethylene glycol) thiotic acid ester and the protected biotin LA derivative was accomplished on a gold surface. The structure of the caged-biotin moiety is illustrated in **Figure 5.8**.

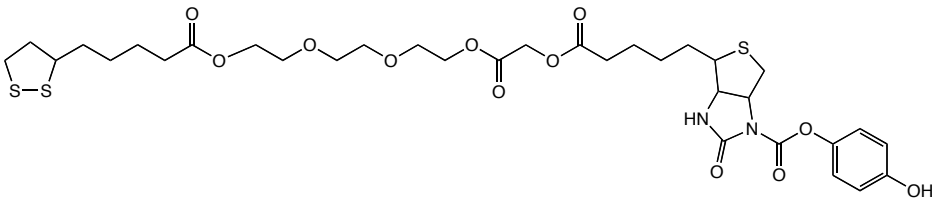

Figure 5.8: Structure of the caged-biotin moiety.[266]

After electrochemical oxidation hydroquinone and carbon dioxide were released to result in a bioactive biotin surface, which enabled a selective protein pattering on the surface. This approach might be used to fabricate protein chips.[266]

Zhang and Echegoyen described the synthesis of porphyrin derivatives, which were also fixed to gold surfaces via LA as anchoring groups. The substituted porphyrin is shown in **Figure 5.9**. The covered substrates were used to accomplish the non-covalent immobilization of C_{60}. In addition, the formed SAMs were investigated by cyclic voltammetry and the first two reduction processes of C_{60} were detected.[267]

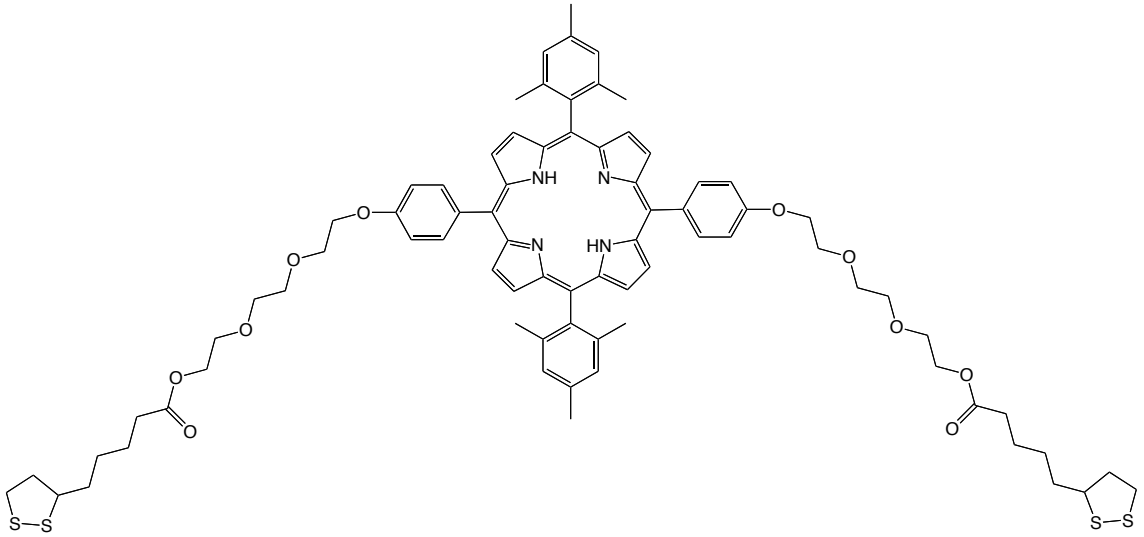

Figure 5.9: Structure of the porphyrin derivatives.[267]

This group also investigated different calix[n]arenes (n = 4, 6, 8) with LA as anchoring groups. These moieties were used to generate SAMs on gold electrodes and cyclic voltammetry measurements were conducted. Non-covalent immobilization of C_{60} was also tested on these modified surfaces. However, solely the adsorbed calix[8]arene derivative accomplished the ability to immobilize C_{60}.[268] The gold surface modified with a *p-tert*-butylcalix[4]crown-6 derivative revealed a selective binding of alkaline metal cations such as calcium and barium. The structure of the used *p-tert*-butylcalix[4]crown-6 derivative with LA linkers for gold attachment is shown in **Figure 5.10**.[269]

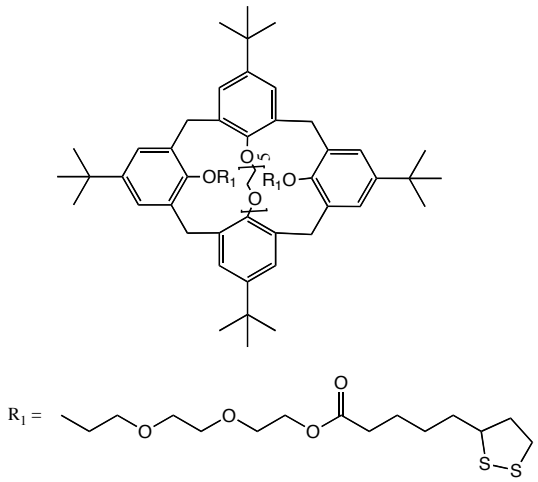

Figure 5.10: Structure of the *p-tert*-butylcalix[4]crown-6 derivatives.[269]

Additionally, two isomers of the *p-tert*-butylcalix[4]crown-6 derivative were investigated regarding the recognition of cesium ions. Both isomers formed stable SAMs on the surface of gold electrodes, but the ion recognition was significantly influenced by the conformation. Only the 1,3-alternating isomer was enabled to bind cesium ions.[270] In contrast, SAMs of *p-tert*-butylcalix[6]crown-4 derivative with LA as linker group were observed to form sensors for ammonium cations. The study via cyclic voltammetry and impedance spectroscopy manifested a selective binding of anilinium. The authors suggested a proper size fit between the *p-tert*-butylcalix[6]crown-4 derivative as host and the anilinium as a guest.[271]

In 2005, the Stoddart group described the use of a photoactive triad as a nanoscale power supply for a supramolecular machine. The molecular triad contained a tetrathiofulvalene-porphyrin-fullerene triad, which was attached to a gold electrode via LA as anchoring group. This system was enabled to generate electrical current by harnessing light energy. Three electroactive compounds were involved in the system: C_{60} as electron acceptor, porphyrin as chromophoric unit and tetrathiofulvalene as electron donor. The molecular triad is illustrated in **Figure 5.11**.[272]

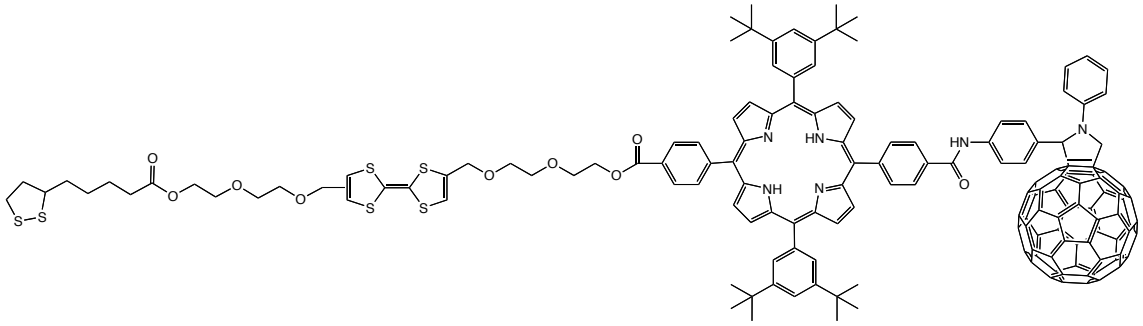

Figure 5.11: Structure of the molecular triad.[272]

Furthermore, the same group investigated a synthetic motor-molecule. Steric and electrostatic interactions of the mechanical switching of a synthesized bistable redox-controllable [2]rotaxane were measured via single molecule spectroscopy. The structure of both stable states, R^{4+} and R^{6+}, of the rotaxane are illustrated in **Figure 5.12**. The LA substituent featured the anchoring group to the gold AFM tip and the rotaxane derivative was covalently bond to a silicon wafer by isocyanatopropyl tethers. Repulsive electrostatic interaction was responsible for the molecular actuation and a value of 65 kcal·mol^{-1} was detected.[273]

LA was also used to attach macromolecules to gold surfaces, which will be introduced by selected examples in the following. In several approaches LA and its derivatives were used to adsorb proteins and poly(amino acids) onto gold substrates. In 2007, Voyer et al. reported the synthesis of a helical peptide with six crown ether side chains, which formed artificial ion channels. Both termini were converted, a lipoic acid derivative was attached to the carboxy-terminus to provide the anchoring group for the adsorption onto gold surfaces and biotin was tethered on the amine-terminus. The structure of the synthesized moiety is shown in **Figure 5.13**. The synthesized peptides were used to modify the surface of bare gold substrates and gold nanoparticles. Characterization of the gold surfaces indicated an oriented adsorption of the helical peptides on the metal surface with a tilt angle of about 55° to the surface.[275]

Synthesis of linear artificial molecular muscles was also accomplished with a similar structure. Surface attachment to gold was again enabled via LA as linker group. The synthesized molecular muscle exhibited two different states, a contracted state (TPR^{8+}) and an extended state (TPR^{12+}), which are shown in **Figure 5.14**.[274]

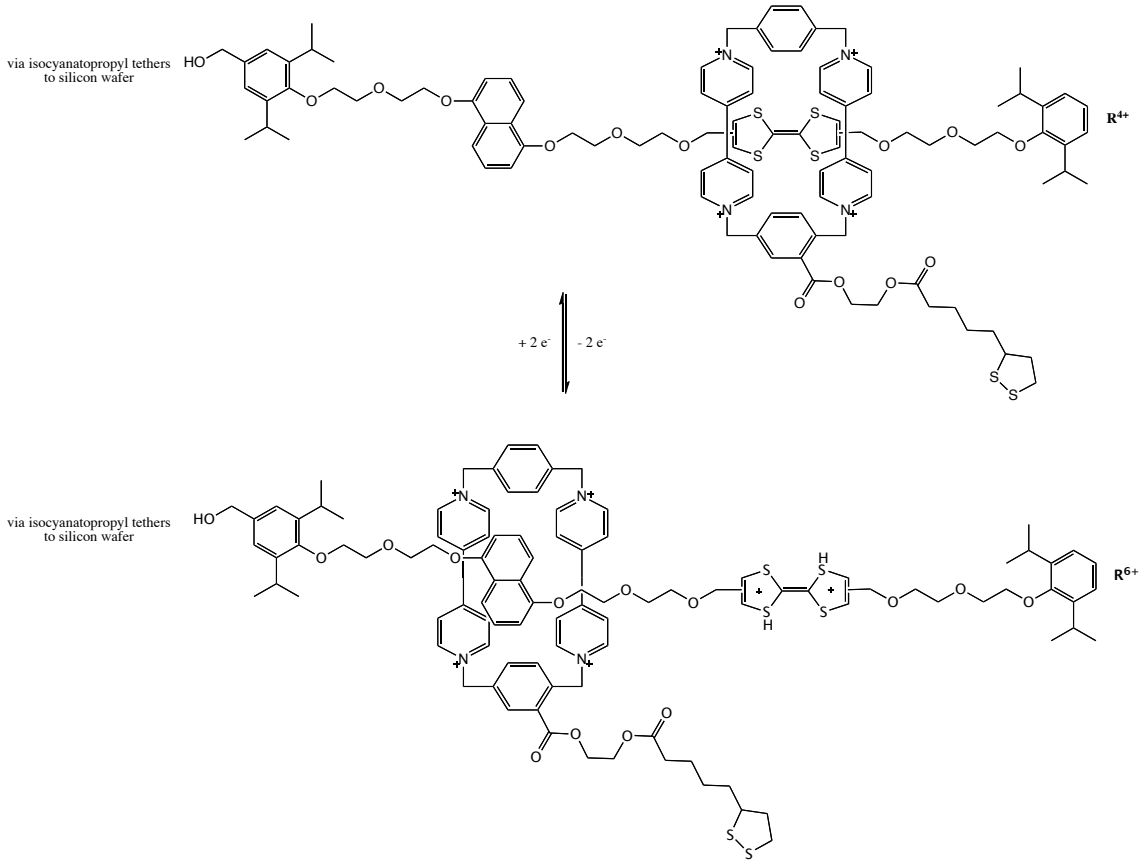

Figure 5.12: Structure of the stable states R^{4+} and R^{6+} of the rotaxane.[273]

The use of LA-modified poly(*L*-glutamic acid) led to reversible end-to-end assembly of gold nanorods. The structure of the synthesized poly(amino acid) is illustrated in **Figure 5.15**. The polyacid was adsorbed onto the end of the gold nanorods by LA as anchoring group. Subsequently, a layer of poly(vinyl pyrrolidone) was adsorbed onto the positively charged polyacid film to generate a stable gold nanorod dispersion. At a pH of about 3.5 poly(*L*-glutamic acid) exhibited a α-helical conformation and the shielded gold nanorods self-assembled into one-dimensional objects. This process was reversible by change of the pH conditions. At a pH of about 8.5 the poly(amino acid) changed its conformation to a random coil and the linkage to the gold nanorods was cleaved.[276,277]

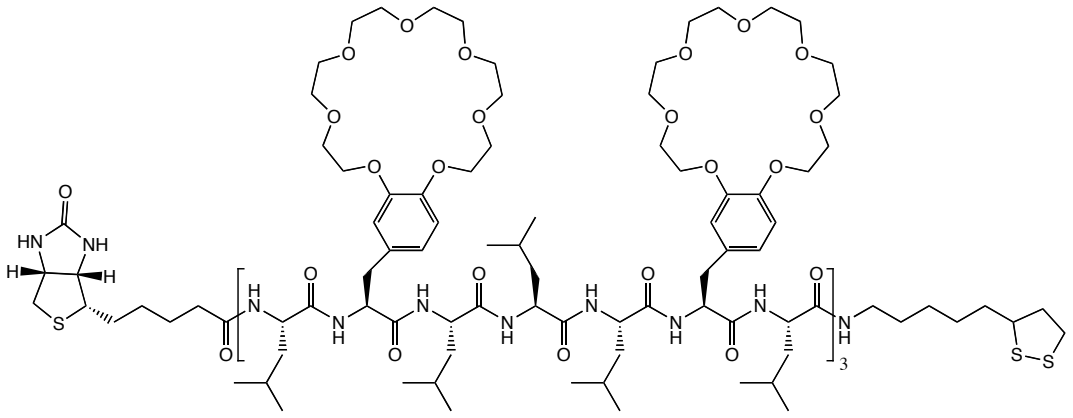

Figure 5.13: Structure of the synthesized peptide.[275]

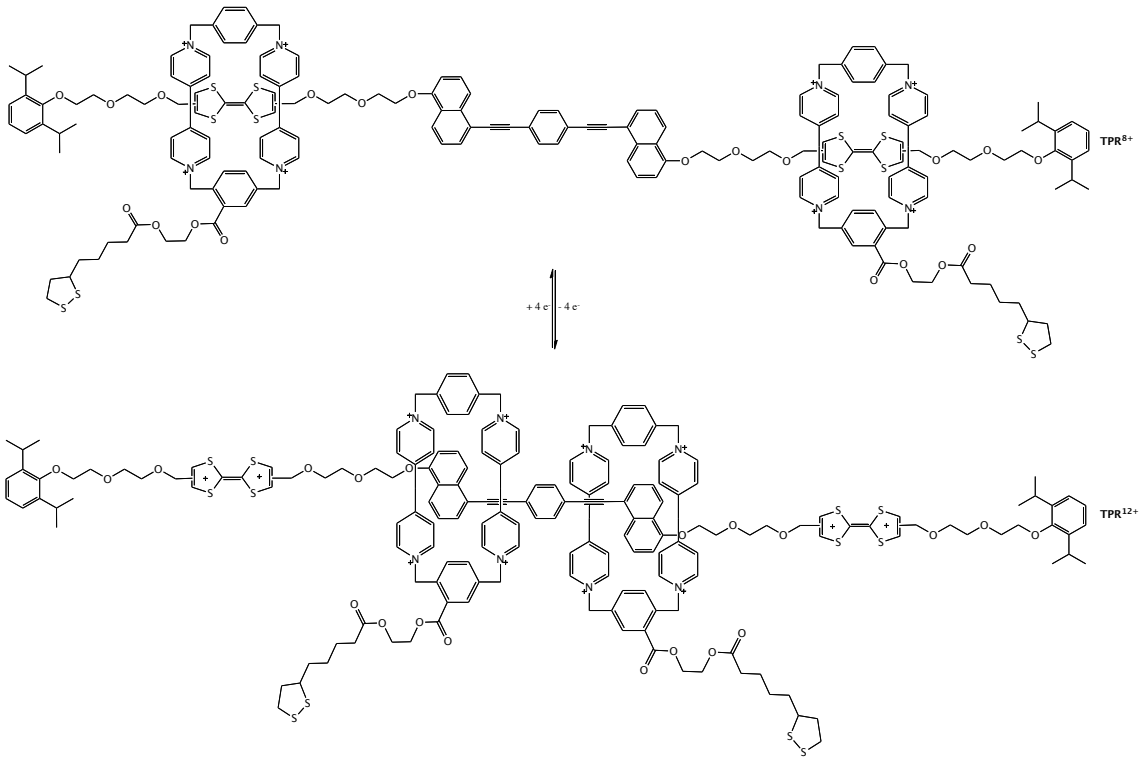

Figure 5.14: Structure of the contracted state (TPR^{8+}) and an extended state (TPR^{12+}).[274]

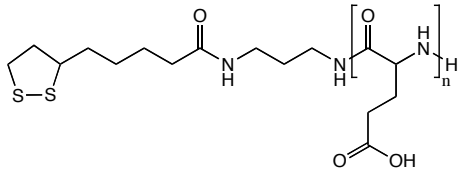

Figure 5.15: Structure of the LA-modified poly(*L*-glutamic acid).[276,277]

The same authors also introduced the synthesis of LA modified poly(*γ*-benzyl-*L*-glutamate) by the polymerization of the *N*-carboxyanhydride of *γ*-benzyl-*L*-glutamate and *N*-lipoyl-1,3-diaminopropane as initiator. **Figure 5.16** shows the affected polymerization. Additionally, the synthesized helical, rigid and rod-like polymer was used for the formation of SAMs on gold substrates. With increasing molecular weight of the polymer the average tilt angle of the helices to the surface normal increased. The tilt angle also increased with increasing desorption time and decreasing surface coverage. However, this effect occurred more significantly for short polypeptides.[278,279]

Enriquez et al. investigated the adsorption of LA-modified poly(*γ*-benzyl-*L*-glutamate) to gold.[280-282]

In a further study, Dondapati et al. published the immobilization of enzymes onto electroactive SAMs by electrochemical cleavage of aldehyde moieties. They used LA-modified benzo[1,3]dioxinol to form SAMs on gold electrodes. The protected aldehyde groups on the adsorbed layer were selectively released by electro-activation. This reaction is shown in **Figure 5.17**. Subsequently, the aldehyde functionalities were enabled to form Schiff bases with amine groups of the different enzymes, such as glucose oxidase and horseradish peroxidase. Thus, covalent pattering of enzymes onto SAMs was obtained.[283]

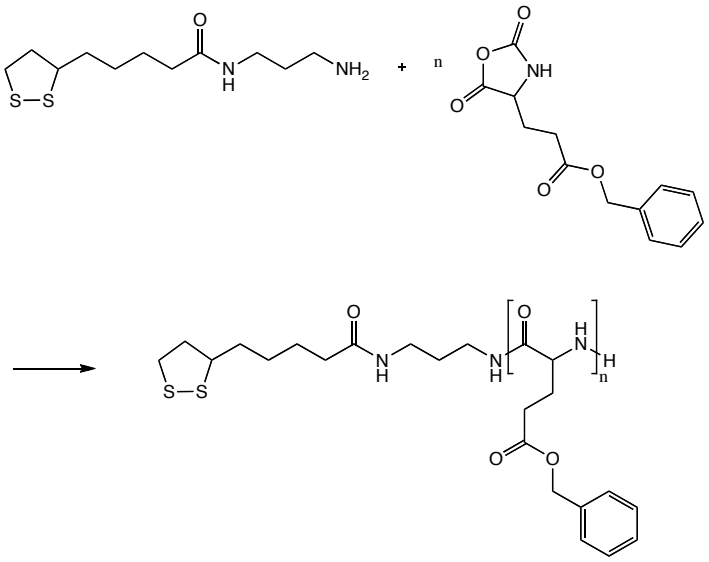

Figure 5.16: Polymerization of the *N*-carboxyanhydride of *γ*-benzyl-*L*-glutamate with *N*-lipoylamin.[278,279]

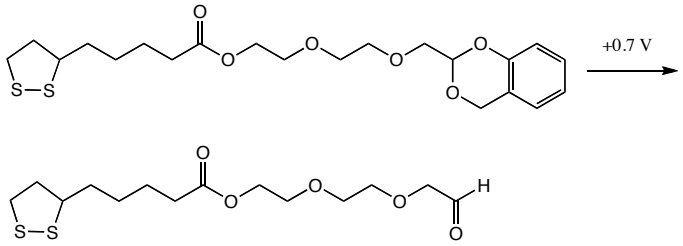

Figure 5.17: Electrochemical cleavage of the aldehyde derivative of LA.[283]

In 2007, the oriented immobilization of immunoglobulin antibodies on a gold surface was described. Hence, glutathione *S*-transferase proteins were fabricated to bind to gluthathione-derivatized LA, which was adsorbed to gold supports. LA was attached via a biaminated tri(ethylene glycol) to gluthathione. The gluthathione-derivatized LA and a scheme of the immobilization are illustrated in **Figures 5.18a** and **b**.[284]

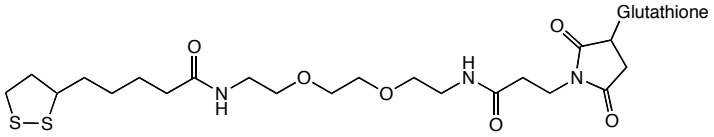

Figure 5.18a: Structure of the gluthathione-derivatized LA.[284]

In a further investigation, the formation and the structure of SAMs of LA-terminated polyproline on gold substrates were studied. The primary structure of the used polyproline was LA-glycine-proline$_{15}$-troptophan-NH_2. The conformation of the poly(amino acid) film changed by the change of the solvent from water to methanol and vice-versa. The same behavior was also observed for polyproline in solution. The monolayer exhibited an orientation of 32° to the normal of the surface at maximum coverage.[285]

In 2006, the esterification of cellulose α-lipoates was investigated under different activation condition of the carboxylic acid. The achieved degree of substitution ranged between 0.11 and 1.45. LA-modified cellulose, shown in **Figure 5.19**, was used to self-assemble onto gold surfaces. [286]

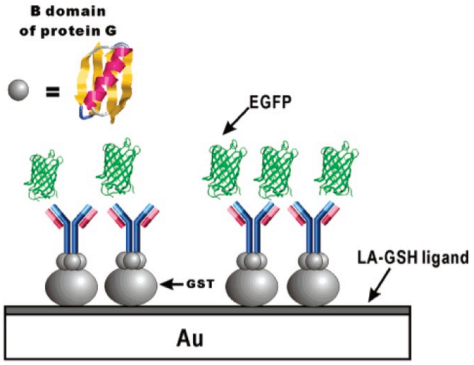

Figure 5.18b: Scheme of the antibody immobilization (LA-GSH ligand = gluthathione-derivatized LA; GST = glutathione *S*-transferase protein; EGFP = enhanced green fluorescent protein) [scheme taken from[284]].

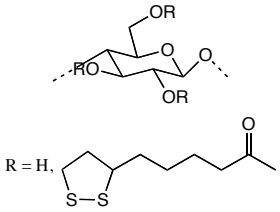

Figure 5.19: Structure of the synthesized cellulose α-lipoates.[286]

LA was also described as anchoring group for various synthetic polymers in several publications. Denditic polyglycerol (PG) with a polyether-polyol structure was adsorbed to gold substrates by Haag et al. Hydroxyl functionalities of different PG derivatives were partially converted in an esterification reaction with LA. In **Figure 5.20** one LA-modified PG is shown as example. On average, every polymer carried one LA as linker group to accomplish the modification of bare gold supports. These shielded substrates exhibited high resistance against protein adsorption, which could be further improved by methylation of the remaining hydroxyl functionalities of the PG core. The obtained protein-resistance was comparable to SAMs of PEG, which are known to be highly protein-resistant.[287,288]

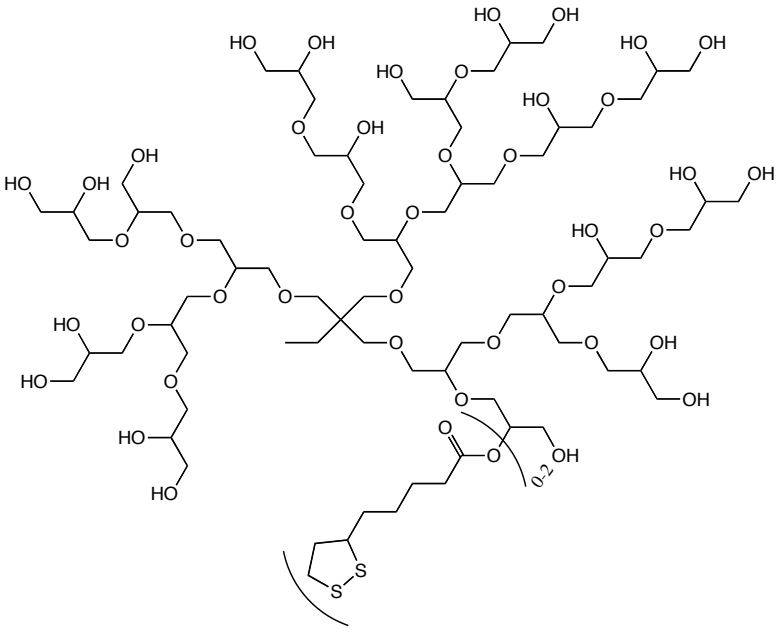

Figure 5.20: Structure of a LA-modified PG.[287,288]

A group of Finnish researchers published the use of a LA-modified polyacrylamide derivative to stabilize colloidal gold coated with antibody fragments. An azo-LA derivate was used as radical initiator for the thermal polymerization of *N*-[tris-(hydroxymethyl)methyl]acrylamide, which is illustrated in **Figure 5.21**. The flocculation of the antibody-shielded Au NPs was efficiently avoided by the synthesized tris(hydroxymethyl)-functionalized polyacrylamide.[289]

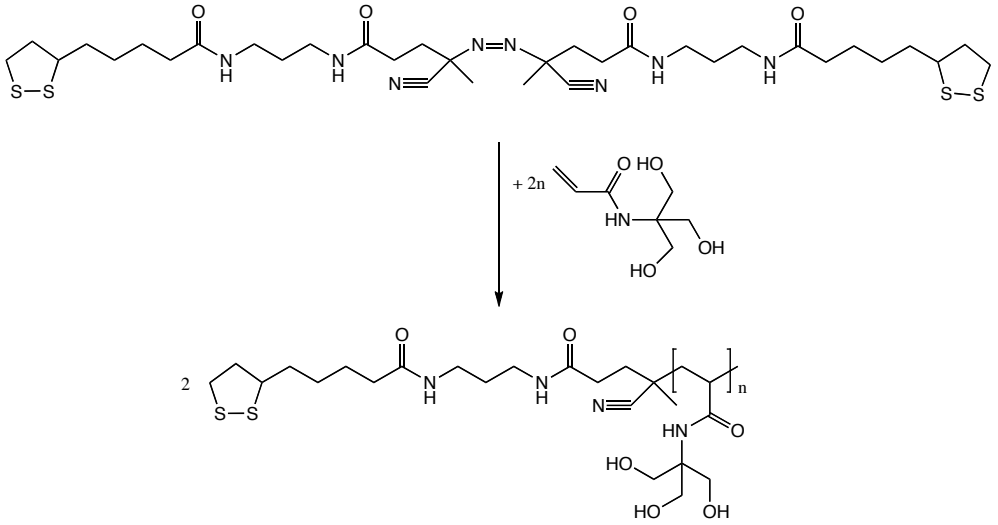

Figure 5.21: Thermal Polymerization of *N*-[tris-(hydroxymethyl)methyl]acrylamide with an azo-initiator.[289]

In addition, permethoxylated-ε-caprolactone as well as block-copolymers consisting of permethoxylated-ε-caprolactone and ε-caprolactone were used to synthesize protein-resistant functional polymers. The synthesized polymers were functionalized with LA and subsequently these materials self-assembled on gold surfaces and were investigated via surface plasmon resonance spectroscopy. In **Figure 5.22** the structure of poly(permethoxylated-ε-caprolactone) functionalized with LA is shown.[290,291]

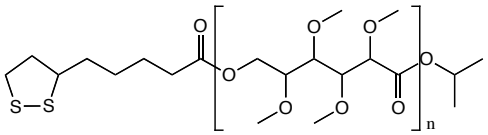

Figure 5.22: Structure of poly(permethoxylated-ε-caprolactone) functionalized with LA.[290,291]

In a further study, the interfacial activity of polymer-coated Au NPs was investigated. Polybutadiene and polydimethylsiloxane with one LA substituent as an anchoring group were fabricated by esterification of functional groups, such as hydroxyl or amino functionalities, with LA.[292]

Mourato et al. published the electropolymerization of pyrrole on functionalized SAMs. Hence, a pyrrolyl LA derivative (**Figure 5.23**) was coated onto gold substrates. The obtained results were compared to those detected on bare substrates.[293]

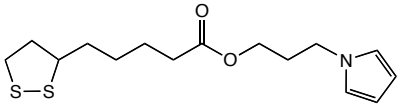

Figure 5.23: Structure of pyrrolyl LA derivative.[293]

The surface of Co@Pt-Au nanoparticles was also modified with different LA-functionalized PEG derivatives (**Figure 5.24)**. These nanoparticles were coated with a mixture of PEG polymers, which carried a LA

substituent on one terminus and a hydroxyl function or a carboxyl functionality on the other terminus. The carboxyl group was subsequently functionalized with neutravidin via an amide linkage, which affected the recognition of biotinylated assemblies. The fabricated Co@Pt-Au NPs exhibited enhanced magnetism and were highly stable in aqueous solution. These moieties might have potential applications in magnetic resonance imaging for therapeutic approaches in Alzheimer's disease.[294]

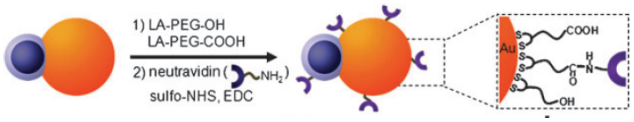

Figure 5.24: Scheme of the PEGylated Co@Pt-Au nanoparticles [scheme taken from[294]].

LA was also described as linker to other metals and in the following a few examples will be given. Various PEG oligomers and polymers were converted in an esterification reaction with LA and subsequently the disulfide bonds of the obtained moieties were reduced to the dihydrolipoic analog. This procedure is illustrated in **Figure 5.25**.

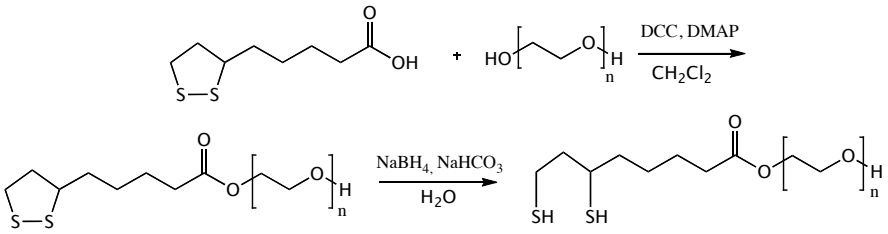

Figure 5.25: Synthesis of the LA-PEG derivatives (DCC = *N,N'*-dicyclohexylcarbodiimide; DMAP = 4-dimethylaminopyridine).[295]

The different dithiol-functionalized PEG derivatives exhibit the ability to stabilize cadmium selenide-zinc sulfide core shell quantum dots in aqueous solution as well as in other polar solvents for several months. These compounds did not indicate cytotoxic effects over a period of two days and they might be used for intracellular labeling and long-term imaging.[295]

In a follow up work of the same group, the stabilization of nanoparticles was further improved. The use of PEG with a terminal bis-LA-based substituent as anchoring group and a terminal methoxide group enabled the stabilization of cadmium selenide-zinc sulfide core shell quantum dots as well as Au NPs under extreme buffer conditions in a range of pH ~ 1.1 to pH ~ 13.9. Michael addition was used to introduce a branching point at one end of a mono-amino PEG to accomplish the attachment of two LA linkers. Subsequently, the disulfide bonds were again cleaved to thiols by the reduction with sodium borohydride. These PEG-based ligands exhibited the ability to chelate to the surface of different nanocrystals and led to an enhanced colloidal stability. The synthesis is shown in **Figure 5.26**.[296]

Algar and Krull attached a LA derivative onto fused silica surfaces to enable the immobilization of cadmium selenide-zinc sulfide quantum dots. The synthesized linker for the modification of nanocrystals is illustrated in **Figure 5.27.** Quantum dots were adsorbed to the multidentate modified surface by ligand exchange.[297]

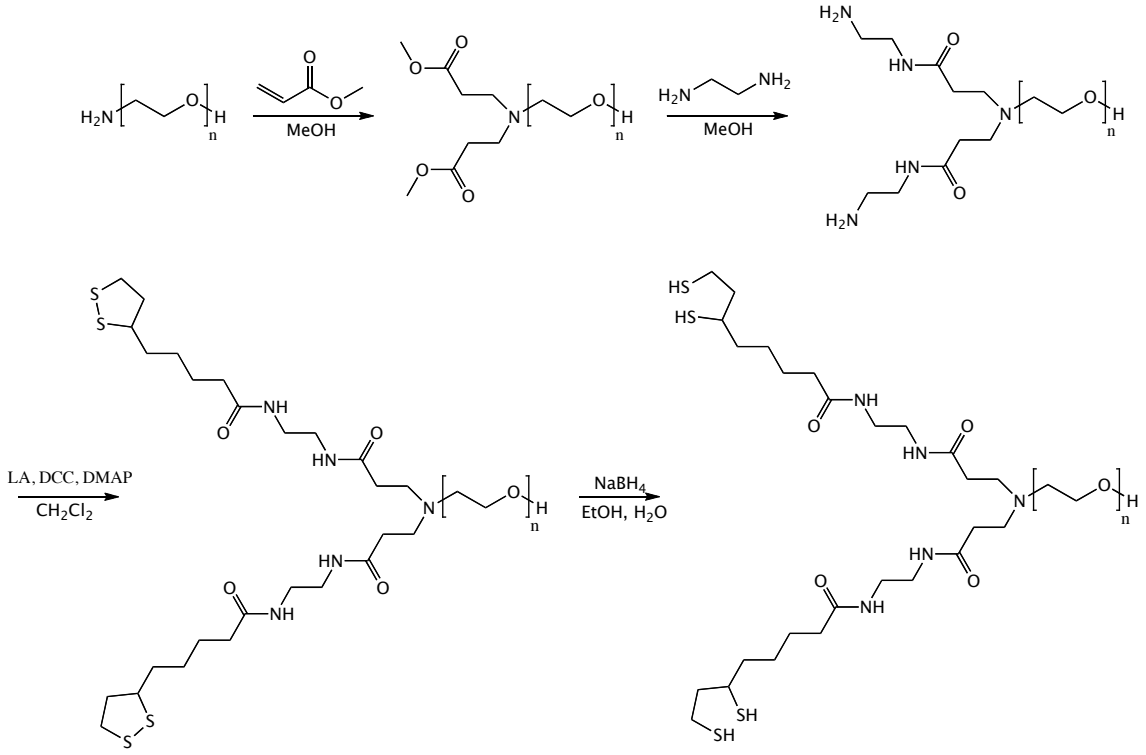

Figure 5.26: Synthesis of the bis-LA-PEG derivatives.[296]

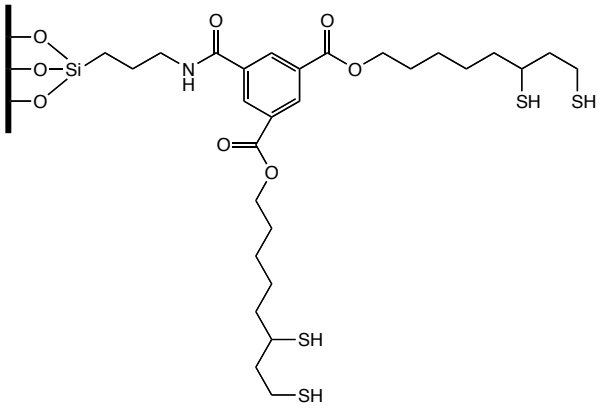

Figure 5.27: Multidentate linker for cadmium selenide-zinc sulfide quantum dots.[297]

In a further study, ferrocene was attached to LA via two different linkers to synthesize different platinum complexes. The complexation was based on the oxidative addition of the disulfide to platinum(0). Two different LA-based ligands are shown in **Figure 5.28**.[298]

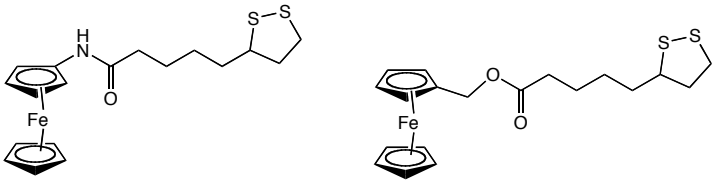

Figure 5.28: Ferrocene-based ligands.[298]

5.1.2 Poly(lactic acid) (PLA)[299-333]

Poly(lactic acid) (PLA) is a widely used biodegradable polyester and its structure is shown in **Figure 5.29**. The one asterisked carbon atom of the polymer backbone is an asymmetric carbon atom, and three different stereoforms are known: the poly(*L*-lactic acid) (PLLA), poly(*D*-lactic acid) (PDLA) as well as poly(*DL*-lactic acid) (PDLLA). PLLA and PDLA are semicrystalline and in contrast, PDLLA is more amorphous with a random distribution of the *D*- and the *L*- enantiomer of lactic acid.[299]

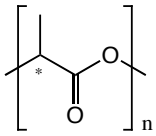

Figure 5.29: Structure of PLA.

PLA has been prepared by different methods. The direct polycondensation of lactic acid as well as the ring-opening polymerization of the cyclic dilactide was successfully accomplished.[300] The different synthesis methods to obtain high molecular weight PLA is illustrated in **Figure 5.30**.[301,302]

Lactic acid can be produced by bacterial fermentation of carbohydrates as well as by hydrolysis of lactonitrile. Until 1990, the petrochemical route was primarily used to synthesize the monomer, since then a more economic fermentation approach was introduced. Nowadays, approximately 90% of the lactic acid production is based on fermentation processes, which produces optically pure lactic acid.[303,304]

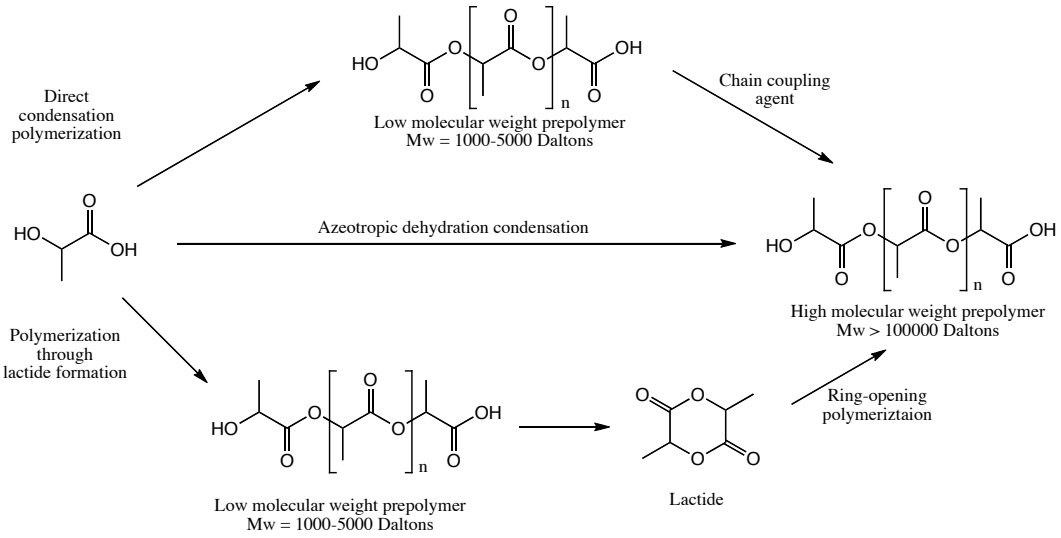

Figure 5.30: Synthesis methods of high molecular PLA.[301,302]

The type of the used bacteria distinguishes the fermentation of carbohydrates. The *Homofermentation* majorly uses a genus of Lactobacilli and averagely 1.8 moles of lactic acid per mole of hexose are obtained. This means more than 90 g lactic acid per 100 g glucose and minor levels of further metabolites are obtained. The *Heterofermentative* method produces less than 1.8 moles of lactic acid and a higher amount of other metabolites such as ethanol, acetic acid and carbon dioxide. Hence, the *Homofermentative* route is mainly used. The production of lactic acid is majorly based on renewable sources. Glucose and maltose obtained from potatoes or corn and additionally lactose from cheese whey and sucrose from cane are used.[301]

The optical purity of lactide influences the physical properties of the obtained PLA.[304] Four different types of polymerizations were reported for the ring-opening polymerization (ROP) of lactide: the cationic as well as

anionic polymerization, the enzymatic polymerization and a coordination-insertion mechanism.[300] In the following, a few examples for each polymerization approach are given.

The first successful cationic polymerization of lactide was described by Kricheldorf et al. in 1986. They used trifluoromethanesulfonic acid and methyl triflate as initiators. The conducted synthesis with trifluromethansulfonic acid as an initiator is illustrated in **Figure 5.31**.[305-308] In principal, the cationic ROP of lactide is less important and rarely used.

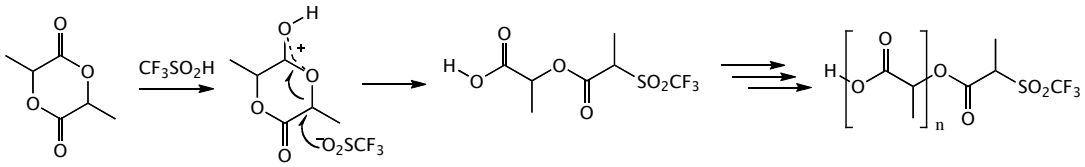

Figure 5.31: Mechanism of the cationic polymerization with trifluoromethanesulfonic acid as initiator.[305-308]

The anionic ROP of lactide with lithium and potassium alkoxides as well as metal alkyls is well known. As an example the anionic ROP of lactide with potassium alkoxyl is shown in **Figure 5.32**.

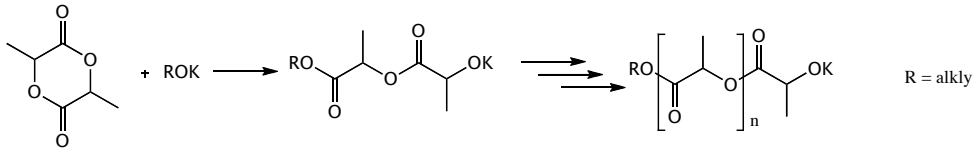

Figure 5.32: Mechanism of the anionic polymerization with potassium alkoxide as initiator.[305,306]

In the first reports, the monomer was not completely converted and the molecular weight of the resulting polymer was not adjustable via the monomer-to-initiator ratio.[305,306]

The enzymatic polymerization with, for example, lipase and the polymerization with organocatalysts such as amines and phosphines can be considered as nucleophilic polymerizations. These metal-free catalysts are more economical and environmentally friendly.[305]

Matsumura et al. were the first who described the lipase-catalyzed ROP of lactide in 1997. They obtained PLA with molecular weighs up to 126000 $g \cdot mol^{-1}$. Surprisingly, the *D*,*L*-lactide led to higher molecular weight polymers than the *D*,*D*-lactide and *L*,*L*-lactide.[309] Different commercially available lipases were tested as catalyst for the ROP of lactide. The highest catalytic activity was reported for *Pseudomonas cepacia* lipase. Under catalysis of the named lipase the polymerization led to high monomer conversions as well as high molecular weight products with narrow polydispersity indices.[305]

The use of organocatalysts attended to a living character of the ROP of lactide with a linear correlation between monomer conversion and achieved molecular weight of the polymer. Hence, the synthesis of PLA with controlled molecular weight and narrow distributions was accomplished.[305,306] The wide range of organocatalysts included amines, such as pyridine derivatives, amidines as well as guanidines, such as DBU and 1,4,7-triazabicyclodecene (TBD), phosphines, such as TBP, and *N*-heterocyclic carbenes, such as imidazole-2-ylidene IMes (**Figure 5.33**).[305,306,310]

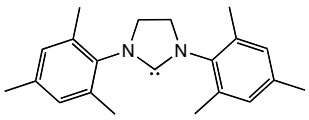

Figure 5.33: Structure of the imidazole-2-ylidene IMes.[305]

In the following, 4-dimethylaminopyridine (DMAP)-catalyzed ROP should be explained as an example. An alcohol derivative acted as an initiator in this polymerization approach. Originally, a nucleophilic monomer activation mechanism, as illustrated in **Figure 5.34**, was proposed.[310]

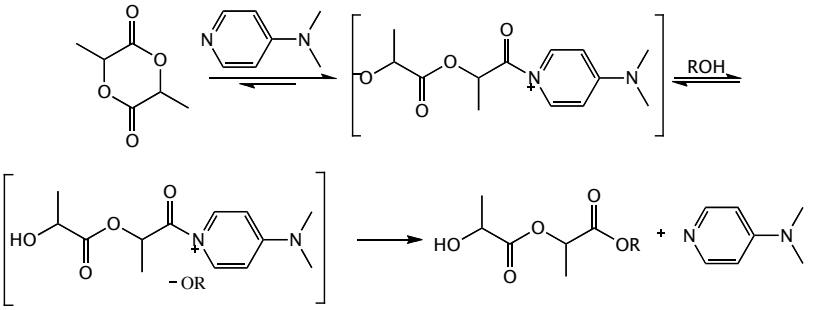

Figure 5.34: Proposed nucleophilic mechanism of the ROP with DMAP.[310]

A concentrated or stepwise alcohol activation mechanism was subsequently proposed after computational investigation. This mechanism is shown in **Figure 5.35**. The energy of both pathways was calculated, showing that the alcohol activation mechanism seemed to be preferred in polar aprotic solvents as well as in gas phase. In contrast, the nucleophilic mechanism took place either in absence of the initiator or at high monomer-to-initiator ratios.[310]

In general, organocatalysts hold the triad of versatility: tolerance of various functional groups, convenience as well as synthesis of well-defined polymers with precise architecture for specific applications.[310]

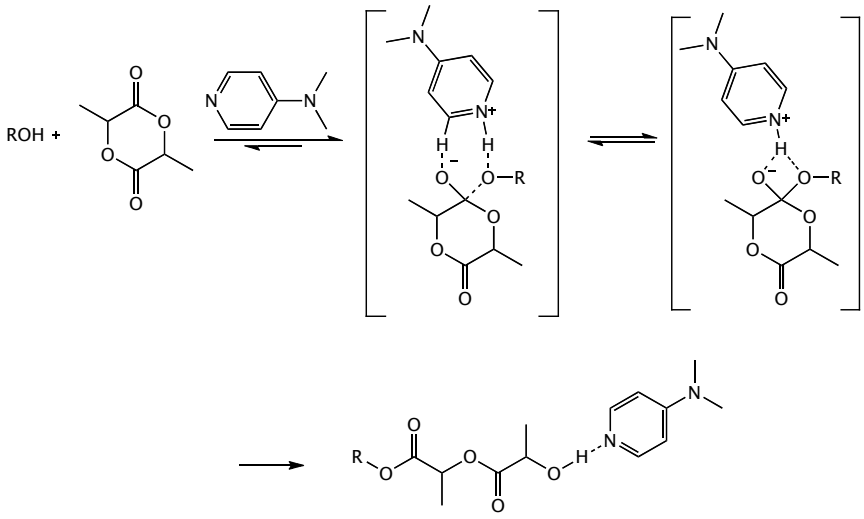

Figure 5.35: Proposed general-base mechanism of the ROP with DMAP.[310]

Tin(II) bis(2-ethylhexanoate), also known as tin(II) octanoate, is the most common complex for the industrial production of PLA via coordination-insertion polymerization. This complex is also important for the polymerization of lactide in the field of research. It has several benefits: tin(II) octanoate is commercially available and exhibit a good solubility in common organic solvents as well as in molten polymers. In addition, the U.S. Food and Drug Administration has licensed it as a food additive, although most tin compounds are toxic. The predicted mechanism of the tin(II) octanoate-catalyzed lactide polymerization in the presence of methanol is shown in **Figure 5.36**.[305]

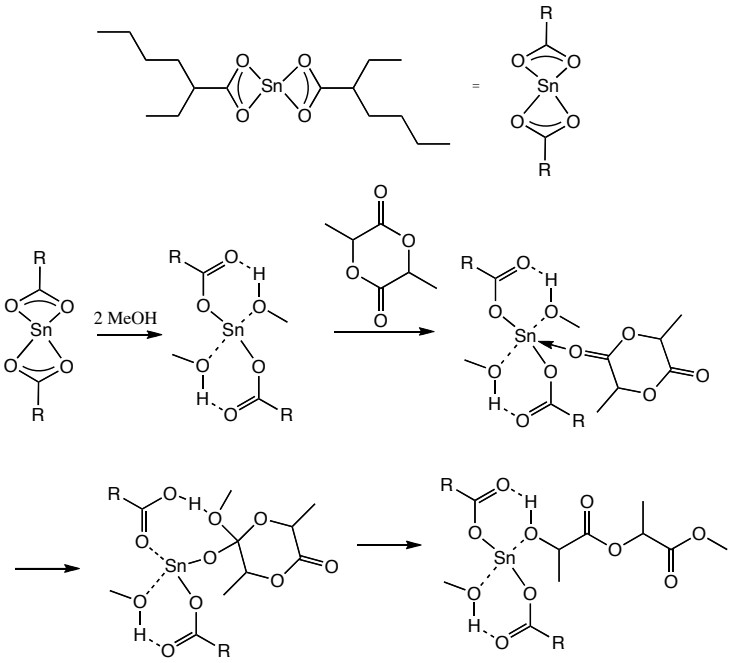

Figure 5.36: Predicted mechanism of the tin(II) octanoate-catalyzed lactide polymerization with methanol.[305]

Aluminum alkoxides such as aluminium(III) isopropoxide and zinc(II) lactate were also tested as effective catalysts for ROP of lactide.[305]

PDLLA with a random sequence is amorphous with a glass transition temperature in the range of 50 to 60 °C, which is influenced by the molecular weight. In contrast, optically pure PLLA is crystalline with a melting temperature in the range of 175 to 185 °C, depending on the molecular weight. It is a hard and brittle material, but the brittleness can be reduced by different approaches.[300] The polyester holds good mechanical properties. Beside the ability to produce PLA from renewable sources, this material exhibit the benefit of biocompatibility with low immunogenicity as well as biodegradability by enzymes and hydrolysis under physiological conditions. The U.S. Food and Drug Administration allowed the clinical use of PLA.[311] In 1994, Albertsson and Karlsson defined biodegradation as decomposition, which is initiated by enzymes or chemically by association with living organisms and its secretion products.[312,313] Degradation of crystalline PLA parts was described to be slow compared to the one of amorphous parts. In addition, higher molecular weight polymers as well as polyesters with high melting points showed slower degradation rates.[299] Several approaches reported that some serine proteasen were enabled to hydrolyze PLLA and PDLLA. In contrast, they were not enabled to cleave PDLA. Further more, lipase exhibited the ability to hydrolyze low molecular PLLA as well as random copolymers of PLA such as PDLLA, but the hydrolysis of PDLA and high molecular weight PLLA was not observed.[299]

In a recent review Platel et al. summarized different biocompatible initiators for ROP of lactide. For example zinc complexes were suitable initiators due to a high reactivity and relatively low toxicity. Lanthanide alkoxides, for instance, accomplished a good polymerization activity with no known toxicity.[314]

In 2001, more than ten companies worldwide produced PLA. A US company reported a production of 100000 t of PLLA in the year 2000.[300] PLA is a widely used material with numerous fields of applications, e.g., in the field of biomedicine as implants for bone fixation. A second operation to remove the implants is not necessary due to disappearance upon degradation after a certain time.[303,311] Resorbable sutures compost of PLA are the most common application. Furthermore, PLA films are used in wound dressing and most

notably for large burn wounds, as tissue engineering scaffolds. These films were resorbed after four to six weeks. It was reported that infectious bacteria were not enabled to grow on these film or to penetrate them.[300,311] PLA is also utilized as drug delivery vehicle for pharmaceutical applications.[311] Since the last decades, PLA is used as packaging material and replaces slowly the synthetic ones. It is mainly applied as food packaging, namely, for yoghurt cups, drinking cups and short self-life products such as fruits and vegetables. Further details were summarized in a review article about this topic by Auras et al.[301]
The architecture of PLA can be varied, for example, to star polymers. Cameron and Shaver reviewed this topic in 2011.[316] Furthermore, PLA is known in various copolymer structures with other monomers. To obtain block-copolymers as well as random copolymers, the sequence of the monomer composition was varied. The following examples are only a few examples of a common used copolymer compound with a broad range of applications. Copolymerization of lactide with cyclic ester such as glycolic acid[308] and ε-caprolactone were described.[316] PLA is known in various copolymer structures with ethylene oxide and propylene oxide.[317-320] J. K. Oh summarized the synthesis and application of PLA-based amphiphilic block-copolymers in a recent review. PLA was also incorporated in AB block-copolymer structures with hydrophilic poly(meth)acrylates, polypeptides, polysaccharides and polyurethanes.[311] In an another approach, nanoparticles composed of dextran-PLA block-copolymers were used for drug delivery applications. The size of these biodegradable nanoparticles was precisely adjustable by variation of the two block lengths in the range of 15 to 70 nm. These materials exhibited promising features with a drug payload of 21% for doxorubicin and a sustained release over six days. Accumulation in spleen was lower than comparable PEGylated poly(lactide-*co*-glycolide) nanoparticles.[321] The influence of different modifications on the thermal and mechanical properties of PLA was summarized in a review by Becker et al. PLLA-*block*-poly(isobutylene)-*block*-PLLA triblock-copolymers, for example, were tested as thermoplastic elastomers. ROP of lactide-related monomers such as 3,6-difunctional glycolides enabled the synthesis of different modified PLA.[322] Jing and Hillmyer, for example, reported the synthesis and polymerization of a norbornene-functionalized cyclic diester monomer. The polymerization is illustrated in **Figure 5.37**.[322,323]

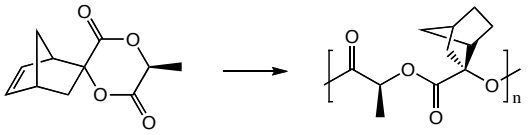

Figure 5.37: ROP of a norbornene-functionalized cyclic diester.[322,323]

In this work, the main focus is on PLA with thiol, disulfide and sulfide functionalities as well as further methods to attach PLA to gold surfaces. Song et al. introduced the use of PLLA-stabilized Au NPs to detect arsenic (III) ions in drinking water. Auric acid was reduced by sodium borohydride in the presence of PLA to form PLA-stabilized Au NPs, which were subsequently used to modify a disposable screen-printed carbon electrode. The detection of As (III) was achieved by differential pulse anodic stripping voltammetry. This method possesses the benefit of no interference with other metals such as copper, cadmium, zinc and nickel and gave reliable results.[324] In 2004, the synthesis of PLA with one thiol functionality was achieved by the use of a protected mercaptan as initiator for lactide. After the polymerization the protecting group of the thiol functionality was removed. **Figure 5.38** shows the affected synthesis. The obtained thiol-modified PLA was used to coat Au NP, which was either accomplished by the reduction of auric acid method in the present of PLA-SH via the Burst method or by partial ligand exchange of undecanethiol-stabilized Au NPs.[325]

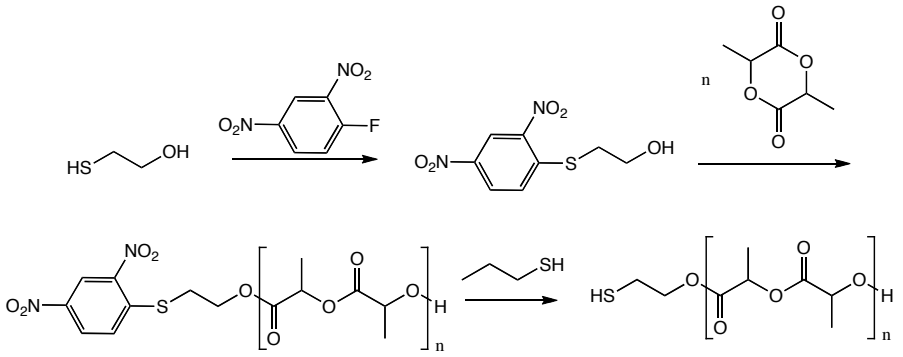

Figure 5.38: Synthesis of PLA with one thiol functionality.[325]

Another possibility to synthesize PLA with a thiol and a disulfide motif, respectively, was achieved by the use of dihydroxyethyl disulfide as initiator for ROP of lactide. After the polymerization the disulfide bond was cleaved by reduction with tributylphosphine to obtain PLA with a terminal thiol function. The synthesis is illustrated in **Figure 5.39**.[326]

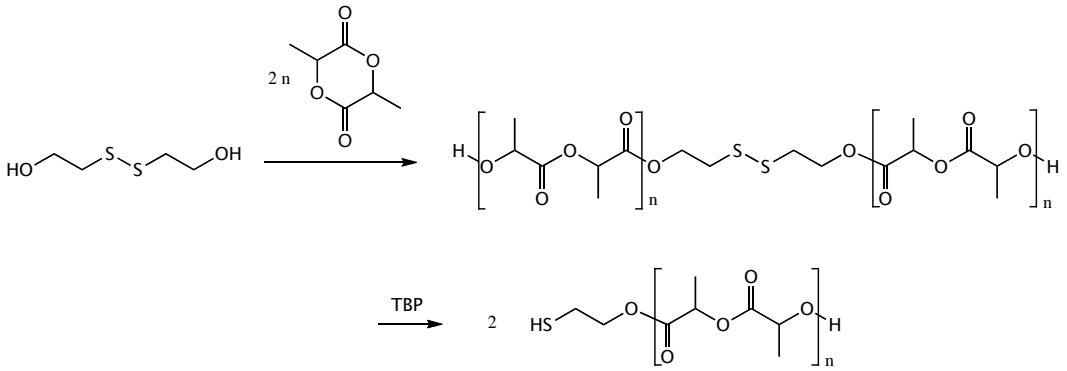

Figure 5.39: Synthesis of PLA with one thiol functionality.[326]

Oh et al. used the same initiator to synthesis block-copolymer micelles with a thiol-responsive corona. They converted dihydroxyethyl disulfide with 2-bromoisobutyric acid to the corresponding mono ester, which was used as initiator for ROP of lactide. The resulting polyester acted subsequently as a macroinitiator for ATRP of oligo(ethylene oxide) monomethyl ether methacrylate (OEOMA). **Figure 5.40** shows the synthetic route. The resulting block-copolymers were used to form micelles and the thiol-responsive degradation was investigated.[327]

Pang et al. described the synthesis of similar unimolecular micelles in a polymer analog approach. The commercial available hyperbranched aliphatic polyester Boltorn® H40 was used as macroinitiator for lactide to synthesis star-shaped PLA copolymers. These star polymers with multiple hydroxyl groups were subsequently reacted in a *N,N'*-dicyclohexylcarbodiimide (DCC)-catalyzed esterification with disulfide-linked carboxyl-terminal mPEG, which is illustrated in **Figure 5.41**.[328] The same authors used a similar protocol to obtain biodegradable micelles with a star-shaped PLA shell, which was linked via a disulfide bond to a hydrophobic polyester core. These amphiphilic block-copolymers self-assembled in aqueous medium into micelles with an average diameter of 70 nm and were tested as drug delivery carrier for doxorubicin, which was released after glutathione induced reduction.[329]

The Leroux group introduced the synthesis of PEG-PLA block-copolymers with a terminal thiol functionality. *tert*-Butyl mercaptan was utilized as initiator for the anionic polymerization of ethylene oxide.

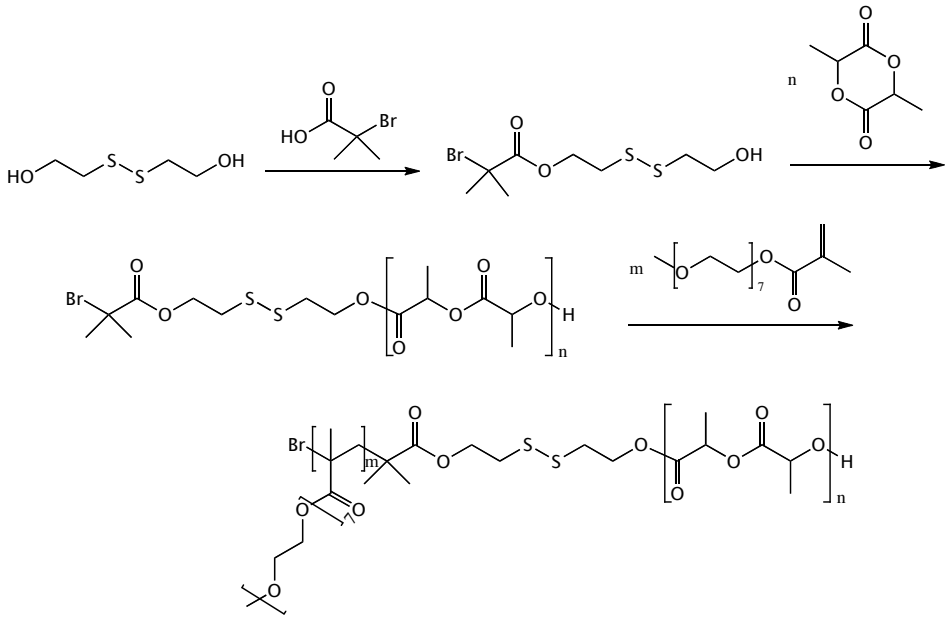

Figure 5.40: Synthesis of PLA with one thiol functionality.[327]

The *tert*-butyl thioethers were cleaved to thiols under acidic condition, which dimerized immediately to disulfides under these conditions.

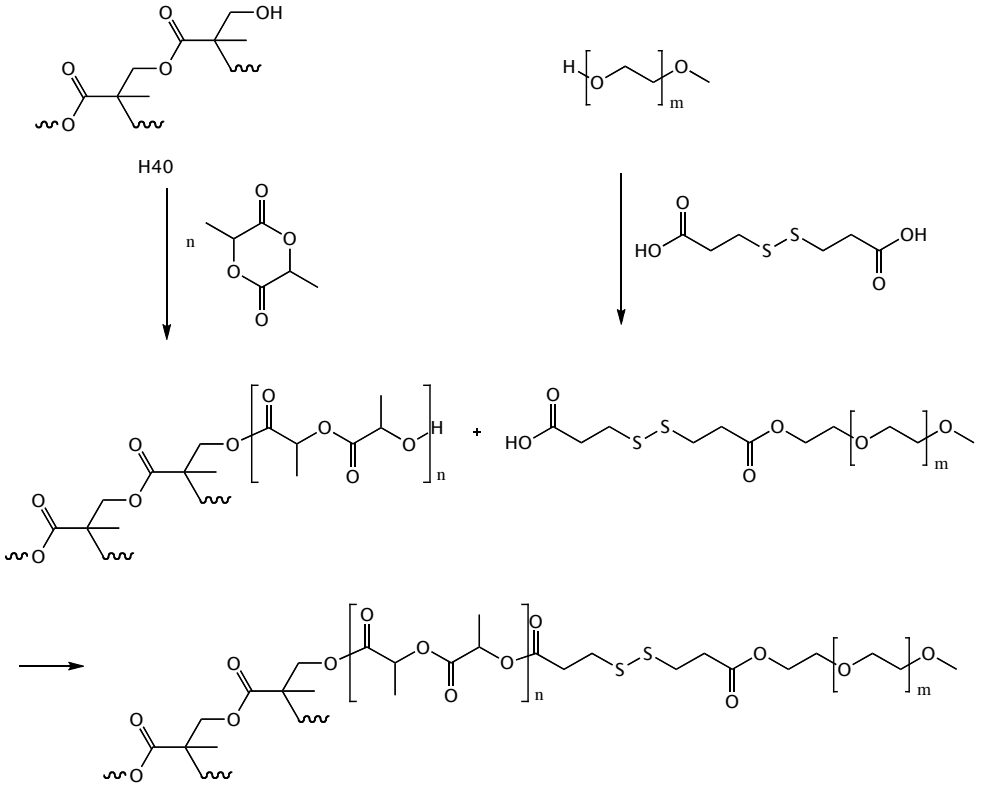

Figure 5.41: Synthesis of PLA with one thiol functionality.[328]

The resulting PEG was used as macroinitiator for ROP of lactide and after reduction with TBP and PEG-PLA copolymers with a thiol functionality were obtained. The synthetic route is shown in **Figure 5.42**. The

aqueous solution of these block-copolymers exhibited a gel-sol transition by increasing the temperature. The formed gels were decomposed under reductive conditions.[330]

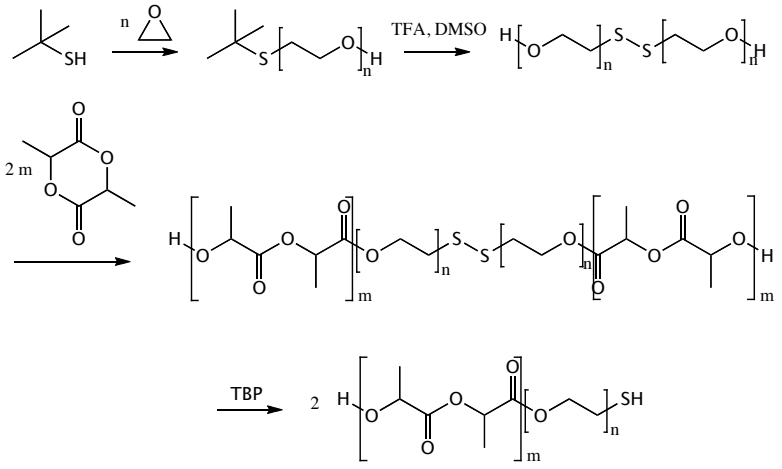

Figure 5.42: Synthesis of PEG-PLA block-copolymers with one thiol functionality.[330]

In a further approach, the synthesis of poly(*L*-lactide)-*block*-poly(*L*-cysteine) copolymers was described. A protected amine was used as initiator for ROP of lactide and subsequently the protected group was cleaved. PLA with a terminal amino functionality acted afterwards as macroinitiator for the polymerization of *N*-carboxyanhydride of *β*-benzyloxycarbonyl-*L*-cysteine. After cleavage of the monothiocarbonate an amphiphilic block-copolymer consisting of a polyester segment and a segment with multiple thiol groups was obtained. The conducted synthesis is illustrated in **Figure 5.43**. These copolymers self-assembled in aqueous medium to form micelles with a PLA core and a cross-linked poly(cysteine) shell, which was reversible under reductive conditions.[331]

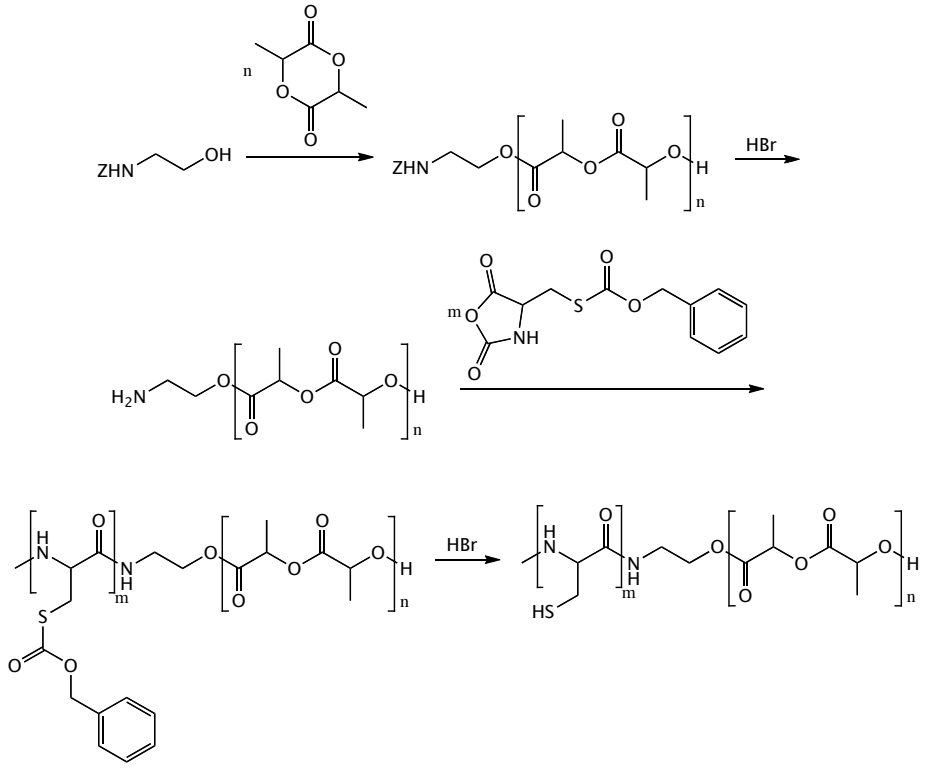

Figure 5.43: Synthesis of poly(*L*-cysteine)-PLA block-copolymers with one thiol functionality.[331]

The group around Nagai synthesized block-copolymers composed of PLA and a disulfide-containing block. They prepared PLA-poly(lipoic acid) nanosphere for drug targeting applications.[332]
In a further study, the surface of PLA nanoparticles was modified by covalent attachment of thiol groups. The modification was accomplished by activation of some carboxyl groups on the surface of the PLA nanoparticle. Subsequently an amide bond was formed by reaction of the synthesized active ester derivative and cysteine or cystamine. In case of the cystamine, the thiol was released by reduction of the disulfide bond with 1,4-dithio-*DL*-threitol or tris(2-carboxyethyl)-phosphine hydrochloride.[333]

5.1.3 Poly(ethylene glycol) (PEG)[334-350]

Poly(ethylene oxide) (PEO) or poly(ethylene glycol) (PEG) is one of the most used synthetic polymer and is present in nearly every area of the daily life. The structure of the simple aliphatic polyether is shown in **Figure 5.44**.[334]

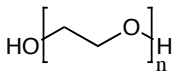

Figure 5.44: Structure of PEG.

In 1859, Wurtz was the first who synthesized ethylene oxide (EO) by reaction of 2-chloroethanol and potassium hydroxide. He also observed that the reaction of EO and zinc chloride or alkali chloride led to a crystalline product.[334,335] PEG is synthesized by ionic polymerization of ethylene oxide (EO). The polymerization was accomplished under anionic and cationic catalysis as well as coordination mechanisms. Cationic polymerization of EO was enabled in two different mechanisms, the active chain end mechanism and the activated monomer mechanism. However, the activated monomer mechanism was preferred, because less backbiting reactions, which led to cyclic oligomers, were observed. The different mechanisms are shown in **Figure 5.45**. Lewis acids such as boron trifluoride and antimony trifluoride were used to catalyze the cationic ring-opening polymerization of EO.[334]

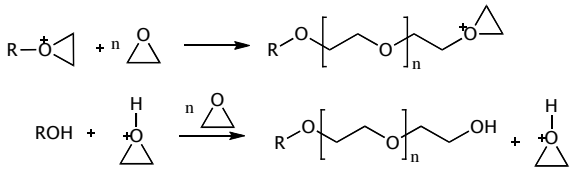

Figure 5.45: Mechanisms of the cationic polymerization of EO.[334]

The anionic ring-opening polymerization is mostly used to synthesis PEG due to the absence of any side-reactions as well as the well controllable molecular weight and polydispersity. Potassium and cesium alkoxides, for example, were used to catalyze the anionic polymerization of EO. The reaction is illustrated in **Figure 5.46**.[334]

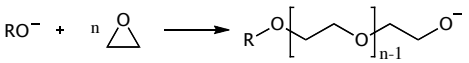

Figure 5.46: Mechanisms of the cationic polymerization of EO.[334]

The physical properties of PEG are influenced by the molecular weight. PEG with a molecular weight upon 400 g·mol^{-1} is a liquid and polymers with higher molecular weights exceeding 2000 g·mol^{-1} are crystalline. The melting temperature is increasing with increasing molecular weight upon a constant value of 60 °C. PEG with a molecular weight between 400 and 2000 g·mol^{-1} is cereous with a characteristic melting range.[334]

PEG exhibits nearly no toxicity and good solubility in water due to the formation of a large network of hydrogen bonds between the PEG-chain and the water molecules. It is thermoresponsive and the formation of the hydration sphere is solely enabled below the lower critical solution temperature. PEG is only soluble in water below this point and the water solubility of PEG only increases with increasing temperature until a certain point.[334]

PEG is often used as a hydrophilic segment of nonionic surfactants due to the positive characteristics mentioned. Furthermore, PEG and its copolymers with poly(dimethylsiloxane), for example, are widely employed in many cosmetic products, such as toothpaste, shampoo and lotion as emulsifiers and surfactants. A further field of application is pharmacy. For instance, a mixture of liquid and solid PEG can be used as base for ointment or as compound for contact lenses to improve the wettability. PEGylation[340] is used to extend the circulation time of drugs and proteins in the human body by the covalent attachment of a PEG chain.[334] In 2003, Duncan summarized the first results and potentials on polymer therapeutics, hybrids materials of synthetic polymers and proteins or drugs, respectively.[341] In addition, many food additives, which act as emulsifiers, are composed of PEG. However, there are some more unexpected applications for PEG. It is used in batteries to enable lithium ion mobility, preservatives for archaeological finds, submarine technology and in breathable fabrics.[334]

PEG is a universally used polymer in nearly every research area and it is know in many applications as homopolymer or in copolymer structures, as already described. In the following a few more examples will be introduced. Unmodified PEG exhibites solely two functional groups on the terminal ends of the polymer chain. The group around Riffle summarized the different possibilities to synthesize and utilize heterobifunctional PEG oligomers with tailored functionalities. There were mainly two strategies to accomplish the synthesis of α, ω-functionalized PEG. The first strategy involved the use of an initiator with a protected or latent functional groups and a terminating agent. The second strategy used various post-polymerization modifications to introduce different functionalities to the terminal ends of the PEG chain.[336]

The homopolymerization of a substituted epoxide, which carried in some cases a protected functionality, or the copolymerization of this type of monomer together with EO led to functionalities at the polyether backbone. In a recent review Obermeier et al. summarized the sequential polymerization as well as the concurrent polymerization of EO and allyl glycidyl ether (AGE), ethoxy ethyl glycidyl ether (EEGE), isopropylidene glyceryl glycidyl ether (IGG) or *N*,*N*-dibenzyl amino glycidol (DBAG) resulting in polyether structures with allyl groups, and after cleavage of the protecting groups one or two hydroxyl functionalities or an amine function, respectively. The different polyether structures are shown as examples in **Figure 5.47**. Additionally, further variety was accomplished by post-polymerization modifications of the functional groups along the polymer backbone. Thus a library of various functional PEG polymers could be achieved.[337]

In 2010, Mizrahi et al. introduced the use of different PEG mono methacrylate esters with various functionalities such as amines, thiols and carboxylates as polymerizable macromonomers. In **Figure 5.48** the structure of the macromonomers is illustrated. Additionally, a macromonomer with a terminal epoxide was synthesized, which might be used to obtain dendritic structures. Nanoparticles for drug delivery applications could be coated with PEG brushes by polymerization of these macromonomers via the acrylate groups.[338]

The synthesis and biomedical applications of PEG-dendritic block-copolymers were published in a recent review. The synthesis of PEG-dendritic block-copolymers with tailored solubility, supramolecular interactions as well as defined assembly properties were accomplished by variation of the length of the block, the generation and the structure of the dendritic block as well as the peripheral functionalities. Such

dendrimers were tested in diagnostics, in tissue engineering as well as for drug and gene delivery applications.[339]

A further approach to obtain PEG with multiple hydroxyl functionalities was recently introduced by Wilms et al. The random anionic ring-opening copolymerization of EO and glycidol led to hyperbranched PEG, a biocompatible, amorphous polyether polyol. The structure of the obtained copolymer is illustrated in **Figure 5.49**. The incorporation of glycidol into the growing PEG chains generated branching points and hence, hyperbranching.[342]

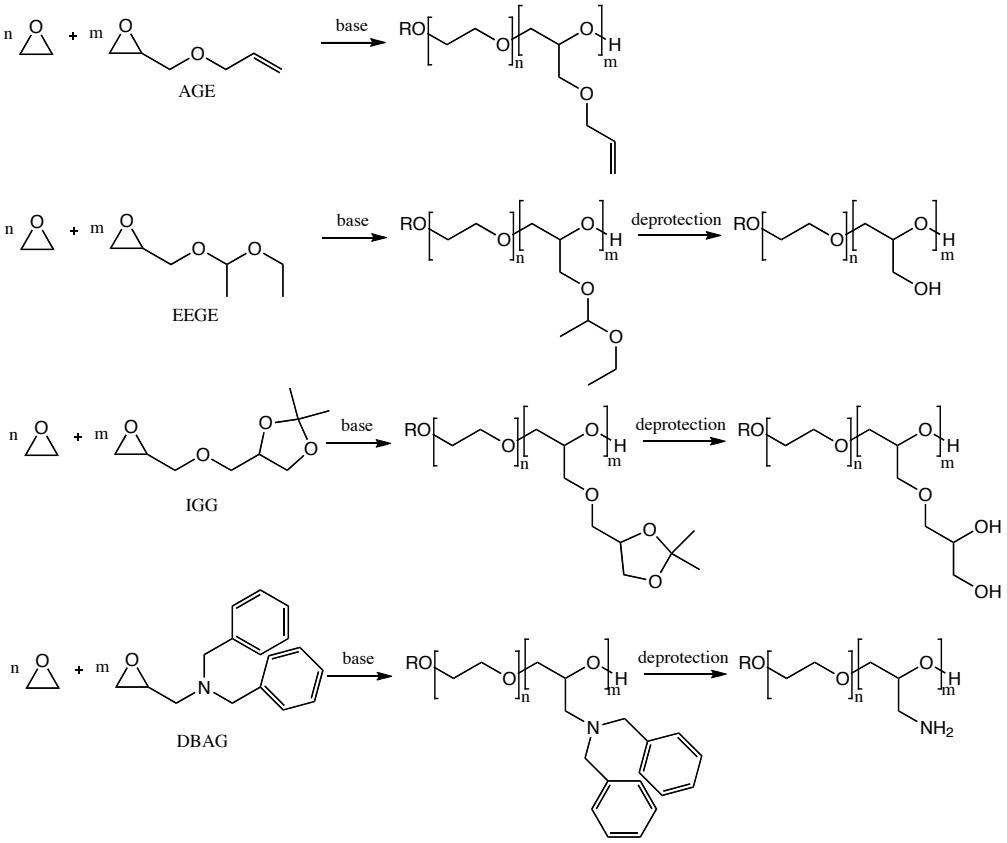

Figure 5.47: Synthesis of different functional PEGs.[337]

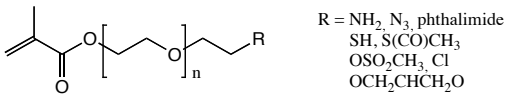

Figure 5.48: Structure of different PEG mono methacrylate esters macromonomers.[338]

In 2002, Kissel et al. published a summary on the use of PEG-polyester ABA-triblock-copolymers as potential candidate of hydrogel delivery systems. The A block consisted of a hydrophobic polyester and the hydrophilic B block was composed of PEG. Hydrogels were preferred as delivery systems for sensitive hydrophilic biomacromolecules such as DNA and proteins. They formed a protective shielding and the incorporation of the carriage was accomplished under mild conditions, while the cross-linking density controlled the diffusion. These triblock-copolymers might be an alternative to poly(lactide-*co*-glycolide) for the use of biodegradable drug delivery systems.[343]

As already mentioned PEG was often used to stabilize inorganic nanoparticles such as Au NPs. In most cases PEG was bond to the gold surface via thiol, disulfide or amine anchoring groups. However, there were also a few approaches where pure PEG was used to physiosorb on the nanoparticle surface.[49]

PEGylation shows several benefits. The shielded surface led to a higher hydrophilicity, which reduced the interaction and identification by opsonin proteins due to highly mobile and flexible PEG chains on the surface. The interfacial free tension of nanoparticles was lowered, hence the interaction with proteins was decreased in fluids. Furthermore, PEGylation increased the binding to dysopsonin proteins, which prevent the uptake by phagocytes.[49]

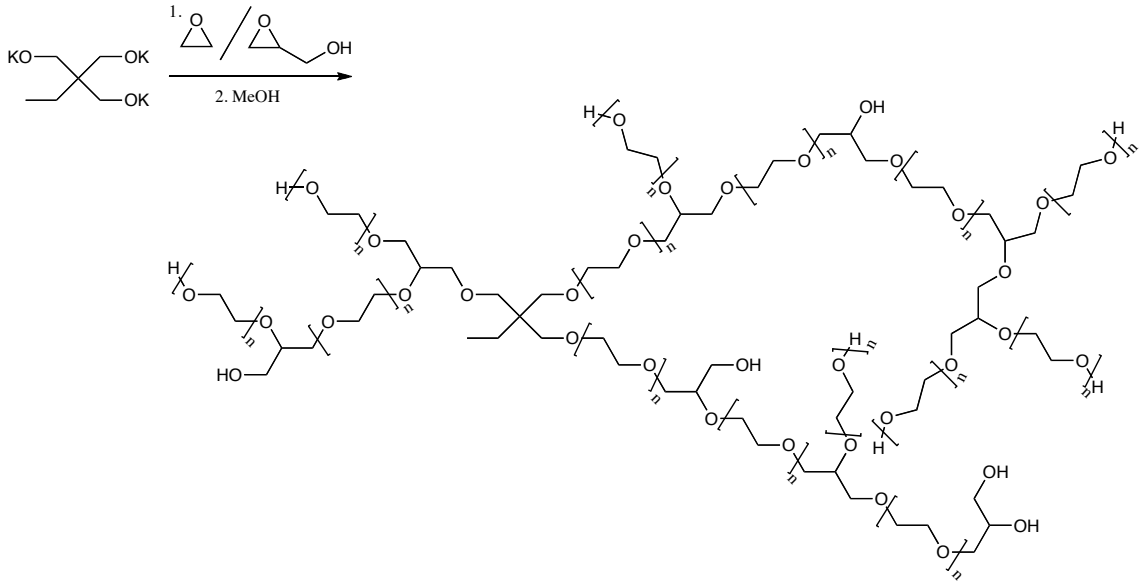

Figure 5.49: Structure of hyperbranched PEG.[342]

The following approach is an example for the application of PEGylated Au NPs. Heterobifunctional PEG with a carboxy terminus and a terminal dithiol was synthesized via termination with a carboxylate derivative and post-polymerization modification. The dithiol was utilized as anchoring group to the surface of the Au NPs and the carboxy terminus facilitated the covalently binding of specific antibodies onto the nanoparticle shell. These hybrid materials were tested as efficient labels of tumor stroma of pancreatic adenocarcinoma. The labeled tumor cells were imaged via darkfield microscopy, while the blind test with nonspecific antibody as well as with noncancerous pancreatic tissues gave a negative result.[344]

As already mentioned in the beginning of this chapter, PEG was attached to lipoic acid to enable the attachment to gold. Bis-lipoic acid modified oligoethylene oxide was used to self-assemble onto the surface of gold electrodes. Subsequently, cyclic voltammetry and impedance spectroscopy were used to investigate the recognition selectivity of alkali metal ions. The synthesized oligoethylene oxide recognized selectively potassium ions over sodium ions.[345] In a follow-up work, the same authors reported that the number of EO repeating units constituted the alkali ion selectivity. SAMs of LA-modified oligoethylene oxide with four repeating units were sensitive against sodium ions and SAMs formed by the oligoethylene oxide derivative with five EO repeating units recognized specifically potassium. The synthesized LA-modified oligomers are illustrated in **Figure 5.50**.[346]

The observed selectivity of the different oligoethylene oxide derivative corresponded to the cation binding of 15-crown-5 and 18-crown-6, respectively, with the same number of oxygen atoms in the binding region.

Although, the oligoethylene oxide derivative exhibited higher selectivity compared to the crown ethers. The structures of the corresponding crown ethers are shown in **Figure 5.51**.[346]

In a different study, PEG with a molecular weight of 2000 $g \cdot mol^{-1}$ was functionalized with LA and tested as anti-melanogenic agent. The used LA-derivative was synthesized in a DCC and DMAP-catalyzed esterification and exhibited lower cytotoxicity than LA. The obtained results suggested that the LA-derivative was able to suppress the melanin biosynthesis by down-regulation and expression of the activity of the tyrosinase, which is known as melanogenic enzyme.[347]

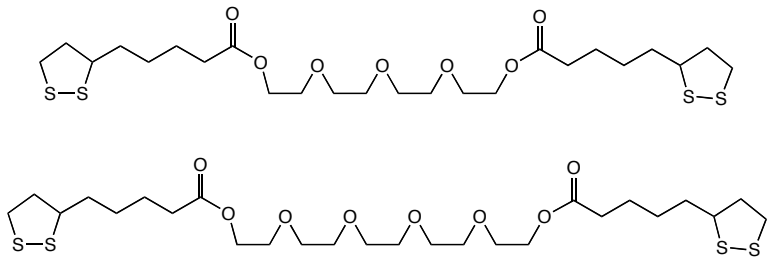

Figure 5.50: Structure of different bis-lipoic acid-modified oligoethylene oxides.[346]

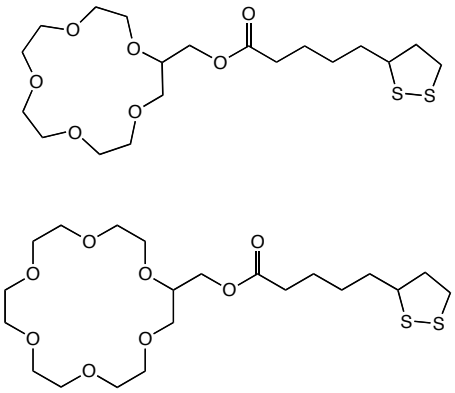

Figure 5.51: Structure of corresponding lipoic acid-modified crown ethers.[346]

In the following three examples, PEG was modified with at least one sulfur atom. The Leroux group used a synthesized block-copolymer composed of PEG, a poly(methacrylate) and a terminal thiol group. This group utilized a similar approach to synthesize PEG-PLA block-copolymers with a terminal thiol functionality,[330] as mentioned above. The synthetic route used a *tert*-butyl mercaptan as initiator for the anionic ring-opening polymerization of EO, which was subsequently reacted with 2-bromoisobutyryl bromide. The modified PEG acted as macroinitiator of the ATRP of (*N*,*N*-dimethylamino)ethyl methacrylate. Afterwards the *tert*-butyl substituent was cleaved and the formed disulfide was reduced by the addition of sodium borohydride. The obtained block-copolymer with a terminal thiol group was converted with biotin-maleimide. **Figure 5.52** illustrates the conducted synthesis. The biotin-modified block-copolymers self-assembled with oligonucleotides in aqueous solution to polyion micelles, which presented the biotin groups on the surface. Hence, these micelles exhibited a specific recognition of streptavidin. Additionally, the block-copolymers with a terminal thiol group self-assembled also in water and showed an increased mucoadhesion due to the ability of the free thiols to form disulfide bonds with mucin. Furthermore, micelles with intermolecular disulfide bonds might be used as stimuli-responsive networks.[348]

In 2011, Lokanathan et al. investigated the backfilling of SAM of PEG with oligoethylene oxides end-capped alkane thiol. **Figure 5.53** illustrates the synthesis. The protein and bacterial adhesion was decreased in case of mixed PEG-layers compared to pure PEG SAMs. Investigation via AFM negated the phase separation of thiol-functionalized PEG with different lengths, which was observed for SAMS of pure alkyl thiols of different lengths. The authors concluded, that backfilling of SAMs of PEG with oligoethylene oxides led to underbrush formation.[349]

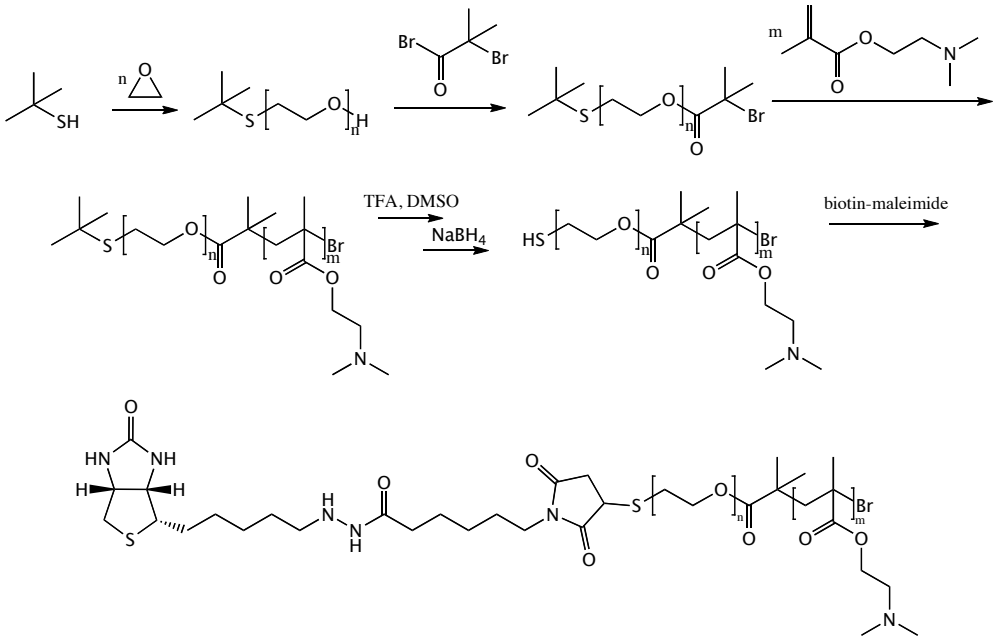

Figure 5.52: Synthesis of biotin-modified copolymers.[348]

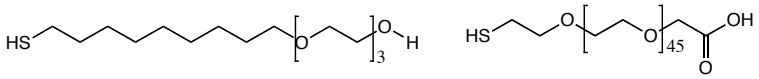

Figure 5.53: left: oligoethylene oxide end-capped by an alkyne thiol; right: α-carboxyl-ω-thiol PEG.[349]

In a further study, the surface coverage and the nanomechanical properties of SAMs of thiol-functionalized PEG on gold were investigated via AFM measurements. The surface coverage was not equal. It was found that PEG chains arranged in brush-like islands on flat gold surfaces.[350]

5.2 Motivation

The aim of this project was the synthesis and characterization of a lipoic acid derivative, which can be used as initiator for different ring-opening polymerizations.

Lipoic acid is a commonly used anchoring group for the attachment to gold surfaces. In most cases, the disulfide linker is attached via post-polymerization modifications, which hold the drawback of a random or incomplete modification as well as elaborate purification of unreacted polymer or unreacted compound, which carries the anchoring group. Additionally, the use of an initiator, which carries the linker group, facilitates the tailored synthesis of polymers, corresponding to the desired application.

The synthesized lipoic acid-derivative should act as initiator for the ring-opening polymerization of cyclic esters and epoxides, which are common used polymers with a wide range of different applications.

In here, *L*-lactide and ethylene oxide were polymerized as examples for these classes of monomers. The structure of the synthesized polymers has been characterized via SEC, ^{1}H as well as ^{13}C NMR spectroscopy and MALDI-ToF mass spectrometry. The thermal behavior of the disulfide-modified polymers was investigated by DSC measurements.

In addition, these polymers have been used to adsorb onto gold surfaces. The lipoic acid-functionalized polymers exchanged the citrate stabilizers of aqueous gold nanoparticles and the polymer-shielded nanoparticles were characterized via UV-vis spectroscopy. Additionally, the prepared polymers were adsorbed onto bare flat gold surfaces. The wettability of the modified-gold substrates was explored by static contact angle measurements and the surface topography was determined by AFM characterization.

5.3 Synthesis of a lipoic acid derivative as initiator

The use of a lipoic acid derivative as initiator for the ring-opening polymerization of epoxides and lactones accomplished the synthesis of well-defined polymers with a lipoic acid anchoring groups. The desired length of the polymer is directly adjustable by monomer to initiator ratio.

In two recent publications, the use of dihydroxyethyl disulfide as an initiator for the ring-opening polymerization of lactide as well as glycidol was described. In both approaches the concentric disulfide functionality was not affected under the polymerization conditions.[326,351]

The ring-opening polymerization of cyclic esters and epoxides requires a hydroxyl, amine or thiol functionality. Lipoic acid carries a carboxyl function and is not capable of initiating the ring-opening polymerization of these named monomer classes.

The simplest strategy to obtain lipoic acid with a terminal hydroxyl functionality might be the reduction of the carboxyl functionality to obtain the corresponding lipoic alcohol. The use of common reduction agents led to the undesired reduction of the disulfide bond. Algar and Krull obviated this problem by a subsequent oxidation reaction. In the first step, lipoic acid was completely reduced with lithium aluminium hydride to 6,8-dimercaptooctan-1-ol. Subsequently, the disulfide bond was retrieved by oxidation of the thiol functionalities with copper(II) ions in a mixture of ethanol and water. The solvent of the dissolved product was not removed completely, otherwise an insoluble product was obtained.[297] In a further approach, catecholborane was used as a versatile reducing agent, which selectively reduced the carboxyl group to a hydroxyl function without cleavage of the disulfide bond. The lipoic alcohol was described as notoriously unstable and was not completely characterized.[352]

The polymerization of EO and *L*-lactide is highly sensitive against traces of water and other protic solvents and complete desiccation is essential. Hence, lipoic alcohol was not tested as initiator for ROP.

In 2011, the group around Möller introduced the successful synthesis of oligoglycidol macromonomers with three to six repeating units of glycidol or EEGE via anionic ring-opening polymerization and *N*-(2-hydroxyethyl)methacroyl amide was used as an initiator among others.[353]

Dougan et al. introduced the synthesis of an amide composed of lipoic acid and aminohexanol.[354]

In this thesis, lipoic acid was modified with 5-aminopentan-1-ol to attach a terminal hydroxyl functionality to LA via an amide bond. The conducted synthesis to obtain the novel lipoic acid derivative is shown in **Figure 5.54**.

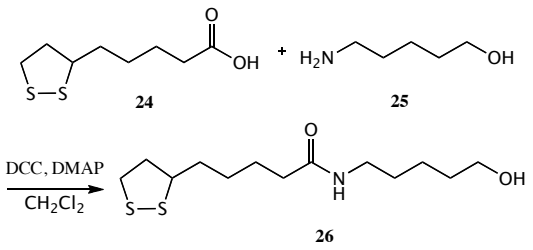

Figure 5.54: Synthesis of *N*-(5-hydroxypentyl)-5-(1,2-dithiolan-3-yl)pentamide.

The synthesis of *N*-(5-hydroxypentyl)-5-(1,2-dithiolan-3-yl)pentamide (**26**) was successfully realized. The required product was formed in a reasonable yield of 68%. The desired structure was proven by NMR spectroscopy and field desorption mass spectrometry (FD-MS). The ^{1}H NMR spectrum, after chromatography on silica, of *N*-(5-hydroxypentyl)-5-(1,2-dithiolan-3-yl)pentamide is illustrated in **Figure 5.55**. The peaks were assigned by the means of two-dimensional NMR spectroscopy. The proton signal of the amide bond at 5.62 ppm clearly indicates the linkage of the starting materials in the desired way.

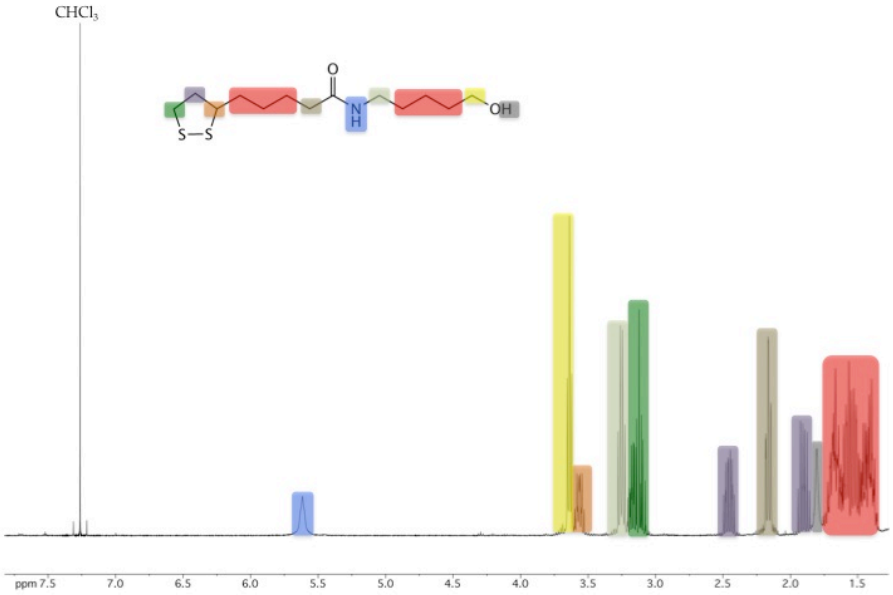

Figure 5.55: ^{1}H NMR spectrum of *N*-(5-hydroxypentyl)-5-(1,2-dithiolan-3-yl)pentamide.

The ^{13}C NMR spectrum as well as the corresponding peak assignment is shown in **Figure 5.56**.

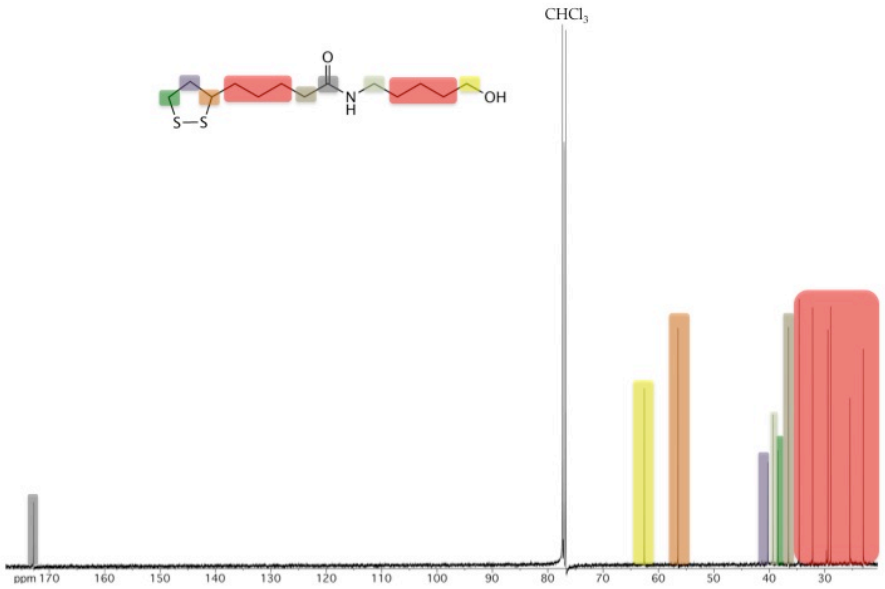

Figure 5.56: ^{13}C NMR spectrum of *N*-(5-hydroxypentyl)-5-(1,2-dithiolan-3-yl)pentamide.

In the following, the use of this compound as an initiator for the ring-opening polymerization of lactide and ethylene oxide was investigated.

5.4 Poly(*L*-lactic acid) with a terminal lipoic acid anchoring group

5.4.1 Synthesis

The synthesized LA-derivative was explored as initiator for ROP of *L*-lactide as a representative of the class of lactones. This approach exhibited the benefit of the immediate synthesis of LA-functionalized PLLA in one reaction step. Additionally, the desired polymer length can be influenced by the amount of monomer, which is polymerized.

Different polymerization catalysts and conditions have been investigated. The commonly used coordination-insertion polymerization catalyzed by tin(II) octanoate at 110 °C in toluene failed. This might be caused by interactions between the disulfide bond of the initiator and the tin species. Additionally, the rather high temperature might raise problems, because the disulfide bond of LA was reported to be sensitive against high temperature and tends to thermal polymerization, as mentioned before.[258,354]

The enzymatically catalysis with Novozym 435, a lipase from *Candida antarctica*, as well as the organocatalysis with DBU or 1,4,7-triazabicyclodecene (TBD) did not lead to the desired polymer.

In contrast, the polymerization of *L*-lactide was successfully conducted with DMAP as organocatalyst in toluene at 60°C and is illustrated in **Figure 5.57**. The used polymerization conditions were similar to those described for dihydroxyethyl disulfide.[326]

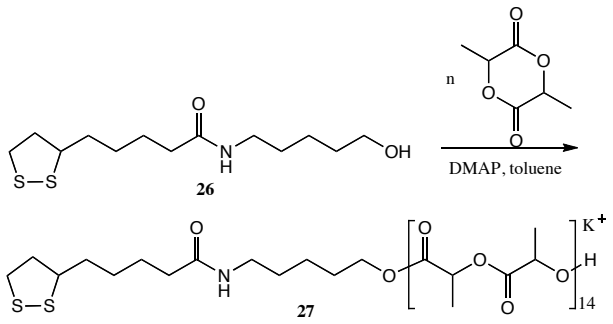

Figure 5.57: ROP of *L*-lactide with *N*-(5-hydroxypentyl)-5-(1,2-dithiolan-3-yl)pentamide as initiator.

Five different PLLA with a LA anchoring group were successfully synthesized. SEC, ^{1}H as well as ^{13}C NMR spectroscopy and MALDI-ToF mass spectrometry were used to characterize the structure of the obtained polylactides. The degree of polymerization was varied in the range of seven to twenty repeating units. The results are summarized in **Table 5.1**. Additionally, the thermal properties were investigated via DSC measurements.

Table 5.1: Summary of the synthesized LA-modified poly(*L*-lactide)s.

	$\overline{DP_n}$ (^{1}H NMR)	$\overline{M_n}$ (^{1}H NMR) [g·mol^{-1}]	$\overline{M_n}$ (SEC)* [g·mol^{-1}]	PDI (SEC)*	T_g (DSC)** [°C]	T_m (DSC)** [°C]
LA-PLLA 1	7	1300	1100	1.16	15	95
LA-PLLA 2	11	1900	1700	1.16	25	119
LA-PLLA 3	15	2500	2500	1.05	29	124
LA-PLLA 4	17	2700	2500	1.06	28	128
LA-PLLA 5	20	3200	2300	1.09	33	129

*SEC: eluent: DMF; PEG standard calibration; ** DSC: temperature range: 0 °C – 200 °C with 10 °C·min^{-1}

The proton spectrum of **LA-PLLA 3** is shown as an example in **Figure 5.58**. All proton signals were clearly visible except some signals of the aliphatic methylene groups (highlighted in red), which were below the signal of the methyl groups of the PLLA backbone. A successful initiation of lactide by the synthesized LA-derivative was indicated by the shift of the proton signal of the methylene group next to the initiating hydroxyl functionality (highlighted in yellow). This signal was shifted from 3.64 ppm for the initiator to 4.11 ppm after the polymerization. This low-field shift occurred due to a change in the proximity of the methylene group from a hydroxyl functionality to an ester group after the polymerization.

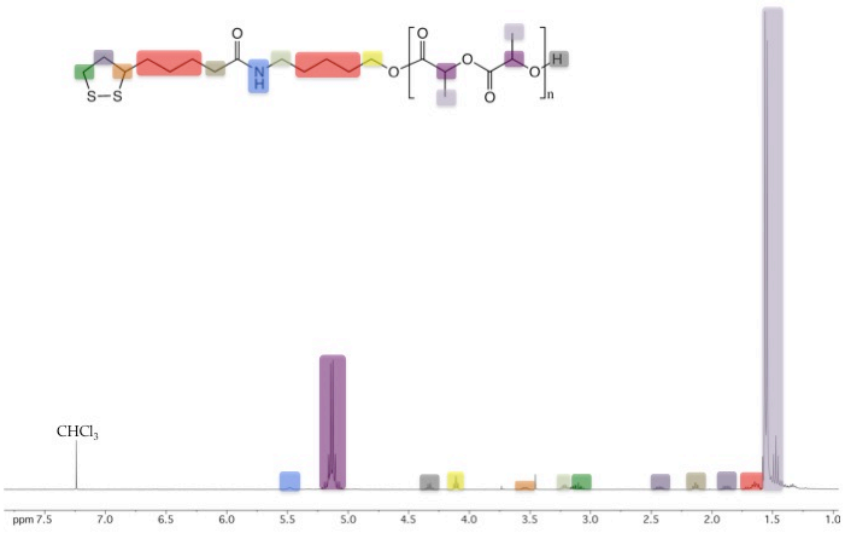

Figure 5.58: ^{1}H NMR spectrum of **LA-PLLA 3**.

The ratio of one proton signal of the dithiolane at 2.45 pm (highlighted in dark purple) and the signal of the methine protons of the PLLA was used to determine the degree of polymerization. The molecular weight of the formed modified polylactides was varied in the range of 1300 to 3200 g·mol^{-1}.
The carbon NMR spectrum of **LA-PLLA 4** is illustrated in **Figure 5.59**.

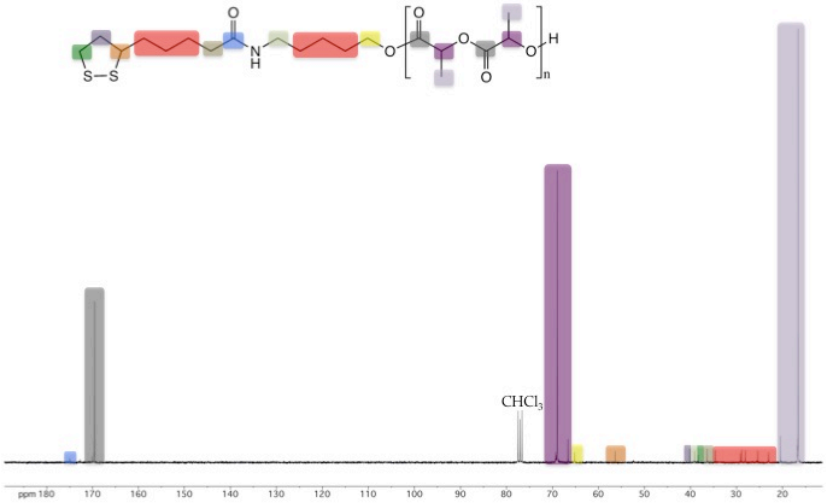

Figure 5.59: ^{13}C NMR spectrum of **LA-PLLA 4**.

MALDI-ToF mass spectrometry was further used to prove the proposed structure. The MALDI-ToF spectrum of **LA-PLLA 3** is illustrated in **Figure 5.60**. The difference between two peaks mounted 144.1 g·mol^{-1} and correlated to one lactide unit. The detected peak distribution corresponded to the desired polymer, after ionization with potassium. In addition, no further distribution, which might be caused by transesterification or a side-product such as PLLA initiated by humidity, was observed. The detected peak at 2347 g·mol^{-1} corresponded well to the molecular weight determined from proton NMR spectroscopy with 2500 g·mol^{-1}.

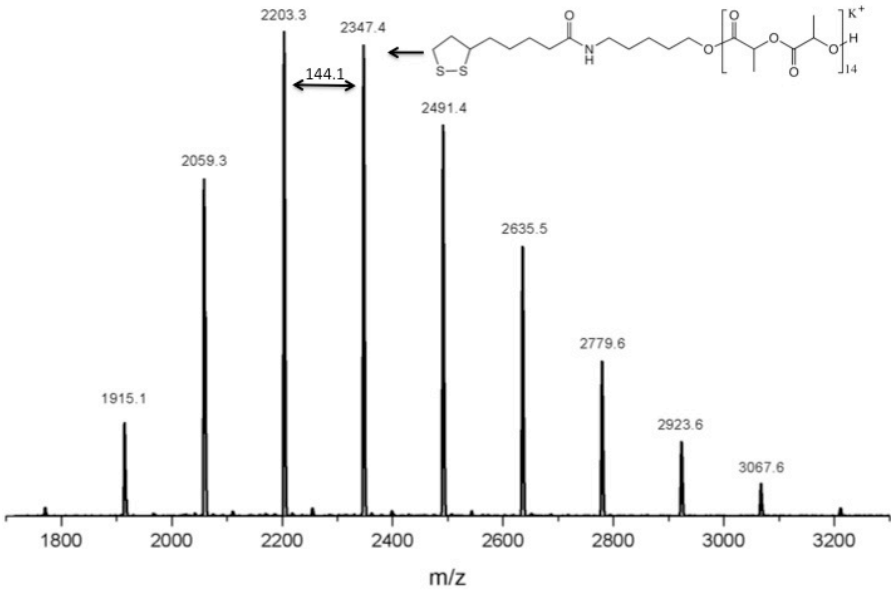

Figure 5.60: MALDI-ToF MS spectrum of **LA-PLLA 3**.

The molecular weights measured by SEC measurements in DMF were in nearly all cases smaller than the molecular masses calculated via NMR spectroscopy. The molecular mass of the polymers upon fifteen lactide repeating units was nearly constant and detected at 2300 to 2500 g·mol^{-1} in SEC. This might be caused by interactions with the material of the SEC column. However, the molecular weight determined by ^{1}H NMR spectrometry might be reliable. The polydispersity of the formed polymers, as obtained by SEC was narrow with PDIs below 1.20. The SEC traces are illustrated in **Figure 5.61**.

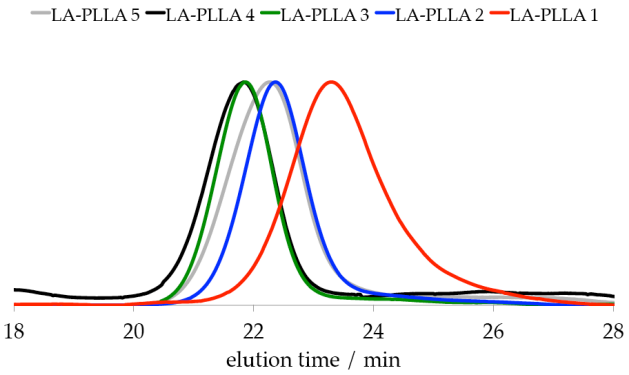

Figure 5.61: SEC traces (eluent: DMF; PEG standard calibration) of **LA-PLLA 1-5**.

The thermal behavior of the obtained light yellow solids was investigated by DSC measurements. For the modified PLLA a melting point as well as glass transition temperature was detected. These values increased with increasing molecular weight. The T_g was shifted from 15 °C for the polylactide with seven monomer units to 33 °C for the sample with twenty repeating units, while the T_m of **LA-PLLA 1** was detected at 95 °C and increased to 129 °C for **LA-PLLA 5**. The Spassky group reported the melting point of optically pure PLLA at 169 °C, which is significantly higher than the detected values.[355] The increasing glass transition temperature and melting point with increasing molecular weight supported the molecular weight calculation by NMR spectroscopy in contrast to the SEC measurements.
The increase of the melting point as well as the glass transition temperature was pronounced on going from **LA-PLLA 1** to **LA-PLLA 2**, compared to the increase between **LA-PLLA 2** to **LA-PLLA 3** and **LA-PLLA 3** to **LA-PLLA 5**, respectively. The difference between **LA-PLLA 1** and **LA-PLLA 2** was four lactide repeating units and the detected T_g increased by 10 °C, and the T_m was 14 °C higher. The difference between **LA-PLLA 2** and **LA-PLLA 3** as well as between **LA-PLLA 3** and **LA-PLLA 5** was also four or five lactide repeating units. However, in both cases the glass transition temperature was 4 °C higher and the melting temperature increased about 5 °C. This observation might be caused by interference with the LA-based initiator, which might be significantly higher in case of seven lactide units compared to eleven, fifteen or twenty repeating units.
In summary, the ring-opening polymerization of *L*-lactide with a novel lipoic acid-based initiator under DMAP-catalysis was successfully conducted as demonstrated by different characterization methods.

5.4.2 Surface attachment

As a proof of principal experiment, the synthesized LA-modified polyester moieties were attached to gold surfaces. This was again realized by the adsorption onto flat gold substrates as well as gold nanoparticles. The respective procedures have already been described in chapter 4.7.

5.4.2.1 Gold nanoparticles

A solution of LA-modified polylactide in dichloromethane was extracted for one hour with aqueous Au NPs solution to exchange the citrate stabilizers at the nanoparticle surface by disulfide-functionalized polymers. Subsequently, the aqueous solution as well as the organic phase was analyzed by UV-vis spectroscopy. Additionally, the extraction efficiency of lipoic acid in dichloromethane solution was investigated under the described conditions and compared to values reported in literature. Three polylactides with different block lengths were investigated. The results are summarized in **Table 5.2**.

Table 5.2: Summary of the UV-vis spectroscopy data.

	$\overline{DP_n}$ (^{1}H NMR)	$\overline{M_n}$ (^{1}H NMR) [g·mol^{-1}]	λ_{max} (H_2O) [nm]	λ_{max} (DCM) [nm]
LA	-	-	522	336
LA-PLLA 1	7	1300	-	525
LA-PLLA 3	15	2500	525*	522
LA-PLLA 5	20	3200	-	520

*weak absorption band

The lipoic acid control experiment exhibit in aqueous solution an absorption maximum at 522 nm in aqueous solution, which was similar to the adsorption maximum of citrate stabilized Au NPs. In dichloromethane an adsorption maximum at 336 nm was detected. This value corresponded to the adsorption of LA in Na_2HPO_4 solution at 333 nm.[357] In contrast, LA was often used to transfer Au NPs synthesized in organic solvents into aqueous solution.[358,359] In a further approach the citrate stabilizers were exchanged against LA mediated by the addition of sodium chloride, as mentioned in the introduction.[262] The obtained results as well as the reported applications excluded any influence of pure lipoic acid on the extraction efficiency of Au NPs from aqueous solution into organic solvents. In contrast, the PLLA polymers functionalized with a lipoic acid anchoring group were enabled to transfer the Au NPs from the water phase into the dichloromethane phase.

Solely the aqueous solution, which was extracted with the polylactide solution of **LA-PLLA 3** with 2500 $g \cdot mol^{-1}$ still exhibited a weak adsorption band at 525 nm. However, the transfer into dichloromethane was carried out successfully. All organic phases indicated an adsorption maximum in the range of 520 to 525 nm. The wavelength of the adsorption band increased with decreasing length of the polylactide. This might be caused by the change of the chemical surrounding due to an exchange of the stabilizers on the nanoparticle surface. The length of the polyester backbone appeared to influence the chemical environment of the nanoparticles and the adsorption maximum. Additionally, **LA-PLLA 1** with seven repeating units might not be enabled to completely prevent the agglomeration of the Au NPs.

The transfer of aqueous Au NPs to dichloromethane was achieved by exchange of the citrate linker groups with LA-functionalized PLLA. In contrast, the extraction of Au NPs under identical conditions with PPS-PLLA block-copolymers failed, as described in chapter 6. Interestingly enough, a polylactide attached to a single disulfide functionality facilitated the extraction of Au NPs. In contrast, a solution of PPS-PLLA block-copolymers with 6wt% PLA and multiple sulfide functions led to an incomplete transfer of the nanoparticles from aqueous solution. Block-copolymers with higher PLA contents did not feature the linker exchange at all.

5.4.2.2 Gold substrates

In a further approach, the poly(*L*-lactide)s initiated by a lipoic acid derivative were adsorbed onto bare gold supports. The surface of the modified gold substrates was subsequently studied by static contact angle measurements and AFM imaging. Two different polylactides **LA-PLLA 1** and **LA-PLLA 2** as well as pure lipoic acid were used to coat gold substrates. LA was again used for comparison. The height images obtained by AFM measurements are shown in **Figure 5.61**. The obtained surface topography of the coated supports was in all cases rather flat, and the structure was similar to bare template-stripped gold (TSG), except for some higher spots. The surface coverage appeared in case of LA more even (**Figure 5.62 A**) compared to the substrates shielded with modified PLLA (**Figure 5.62 B**, **C**). The AFM height images did not reveal a uniform result, if the coating procedure was successful.

Additionally, the modified surface was assessed via the root-mean squared (RMS) roughness and static contact angles of a water droplet. The obtained values of the contact angle goniometry and RMS values are summarized in **Table 5.3**.

The surface roughness of the sample coated with LA as well as with polylactide was slightly higher that the RMS value of the processed TSG, but in the range of the error margin. However, the static contact angle was significantly shifted compared to the TSG blind sample. The surface coated with LA exhibited with approximately 73 ° a slightly higher contact angle than the substrates coated with polylactide. The contact

angle detected for the gold substrates modified with PPS-PLA block-copolymers was 70 to 72 °, dependent on the content of PLA (chapter 6.1). These values were similar to those obtained for the LA-functionalized PLA with 67 to 69 °.

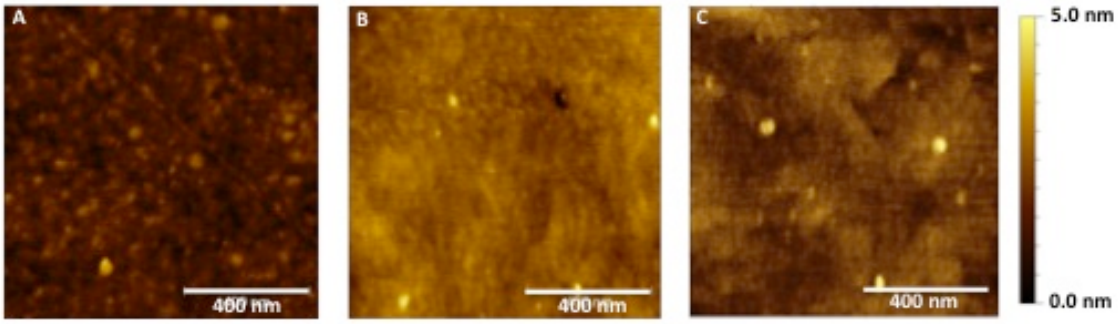

Figure 5.62: AFM height images of different coated gold substrates recorded in tapping mode; (A = LA; B = **LA-PLLA 1**; C = **LA-PLLA 2**).

Table 5.3: Summary of the obtained contact angles and RMS values.

	$\overline{DP_n}$ (^{1}H NMR)	$\overline{M_n}$ (^{1}H NMR) [g·mol^{-1}]	**Static contact angle** (H_2O) [°]	**RMS roughness** (1 x 1 µm^2) [nm]
bare gold**	-	-	88 ± 2	0.3 ± 0.1
LA	-	-	73 ± 3	0.5 ± 0.1
LA-PLLA 1	7	1300	69 ± 2	0.6 ± 0.2
LA-PLLA 2	11	1900	67 ± 2	0.4 ± 0.1

**reference (equally processed)

In summary, the successful adsorption onto flat gold substrates was proven by contact angle measurements, although the surface topography was rather flat and only slightly higher than the TSG. The polysulfides as well as lipoic acid recreated the typical structure of TSG. Similar results were also detected for gold supports modified with polysulfide, as described in chapter 4.

5.5 Poly(ethylene glycol) with a terminal lipoic acid anchoring group

5.5.1 Synthesis

The LA-derivative with a terminal hydroxyl functionality was also investigated as an initiator for the anionic ring-opening polymerization of ethylene oxide. This straightforward approach enabled the synthesis of PEG with lipoic acid as a terminal anchoring group, without post-polymerization modification and the associated drawbacks. Furthermore, the molecular weight of the modified PEG can be directly adjusted by the ratio between the initiator and the monomer.

The anionic ring-opening polymerization of ethylene oxide with the novel LA-based initiator was investigated as an eyample for the general class of epoxide monomers.

The use of cesium hydroxide in benzene for the deprotonation of the LA-based initiator and an efficient initiation failed under different conditions. Neither the use of dimethyl sulfoxide (DMSO) nor a mixture of DMSO and THF showed any improvement. This might be caused by interactions between the cesium ions and the sulfur atoms of the disulfide motif, as well as by an inefficient deprotonation due to low solubility in benzene for the LA-derivative and a discontentedly deprotonation. Additionally, the removal of water, which was formed during the deprotonation and water of hydration from cesium hydroxide, might be challenging. Heating above 90 °C is necessary to ensure efficient drying of the deprotonated initiator, but the dithiolane functionality was reported to be sensitive against higher temperatures, as already mentioned.[258,354]

In further approaches, the deprotonation with potassium *tert*-butoxide solution in THF was investigated. This reagent exhibited the benefit of a dissolved base, and *tert*-butanol was formed during the deprotonation, which should be easier to remove than water due to its lower boiling point at 83 °C.[356] In case of potassium *tert*-butoxide solution the deprotonation or the removal of the *tert*-butanol was incomplete. Hence PEG initiated by *tert*-butoxide was obtained.

Potassium naphthalide solution is on one hand a soluble deprotonating agent and naphthalene, which was formed during the deprotonation of the hydroxyl functionality of the initiator, did not show any interference with the ring-opening polymerization of EO. Hence, the monomer addition was enabled immediately after the deprotonation without drying of the deprotonated initiator. However, potassium naphthalide solution did not lead to satisfactory results, which might be caused by its reductive effect on the disulfide bond.

The deprotonation with diphenylmethyl potassium (DPMK), which was also described for the initiation of dihydroxyethyl disulfide, led to a successful polymerization with the novel LA-based initiator.[351] This reagent exhibited the benefits of a soluble deprotonating agent without drying of the formed initiator salt and did not cause a reductive effect. The conducted synthesis is illustrated in **Figure 5.63**.

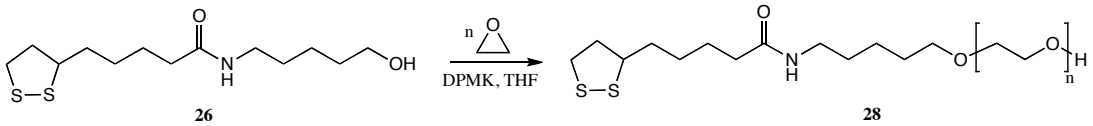

26 **28**

Figure 5.63: Polymerization of EO with *N*-(5-hydroxypentyl)- 5-(1,2-dithiolan-3-yl)pentamide as initiator.

The polymers obtained were investigated via ^{1}H and ^{13}C NMR spectroscopy, MALDI-ToF mass spectrometry as well as SEC measurements. **Table 5.4** summarizes the synthesized PEG polymers with a lipoic acid anchoring group.

Table 5.4: Summary of the synthesized LA-modified poly(ethylene glycol)s.

	$\overline{DP_n}$ (^{1}H NMR)	$\overline{M_n}$ (^{1}H NMR) [g·mol^{-1}]	$\overline{M_n}$ (SEC)* [g·mol^{-1}]	PDI (SEC)*
LA-PEG 1	15	950	1500	1.51
LA-PEG 2	23	1300	1800	1.28
LA-PEG 3	25	1400	1800	1.33
LA-PEG 4	36	1900	2100	1.24

*SEC: eluent: DMF; PEG standard calibration

The polymerization of EO initiated by a LA-derivative was successful, even though the achieved polydispersities were only moderate (i.e., not narrow) with 1.24 to 1.51. The obtained polymers were brown-colored and cereous. The SEC traces are illustrated in **Figure 5.64**.

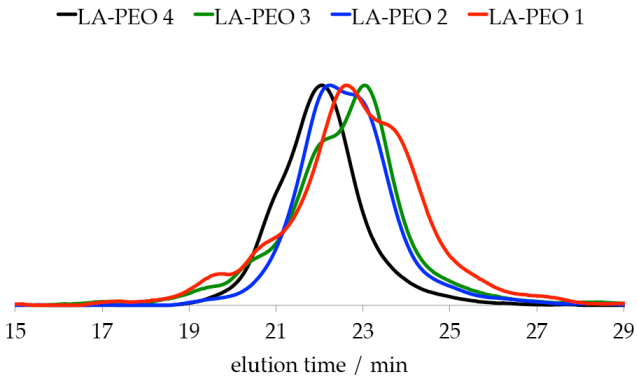

Figure 5.64: SEC traces (eluent: DMF; PEG standard calibration) of **LA-PEG 1-4**.

The MALDI-ToF mass spectrum of **LA-PEG 2** is illustrated in **Figure 5.65**.

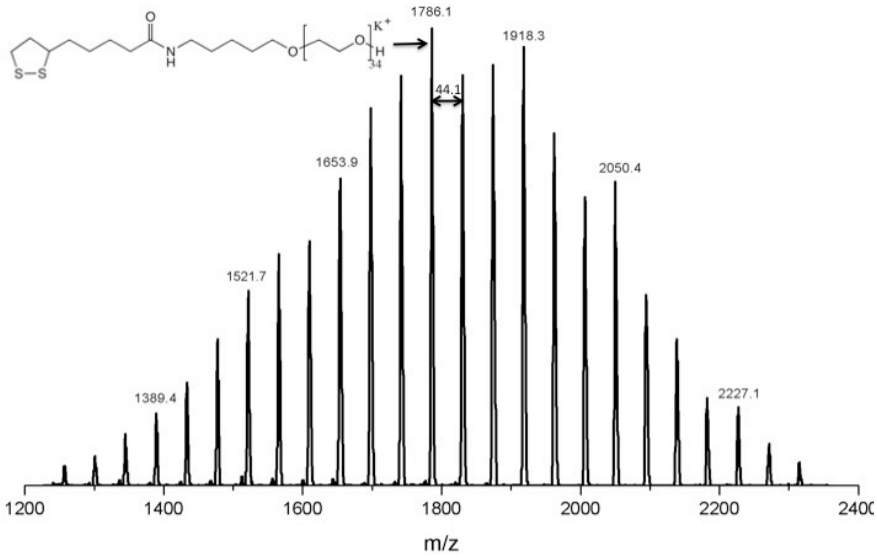

Figure 5.65: MALDI-ToF MS spectrum of **LA-PEG 2**.

In some cases, the SEC traces exhibited a slight shoulder, which might be caused by a side product. Although only one molecular weight distribution appeared in the MALDI-ToF mass spectrum. The difference between two detected molecular masses of the prospected polymer mounted 44.1 g·mol^{-1}, which corresponded to the molecular weight of ethylene oxide. The detected molecular mass maximum of 1786 g·mol^{-1} correlated to PEG with 34 repeating units, which was initiated by *N*-(5-hydroxypentyl)- 5-(1,2-dithiolan-3-yl)pentamide and ionized with potassium. The peak maximum of the mass spectrometric analysis was similar to the one detected by SEC in DMF. The obtained molecular weight varied between 1500 to 2100 g·mol^{-1}. Proton NMR spectroscopy was also used to calculate the molecular weight of the formed polymers. The ^{1}H NMR of **LA-PEG 1** is shown as an example in **Figure 5.66**.

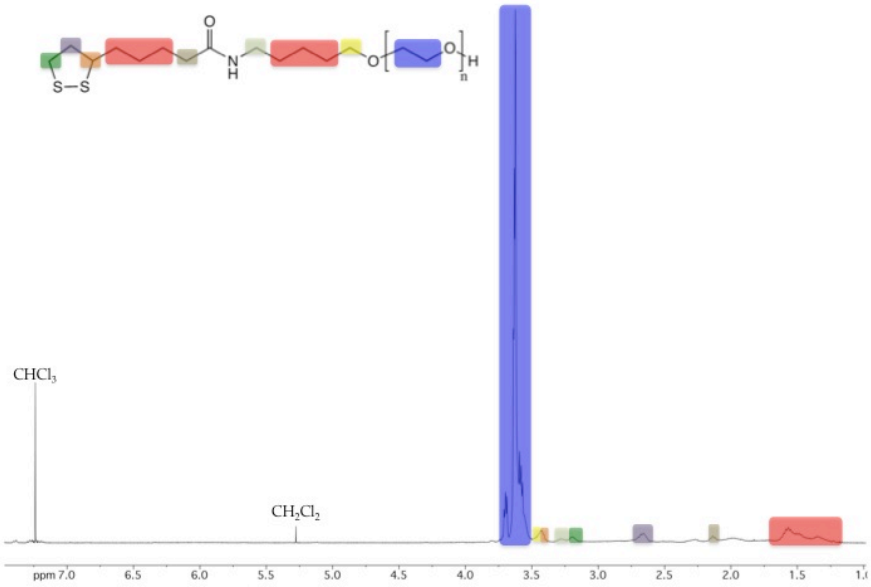

Figure 5.66: ^{1}H NMR spectrum of **LA-PEG 1**.

The peak ratio between the twelve aliphatic methylene protons from 1.23 to 1.62 ppm (highlighted in red) and the protons of the ethylene oxide backbone from 3.57 to 3.75 ppm (highlighted in blue) was used to calculate the obtained molecular weight of the polymers prepared. The error of this calculation might be in case of the synthesized PEG moiety relatively high, because the integral of the polymer backbone was high, compared to the initiator signal, even for the sample with only fifteen repeating units. Some of the initiator signals were nearly non-distinguishable from the baseline. The molecular weights calculated by NMR were in all cases slightly lower than those obtained by SEC. The reckoned length of the polymers amounted to fifteen to thirty-six repeating units and hence a molecular weight between 950 and 1900 g·mol^{-1}. The synthesis of polymers with higher molecular weights was challenging under the named conditions. However, for most applications the desired molecular weight for surface modification was below 2000 g·mol^{-1}, as described in the beginning of this chapter.

The structure of the PEG initiated by a LA-derivative was also investigated by ^{3}C NMR spectroscopy. The ^{13}C NMR spectrum of a LA-PEG is illustrated in **Figure 5.67**. The carbon signals of the initiator were hardly observable due to the large difference of the peak intensity of the initiator and the polyether backbone. The aromatic carbon signals at approximately 130 ppm were caused by diphenylmethane, which was formed during the deprotonation of the initiator. It was demanding to remove the side-product completely. However, the small impurity did not interfere with the following applications as adsorbents.

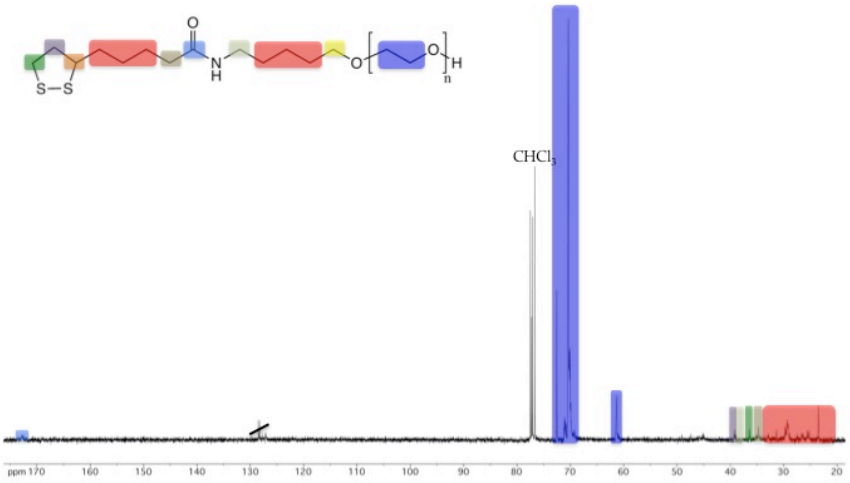

Figure 5.67: ^{13}C NMR spectrum of **LA-PEG 1**.

The synthesis of PEG with a LA-derivate as initiator was successfully conducted, as proven by MALDI-ToF mass spectrometry, but the achieved polydispersity was only moderate for anionic ring-opening polymerization. The synthesis of high molecular weight polymers was demanding.

5.5.2 Surface attachment

The synthesized PEGs functionalized with lipoic acid as an anchoring group were used to adsorb onto the surface of gold nanoparticles and bare template-stripped gold substrates. The adsorption was conducted as described in chapter 4.7 for polysulfides and analyzed via UV-vis spectroscopy or AFM and static contact angle measurements, respectively.

5.5.2.1 Gold nanoparticles

One of the main benefits of PEG is its good solubility in water. The transfer of Au NPs from aqueous solution into the organic phase was not possible. However, the LA-modified polyethers should accomplish the exchange of the citrate linker at the nanoparticle surface. The results of the UV-vis spectroscopy are summarized in **Table 5.5**.

Table 5.5: Summary of the UV-vis spectroscopy data.

	$\overline{DP_n}$ (^{1}H NMR)	$\overline{M_n}$ (^{1}H NMR) [g·mol^{-1}]	λ_{max} (H_2O) [nm]	λ_{max} (DCM) [nm]
LA-PEG 1	15	950	521	-
LA-PEG 2	23	1300	521	-
LA-PEG 4	36	1900	522	-

The adsorption behavior onto aqueous Au NPs was studied with three LA-functionalized PEGs, the molecular weight was varied from approximately 950 to 1900 g·mol^{-1}. The detected adsorption maxima of the aqueous solution were 521 and 522 nm, respectively, thus similar to the citrate-stabilized nanoparticles

with 519 nm. This slight bathochromic shift might occur due to the change of the stabilizers at the nanoparticle surface. In contrast to the LA-functionalized polylactides, the adsorption maximum increased with increasing polymer chain length. In case of the polyester-modified Au NPs this effect was more marked. The organic phase did not exhibit an adsorption band, as expected.

5.5.2.2 Gold substrates

The gold supports were dipped into a solution of LA-modified PEG in dichloromethane. Subsequently, the shielded gold substrates were investigated by AFM and contact goniometry.

The gold substrates were coated with **LA-PEG 2** and **LA-PEG 4**. The obtained AFM height images are illustrated in **Figure 5.68**.

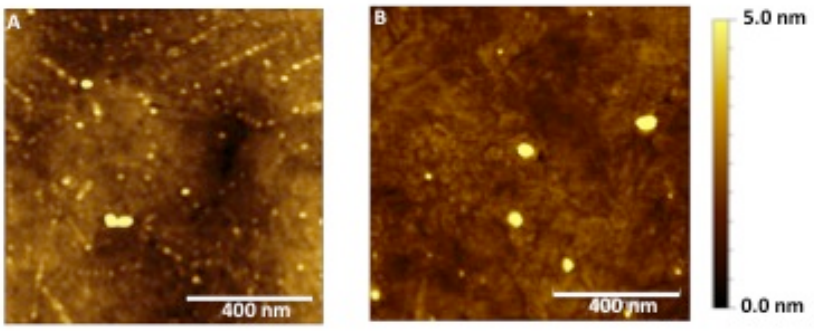

Figure 5.68: AFM height images of different coated gold substrates recorded in tapping mode; (A = **LA-PEG 2**; B = **LA-PEG 4**).

The surface covered with **LA-PEG 2** appeared relatively homogenous covered by mostly small aggregates and in contrast, the surface coverage with **LA-PEG 4** seemed less dense and the aggregates were larger. A profile of topology of sample **LA-PEG 4** is shown in **Figure 5.69**.

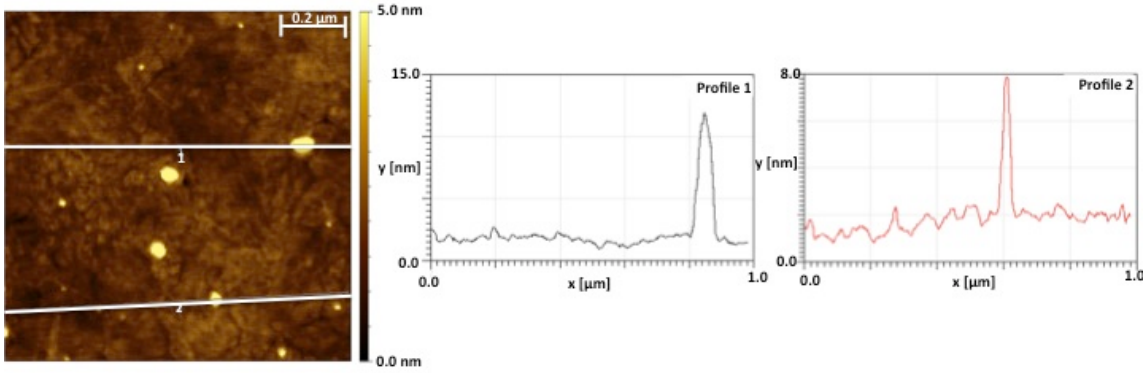

Figure 5.69: Profiles of the AFM height image of **LA-PEG 4** coated gold substrate.

The "spikes" on the surface exhibited different proportions, the larger ones were nearly 12 nm high, in contrast the smaller ones were thinner and approximately 6 nm high.

In addition, the wettability of the PEG-coated surfaces was investigated. **Table 5.6** summarizes the obtained static contact angles of a water droplet as well as the values of the RMS roughness.

The obtained surface roughness was 0.8 nm, i.e., markedly rougher than the TSG comparison with 0.3 nm (**Table 5.3**). The static contact angle detected for the PEG-modified surfaces was about 36 ° and significantly

different from the bare TSG with 88 ° (**Table 5.3**). The small contact angle revealed a hydrophilic surface, as expected after coating with PEG.

The LA-functionalized PEG was successfully coated onto the gold surfaces as proven by the surface roughness and the significant change of the wettability.

Table 5.6: Summary of the obtained contact angles and RMS values.

	$\overline{DP_n}$ (^{1}H NMR)	$\overline{M_n}$ (^{1}H NMR) [g·mol^{-1}]	**Static contact angle** (H_2O) [°]	**RMS roughness** (1 x 1 μm^2) [nm]
LA-PEG 2	23	1300	37 ± 2	0.8 ± 0.3
LA-PEG 4	36	1900	36 ± 3	0.8 ± 0.2

5.6 Summary and conclusion

The chemical derivatization of lipoic acid, a widely used anchoring group to attach numerous structures onto metal surfaces, enabled the synthesis of a variety of polymers with a terminal lipoic acid functionality. The novel lipoic acid-containing initiator was successfully synthesized in a straightforward approach by the reaction of lipoic acid and 5-aminopentan-1-ol. The respective amide with one terminal hydroxyl functionality was obtained in good yields.

This initiator was used to initiate the ring-opening polymerization of lactide. The polymerization conditions were adjusted to the novel disulfide-containing initiator. The use of DMAP as organocatalyst in toluene at 60 °C exhibited the best results. The desired functionalized polyester structure was proven by MALDI-ToF MS as well as NMR spectroscopy. The obtained polymers exhibited narrow polydispersities below 1.2. The results of the thermal behavior of the synthesized moieties were characteristic for PLLA. Additionally, the synthesized polymers were adsorbed onto gold surfaces. The successful transfer of aqueous gold nanoparticles into organic solvents was accomplished after exchange of the citrate linkers by LA-functionalized polylactides. The adsorption to bare gold substrates was also feasible, as confirmed by the RMS roughness and static contact angle measurements.

Furthermore, the functionalized LA was tested as an initiator for the anionic ring-opening polymerization of epoxides. Ethylene oxide was studied as an important representative of this class of monomers and the reaction conditions were investigated. The full deprotonation with DPMK in THF and the polymerization at room temperature for seven days gave satisfactory products. However, the synthesis of high molecular weight polymers was difficult and the achieved polydispersities were in the range of 1.24 to 1.5. Successful successful initiation was proven by MALDI-ToF MS. The detected molecular masses corresponded to PEG initiated by the modified lipoic acid. The obtained functionalized polyethers were used to coat different gold surfaces. The citrate linker exchange on aqueous Au NPs was investigated via UV-vis spectroscopy. A transfer to organic solution was not possible due to of the good water-solubility of PEG. This consideration was used to change the surface characteristic of gold surfaces. After the adsorption of disulfide-functionalized PEG onto gold supports, the surface was hydrophilic with a good wettability for water, which was confirmed by static contact angle measurements. Additionally, the surface topography of the modified substrates was investigated by AFM measurements.

In summary, an straithforward synthesis of a new initiator with a dithiolane function has been introduced. The use of this initiator enabled the synthesis of tailored polymers with a disulfide anchoring group, which can be used for various applications such as surface modification. The successful polymerization was confirmed at least for two classes of monomers: epoxides and lactones.

The synthesis was in some cases limited to molecular weights up to 2000 $g \cdot mol^{-1}$. However, for most applications, such as surface attachment, the obtained molecular weights are sufficient.

5.7 Experimental

5.7.1 Materials

The aqueous gold nanoparticle solution was obtained according to a described procedure.[72] The size of the gold nanoparticles were controlled by measurement of Z-average. For the preparation of gold substrates the protocol for template-stripped gold was used.[238] The synthesis of diphenylmethyl potassium (DPMK) by the reaction of potassium naphthalenide and diphenylmethane in THF was described before.[360] THF was distilled from sodium under nitrogen. MN silica gel 60 M with a mesh size of 230-400 was purchased from Macherey-Nagel GmbH & Co. KG. Absolut toluene stored over molecular sieve was commercially available from Sigma Aldrich Germany. The used deuterated solvent chloroform-*d* (99.8%) was purchased from Deutero GmbH. All other chemicals were commercially available from Sigma-Aldrich Germany, Acros or Fluka and used as received, unless otherwise noted. The analytical data are shown on the basis of one example per class of polymers.

5.7.2 *N*-(5-hydroxypentyl)-5-(1,2-dithiolan-3-yl)pentamide (**26**)

1 g DCC (4.8 mmol, 1 eq) and 0,05 g DMAP dissolved in 10 ml dichloromethane were slowly added to a stirred solution of 1 g (4.8 mmol, 1 eq) lipoic acid dissolved in 10 ml dichloromethane under argon. After 20 minutes 0,5 g (4.8 mmol, 1 eq) 5-aminopentan-1-ol dissolved in 5 ml dichloromethane was slowly added and the reaction mixture was stirred for 16 hours under argon. The reaction mixture was filtered and the solvent was nearly completely removed at a rotary evaporator (please note: the complete removal led to an insoluble fraction). The crude product was purified by column chromatography on silica gel with ethyl acetate / methanol (95:5) (R_f = 0.25).

Characterization:

Yield: 68%; m.p.: 50.5 °C; FD-MS: m / z = 291.4 (100%) [M^+]; FT-IR (on ATR crystal) [in cm^{-1}]: 3302, 2934, 2859, 1626, 1541, 1041. ^{1}H NMR (400 MHz, $CDCl_3$-*d*): δ (ppm) = 5.62 (s, 1 H, -CO-N**H**-); 3.64 (t, 2 H, -**CH$_2$**-OH); 3.60-3.53 (m, 1 H, -S-**CH**-[CH_2]$_2$-); 3.28-3.23 (m, 2 H, -NH-**CH$_2$**-CH_2-); 3.19-3.08 (m, 2 H, -S-**CH$_2$**-CH_2-); 2.49-2.42 (m, 1 H, diastereotopic H, -S-CH_2-**CH$_2$**-CH-); 2.19-2.14 (t, 2 H, -CH_2-**CH$_2$**-CO-); 1.94-1.86 (m, 1 H, diastereotopic H, -S-CH_2-**CH$_2$**-CH-); 1.81 (s, 1 H, -CH_2-**OH**); 1.72-1.38 (m, 12 H, -CH-**CH$_2$-CH$_2$-CH$_2$**-CH_2-CO, -CH_2-**CH$_2$-CH$_2$-CH$_2$**-CH_2-OH). ^{13}C-NMR (75.5 MHz, $CDCl_3$-*d*): δ (ppm) = 172.80 (-**CO**-NH-); 62.58 (-**CH$_2$**-OH); 56.49 (-S-**CH**-[CH_2]$_2$-); 40.27 (-S-CH_2-**CH$_2$**-CH-); 39.35 (-CH_2-**CH$_2$**-CO-); 38.49 (-S-**CH$_2$**-CH_2-); 36.55 (-NH-**CH$_2$**-CH_2-); 34.63, 32.18, 29.43, 28.92, 25.45, 23.05 (-CH-**CH$_2$-CH$_2$-CH$_2$**-CH_2-CO, -CH_2-**CH$_2$-CH$_2$-CH$_2$**-CH_2-OH).

5.7.3 General protocol for poly-(*L*-lactide) initiated with *N*-(5-hydroxypentyl)-5-(1,2-dithiolan-3-yl) pentamide (**27**)

In a typical experiment, 1 eq *N*-(5-hydroxypentyl)-5-(1,2-dithiolan-3-yl)pentamide (**26**), 2 eq DMAP and 7-20 eq *L*-lactide were charged into a Schlenk flask equipped with a magnetic stir bar and closed with a rubber septum. The reaction vessel was evacuated three times under high vacuum and purged again with argon. Subsequently, 10 ml absolute toluene were added and the reaction mixture was stirred under argon at 60°C for 16 hours. The solvent was completely removed and the raw product was dissolved in 2-5 ml dichloromethane. The crude polymer was precipitated into methanol or a mixture of cold diethyl ether and petroleum ether (3:1) (for polymers with < 1500 $g \cdot mol^{-1}$) and dried in vacuum.

Characterization:

Yield: 34-66%; FT-IR (on ATR crystal) [in cm^{-1}]: 2997, 2945, 1747, 1651, 1539, 1455, 1383, 1181, 1128, 1090, 1043. ^{1}H NMR (400 MHz, $CDCl_3$-*d*): δ (ppm) = 5.50 (s, -CO-N**H**-); 5.24-5.08 (m, **-CH-** PLLA chain); 4.38-4.32 (m, PLLA-**OH**); 4.13 (t, -**CH_2**-O-PLLA); 3.60-3.53 (m, -S-**CH**-$[CH_2]_2$-); 3.29-3.19 (m, -NH-**CH_2**-CH_2-); 3.19-3.08 (m, -S-**CH_2**-CH_2-); 2.49-2.42 (m, diastereotopic H, -S-CH_2-**CH_2**-CH-); 2.16 (t, -CH_2-**CH_2**-CO-); 1.94-1.86 (m, diastereotopic H, -S-CH_2-**CH_2**-CH-); 1.74-1.62 (m, -CH-**CH_2-CH_2-CH_2**-CH_2-CO, -CH_2-**CH_2-CH_2-CH_2**-CH_2-O-), 1.60-1.54(m, -**CH_3**- PLLA chain). ^{13}C-NMR (75.5 MHz, $CDCl_3$-*d*): δ (ppm) = 175.03 (-**CO**-NH-); 1.69.54 (-**CO**- PLLA chain); 68.95, 66.63 (**-CH-** PLLA chain); 65.19 (-**CH_2**-O-PLLA); 56.37 (-S-**CH**-$[CH_2]_2$-); 40.20 (-S-CH_2-**CH_2**-CH-); 39.13 (-CH_2-**CH_2**-CO-); 38.40 (-S-**CH_2**-CH_2-); 36.39 (-NH-**CH_2**-CH_2-); 34.56, 29.14, 28.84, 28.06, 25.35, 23.00 (-CH-**CH_2-CH_2-CH_2**-CH_2-CO, -CH_2-**CH_2-CH_2-CH_2**-CH_2-O-); 20.45, 16.59 (-**CH_3**- PLLA chain).

5.7.4 General protocol for poly-(ethylene oxide) initiated with *N*-(5-hydroxypentyl)- 5-(1,2-dithiolan-3-yl)pentamide (**28**)

In a typical experiment, a suspension of 1 eq *N*-(5-hydroxypentyl)-5-(1,2-dithiolan-3-yl)pentamide (**26**) in benzene was charged into a Schenk flask and evacuated for 24 hours at room temperature. The initiator was dissolved by addition of 20 ml THF, which was freshly distilled from sodium, via cryo transfer. 1 eq of DPMK (0.5 M in THF) was introduced via a cannula and the reaction was stirred for 30 minutes. 15-36 eq ethylene oxide were first cryo transferred to a graduated ampule and subsequently into the Schenk flask with the deprotonated initiator. The polymerization was conducted in vacuum at room temperature for 7 days. The polymerization was terminated by the addition of methanol and acidic ion-exchange resin (Dowex 50WX8, 200-400 mesh). After filtration, the crude polymer was precipitated twice in ice-cold diethyl ether and dried in vacuum.

Characterization:

Yield: 25-61%; FT-IR (on ATR crystal) [in cm^{-1}]: 3478, 2863, 1640, 1455, 1348, 1294, 1248, 1099. ^{1}H NMR (400 MHz, $CDCl_3$-*d*): δ (ppm) = 5.14 (s, -CO-N**H**-); 3.77-3.59 (m, -**CH_2-CH_2**-O- PEG chain); 3.50-3.41 (m, -**CH_2**-O-PEG, -S-**CH**-$[CH_2]_2$-); 3.31-3.27 (m, -NH-**CH_2**-CH_2-); 3.25-3.19 (m, -S-**CH_2**-CH_2-); 2.72-2.63 (-S-CH_2-**CH_2**-CH-); 2.15 (t, -CH_2-**CH_2**-CO-); 1.64-1.25 (m, -CH-**CH_2-CH_2-CH_2**-CH_2-CO, -CH_2-**CH_2-CH_2-CH_2**-CH_2-O-). ^{13}C-NMR (75.5 MHz, $CDCl_3$-*d*): δ (ppm) = 172.80 (-**CO**-NH-); 72.56 (-**CH_2**-**CH_2**-OH); 71.09-69.94 (-**CH_2**-**CH_2**-O- PEG chain); 61.35 (-**CH_2**-**CH_2**-OH); 39.19 (-CH_2-**CH_2**-CO-); 36.34 (-S-**CH_2**-CH_2-); 34.77 (-NH-**CH_2**-CH_2-); 32.89, 31.34, 29.74-29.15, 26.66, 25.56 (-CH-**CH_2-CH_2-CH_2**-CH_2-CO, -CH_2-**CH_2-CH_2-CH_2**-CH_2-O-).

5.7.5 General protocol for the adsorption of polymers with a lipioc acid anchoring group

5.7.5.1 Adsorption of polymers with a lipioc acid anchoring group onto Au NPs

5 ml of the aqueous gold particle solution was extracted with 5 ml polymer solution (1 $mg \cdot ml^{-1}$ in dichloromethane or toluene) via shaking at a frequency of 500 min^{-1} at room temperature for 60 minutes. Immediately after this time the water phase as well as the organic phase were characterized using a UV-vis spectrometer.

5.7.5.2 Adsorption of polymers with a lipioc acid anchoring group onto bare gold substrates

A bare template-stripped gold substrate was dipped in polymer solution (1 $mg \cdot ml^{-1}$) in dichloromethane at room temperature for 15 minutes to 30 minutes. The substrates were rinsed 10 times with dichloromethane, dried under argon stream and stored under argon atmosphere until the AFM and static contact angle measurements.

5.8 References

(246) Safety data sheet: DL-alpha-Liponsäure from Sigma-Aldrich.com retrieved on May 14, 2012
(247) Singh, U.; Jialal, I.; *Nutrition Reviews* **2008**, *66*, 646.
(248) Smith, A. R.; Shenvi, S. V.; Widlansky, M.; Suh, J. H.; Hagen, T. M.; *Current Medicinal Chemistry* **2004**, *11*, 1135.
(249) Reed, L. J.; DeBusk, B. G.; Gunsalus, I. C.; Hornberger Jr., C. S.; *Science* **1951**, *114*, 93.
(250) *Biochemie 5. Auflage* (Berg, J. M.; Tymoczko, J. L.; Stryer, L.) *Spektrum Akademischer Verlag GmbH*, Heidelberg · Berlin, Deutschland, Kapitel 17, 509.
(251) Valko, M.; Morris, H.; Cronin, M. T.; *Current Medicinal Chemistry* **2005**, *12*, 1161.
(252) Suh, J. H.; Moreau, R.; Heath, S. H.; Hagen, T. M.; *Redox Report* **2005**, *10*, 52.
(253) Maczurek, A.; Hager, K.; Kenklies, M.; Sharman, M.; Martins, R.; Engel, J.; Carlson, D. A.; Münch, G.; *Advanced Drug Delivery Reviews* **2008**, *60*, 1463.
(254) Halıcı, M.; İmik, H.; Koç, M.; Gümüş, R.; *Animal Physiology and Animal Nutrition* **2012**, *96*, 408.
(255) Koga, H.; Hagiwara, S.; Kusaka, J.; Goto, K.; Uchino, T.; Shingu, C.; Kai, S.; Noguchi, T.; *Journal of Surgical Research* **2012**, *174*, 352.
(256) Zheng, M.; Zhong; Y.; Meng, F.; Peng, R.; Zhong, Z.; *Molecular Pharmaceutics* **2011**, *8*, 2434.
(257) Bienvenu, C.; Greiner, J.; Vierling, P.; Di Giorgio, C.; *Tetrahedron Letters* **2010**, *51*, 3309.
(258) Thomas, R. C.; Reed, L. J.; *Journal of the American Chemical Society* **1956**, *78*, 6148.
(259) Kisanuki, A.; Kimpara, Y.; Oikado, Y.; Kado, N.; Matsumoto, M.; Endo, K.; *Journal of Polymer Science: Part A: Polymer Chemistry* **2010**, *48*, 5247.
(260) Endo, K.; Yamanaka, T.; *Macromolecules* **2006**, *39*, 4038.
(261) Endo, K.; Yamanaka, T.; *Polymer Journal* **2007**, *39*, 1360.
(262) Volkert, A. A.; Subramaniam, V.; Ivanov, M. R.; Goodman, A. M.; Haes, A. J.; *ACS Nano* **2011**, *5*, 4570.
(263) Tappura, K.; Vikholm-Lundin, I.; Albers, W. M.; *Biosensors and Bioelectronics* **2007**, *22*, 912.
(264) Wang, Y.; El-Boubbou, K.; Kouyoumdjian, H.; Sun, B.; Huang, X.; Zeng, X.; *Langmuir* **2010**, *26*, 4119.
(265) Kunze, J.; Leitch, J.; Schwan, A. L.; Faragher, R. J.; Naumann, R.; Schiller, S.; Knoll, W.; Dutcher, J. R.; Lipkowski, J.; *Langmuir* **2006**, *22*, 5509.
(266) Kim, K.; Yang, H.; Jon, S.; Kim, E.; Kwak, J.; *Journal of the American Chemical Society* **2004**, *126*, 15368.
(267) Zhang, S.; Echegoyen, L.; *Tetrahedron* **2006**, *62*, 1947.
(268) Zhang, S.; Echegoyen, L.; *Journal of Organic Chemistry* **2005**, *70*, 9874.
(269) Zhang, S.; Song, F.; Echegoyen, L.; *European Journal of Organic Chemistry* **2004**, *2004*, 936.
(270) Zhang, S.; Echegoyen, L.; *Tetrahedron Letters* **2003**, *44*, 9079.
(271) Zhang, S.; Echegoyen, L.; *Organic Letters* **2004**, *6*, 791.
(272) Saha, S.; Johansson, E.; Flood, A. H.; Tseng, H.-R.; Zink, J. I.; Stoddart, J. F.; *Chemistry – A European Journal* **2005**, *11*, 6846.
(273) Brough, B.; Northrop, B. H.; Schmidt, J. J.; Tseng, H.-R.; Houk; K. N.; Stoddart, J. F.; Ho, C.-M.; *Proceedings of the National Academy of Sciences* **2006**, *103*, 8583.
(274) Lui, Y.; Flood, A. H.; Bonvallet, P. A.; Vignon, S. A.; Northrop, B. H.; Tseng, H.-R.; Jeppesen, J. O.; Huang, T. J.; Brough, B.; Baller, M.; Magonov, S.; Solares, S. D.; Goddard, W. A.; Ho, C.-M.; Stoddard, J. F.; *Journal of the American Chemical Society* **2005**, *127*, 9745.
(275) Boutin, J. M.; Richer, J.; Tremblay, M.; Bissonette, V.; Voyer, N.; *New Journal of Chemistry* **2007**, *31*, 741.
(276) Walker, A. D.; Gupta, V. K.; *Nanotechnology* **2008**, *19*, 9.
(277) Shim, J.-Y.; Gupta, V. K.; *Journal of Colloid and Interface Science* **2007**, *316*, 977.
(278) Walker, A. D.; Gupta, V. K.; *Journal of Physical Chemistry B* **2001**, *105*, 5223.
(279) Walker, A. D.; Gupta, V. K.; *Thin Solid Films* **2003**, *423*, 228.
(280) Hadjichristidis, N.; Iatrou, H.; Pitsikalis, M.; Sakellariou, G.; *Chemical Reviews* **2009**, *109*, 5528.
(281) Enriquez, E. P.; Gray, K. H.; Guarisco, V. F.; Linton, R. W.; Mar, K. D.; Samulski, E. T.; *Journal of Vacuum Science & Technology A* **1992**, *10*, 2775.
(282) Enriquez, E. P.; Samulski, E. T.; *Materials Research Society Symposium Proceedings* **1992**, *255*, 423.
(283) Dondapati, S. K.; Montornes, J. M.; Sanchez, P. L.; Sanchez, J. L. A.; O'Sullivan C.; Katakis, I.; *Electroanalysis* **2006**, *19-20*, 1879.

(284) Ha, T. H.; Jung, S. O.; Lee, J. M.; Lee, K. Y.; Lee, Y.; Park, J. S.; Chung, B. H.; *Analytical Chemistry* **2007**, *79*, 546.
(285) Han, Y.; Noguchi, H.; Sakaguchi, K.; Uosaki, K.; *Langmuir* **2011**, *27*, 11951.
(286) Liebert, T.; Hussain, M. A.; Tahir, M. N.; Heinze, T.; *Polymer Bulletin* **2006**, *57*, 857.
(287) Siegers, C.; Biesalski, M.; Haag, R.; *Chemistry – A European Journal* **2004**, *10*, 2831.
(288) Calderón, M.; Quadir, M. A.; Sharma, S. K.; Haag, R.; *Advanced Materials* **2010**, *22*, 190.
(289) Albers, W. M.; Munter, T.; Laaksonen, P.; Vikholm-Lundin, I.; *Journal of Colloid and Interface Science* **2010**, *348*, 1.
(290) Urakami, H.; Guan, Z.; *Biomacromolecules* **2008**, *9*, 592.
(291) Meyers, S. R.; Grinstaff, M. W.; *Chemical Review* **2012**, *112*, 1615.
(292) Borrell, M.; Leal, L. G.; *Langmuir* **2007**, *23*, 12497.
(293) Mourato, A.; Viana, A. S.; Montforts, F.-P.; Abrantes, L. M.; *Journal of Solid State Electrochemistry* **2010**, *14*, 1985.
(294) Choi, J.; Choi, H. J.; Jung, D. C.; Lee, J.-H.; Cheon, J.; *Chemical Communications* **2008**, *19*, 2197.
(295) Uyeda, H. T.; Medintz, I. L.; Jaiswal, J. K.; Simon, S. M.; Mattoussi, D.; *Journal of the American Chemical Society* **2005**, *127*, 3870.
(296) Stewart, M. H.; Susumu, K.; Mei, B. C.; Medintz, I. L.; Delehanty, J. B.; Blanco-Canosa, J. B.; Dawson, P. E.; Mattoussi, H.; *Journal of the American Chemical Society* **2010**, *132*, 9804.
(297) Algar, W. R.; Krull, U. J.; *Langmuir* **2008**, *24*, 5514.
(298) Najafabadi, B. K.; Hesari, M.; Workentin, M. S.; Corrigan, J. F.; *Journal of Organometallic Chemistry* **2012**, *703*, 16.
(299) Tokiwa, Y.; Calabia, B. P.; *Applied Microbiology and Biotechnology* **2006**, *72*, 244.
(300) Kricheldorf, H. R.; *Chemosphere* **2001**, *43*, 49.
(301) Auras, R.; Harte, B.; Selke, S.; *Macromolecular Bioscience* **2004**, *4*, 835.
(302) *Biopolymers from Renewable Resources, 1st edition* (Kaplan, D. L.; Hartmann, M. H.) Ed., *Springer-Verlag* Berlin Heidelberg, Berlin 1998, 367.
(303) Lasprilla, A. J. R.; Martinez, G. A. R.; Lunelli, B. H.; Jardini, A. L.; Filho, R. M.; *Biotechnology Advances* **2012**, *30*, 321.
(304) Inkinen, S.; Hakkarainen, M.; Albertsson, A.-C.; Södergård, A.; *Biomacromolecules* **2011**, *12*, 523.
(305) Dechy-Cabaret, O.; Martin-Vaca, B.; Bourissou, D.; *Chemical Review* **2004**, *104*, 6147.
(306) Kamber, N. E.; Jeong, W.; Waymouth, R. M.; Pratt, R. C.; Lohmeijer, B. G. G.; Hedrick, J. L.; *Chemical Review* **2007**, *103*, 5813.
(307) Kricheldorf, H. R.; Dunsig, R.; *Die Makromolekulare Chemie* **1986**, *187*, 1611.
(308) Kricheldorf, H. R.; Kreiser, I.; *Die Makromolekulare Chemie* **1987**, *188*, 1861.
(309) Matsumura, S.; Mabuchi, K.; Toshima, K.; *Macromolecular Rapid Communication* **1997**, *18*, 477.
(310) Kiesewtter, M. K.; Shin, E. J.; Hedrick, J. L.; Waymouth, R. M.; *Macromolecules* **2010**, *43*, 2093.
(311) Oh, J. K.; *Soft Matter* **2011**, *7*, 5096.
(312) *Chemistry and technology of biodegradable polymers* (Albertsson, A. C.; Karlsson, S.) *Blackie*, Glasgow, *7*.
(313) Luckachan, G. E.; Pillai, C. K. S.; *Journal of Polymers and the Environment* **2011**, *19*, 637.
(314) Platel, R. H.; Hodgson, L. M.; Williams, C. K.; *Polymer Reviews* **2008**, *48*, 11.
(315) Cameron, D. J. A.; Shaver, M. P.; *Chemical Society Reviews* **2011**, *40*, 1761.
(316) Darensbourg, D. J.; Karroonnirun, O.; *Macromolecules* **2010**, *43*, 8880.
(317) Aubrecht, K. B.; Grubbs, R. B.; *Journal of Polymer Science: Part A: Polymer Chemistry* **2005**, *43*, 5156.
(318) Yang, D. Lu, Q.; Fan, Z.; Li, S.; Tu, J.; Wang, W.; *Journal of Applied Polymer Science* **2010**, *118*, 2304.
(319) Chrisholm, M. H.; Navarro-Llobet, D.; Simonsick, Jr, W. J.; *Macromolecules* **2001**, *34*, 8851.
(320) Otsuka, H.; Nagasaki, Y.; Kataoka, K.; *Biomacromolecules* **2000**, *1*, 39.
(321) Verma, M. S.; Liu, S.; Chen, Y. Y.; Meerasa, A.; Gu, F. X.; *Nano Research* **2012**, *5*, 49.
(322) Becker, J. M.; Pounder, R. J.; Dove, A. P.; *Macromolecular Rapid Communications* **2010**, *31*, 1923.
(323) Jing, F.; Hillmyer, M. A.; *Journal of the American Chemical Society* **2008**, *130*, 13826.
(324) Song, Y.-S.; Muthuraman, G.; Chen, Y.-Z.; Lin, C.-C.; Zen, J.-M.; *Electroanalysis* **2006**, *18*, 1763.
(325) Qui, H.; Rieger, J.; Gilbert, B.; Jérôme, R.; Jérôme, C.; *Chemistry of Materials* **2004**, *16*, 850.
(326) Hou, X.; Li, Q.; Jia, L.; Li, Y., Zhu, Y.; Cao, A.; *Macromolecular Bioscience* **2009**, *9*, 551.
(327) Sourkohi, B. K.; Cunningham, A.; Zhang, Q.; Oh, J. K.; *Biomacromolecules* **2011**, *12*, 3819.
(328) Pang, Y.; Liu, J. Y.; Su, Y.; Zhu, B. S.; Huang, W.; Zhou, Y. F.; Zhu, X. Y.; Yan, D. Y.; *Science China Chemistry* **2010**, *53*, 2497.

(329) Liu, J.; Pang, Y., Huang, W.; Huang, X.; Meng, L.; Zhu, X.; Zhou, Y.; Yan, D.; *Biomacromolecules* **2011**, *12*, 1567.
(330) Kalarickal, N. C.; Rimmer, S.; Sarker, P.; Leroux, J.-C., *Macromolecules* **2007**, *40*, 1874.
(331) Sun, J.; Chen, X.; Lu, T.; Liu, S.; Tian, H.; Guo, Z.; Jing, X.; *Langmuir* **2008**, *24*, 10099.
(332) Arai, K.; Takayama, K.; Nambu, Y.; Nambu, N.; Ueda, H.; Machida, Y.; Nagai, T.; *Drug Design and Delivery* **1987**, *2*, 109.
(333) Nobs, L.; Buchegger, F.; Gurny, R.; Allémann, E.; *International Journal of Pharmaceutics* **2003**, *250*, 327.
(334) Dingels, C.; Schömer, M.; Frey, H.; *Chemie in unserer Zeit* **2011**, *45*, 338.
(335) Wurtz, M. A.; *Comptes rendus hebdomadaires des séances de l´Académie des sciences* **1859**, *48*, 101.
(336) Thompson, M. S.; Vadala, T. P.; Vadala, M. L.; Lin, Y.; Riffle, J. S.; *Polymer* **2008**, *49*, 345.
(337) Obermeier, B.; Wurm, F.; Mangold, C.; Frey, H.; *Angewandte Chemie Internetional Edition* **2011**, *50*, 7988.
(338) Mizrahi, D. M.; Omer-Mizrahi, M.; Goldshtein, J.; Askinadze, N.; Margel, S.; *Journal of Polymer Science: Part A: Polymer Chemistry* **2010**, *48*, 5468.
(339) Sousa-Herves, A.; Riguera, R.; Fernandez-Megia, E.; *New Journal of Chemistry* **2012**, *36*, 205.
(340) Veronese, F. M.; *Biomaterials* **2001**, *22*, 405.
(341) Duncan, R.; *Nature Reviews* **2003**, *2*, 347.
(342) Wilms, D.; Schömer, M.; Wurm, F.; Hermanns, I.; Kirkpatrick, C. J.; Frey, H.; *Macromolecular Rapid Communications* **2010**, *31*, 1811.
(343) Kissel, T.; Li, Y.; Unger, F.; *Advanced Drug Delivery Reviews* **2002**, *54*, 99.
(344) Eck, W.; Craig, G.; Sigdel, A.; Ritter, G.; Old, L. J.; Tang, L.; Brennan, M. F.; Allen, P. J.; Mason, M. D.; *ACS Nano* **2008**, *2*, 2263.
(345) Bandyopadhyay, K.; Liu, H.; Liu, S.-G.; Echegoyen, L.; *Chemical Communications* **2000**, 141.
(346) Bandyopadhyay, K.; Liu, S.-G.; Liu, H.; Echegoyen, L.; *Chemistry – A European Journal* **2000**, *6*, 4385.
(347) Kim, J.-H.; Sim, G.-S.; Bae, J.-T.; Oh, J.-Y.; Lee, G.-S.; Lee, D.-H.; Lee, B.-C.; Pyo, H.-B.; *Journal of Pharmacy and Pharmacology* **2008**, *60*, 863.
(348) Dufresne, M.-H.; Gauthier, M. A.; Leroux, J.-C.; *Bioconjugate Chemistry* **2005**, *16*, 1027.
(349) Lakanathan, S. R.; Zhang, S.; Regina, V. R.; Cole, M. A.; Ogaki, R.; Dong, M.; Besenbacher, F.; Meyer, R. L.; Kingshott, R.; *Biointerphases* **2011**, *6*, 180.
(350) Stan, G.; DelRio, F. W.; MacCuspie, R.; Cook, R. F.; *Journal of Physical Chemistry B* **2012**, *116*, 3138.
(351) Yeh, P.-Y. J.; Kainthan, R. K.; Zou, Y.; Chiao, M.; Kizhakkedathu, J. N.; *Langmuir* **2008**, *24*, 4907.
(352) Kabalka, G. W.; Baker, Jr., J. D.; Neal, G. W.; *Journal of Organic Chemistry* **1977**, *42*, 512.
(353) Pargen, S.; Omeis, J.; Jaunky, G.; Keul, H.; Möller, M.; *Macromolecular Chemistry and Physics* **2011**, *212*, 1791.
(354) Dougan, J. A.; Reid, A. K.; Graham, D.; *Tetrahedron Letters* **2010**, *51*, 5787.
(355) Sarasua, J.-R.; Prud'homme, R. E.; Wisniewski, M.; Le Borgne, A.; Spassky, N.; *Macromolecules* **1998**, *31*, 3895-3905.
(356) Safety data sheet: *tert*-Butanol from Sigma-Aldrich.com retrieved on June 2, 2012.
(357) Wada, N.; Wakami, H.; Konishi, T.; Matsugo, S.; *Journal of Clinical Biochemistry and Nutrition* **2009**, *44*, 218.
(358) Lin, C.-A. J.; Yang, T.-Y.; Lee, C.-H.; Huang, S. H.; Sperling, R. A.; Zanella, M.; Li, J. K.; Shen, J.-L.; Wang, H.-H.; Yeh, H.-I.; Parak, W. J.; Chang, W. H.; *ASC Nano* **2009**, *3*, 395.
(359) Abad, J. M.; Mertens, S. F. L.; Pita, M.; Fernández, V. M.; Schiffrin, D. J.; *Journal of the American Chemical Society* **2005**, *127*, 5689.
(360) Francis, R.; Taton, D.; Logan, J. L.; Masse, P.; Gnanou, Y.; Duran, R. S.; *Macromolecules* **2003**, *36*, 8253.
(361) *Biochemie 1. Auflage* (Müller-Esterl, W. et al.) *Elsevier GmbH*, München, *Spektrum Akademischer Verlag GmbH*, Deutschland, Kapitel 36, 500.

Chapter 6

Combining Polysulfides with Polyesters to Degradable Copolymers

Combining Polysulfides with Polyesters to Block Copolymers[♦,*]

ABSTRACT: A new type of block copolymer composed of poly(propylene sulfide) and poly(lactide) was synthesized. Propylene sulfide was polymerized and terminated with 2-bromoethanol to gain a hydroxyl functionality at the end of the polysulfide backbone. Subsequently, *L*- or *D*-lactide was reacted via 1,8-diazabicyclo[5.4.0]undec-7-ene (DBU)-catalyzed ring-opening polymerization. The synthesized copolymers with different molar content of poly(lactide) were characterized with size exclusion chromatography (SEC), nuclear magnetic resonance spectroscopy (NMR) and differential scanning calorimetry (DSC). Furthermore the adhesion to gold was investigated. Both gold nanoparticles as well as flat gold substrates were coated with the sulfur-containing copolymer and analyzed via UV-vis spectroscopy and atomic force microscope (AFM).

Poly(lactide) (PLA) is a biocompatible and biodegradable polymer.[362] It has been incorporated in various copolymers for example with poly(ε-caprolactone) (PCL)[363], poly(glycolide) (PGA)[364], poly(ethylene glycol) (PEG)[365], poly(allyl glycidyl ether) (PAGE)[366] and poly(propylene oxide) (PPO)[367]. PLA copolymers have been successfully employed in numerous biomedical and pharmaceutical applications like in drug delivery systems and implants for bone fixation.[362]

The sulfur-analog of PPO, poly(propylene sulfide) (PPS) has been used for copolymer structures, mostly in copolymers with PEG.[368-370] The amphiphilic structures of these copolymers are well-characterized, for example with regard to the aggregation behavior in aqueous media, which leads to potential applications for drug delivery.[371-373] Furthermore, different architectures of these species were characterized via polarized light optical microscopy (POM) to investigate the hydration of polymer films.[374,375] In addition, the attraction between sulfur and gold was used to coat surfaces with these poly(thioethers) and the adsorption of proteins has been explored[376-378] In a recent work the synthesis of triblock copolymers of PEG, PPS and poly(ethylene imine) (PEI) was reported.[379] In all approaches mentioned, the copolymer structure is achieved by post-polymerization modification. The first strategy pursues the use of a polymer-based macroinitiator for the anionic ring-opening polymerization of propylene sulfide. The second strategy uses a polymer-based end-capping reagent to terminate the living PPS chain. The combination of both methods leads to triblock copolymers.

Here we describe a novel approach, wherein the living PPS chain is end-capped with 2-bromoethanol to introduce a hydroxyl functionality at the end of the polysulfide backbone, which can be addressed directly in the DBU-catalyzed polymerization of *L*- or *D*-lactide. To our knowledge, it is the first approach that uses PPS as a macroinitiator. This synthetic strategy leads to tailored copolymers with adjustable block length through the monomer to initiator ratio. The composition of PPS and PLA leads to sensitive copolymers under different conditions. In case of PLA the polymer is completely degradable under enzymatic and hydrolytic conditions[380] through cleavage of the polyester backbone. In contrast, the sulfur atoms of the PPS polymer backbone are oxidation sensitive and have been oxidized to sulfoxides[381], which leads to hydrophilic materials properties. The former hydrophobic polymer is then enabled to swell in water.

A protected thiol acted as an initiator for the anionic ring-opening polymerization of propylene sulfide, namely benzyl thioacetate **1**. As described elsewhere,[369] the reaction is carried out in degassed THF under

♦ This chapter was developed in cooperation with Dipl. Chem. Anna Fischer

* *ACS Macro Letters*: in preparation

argon atmosphere with tributylphosphine as a reducing agent and an *in-situ* deprotection of the thioacetate in basic media. Subsequent to the polymerization, the termination reaction is performed in acetic acid and DBU buffered solution. The reaction between a thiol and an aliphatic bromo substituted alcohol has previously been described for small molecules under basic conditions and as termination reaction for poly(propylene sulfide) star polymers.[382,383]

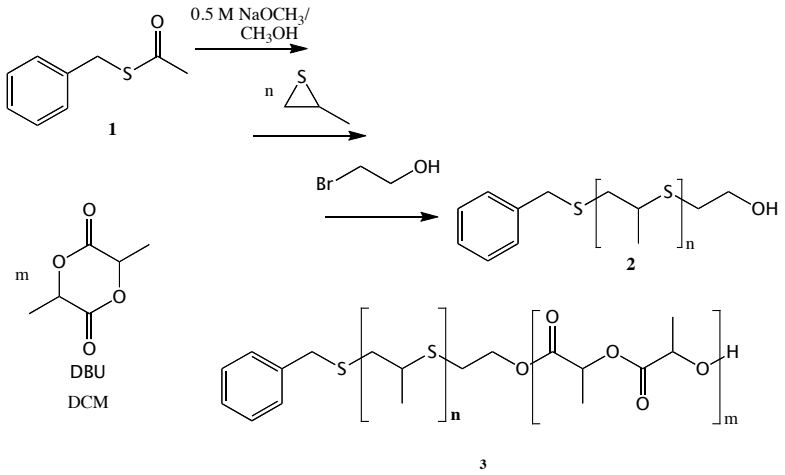

Figure 6.1. Synthesis of the poly(propylene sulfide)-*block*-poly(lactide) copolymers in a two step protocol.

In the present work we achieved an end-capping yield of the polymers **2** exceeding 85mol%, in most cases even exceeding 90mol%. We used an excess of DBU before 2-bromoethanol was added. The end-capping yield was calculated via the ratio of the ^{1}H NMR signals of the methylene group next to the benzene ring of the initiator at 3.77 ppm and the methylene group of the terminating agent adjacent to the hydroxyl function at 3.52 ppm. The infrared (IR) spectra of the synthesized PPS polymers show an adsorption band at 3463 cm^{-1}, which is typical for a hydroxyl functionality. This result confirms the successful termination reaction of the polysulfide with 2-bromoethanol and thereby the introduction of a hydroxyl group at the end of the polymer. The polymers **2** have also been characterized with size exclusion chromatography (SEC). The polydispersity index (PDI) is below 1.25 for all samples, and, as expected for a controlled anionic ring-opening polymerization the mass distribution is monomodal and narrow.

After purification of the first block, these polymers were used as PPS-based macroinitiators for the ROP of poly(lactide). In a second step *L*- or *D*-lactide was reacted in a DBU-catalyzed ring-opening polymerization in dichloromethane to synthesize the PPS-*b*-PLA copolymers **3**.[384] **Table 6.1** summarizes the results of the synthesis of PPS-PLA block copolymers **3**. The weight fraction of poly(lactide) was varied between 6 and 79 weight percent (wt%). The degree of polymerization (DP) has been calculated via ^{1}H NMR signal ratios of the methylene group next to the benzene ring of the initiator of the PPS block at 3.77 ppm and the signals of the PPS backbone at 2.95-2.77 ppm, 2.67-2.57 ppm plus 1.33-1.30 ppm and accordingly to the signals of the PLA backbone at 5.15 ppm and 1.54-1.44 ppm. The synthesis of the novel copolymers is conducted in a controlled fashion with PDIs below 1.35. **Figure 6.2** shows as an example the SEC traces of one PPS- based macroinitiator and three PPS-*b*-PLLA copolymers. A clear shift between the trace of the macroinitiator and the different copolymer traces to shorter retention times is observed, which indicates successful diblock copolymer formation.

Table 6.1. Characterization data of poly(propylene sulfide)-*b*-poly(lactide) copolymers.

Copolymer	Initiator	Sample	DP PPS[i]/ DP PLA[i]	PLA content [wt%]	M_n[i] NMR [g·mol^{-1}]	M_n[ii] SEC [g·mol^{-1}]	PDI[ii]	Yield [%]
3a	**2e**	PPS-*b*-PLLA	63/2	6	5150	4000	1.15	quan
3b	**2e**	PPS-*b*-PLLA	59/9	23	5850	4400	1.31	71
3c	**2d**	PPS-*b*-PDLA	49/10	28	5250	4900	1.19	67
3d	**2a**	PPS-*b*-PLLA	30/18	54	5000	5800	1.15	68
3e	**2a**	PPS-*b*-PLLA	31/31	66	6950	7400	1.20	55
3f	**2a**	PPS-*b*-PLLA	35/69	79	12700	10800	1.21	60

[i]calculated by ^{1}H NMR, ratio of the CH_2-signal of the initiator (benzyl group) and the PPS backbone signals, accordingly to the PLA backbone. [ii]SEC with chloroform as eluent, calibrated with polystyrene standards.

In the IR spectra an intensive band is found at 1750 cm^{-1}, the band of the carbonyl group of an ester compound. This also confirms polyester formation. Further hints at the proposed structure are given by ^{1}H NMR spectroscopy. The proton signal of the CH_2-group next to the hydroxyl function of the PPS-based macroinitiator is at 3.52 ppm. This signal is shifted to 4.26-4.36 ppm in the NMR spectra of the PPS-*b*-PLA copolymers. The shift occurs due to the ester formation, which clearly demonstrates initiation of the poly(lactide) block by the poly(propylene sulfide) macroinitiator.

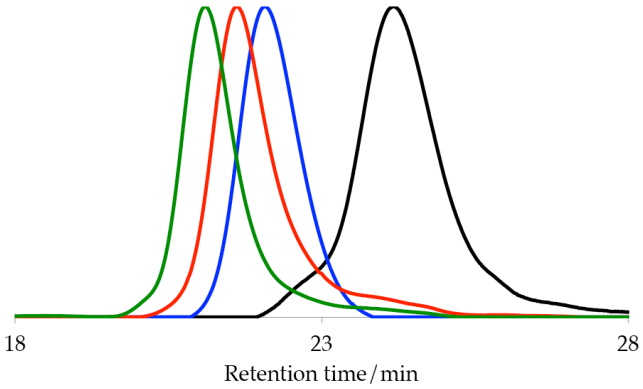

Figure 6.2. SEC traces (RI signal) in chloroform of the initiator (2a, black line) and three PPS-*b*-PLLA copolymers (3d blue line, 3e red line, 3f green line).

The thermal properties of the synthesized PPS-*b*-PLA copolymers **3** were investigated with differential scanning calorimetry. The results are summarized in **Table 6.2**. As a reference one PPS-macroinitiator is also noted. The glass transition temperature (T_g) of the PPS homopolymer is at -48°C, and with increasing PLA content of the copolymers the T_g of the PPS block increases to around -40°C. In the sample with the highest PLA content of 79wt% the T_g of PPS is not observable anymore. This shows the influence of the less flexible poly(lactide) on the thermal behavior of the poly(propylene sulfide). The crystallization of the poly(lactide) block is first detectable with the copolymer **3b** with 23wt% PLA. This structure shows a melting point (T_m) at 110°C. The T_m of PLA also increases with increasing poly(lactide) content up to 137°C, as expected. The melting point of PLLA with 100% optical purity with 169°C is not achieved.[385] Furthermore the degree of crystallization of the poly(lactide) block has been calculated.[386,387] The degree of crystallization rises with increasing PLA content.

Table 6.2. Thermal properties of the PPS-*b*-PLA samples.

Sample	PLA content [wt%]	T_g [i] [°C]	T_m [°C]	dH_m [J g^{-1}]	χ_c [ii] [%]
2c	0	-48	-	-	-
3a	6	-42	-	-	-
3b	23	-41	104	4.5	1.11
3c	28	-40	111	7.8	2.34
3d	54	-38	120	14.2	8.25
3e	66	-41	124	10.4	7.39
3f	79	-	137	14.7	12.49

[i]glass temperature PPS block; [ii]degree of crystallization[386] of the PLA determined via $\chi c = \frac{\Delta H_m}{\Delta H_m^{\infty}} \times f_w^{LA}$ with $\Delta H_m^{\infty} = 93\ J\ g^{-1}$

The attraction between sulfur and gold can be used to coat poly(propylene sulfide) containing polymers to the gold surfaces and gold nanoparticles. The adsorption of the PPS-*b*-PLA copolymers to bare template-stripped gold (TSG) substrates has been demonstrated to be successful. The static contact angle of a water droplet on the polymer coated surface with about 70° differs from the contact angle of the bare substrate with 88°, which is used as a reference. The reference sample has been equally processed, but was been dipped in dichloromethane instead of a polymer solution to exclude any influence by the used solvent.
The surface topography of the coated-gold substrates has been investigated via AFM measurements. **Figure 6.3** shows AFM height and phase images of a polymer-coated gold support.

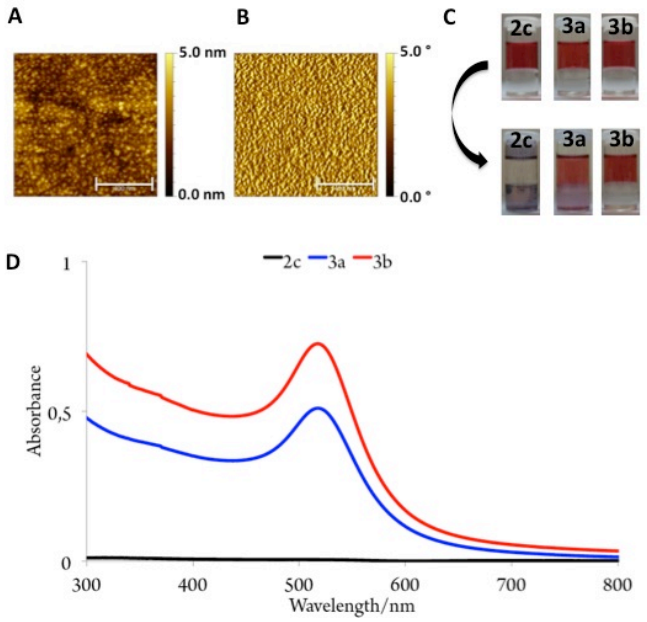

Figure 6.3. (A) AFM height image of copolymer **3d** on a gold substrate (scale bar 400 nm) (B) AFM phase image of copolymer **3d** on a gold substrate (scale bar 400 nm) (C) photographs of the gold nanoparticle extraction (D) UV-vis adsorption of the aqueous solutions of gold nanoparticle extraction.

The surface structure of the coated substrate is significantly different compared to the surface topology of the bare gold reference. The comparison of the phase contrast of the reference and the coated supports shows similar results. In addition, the root mean square (RMS) roughness of the height images was

calculated. The RMS roughness describes the standard deviation of the surface height and is a common value to determinate the roughness of a surface.[388] The RMS roughness (1 x 1 μm^2) of the TSG amounted about 0.3 nm, which is used as reference. The values of the polymer-coated surfaces were slightly higher with 0.4 nm and 0.5 nm respectively, but it was in the range of the measurement error. Hence, it is assumed, that the copolymer recreated the relatively flat surface structure of the TSG. However, the gold surfaces were not in all cases completely covered by the PPS-*b*-PLA copolymers. In a further approach the copolymers were employed for the surface modification of citrate-stabilized gold nanoparticles.[389] The aqueous gold nanoparticle solution was extracted with a polymer solution in dichloromethane. **Figure 6.3** illustrates photographs of the different solutions before extraction and afterwards. The PPS macroinitiator **2c** acts as a reference (i.e. 0wt% PLA) and the copolymers with 6wt% (**3a**) and 23wt% (**3b**) poly(lactide) content is are shown. It is clearly observable that only the PPS homopolymer capable of removing the red colored gold nanoparticles from the water phase. This observation was investigated with UV-vis spectroscopy in more detail. The results are shown in the **Figure 6.3** as well. In case of the macroinitiator no absorbance remains in the water phase, which means the gold nanoparticles are removed completely from the aqueous solution. The copolymer **3a** with a content of 6wt% of PLA is capable of transferring a fraction of gold nanoparticles, indicated through the partially reduced absorbance of the water phase. All other copolymer samples with higher poly(lactide) content as 6wt% are not able to bind to the gold nanoparticles and extract them from the aqueous solution. This suggests that the PLA block prevents the binding of the polysulfide block to gold nanoparticles. We tentatively ascribe this to shielding of the PPS block by PLA, considering that the sulfur atoms of the PPS cannot interact with the gold surface of the gold nanoparticles in the water phase.

In summary, the successful synthesis of hydroxyl-terminated poly(propylene sulfide) with narrow molecular mass distribution has been presented. In a second step the PPS was shown to act as a macroinitiator for the ring-opening polymerization of *D*- or *L*-lactide to form a novel type of copolymer in a controlled manner. The proposed structures of the samples were confirmed by NMR spectroscopy, DSC and IR spectroscopy. Furthermore the adsorption to gold substrates and gold nanoparticles was analyzed with AFM and UV-vis spectroscopy. The adsorption of the copolymers from dichloromethane solutions to gold supports was demonstrated, as shown via static contact angle and AFM measurements. In case of the gold nanoparticles the adhesion of the PPS block was impeded by larger PLA blocks. For PPS-PLA block copolymers in dichloromethane with higher molar content than 6wt% poly(lactide) the binding to gold nanoparticles in aqueous solution is not viable.

REFERENCES

(362) Oh, J. K.; *Soft Matter* **2011**, *7*, 5096-5108.
(363) Darensbourg, D. J.; Karroonnirun, O.; *Macromolecules* **2011**, *43*, 8880-8886.
(364) Kricheldorf, H. R.; Kreiser, I.; *Makromolekulare Chemie* **1987**, *188*, 1861-1873.
(365) Zhu, K. J.; Xiangzhou, L.; Shilin, Y.; *Journal of Applied Polymer Science* **1990**, *39*, 1-9.
(366) Hu, Z.; Fan, X.; Wang, H.; Wang, J.; *Polymer* **2009**, *50*, 4175-4181.
(367) Chisholm, M. H.; Navarro-Llobet, D.; *Macromolecules* **2001**, *34*, 8851-8857.
(368) Napoli, A.; Tirelli, N.; Kilcher, G.; Hubbell, J. A.; *Macromolecules* **2001**, *34*, 8913-8917.
(369) Wang, L.; Kilcher, G.; Tirelli, N.; *Macromolecular Bioscience* **2007**, *7*, 987-998.
(370) Domb, A.; Avny, Y.; *Journal of Applied Polymer Science* **1984**, *29*, 2517-2528.
(371) Cerritelli, S.; Fontana, A.; Velluto, D.; Adrian, M.; Dubochet, J.; De Maria, P.; Hubbell, J.A.; *Macromolecules* **2005**, *38*, 7845-7851.
(372) Cerritelli, S.; O´Neil, C. P.; Velluto, D.; Fontana, A.; Adrian, M.; Dubochet, J.; Hubbell, J. A.; *Langmuir* **2009**, *25*, 11328-11335.

(373) O´Neil, C. P.; van der Vlies, A. J.; Velluto, D.; Wandrey, C.; Demurtas, D.; Dubochet, J.; Hubbell, J. A.; *Journal of Controlled Release* **2009**, *137*, 146-151.
(374) Napoli, A.; Tirelli, N.; Wehrli, E.; Hubbell, J. A.; *Langmuir* **2002**, *18*, 8324-8329.
(375) Wang, L.; Hu, P.; Tirelli, N.; *Polymer* **2009**, *50*, 2863-2873.
(376) Bearinger, J. P.; Stone, G.; Hiddessen, A. L.; Dugan, L. C.; Wu, L.; Hailey, P.; Conway, J. W.; Kuenzler, T.; Feller, L.; Cerritelli, S.; Hubbell, J. A.; *Langmuir* **2009**, *25*, 1238-1244.
(377) Bearinger, J. P.; Terrettaz, S.; Michel, R.; Tirelli, N.; Vogel, H.; Textor, M.; Hubbell, J. A.; *Nature Materials* **2003**, *2*, 259-264.
(378) Feller, L.; Bearinger, J. P.; Wu, L.; Hubbell, J. A.; Tosatti, S.; *Surface Science* **2008**, *602*, 2305-2310.
(379) Velluto, D.; Thomas, S. N.; Simeoni, E.; Schwartz, M. A.; Hubbell, J. A.; *Biomaterials* **2011**, *32*, 9839-9847.
(380) Tokiwa, Y.; Calabia, B. P.; *Applied Microbiology and Biotechnology* **2006**, *72*, 244-251.
(381) Vo, C. D.; Kilcher, G.; Tirelli, N.; *Macromolecular Rapid Communications* **2009**, *30*, 299-315.
(382) Dzhafarov, I. A.; Mamedbeili, E. G.; Kyazimova, T. G.; Gasanov, Kh. I.; Suleimanova, E. I.; *Russian Journal of Applied Chemistry* **2010**, *5*, 854-857.
(383) Nicol, E.; Bonnans-Plaisance, C.; Dony, P.; Levesque, G.; *Macromolecular Chemistry and Physics* **2001**, *202*, 2843.
(384) Kamber, N. E.; Jeong, W.; Waymouth, R. M.; Pratt, R. C.; Lohmeijer, B. G. G.; Hedrick, J. L.; *Chemical Reviews* **2007**, *107*, 5813-5840.
(385) Sarasua, J.-R.; Prud'homme, R. E.; Wisniewski, M.; Le Borgne, A.; Spassky, N.; *Macromolecules* **1998**, *31*, 3895-3905.
(386) Rathi, S.; Kalish, J. P.; Coughlin, E. B.; Hsu, S. L.; *Macromolecules* **2011**, *44*, 3410-3415.
(387) Wanamaker, C. L.; Tolman, W. B.; Hillmyer, M. A.; *Macromolecular Symposia* **2009**, *283-284*, 130-138.
(388) Gadelmawla, E. S.; Koura, M. M.; Maksoud, T. M. A.; Elewa, I. M.; Soliman, H. H.; *Journal of Materials Processing Technology* **2002**, *123*, 133.
(389) Porta, F.; Speranza, G.; Krpetić, Ž.; Santo, V. D.; Francescato, P.; Scarì, G.; *Materials Science and Engineering B* **2007**, *140*, 187-194.

6.1 Supporting Information

Experimental Section

Materials and Instrumentation

All chemicals are commercially available from *Sigma-Aldrich Germany*, *Acros* or *Fluka* and were used as received, unless otherwise noted. Tetrahydrofuran (THF) was degassed via five cycles of freeze-pump-thaw. Dichloromethane (DCM) was stored over molecular sieve. 1,8-Diazabicyclo[5.4.0]undec-7-ene (DBU) was dried over calcium hydride and freshly distilled prior to use. The deuterated solvents (dimethyl sulfoxide-d_6 and chloroform-d) were purchased from *Deutero GmbH*. Benzyl thioacetate (**1**) was synthesized as described elsewere.[390] Gold nanoparticles (20 nm) in aqueous solution were synthesized accordingly to the literature.[391] Flat gold substrates were produced via the template stripped gold methode.[392]

The nuclear magnetic resonance spectra (NMR) were recorded on a *Bruker* spectrometer at a frequency of 300 MHz for the proton spectra and the carbon spectra were recorded at 75.5 MHz. All spectra were referred to an internal standard (the proton signal of the deuterated solvents). FT-IR spectra were recorded using a *Thermo Scientific* (Nicolet iS10) spectrometer. For the characterization of the substances only the typical and intensive bonds are given. The size exclusion chromatography (SEC) was performed in chloroform with 1 $ml \cdot min^{-1}$ on a set of three *PSS SDV* columns (10^4/500/50 Å) connected to a RI and an UV detector as well as a *waters 717 plus* auto sampler and a *TSP Spectra Series P 100* pump. A polystyrene standard calibration was used. For the measurements of thermal properties a *Perkin Elmer* DSC 8500, calibrated with indium, in a temperature range from -95°C to 180°C and a heating rate of 10 K per minute was used. The UV-vis spectra were measured on a *Jasco* V-630 Spectrophotometer at 20°C. Static water contact angles were measured on a *data physics* OCA 20 with SCA 20 software. A droplet of deionized water was placed on the surface of the substrate and imaged via a video camera. The contact angle was calculated via software. This procedure was repeated 10 times on different positions of the substrate. The AFM measurements are carried out on a *Veeco* NanoScope Dimension 3100 in tapping mode with silicon cantilevers with a resonance frequency of 300 kHz, a spring constant of 42 $N \cdot m^{-1}$ and a tip height of 11 μm. The data were collected with Nanoscope 5.31r1 and Gwyddion 2.25 was used to analyze the AFM height and phase images as well as the determination of the RMS roughness.

Synthesis of poly(propylene sulfide) with one terminal hydroxyl function (2)

In a typical experiment the reaction vessel was evacuated three times under high vacuum and purged again with argon. 5 ml of degassed THF were added to the reaction flask and benzyl thioacetate **(1)** in 1 ml THF was added. Then 5 equiv tributylphosphine (TBP) in 1 ml THF and 1.05 equiv sodium methoxide solution (0.5 M in methanol) in 1 ml of THF were introduced. After 5 minutes 10, 20, 30 or 40 equiv propylene sulfide in 1 ml THF were added and the reaction mixture was stirred at room temperature for 45 minutes. The pH was adjusted using 1.1 equiv of acetic acid in 1 ml THF and 2.3 equiv DBU in 1 ml THF. 5 equiv of 2-bromoethanol in 1 ml THF were added and the reaction was stirred for 16 hours at room temperature. The solvent was removed at the rotary evaporator, the residue was redissolved in dichloromethane and extracted three times with water. The organic phase was dried over anhydrous sodium sulfate, filtrated and the solvent was completely removed. The viscous oil was extracted 3 times with methanol or petroleum ether and dried in vacuum.

FT-IR (on ATR crystal) [in cm^{-1}]: 3463, 2958, 2919, 2864, 1449, 1308, 1041, 1006, 734, 701. ^{1}H NMR (300 MHz, DMSO-d_6): δ (ppm) = 7.33-7.24 (m, **C_6H_5**-CH_2-); 3.77 (s, C_6H_5-**CH_2**-); 3.52 (t, -S-CH_2-**CH_2**-OH); 2.97-2.85 (broad, diastereotopic H of -**CH_2**- PPS chain, -**CH**- PPS chain); 2.67-2.55 (broad, diastereotopic H of -**CH_2**- PPS chain); 1.27-1.22 (broad, -**CH_3** PPS chain).

^{13}C NMR (75.5 MHz, $CHCl_3$-d): δ (ppm) = 138.22, 128.96-127.18 (**C_6H_5**-CH_2-); 61.05 (-S-CH_2-**CH_2**-OH); 41.32-40.45 (-**CH**- PPS chain); 38.78-37.06 (-**CH_2**- PPS chain); 34.16 (C_6H_5-**CH_2**-); 22.01-20.59 (-**CH_3** PPS chain).

Table 6.S1. Synthesized poly(propylene sulfide)s (PPS) with one terminal hydroxyl function.

Macroinitiator	DP PS[i]	M_n[i] [g·mol^{-1}]	M_n[ii] [g·mol^{-1}]	PDI[ii]	Yield [%]	End-capping[iii] [mol%]
2a	25	2000	1400	1.15	45	90
2b	35	2800	1700	1.15	59	95
2c	39	3100	2500	1.21	30	85
2d	47	3700	2800	1.20	48	91
2e	48	3750	3300	1.24	48	100

[i]calculated by ^{1}H NMR, ratio of the CH_2-signal of the initiator (benzyl group) and the PPS backbone signals. [ii]SEC with chloroform as eluent, calibrated with polystyrene standards. [iii]Ratio of the ^{1}H NMR signal of the CH_2 of the benzyl-group and the CH_2-signal of the end-capping agent.

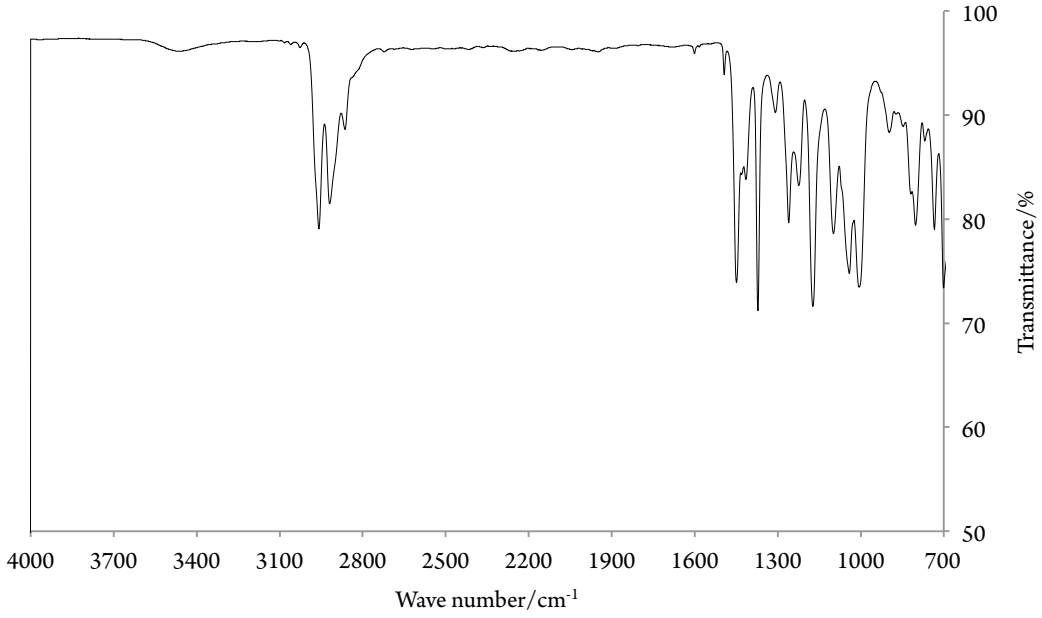

Figure 6.S1. IR spectrum (film on ATR crystal) of PPS with one terminal hydroxyl function.

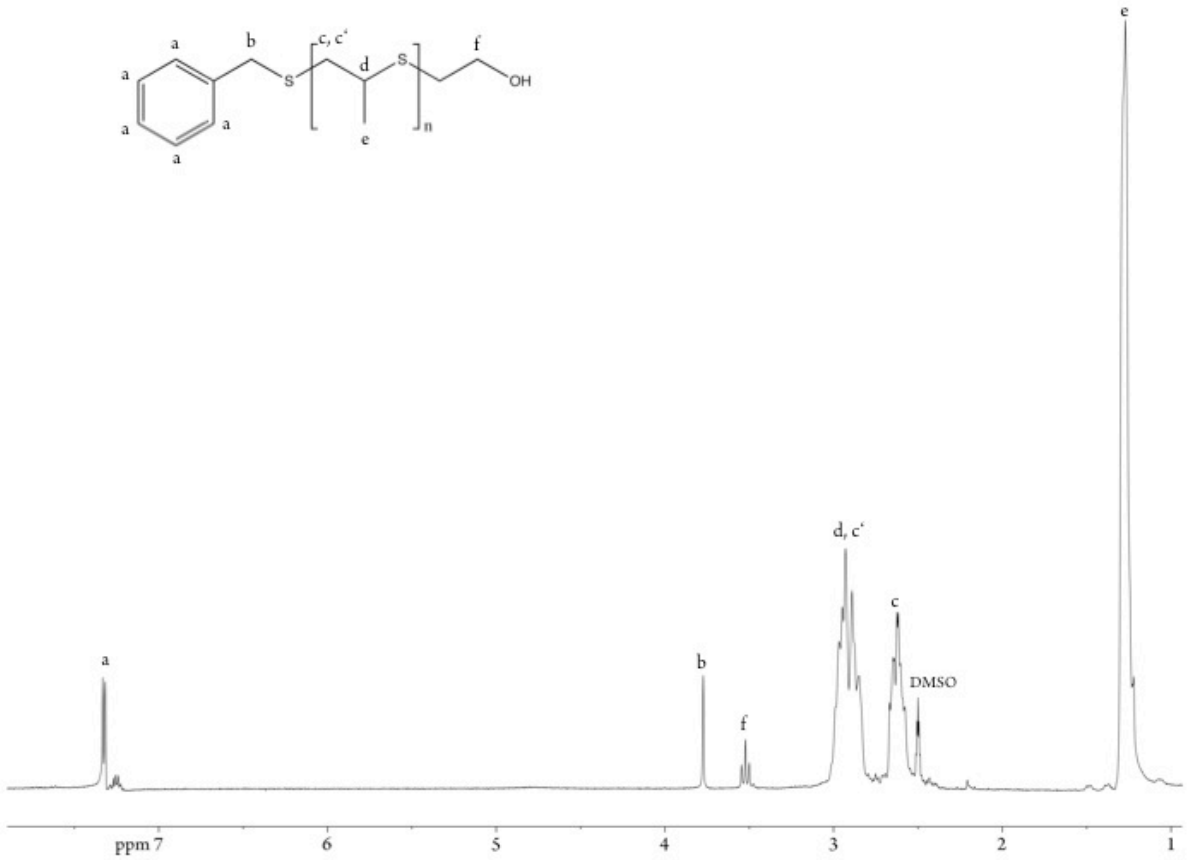

Figure 6.S2. ^{1}H NMR (300MHz, DMSO-d_6) spectrum of PPS with one terminal hydroxyl function **2a**.

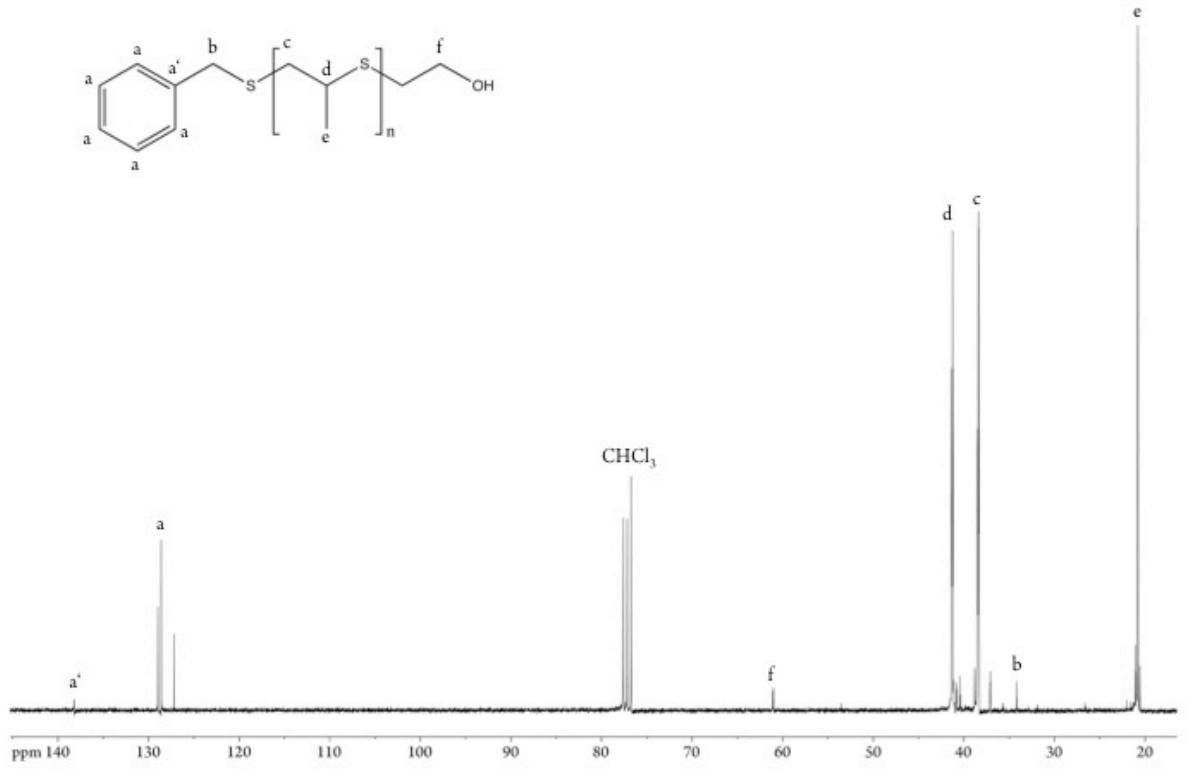

Figure 6.S3. ^{13}C NMR (75.5 MHz, $CHCl_3$-*d*) spectrum of a PPS with one terminal hydroxyl function.

Synthesis of poly(propylene sulfide)-*b*-poly(lactide) copolymers (PPS-*b*-PLA) (3)

Ring-opening polymerization of *D*- or *L*-lactide was performed in solution at room temperature with DBU as catalyst. A Schlenk flask equipped with a magnetic stirrer was charged with PPS initiator and transferred into a glove box, where various equiv *D*- or *L*-lactide were added. The flask was closed with a rubber septum and kept under argon atmosphere. Outside the glove box 2 ml dry dichloromethane were added to dissolve monomer and initiator. After the addition of DBU (monomer/catalyst=100/1) the polymerization was conducted at room temperature for 12 min. After completion, the reaction was quenched with benzoic acid (1.2 equiv according to DBU). The obtained block copolymer was precipitated into methanol or a mixture of diethyl ether and petroleum ether (1:1) (for copolymers with < 2000 g·mol^{-1} PLA chain length). The synthesized products were carefully dried in vacuum at room temperature.

FT-IR (on ATR crystal) [in cm^{-1}]: 2959, 1750, 1451, 1369, 1181, 1128, 1083, 1043, 734. ^{1}H NMR (300 MHz, $CHCl_3$-d): δ (ppm) = 7.33-7.31 (m, **C_6H_5**-CH_2-); 5.15 (q, -**CH**- PLA chain); 4.36-4.26 (m, -S-CH_2-**CH_2**-O-PLA); 3.74 (s, C_6H_5-**CH_2**-); 2.95-2.77 (broad, diastereotopic H of -**CH_2**- PPS chain, -**CH**- PPS chain); 2.67-2.57 (broad, diastereotopic H of -**CH_2**- PPS chain); 1.54-1.44 (m, -**CH_3**- PLA chain); 1.33-1.30 (broad, -**CH_3** PPS chain).

^{13}C NMR (75.5 MHz, $CHCl_3$-d): δ (ppm) = 169.77 (-**CO**- PLA chain); 130.25, 129.10-127.34 (**C_6H_5**-CH_2-); 69.18-66.86 (-**CH**- PLA chain); 64.53 (-S-CH_2-**CH_2**-O-PLA); 41.45-40.98 (-**CH**- PPS chain); 38.95-37.22 (-**CH_2**- PPS chain); 29.16 (C_6H_5-**CH_2**-); 20.70 (-**CH_3** PPS chain); 17.21-16.74 (-**CH_3**- PLA chain).

Table 6.S2. Synthesized PPS-*b*-PLA copolymers.

Copolymer	Initiator	Sample	DP PPS[i]/ DP PLA[i]	PLA content [wt%]	M_n[i] NMR [g·mol^{-1}]	M_n[ii] SEC [g·mol^{-1}]	PDI[ii]	Yield [%]
3a	**2e**	PPS-*b*-PLLA	63/2	6	5150	4000	1.15	quan
3b	**2e**	PPS-*b*-PLLA	59/9	23	5850	4400	1.31	71
3c	**2d**	PPS-*b*-PDLA	49/10	28	5250	4900	1.19	67
3d	**2a**	PPS-*b*-PLLA	30/18	54	5000	5800	1.15	68
3e	**2a**	PPS-*b*-PLLA	31/31	66	6950	7400	1.20	55
3f	**2a**	PPS-*b*-PLLA	35/69	79	12700	10800	1.21	60

[i]calculated by ^{1}H NMR, ratio of the CH_2-signal of the initiator (benzyl group) and the PPS backbone signals and accordingly the PLA backbone. [ii]SEC with chloroform as eluent, calibrated with polystyrene standards.

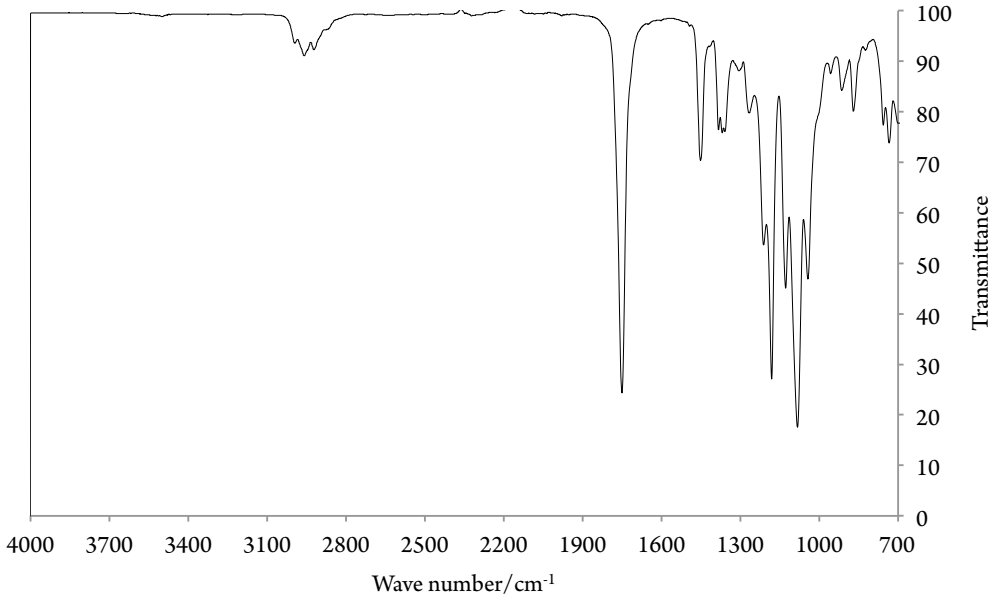

Figure 6.S4. IR spectrum (film on ATR crystal) of PPS-*b*-PLLA.

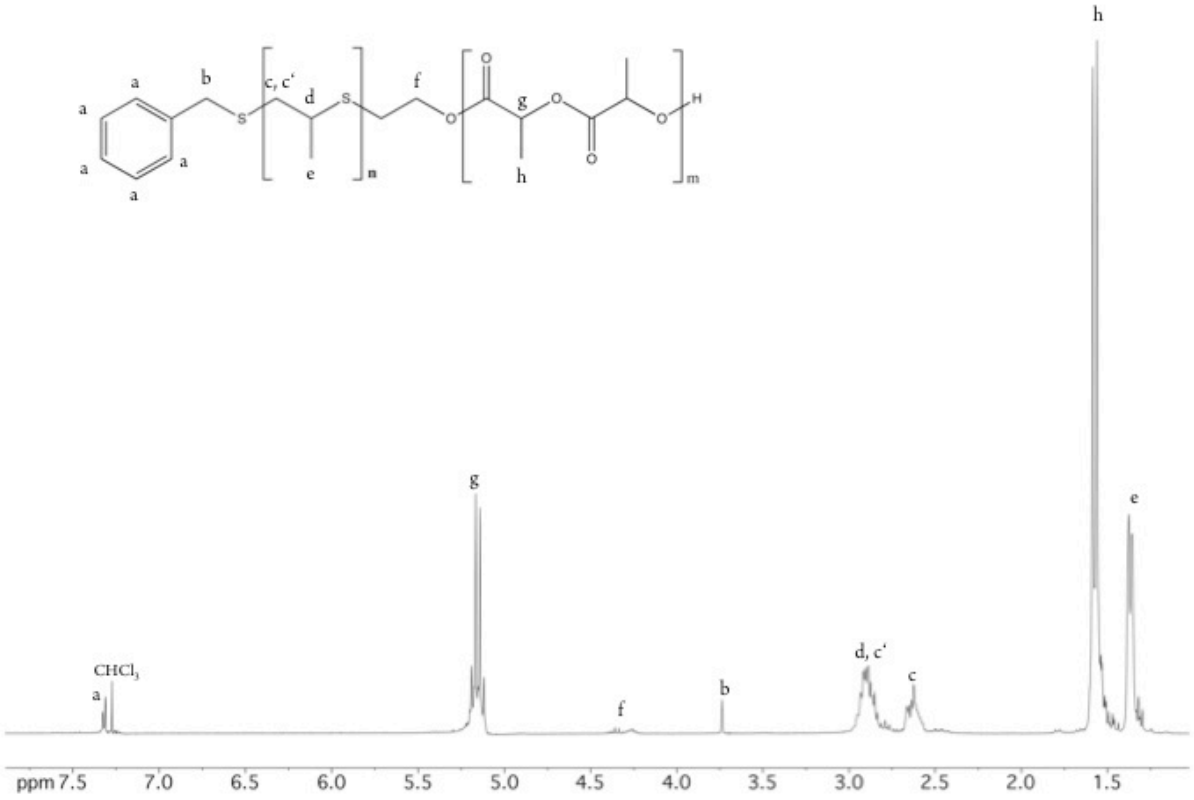

Figure 6.S5. ^{1}H NMR (300MHz, $CHCl_3$-*d*) spectrum of PPS-*b*-PLLA.

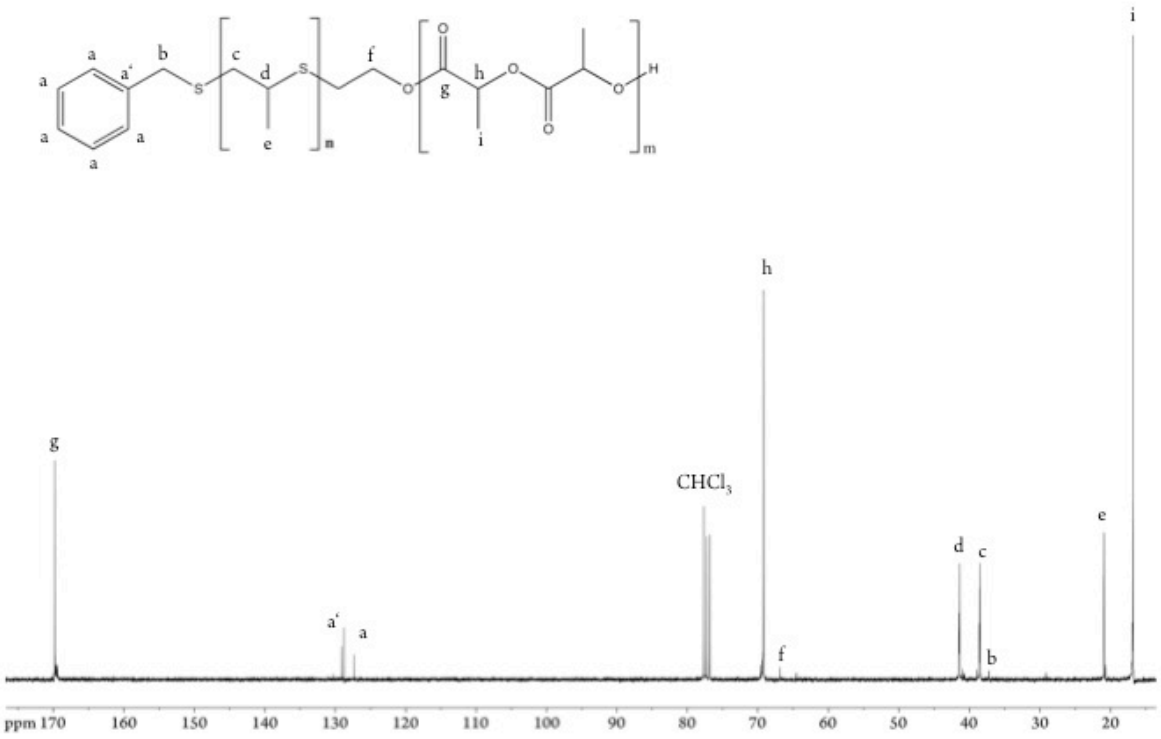

Figure 6.S6. ^{13}C NMR (75.5 MHz, $CHCl_3$-*d*) spectrum of PPS-*b*-PLLA.

Extraction of the gold nanoparticle solution

5 ml of the aqueous gold particle solution was extracted with 5 ml polymer solution (1mg·ml^{-1} in dichloromethane) via shaking at a frequency of 500 min^{-1} at room temperature for one hour. Immediately after this time the water phases were characterized using a UV-vis spectrometer.

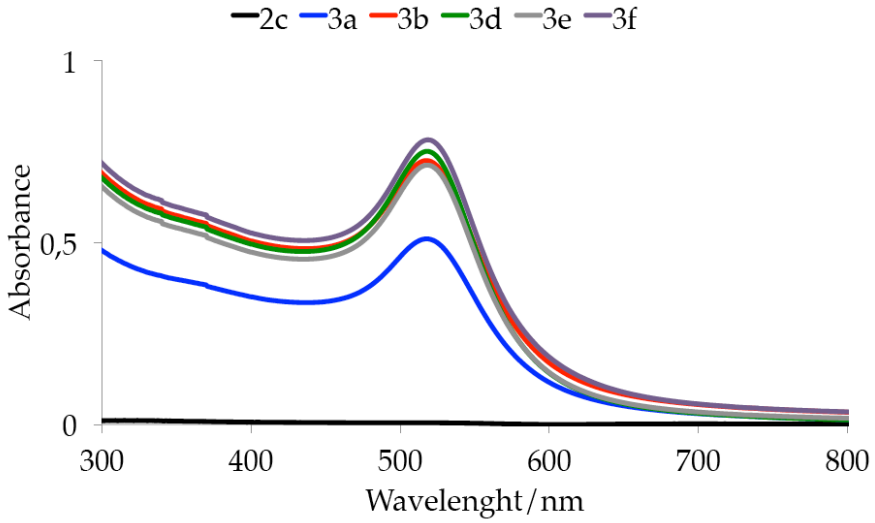

Figure 6.S7. UV-vis spectra of the aqueous solutions.

Adsorption of polymer to gold substrates

A gold substrate was dipped in 5 ml polymer solution (1mg·ml^{-1} in dichloromethane) for 15-30 minutes. The substrates were rinsed 10 times with dichloromethane, dried under argon stream and stored under argon atmosphere until the AFM and static contact angle measurements.

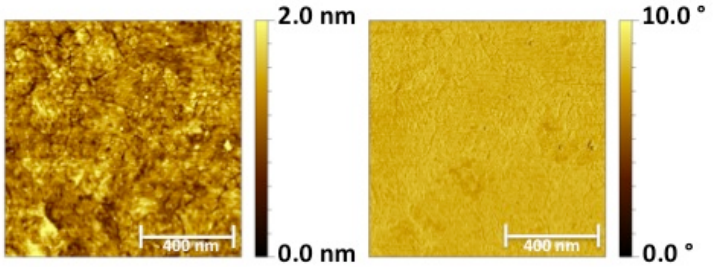

Figure 6.S8. left: AFM height image of bare gold support; right: AFM phase image of bare gold support.

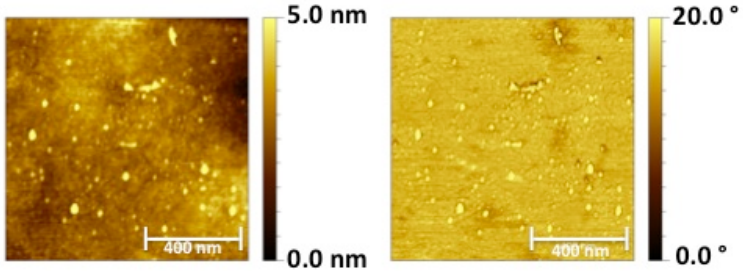

Figure 6.S9. left: AFM height image of **3a**; right: AFM phase image of **3a**.

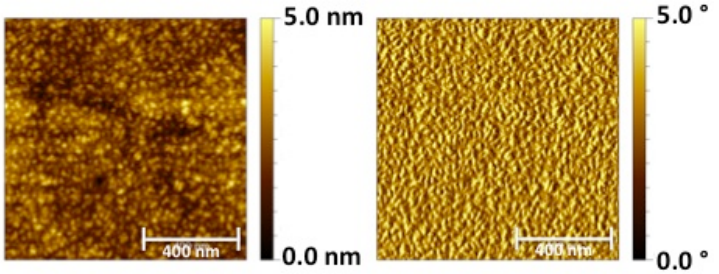

Figure 6.S10. left: AFM height image of **3d**; right: AFM phase image of **3d**.

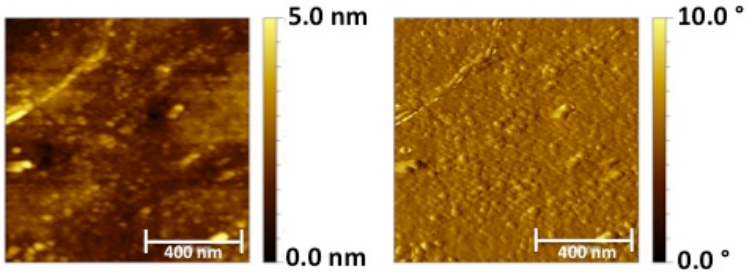

Figure 6.S11. left: AFM height image of **3g**; right: AFM phase image of **3g**.

Table 6.S3. Contact angle measurement.

Sample	Static contact angle [°]	RMS roughness (1 x 1 µm²) [nm]
Bare gold substrate	88 ± 2	0.3 ± 0.1
3a	71 ± 3	0.4 ± 0.1
3d	72 ± 2	0.5 ± 0.1
3g	70 ± 2	0.4 ± 0.1

References

(390) Zheng, T.; Burkhart, M.; Richardson, D. E.; *Tetrahedron Letters* **1999**, *40*, 603-606.
(391) Porta, F.; Speranza, G.; Krpetić, Ž.; Dal Santo, V.; Francescato, P.; Scarì, G.; *Materials Science and Engineering B* **2007**, *140*, 187-194.
(392) Naumann, R.; Schiller, S. M.; Griess, F.; Grohe, B.; Hartmann, K. B.; Kärcher, I.; Köper, I.; Lübben, J.; Vasilev, K.; Knoll, W.; *Langmuir* **2003**, *19*, 5435-5443.

Chapter 7

Summary and Outlook

7.1 Summary

The focus of the present work was the synthesis and characterization of sulfur-containing polymers with specific structures for surface attachment and gold nanoparticle stabilization. This was successfully implemented by three different strategies: The synthesis of polysulfides with a complex architecture, the use of polysulfides as a macroinitiator and the design of a lipoic acid derivative as an initiator of lactones and epoxides.

The first strategy involved the use of polyether-polyols as macroinitiators for thiiranes. These monomers require a thiol as initiating functionality. Thiols are sensitive to oxidants such as oxygen from air. Hence, the use of protected thiols, such as thioacetates, was necessary. The modification of polyglycerol and poly(ethylene glycol)-poly(allyl glycidyl ether) (PEG-PAGE) di- and triblock-copolymers to macroinitiators with multiple thioacetate groups was essential. This modification was accomplished for polyglycerol in a three-step protocol and for PAGE block-copolymers in one post-polymerization modification reaction. The chosen synthetic route enabled the synthesis of polyethers with numerous thiol functionalities. The thioacetates bear the possibility to release thiols in a controlled manner under inert gas without oxidation to disulfide moieties. The use of the synthesized macroinitiators for the ring-opening polymerization of ethylene sulfide and propylene sulfide led to graft-copolymers with various complex architectures. Thioacetate-functionalized linear and hyperbranched polyglycerol enabled the synthesis of brush-like and star-shaped polysulfides, respectively. The use of modified PEG-PAGE block-copolymers led to comb-like structures in case of the diblock-copolymer and in case of the triblock-copolymer to pom-pom-like polysulfides. This synthetic toolkit facilitates the successful synthesis of a variety of polysulfides structures due to the different nature of the macroinitiators and a various number of initiating groups as well as the choice of the monomer. In addition, the length of the polysulfide arms was varied by the ratio of initiator and monomer. The synthesized graft-copolymers were subsequently analyzed by common methods, such as SEC as well as NMR and IR spectroscopy. Thus, the synthesis of soluble ethylene sulfide-containing polymers by the concept of short ethylene sulfide chains, i.e., onto macroinitiators with multiple initiating groups was accomplished for the first time.

The graft-polymerization of propylene sulfide onto macroinitiators-based on PEG-PAGE led to well-defined polymers with different chain lengths and narrow distribution with polydispersities below 1.3. In contrast, homopolymerization of propylene sulfide as side-reaction occurred in polymerizations with polyglycerol-based macroinitiators. The by-product was formed by proton-abstraction of propylene sulfide, which was subsequently enabled to act also as initiator for propylene sulfide. The side-product was removed by machine-aided HPLC, and the purified products exhibited narrow, monomodal PDIs in SEC.

Consecutively, the random copolymerization of ethylene sulfide and propylene sulfide was investigated. The ethylene sulfide content was successfully varied in the range of 9 to 62wt%, but star-shaped copolymers with higher ethylene sulfide contents than 60wt% ethylene sulfide were not soluble in dichloromethane. Compared to propylene sulfide, ethylene sulfide exhibited higher reactivity in the anionic ring-opening polymerization. The content of ethylene sulfide, calculated by ^{1}H NMR spectroscopy was often slightly higher than expected. Additionally, the analysis of the triad signals in ^{13}C NMR spectroscopy suggested a slight gradient for the incorporation of the monomers. At the beginning of the polymerization, the content of ethylene sulfide was enriched in the polysulfide chains and propylene sulfide was enriched at the terminal ends. The obtained distributions were broader and in some cases exceeded two. The polydispersity increased with increasing number of polysulfide chains and additionally with increasing ethylene sulfide content. The best results were obtained for polysulfides with a pom-pom-like architecture, which showed

PDIs in the range of 1.2 to 1.7. The increasing polydispersities might be caused by local insolubility of the growing polymer chains due to partial crystallization after incorporation of ethylene sulfide. The high number of charged and growing polysulfide arms in close proximity might cause higher PDIs, which was also observed for the polymerization of propylene sulfide with polyglycerol-based macroinitiators.
The thermal behavior was investigated by DSC measurements. The melting temperature of poly(ethylene sulfide) graft-copolymers mainly increased with increasing number of polysulfide arms. However, the copolymer with a larger hyperbranched polyether core and a poly(ethylene sulfide) shell still exhibited the glass transition temperature of the PG core and the melting temperature of PES segments was significantly lowered. In contrast, the glass transition temperature of the poly(propylene sulfide) graft-copolymers depended less strictly on the molecular weight as expected. The T_g increased slightly with increasing molecular weight of PPS. The increase corresponded to the increase of the molecular weight per polysulfide arm, independent of the number of polysulfide arms. For the random copolymers no melting point was detected, which supported the existence of a random structure and contradicted a block-like structure. The detected glass transition temperatures seemed to be merely influenced by the content of propylene sulfide per polysulfide arm.
The efficiency for the transfer of gold nanoparticles to organic media from aqueous solution was influenced by the architecture and the number of polysulfide arms as well as by the monomer composition and the length of the polysulfide arms. Brush-like copolymers with thirty-six polysulfide arms enabled the transfer of nanoparticles independent of the polymer length and the monomer composition. The transfer of gold nanoparticles with star-shaped random polysulfides with longer polymer chains was not possible. In case of the comb-like copolymers with an additional PEG chain, transfer was mostly successfully enabled for samples with ten repeating units of propylene sulfide per initiating group. In contrast, the random graft-copolymers with a pom-pom-like structure led to transfer from aqueous solutions for all monomer compositions, but merely the poly(propylene sulfide) sample with ten repeating units per thioacetate unit were capable of solubilizing the nanoparticles. However, the polysulfide-shielded nanoparticles exhibited a characteristic solubility, some of the modified Au NPs were soluble in dichloromethane and toluene. This behavior was important for the ability to functionalize gold nanoparticles to obtain modified Au NPs with a tailored solubility.
The adsorption onto bare gold supports was also conducted for the tested polysulfides. For most copolymers the obtained surface roughness was only slightly higher than the bare gold comparison, but the coating with different polysulfides significantly influenced the static contact angle of a water droplet. The polymer architecture, the number of polysulfide arms as well as the monomer composition influenced the change of the wettability. The used polysulfides recreated the characteristic surface structure of template-stripped gold. Coating with random polysulfides with ethylene sulfide contents higher than 50wt% led to a worm-like surface pattering on the gold substrates, which might be caused by aggregation of polysulfide due to a partial aggregation of the copolymers with such high ethylene sulfide contents. These modified gold supports were used to attach gold nanoparticles in a second adsorption. Polysulfide bore a multiple number of sulfide functionalities, but not all of those were engaged with the gold support and facilitated the adsorption of gold nanoparticles. The gold nanoparticles were homogenously attached to the gold substrate. An influence by the used polymer architecture on the surface patterning was not observed.

The second part of this thesis introduced the successful preparation of a novel lipoic acid derivative, which acted as an initiator for the polymerization of lactones and epoxides to obtain polymers with a dithiolane

anchoring group. These monomers require, for example, a hydroxyl function to initiate the polymerization. The reaction of lipoic acid with a 5-aminopentan-1-ol supported by DCC and DMAP led to a lipoic acid derivative with a terminal hydroxyl functionality in a suiting yield. The use of the novel initiator for the DMAP-catalyzed polymerization of *L*-lactide was achieved. The obtained functionalized polylactides exhibited narrow molecular weight distributions with PDIs below 1.2. Successful initiation was proven by MALDI-ToF mass spectrometry and ^{1}H NMR spectroscopy. The exchange of the citrate stabilizers on the gold nanoparticles surface with this modified polyester led to a nanoparticle transfer from aqueous solution to dichloromethane. The adsorption onto bare template-stripped gold substrates resulted into a recreation of the typical TSG surface structure, but a significant change of the wettability of the functionalized surfaces was detected.

The successful preparation of lipoic acid-modified polyethers was proven by the polymerization of ethylene oxide with the synthesized lipoic acid derivative. The polymerization was limited to molecular weights up to 2000 g·mol^{-1} and the obtained polydispersities were moderate for anionic ring-opening polymerization with PDIs up to 1.5. However, for most applications in surface attachment this might not be a disadvantage. MALDI-ToF mass spectrometry evidenced the initiation by the synthesized lipoic acid derivative. As a proof of principle, the functionalized polymers were adsorbed onto gold surfaces. The polymers were not capable of transferring gold nanoparticles to organic solvents, most probably due to the good water solubility of PEG. The modification of bare gold substrates resulted in a significant change of the wettability. The detected static contact angles of a water droplet were small, as expected for coating with a hydrophilic polymer. Additionally, the surface structure was markedly rougher than the smooth comparison.

The use of a functionalized initiator enabled the direct synthesis of tailored polymers to functionalize metal surfaces. This straightforward approach made the polymerization of different monomer classes possible to obtain polymers with a disulfide-anchoring group for gold without the drawbacks of post-polymerization modifications as well as a complicated purification and potential limited conversion.

The third strategy, the design of a poly(propylene sulfide) with a terminal functionality, which could be addressed in a second polymerization to obtain block-copolymers without post-polymerization modifications, was explored. A terminal hydroxyl functionality was obtained by termination of living poly(propylene sulfide) chains with 2-bromoethanol. The end-capping reaction was quantitatively conducted. The hydroxyl function can be used to initiate a second polymerization, which was proven by the polymerization of lactide in a collaboration project. This is the first approach, in which PPS acted as a macroinitiator. The synthesis of a novel class of block-copolymers was successful. The composition of these copolymers was varied over a wide range from 6 to 79wt% polylactide. The obtained copolymers exhibited narrow molecular weight distributions with PDIs below 1.35. The thermal characteristics were analyzed by DSC measurements. Compared to the glass transition temperature of a hydroxyl-functionalized PPS, the T_g of most PPS block-copolymers was increasing with increasing polylactide content from -48 °C to -38°C. The block-copolymer with a polylactide content of 79wt% did not exhibit a T_g. The melting temperatures also increased with increasing polylactide content from 104 °C to 137 °C and for the block-copolymer with only 6wt% no T_m was detected. Additionally, the adsorption efficiency of these copolymers was investigated. The hydroxyl-terminated poly(propylene sulfide) samples were capable of transferring gold nanoparticles from aqueous solution to organic solution after linker exchange. In contrast, the block-copolymer with 6wt% PLA led to an incomplete transfer of aqueous gold nanoparticles. Block-copolymers with higher PLA content were incapable of transferring nanoparticles from aqueous solution. This behavior might be caused by a

PLA block, which coiled around the polysulfide segment and prevented the interaction between sulfur atoms and the gold surface. This was surprising, due to the fact that lipoic acid functionalized polylactides were able to transfer aqueous nanoparticles to dichloromethane solution. The adsorption of PPS-PLA block-copolymers to bare template-stripped gold supports was also accomplished, which was proven by a change of the static contact angle and a slightly rougher surface patterning.

7.2 Outlook

In the future, the work started with this thesis result in further studies. The polymerization of thiiranes with functionalized polyether-polyols will be further investigated. The use of a more polar solvent such as dimethylformamide might reduce the electrostatic repulsion, which results from the large number of charged growing polysulfide chains in close proximity. The close proximity can also be reduced by use of thioacetate-functionalized random polyether moieties, for example PEG-PAGE random copolymers as well as hyperbranched PEG, which is formed in the random copolymerization of glycidol and ethylene oxide. Additionally, the use of further polyether-based macroinitiators will increase the variety of complex polysulfide architectures. A weaker base such as an amide should be tested to cleave the thioacetate and release the active initiating groups without the ability to deprotonate propylene sulfide and thereby initiate the homopolymerization of propylene sulfide as a side-reaction.

The termination with 2-bromoethanol can also be used for the synthesis of terpolymers with complex architectures via the introduction of a terminal hydroxyl functionality, which can be addressed in a further polymerization. These complex terpolymers might exhibit interesting chemical and physical characteristics. For example, this approach might enable the synthesis of amphiphilic PPS-PEG copolymers, which may form monomolecular micelles. Additionally, the surface attachment to gold surfaces and other metals could by investigated.

The introduced DMAP-catalyzed ring-opening polymerization of *L*-lactide might be also applied to polymerize further lactons such as ε-caprolactone to obtain other lipoic acid-functionalized polyesters. Poly(*D*-lactide)s initiated by the lipoic acid derivative might be used for the formation of stereocomplexes composed of PDLA and PLLA, which can be fixed to gold substrates via their lipoic acid anchoring group. However, the polymerization conditions of ethylene oxide with the novel lipoic acid derivative might be further improved to obtain polymers with higher molecular weights and lower PDIs. Additionally, the novel initiator should be explored for the ring-opening polymerization of substituted epoxides, such as glycidol and 2,3-epoxypropyl-1-ethoxyethyl ether. The surface attachment to gold supports and gold nanoparticles of these dithiolane-modified polymers should be further investigated by wettability measurements, AFM imaging and UV-vis spectroscopy.

The ability to oxidize polysulfide to polysulfoxides represents an additional intriguing facet and could be used to form amphiphilic block-copolymers composed of a hydrophilic polysulfoxide block and a hydrophobic polylactide block for biomedical applications. The sulfide functionalities of the hydroxyl-functionalized PPS should be selectively oxidized to sulfoxides, and subsequently this moiety should act as initiator for the ring-opening polymerization of lactide.

The use of hydroxyl-terminated poly(propylene sulfide) as macroinitiators should be further extended to other lactones to form different polysulfide-polyester block-copolymers. Additionally, this polysulfide macroinitiator should also be investigated to initiate the polymerization of epoxides such as ethylene oxide

and 2,3-epoxypropyl-1-ethoxyethyl ether to obtain polysulfide-polyether copolymers in a straightforward procedure without post-polymerization modification. The adsorption efficiency of these copolymers should also be studied and compared to the results obtained by the PPS-PLA block-copolymers and further reference polymers with a sulfur-containing anchoring group.

Appendix

Appendix

A. List of abbreviations

AA	acetic acid
AFM	atomic force microscope
AGE	allyl glycidyl ether
AIBN	azobisisobutyronitrile
ATE	allyl thioglycidyl ether
ATRP	atom-transfer radical polymerization
Au NP	gold nanoparticle
BSA	bovine serum albumin
BT	benzyl thioacetate
DBU	1,8-diazabicyclo[5.4.0]undec-7-ene
DCC	*N,N'*-dicyclohexylcarbodiimide
DCM	dichloromethane
DHLA	dihydrolipoic acid
DMAP	4-dimethylaminopyridine
DMF	dimethylformamide
DMSO	dimethyl sulfoxide
DP	degree of polymerization
DPMK	diphenylmethyl potassium
DSC	differential scanning calorimetry
EEGE	2,3-epoxypropyl-1-ethoxyethyl ether
EO	ethylene oxide
ES	ethylene sulfide
FAD	flavin adenine dinucleotide
FD	field desorption
FD-MS	field desorption mass spectrometry
FT-IR	Fourier transform infrared spectroscopy
ToF	time of flight
hb	hyperbranched
HMT	hydoxymethylthiirane
HPLC	high-performance liquid chromatography
IBS	isobutylene sulfide
IR	infrared
LA	α-lipoic acid
lin	linear
MALDI	matrix-assisted laser desorption/ionization
MO	molecular orbital
MS	mass spectrometry
NAD^+	nicotinamide adenine dinucleotide
OEGMA	oligo(ethylene glycol) monomethyl ether methacrylate

PAGE	poly(allyl glycidyl ether)
PCL	poly(ε-caprolactone)
PDI	polydispersity index
PEG	poly(ethylene glycol)
PEO	poly(ethylene oxide)
PEI	poly(ethylene imine)
PG	polyglycerol
PGA	poly(glycolide)
PO	propylene oxide
POM	polarized light optical microscopy
PPO	poly(propylene oxide)
PES	poly(ethylene sulfide)
PLA	poly(lactide)
PLLA	poly(*L*-lactide)
PNIPMAA	poly(*N*-isopropylacrylamide-*co*-methacrylic acid)
PPS	poly(propylene sulfide)
PS	propylene sulfide
QCM-D	quartz crystal microbalance with dissipation monitoring
RAFT	radical addition-fragmentation chain transfer
RI	refractive index
RMS	root mean square
ROP	ring-opening polymerization
SAM	self-assembled monolayers
SEC	size-exclusion chromatography
SER	surface enhanced Raman
SOD	superoxide dismutase
STM	scanning tunneling microscopy
TAGT	controlled thioacyl group transfer
TBAB	tetrabutylammonium bromide
TBAC	tetrabutylammonium chloride
TBAI	tetrabutylammonium iodide
TBD	1,4,7-triazabicyclodecene
TBP	tributyl phosphine
TCM	trichloromethane
TEM	transmission electron microscopy
T_g	glass transition temperature
T_m	melting temperature
THF	tetrahydrofuran
ToF	time-of-flight
TOL	toluene
TSG	template-stripped gold
USPIO	ultrasmall superparamagnetic iron oxide
UV	ultraviolet

UV-vis	ultraviolet-visible
XPS	X-ray photoelectron spectroscopy

B. Instrumentation

AFM (atomic force microscope) measurements were carried out on a Veeco NanoScope Dimension 3100 in tapping mode. Silicon cantilevers with a resonance frequency of 300 kHz, a spring constant of 42 $N \cdot m^{-1}$ and a tip height of 11 μm were used. The data were collected with Nanoscope 5.31r1 and Gwyddion 2.25 was used to analyze the AFM height and phase images as well as the determination of the RMS roughness.

DSC (differential scanning calorimetry) was done on a *Perkin Elmer* DSC 8500, calibrated with indium and millipore water, in sealed aluminum pans under nitrogen with a heating rate of 10 K per minute.

FD (field desorption) **mass spectrometry** was performed on a Finningan MAT 95 with a heating rate of 10 $mA \cdot min^{-1}$ and an accelerating voltage of 5 kV.

^{1}H NMR (nuclear magnetic resonance) spectra were recorded on a Bruker AC 300 at a frequency of 300 MHz or on a Bruker AMX 400 at 400 MHz, whereas the **^{13}C NMR** spectra were recorded at a frequency of 75.5 MHz on a Bruker AC 300. All NMR spectra were referred to the proton signal of the deuterated solvent as an internal standard. The online ^{1}H NMR experiments were recorded in the Bruker AMX 400 at 400 MHz.

FT-**IR** (Fourier transform infrared) **spectroscopy** was done in ATR mode either on a Tensor 27 Bruker spectrometer or on a Nicolet iS10 spectrometer from Thermo Scientific. For the characterization of the synthesized substances only the characteristic and intensive bands were given.

MALDI-ToF (matrix-assisted laser desorption/ionization time-of-flight) **mass spectrometry** was performed on a Shimadzu Axima CFR MALDI-TOF mass spectrometer with a nitrogen laser delivering 3 ns laser pulses at 337 nm using potassium triflate as cationizing agent and dithranol (1,8-dihydroxy-9(10H)-anthracetone) as matrices. Linear and reflectron mode of the spectrometer was employed to detect the positive ions.

Recycling preparative HPLC (high-performance liquid chromatography) in chloroform with a flow rate of 3.5 $ml \cdot min^{-1}$ was done in chloroform on a Next LC-9110/9130 from Japan Analytical Industry Co. Ltd equipped with a Jaigel-4H polystyrene gel GPC HPLC column, a RI and UV detector.

SEC (size-exclusion chromatography) was performed in tetrahydrofuran (THF) on a Polymer Laboratories GPC 50 connected to a refractive index (RI) detector or in THF and chloroform on a set of three PSS SDV columns (10^{4}/500/50 Å) connected to a refractive index and an UV (254 nm) detector as well as a Waters 717 plus auto sampler and a TSP Spectra Series P 100 pump. In all cases polystyrene standard calibration with toluene as internal standard and a flow rate of 1 $ml \cdot min^{-1}$ was used.
The SEC measurements in dimethylformamide (DMF) (containing 0.25 $g \cdot L^{-1}$ of lithium bromide) with 1 $ml \cdot min^{-1}$ were carried out on an Agilent 1100 series integrated instrument including a PSS HEMA column ($10^{6}/10^{5}/10^{4}$ $g \cdot mol^{-1}$), RI and UV (254 nm) detector. The calibration was done with poly(ethylene oxide) standards provided by Polymer Standard Service and toluene was added as internal standard.

The glass supports for **TSG** (template-stripped gold) were cleaned with Hellmanex solution (2%) from Hellma Analytics in an ultrasonic bath. Subsequently, the glass supports were carefully rinsed with Milli-Q water for 30 seconds, stored in ethanol and dried in nitrogen flow immediately before used. The silicon substrates were cleaned in a mixture of 50 ml Milli-Q water, 10 ml hydrogen peroxide solution and 10 ml ammonia solution at 75 °C for 60 minutes. Subsequently, the silicon substrates were carefully rinsed with Milli-Q water and isopropyl alcohol. The substrates were stored in ethanol and dried in nitrogen flow immediately before used.
The thermal gold deposition of a 50 nm thick gold layer on clean silicon substrates was done on an Edwards GmbH Auto 306 Turbo system with a deposition rate of 2 $Å \cdot s^{-1}$ under high vacuum.
The epoxy adhesive EPO-TEK® 377 from Epoxy Technology was used as glue. The two components were mixed in a weight ration of 1:1 and degassed under high vacuum for one hour.

The **wettability** of the coated gold substrates were analyzed via static water contact angles, which were measured on a *data physics* OCA 20 with SCA 20 software. A droplet of deionized water was placed on the surface of the substrate and imaged via a video camera. The contact angle was calculated via software. This procedure was repeated ten times on different positions of the substrate.

UV-vis (ultraviolet-visible) **spectroscopy** was measured on a Jasco V-630 Spectrophotometer at 20°C. Excel was used for the illustration and analysis of the adsorption maxima.

Zeta-Potentials and dynamic light scattering data were obtained on a Nano Series Nano ZS Zetasizer from Malvern. The measurements were performed at a fixed scattering angle of 173° and an excitation wavelength of 633 nm in aqueous media at 25 °C. The analysis was repeated three times.

C. UV-vis spectra

C.I Linear polysulfides

Polymer solution in dichloromethane:

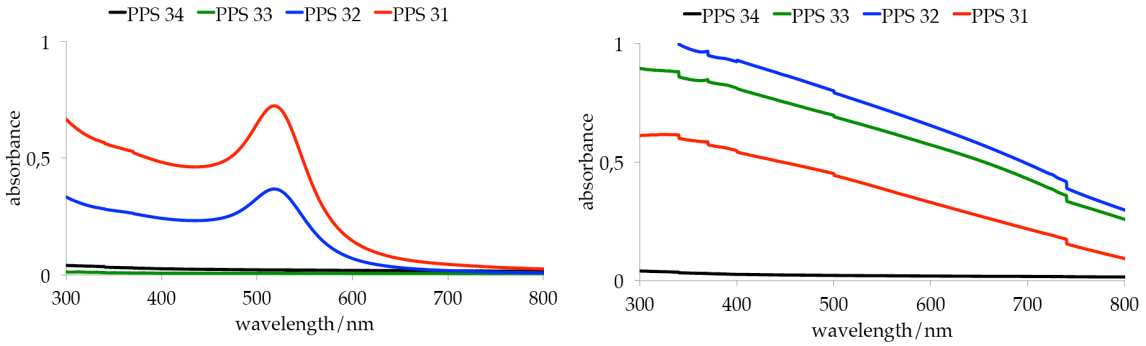

Figure C.1: UV-vis spectra of the extraction with **PPS 31-34** (left: aqueous phase; right: organic phase).

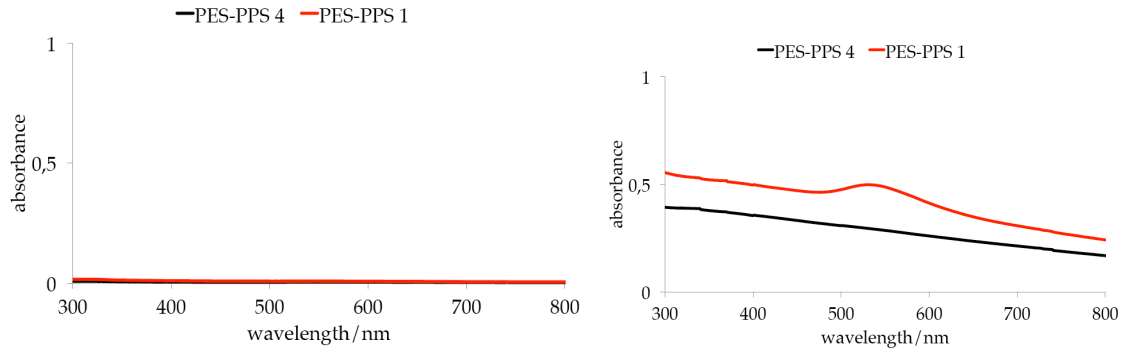

Figure C.2: UV-vis spectra of the extraction with **PES-PPS 1** and **4** (left: aqueous phase; right: organic phase).

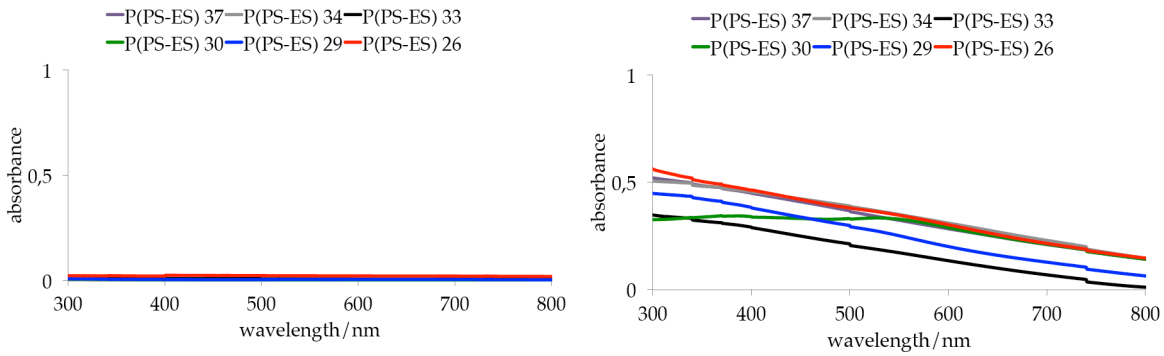

Figure C.3: UV-vis spectra of the extraction with **P(PS-ES) 26**, **29**, **30**, **33**, **34** and **37** (l.: aqueous phase; r.: organic phase).

Polymer solution in toluene:

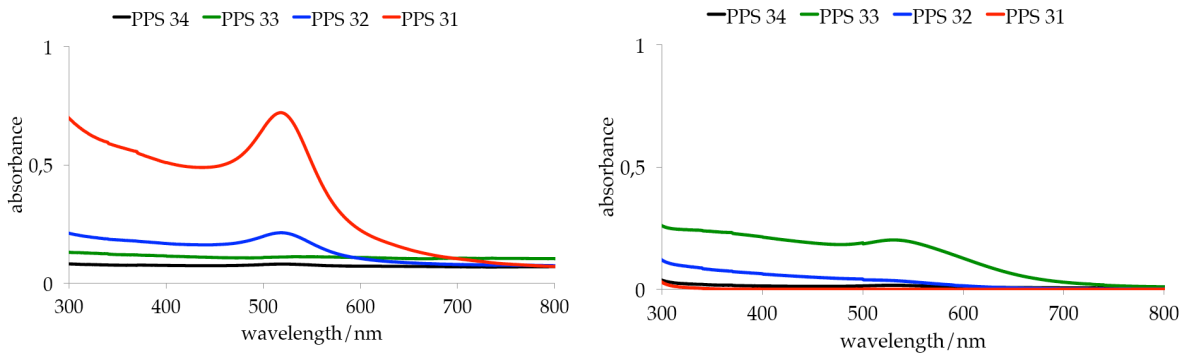

Figure C.4: UV-vis spectra of the extraction with **PPS 31-34** (left: aqueous phase; right: organic phase).

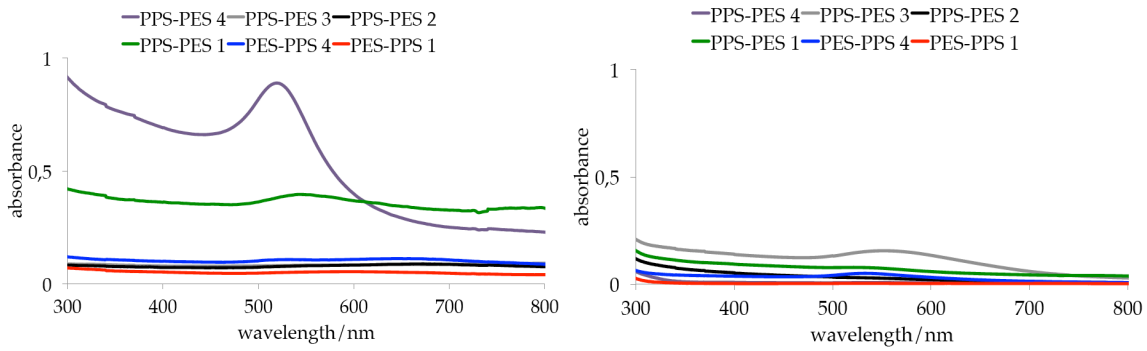

Figure C.5: UV-vis spectra of the extraction with **PES-PPS 1** and **4** (left: aqueous phase; right: organic phase).

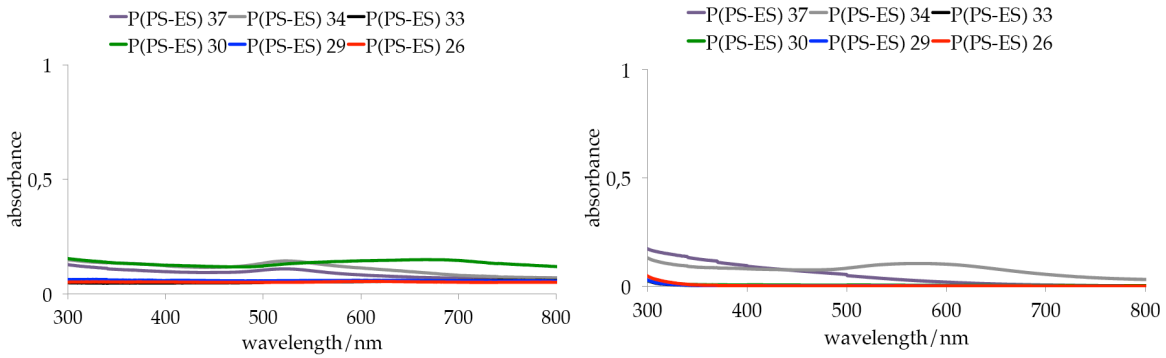

Figure C.6: UV-vis spectra of the extraction with **P(PS-ES) 26**, **29**, **30**, **33**, **34** and **37** (l.: aqueous phase; r.: organic phase).

C.II Star-shaped polysulfides

Polymer solution in dichloromethane:

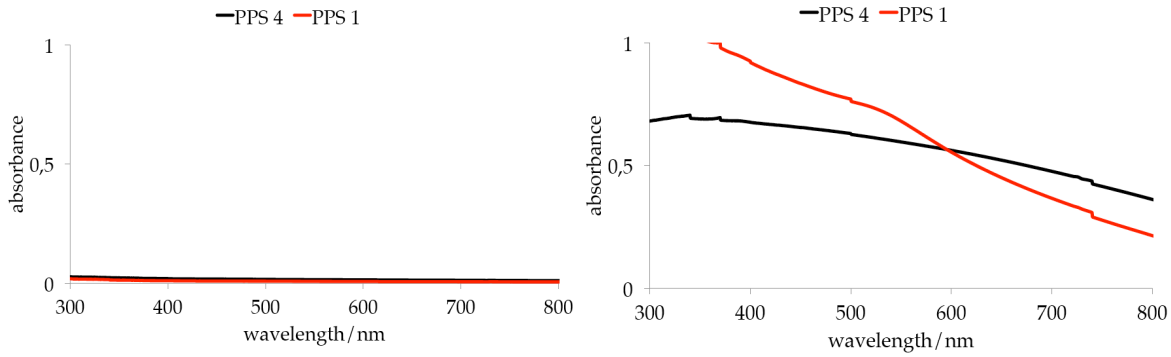

Figure C.7: UV-vis spectra of the extraction with **PPS 1-4** (left: aqueous phase; right: organic phase).

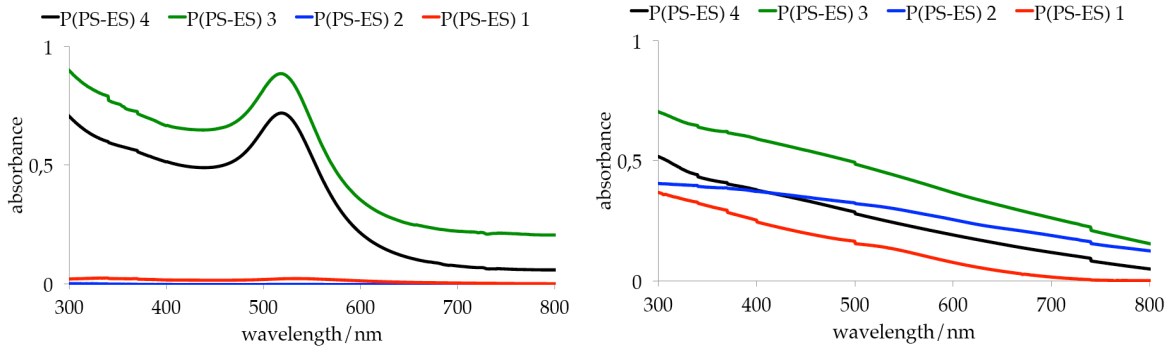

Figure C.8: UV-vis spectra of the extraction with **P(PS-ES) 1-4** (left: aqueous phase; right: organic phase).

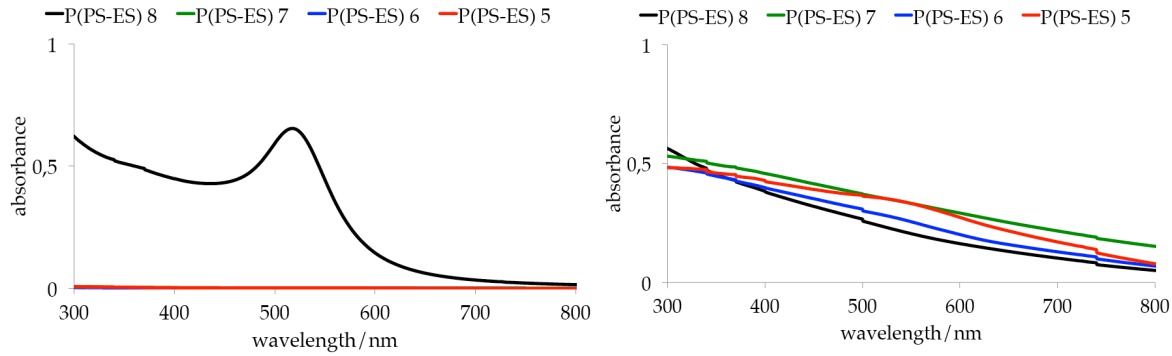

Figure C.9: UV-vis spectra of the extraction with **P(PS-ES) 5-8** (left: aqueous phase; right: organic phase).

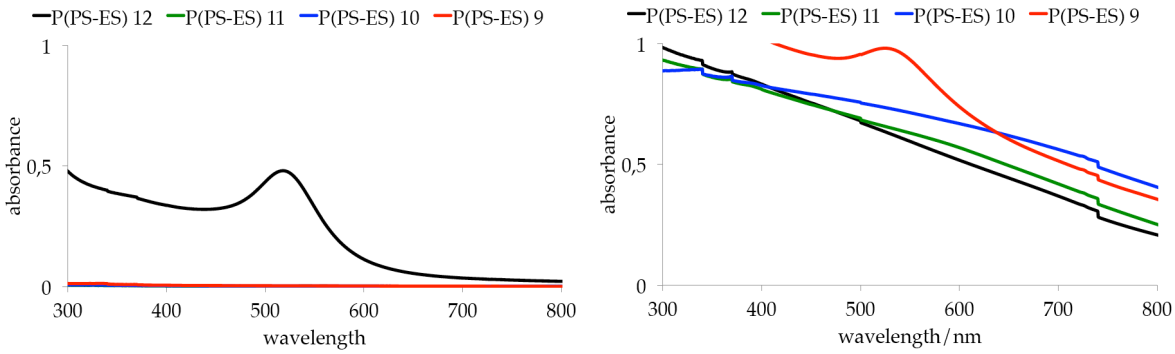

Figure C.10: UV-vis spectra of the extraction with **P(PS-ES) 9-12** (left: aqueous phase; right: organic phase).

Polymer solution in toluene:

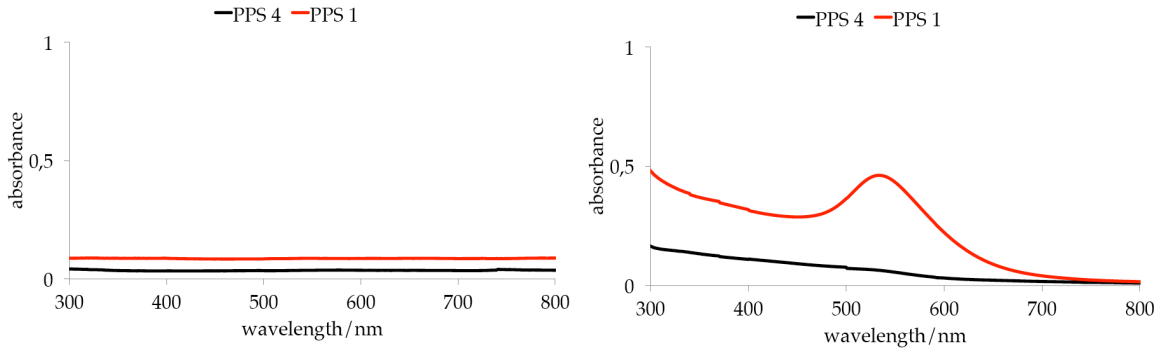

Figure C.11: UV-vis spectra of the extraction with **PPS 1-4** (left: aqueous phase; right: organic phase).

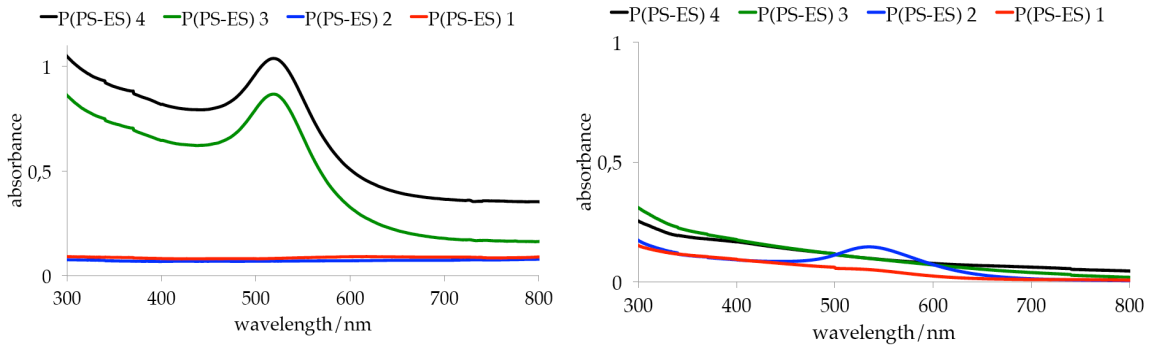

Figure C.12: UV-vis spectra of the extraction with **P(PS-ES) 1-4** (left: aqueous phase; right: organic phase).

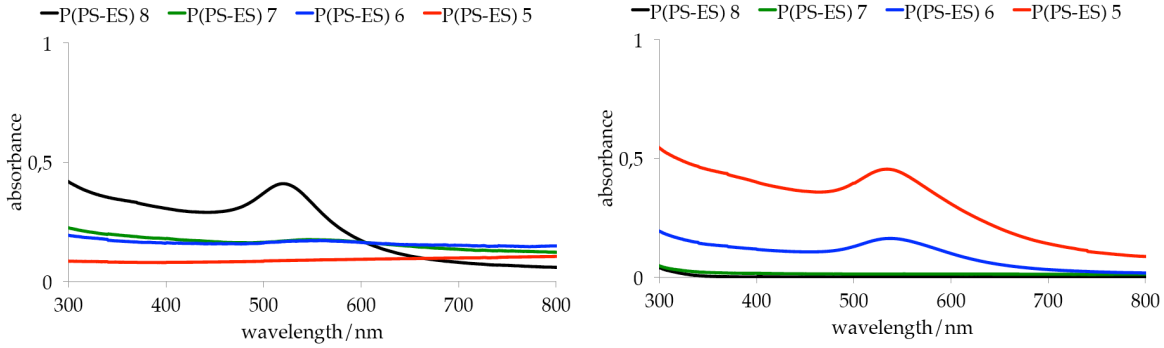

Figure C.13: UV-vis spectra of the extraction with **P(PS-ES) 5-8** (left: aqueous phase; right: organic phase).

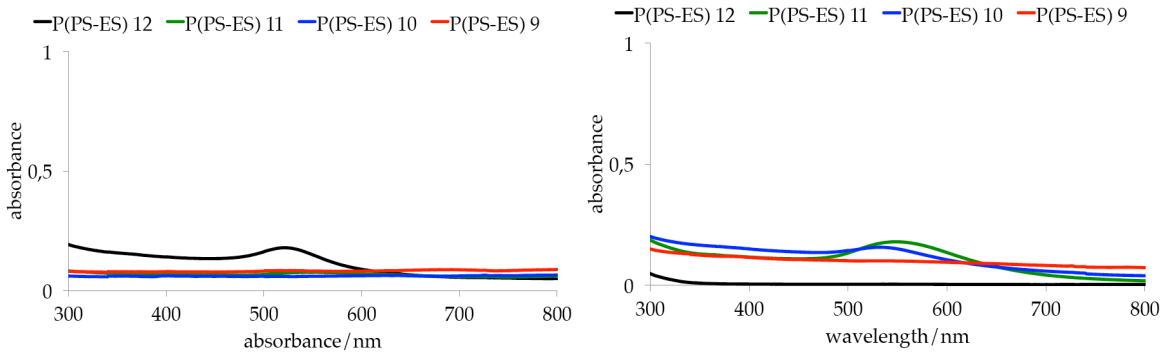

Figure C.14: UV-vis spectra of the extraction with **P(PS-ES) 9-12** (left: aqueous phase; right: organic phase).

C.III Brush-like polysulfides

Polymer solution in dichloromethane:

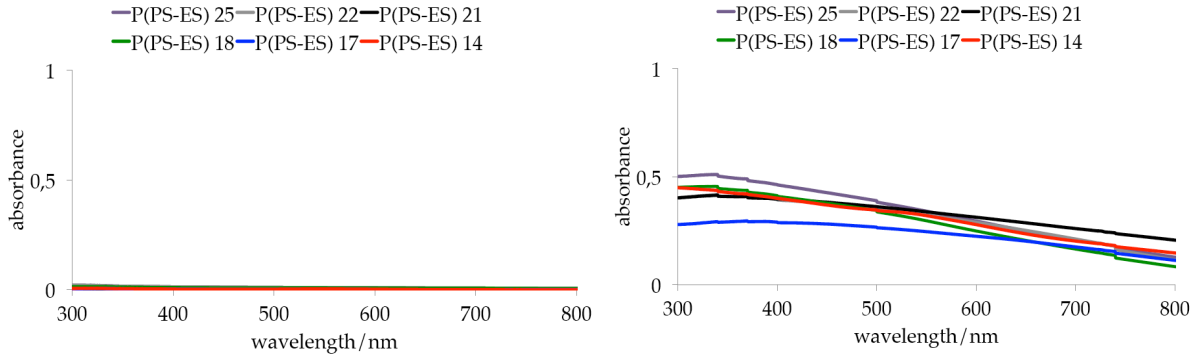

Figure C.15: UV-vis spectra of the extraction with **P(PS-ES) 14**, **17**, **18**, **21**, **22** and **25** (l.: aqueous phase; r.: organic phase).

Polymer solution in toluene:

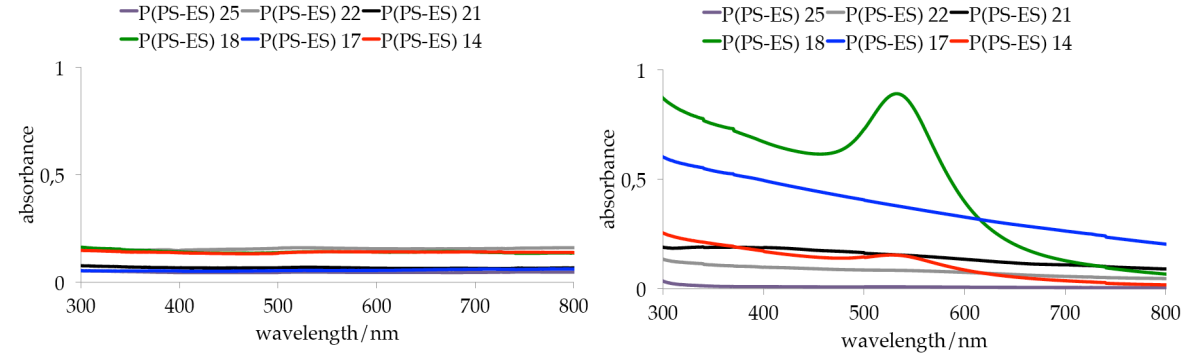

Figure C.16: UV-vis spectra of the extraction with **P(PS-ES) 14**, **17**, **18**, **21**, **22** and **25** (l.: aqueous phase; r.: organic phase).

C.IV Comb-like polysulfides

Polymer solution in dichloromethane:

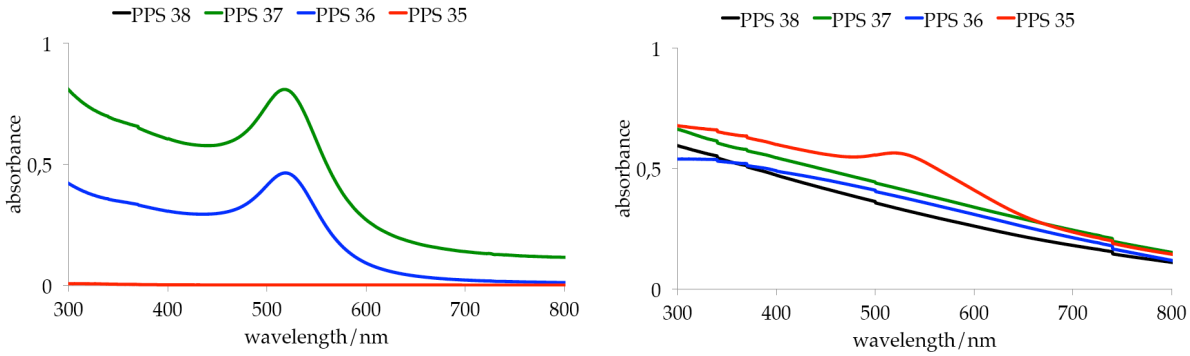

Figure C.17: UV-vis spectra of the extraction with **PPS 35-38** (left: aqueous phase; right: organic phase).

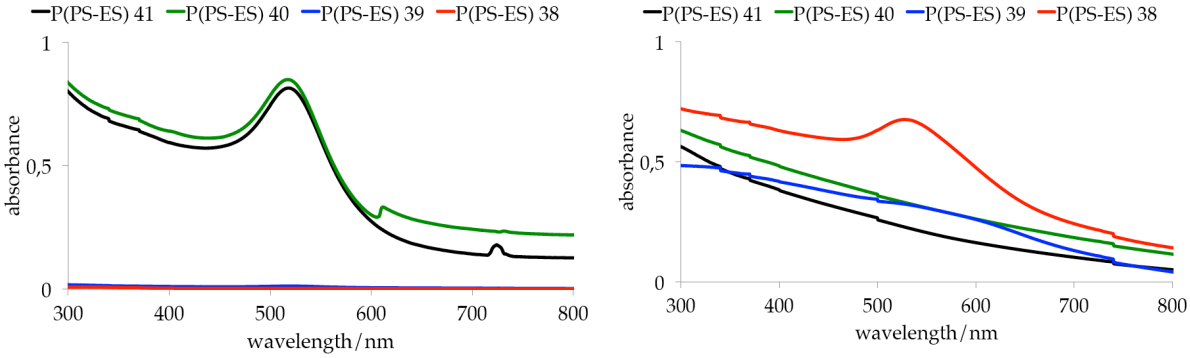

Figure C.18: UV-vis spectra of the extraction with **P(PS-ES) 38-41** (left: aqueous phase; right: organic phase).

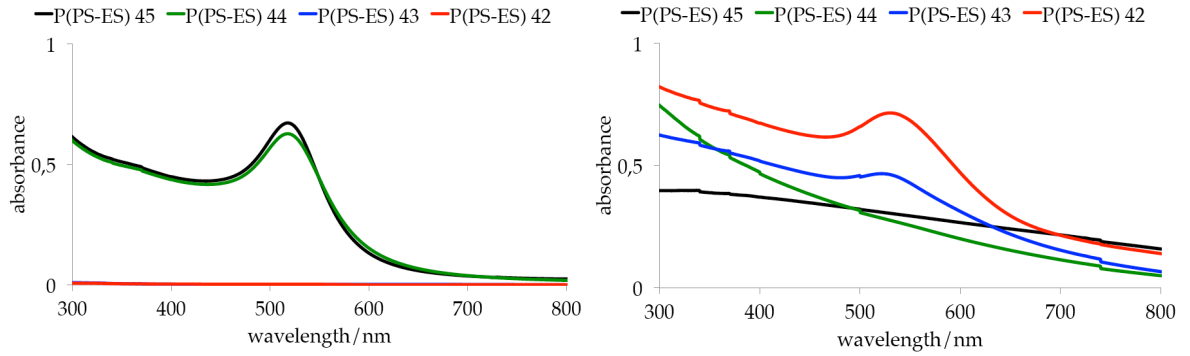

Figure C.19: UV-vis spectra of the extraction with **P(PS-ES) 42-45** (left: aqueous phase; right: organic phase).

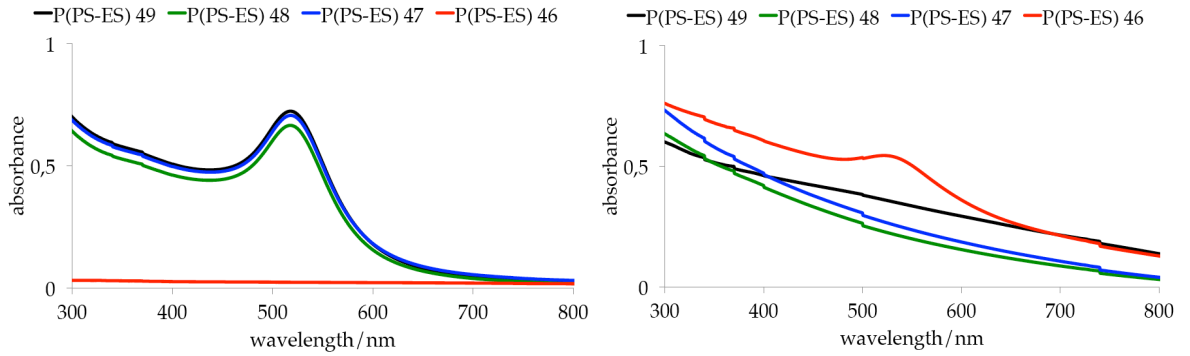

Figure C.20: UV-vis spectra of the extraction with **P(PS-ES) 46-49** (left: aqueous phase; right: organic phase).

C.V Pom-pom-like polysulfides

Polymer solution in dichloromethane:

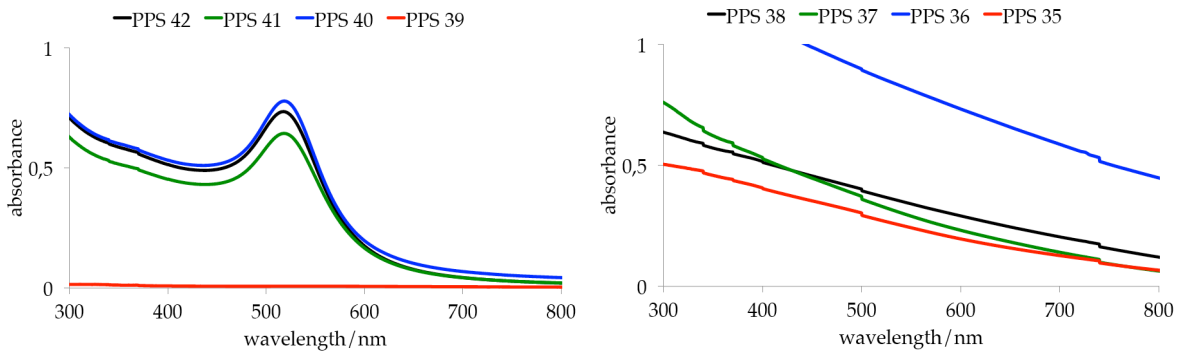

Figure C.21: UV-vis spectra of the extraction with **PPS 35-38** (left: aqueous phase; right: organic phase).

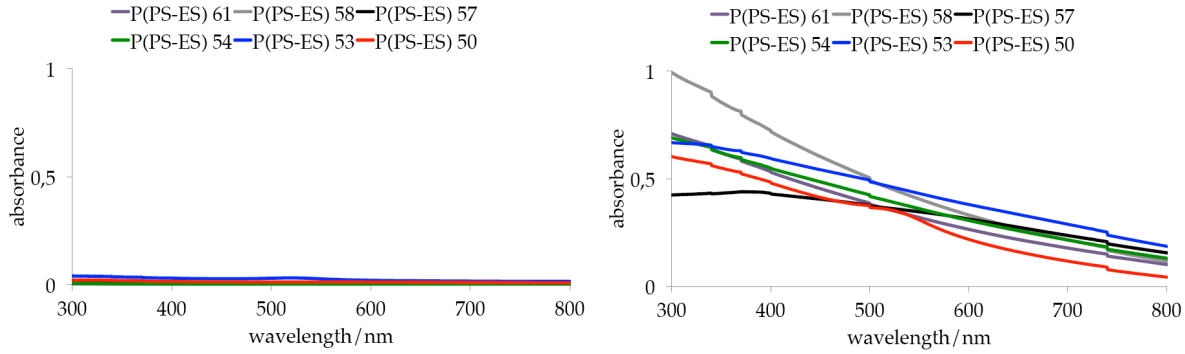

Figure C.22: UV-vis spectra of the extraction with **P(PS-ES) 50**, **53**, **54**, **57**, **58** and **61** (l.: aqueous phase; r.: organic phase).

C.VI Poly(*L*-latide) with a lipoic acid anchoring group

Polymer solution in dichloromethane:

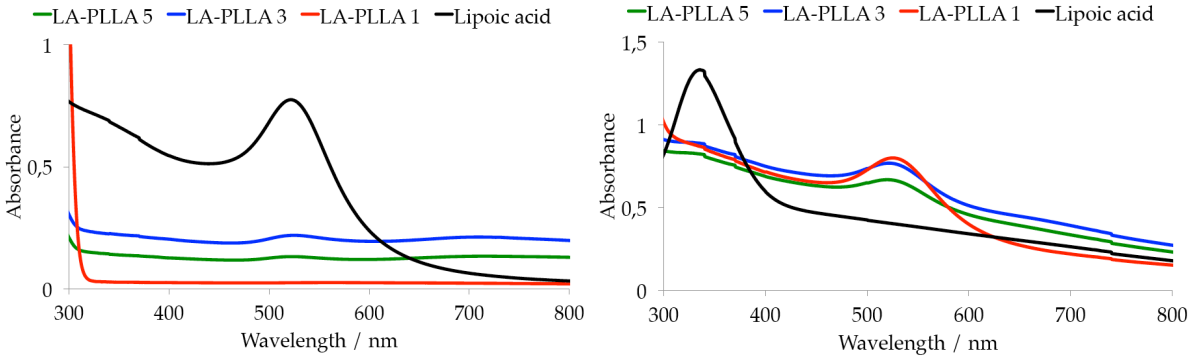

Figure C.23: UV-vis spectra of the extraction with lipoic acid and **LA-PLLA 1**, **3**, **5** (l.: aqueous phase; r.: organic phase).

C.VII Poly(ethylene oxide) with a lipoic acid anchoring group

Polymer solution in dichloromethane:

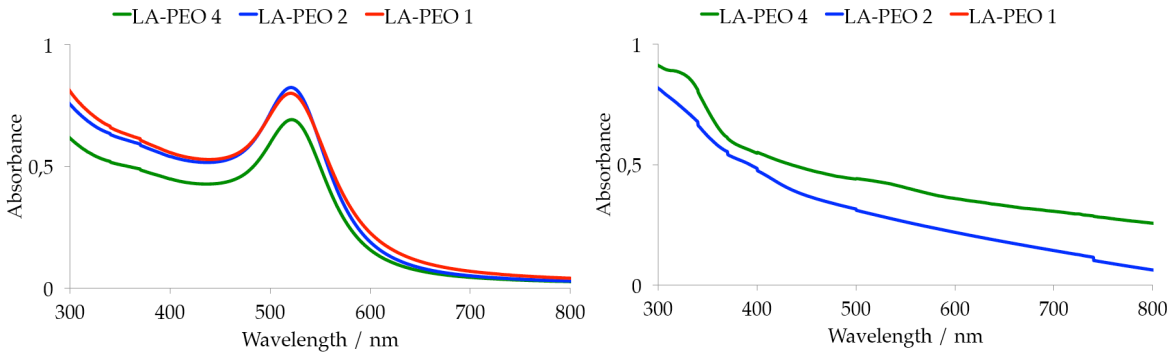

Figure C.24: UV-vis spectra of the extraction with **LA-PEO 1**, **2**, **4** (l.: aqueous phase; r.: organic phase).

		Size (d.n...	% Number	Width (d.n...
Z-Average (d.nm): 19,52	Peak 1:	11,18	100,0	3,019
PdI: 0,300	Peak 2:	0,000	0,0	0,000
Intercept: 0,907	Peak 3:	0,000	0,0	0,000

Result quality Good

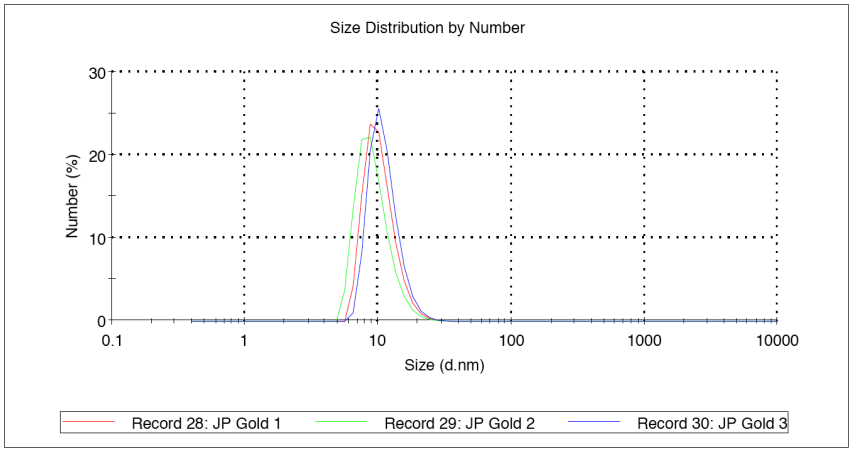

Figure D.1: Data of the Zetasizer measurements of the gold nanoparticle solution (three measurements).

Table D.1: Data of the Zetasizer measurements of the gold nanoparticle solution (three measurements and average).

	T [°C]	Z-Average [d.nm]	PdI	Pk 1 Mean Int [d.nm]	Pk 2 Mean Int [d.nm]
Au NPs	25	19.90	0.31	19.92	258.5
Au NPs	25	19.70	0.31	21.04	296.0
Au NPs	25	19.52	0.30	19.77	591.4
Average		19.71	0.31	20.24	
Deviation		± 0.19	± 0.01		

Jasmin Preis – Curriculum Vitae

Articles

- “Synthesis of Polyether-Based Polysulfides with Complex Architectures” Journal Article, in preparation (Chapter 4).

- “Modified Lipoic Acid as an Initiator for Ring-opening Polymerizations” Journal Article, in preparation (Chapter 5).

- “Combining Polysulfides with Polyesters to Block Copolymers” Preis, J.; Fischer, A. M.; Tabulew, I.; Tirelli, N.; Frey, H.; *ACS Macro Letters*, in preparation (Chapter 6).

- "6-Chloro-3-(3-methylphenyl)-1,2,4-triazolo[4,3-b]pyridazine" Preis, J.; Schollmeyer, D.; Detert, H; *Acta Crystallographica Section E*, **2011**, *67*, o2551.

- "5-Methyl-3-(3-methylphenyl)-7-phenyl-1,2,4-triazolo[4,3-c] pyrimidine" Preis, J.; Schollmeyer, D.; Detert, H; *Acta Crystallographica Section E*, **2011**, *67*, o987.

- "Proton-induced Multiple Changes of the Absorption and Fluorescence Spectra ofAmino-Aza-Oligo-(phenylenevinylene)s" Schmitt, V.; Glang, S.; Preis, J.; Detert, H.; *Advances in Science and Technology*, **2008**, *55*, 36-41.

- "Proton-Induced Multiple Changes of the Absorption and Fluorescence Spectra of Amino-Aza-Oligo-(phenylenevinylene)s" Schmitt, V.; Glang, S.; Preis, J.; Detert, H.; *Sensor Letters*, **2008**, *6*, 1-7.

Posters

- "From Polyglycerol to Novel Poly(propylene) Sulfide Brushes and Multi-Arm Star" Preis, J.; Frey, H.; Tirelli, N.; **International Symposium on Ionic Polymerization**, July **2011**, Akron, Ohio, USA

- “Biocompatible Polymers on Surfaces” Preis, J.; Frey, H.; **IMPRS evaluation meeting**, May **2010**, Mainz

Danksagung